ETS1 Promotes Context-Dependent Activation of Notch Signals in T-Cell Leukemia

by

Anna C. McCarter

A dissertation submitted in partial fulfillment
of the requirements for the degree of
Doctor of Philosophy
(Cellular and Molecular Biology)
in the University of Michigan
2020

Doctoral Committee:

Associate Professor Mark Y. Chiang, Chair
Professor James D. Engel
Professor Elizabeth R. Lawlor
Associate Professor Qing Li
Professor Ivan P. Maillard, University of Pennsylvania

Anna Catherine McCarter

gormleya@umich.edu

ORCID iD: 0000-0003-3828-9797

© Anna C. McCarter 2020

Dedication

To my family, my friends, my lab mates, and my Ph.D. mentor. I could not have matured as a scientist or person without your support, for which I am very grateful.

Acknowledgements

Completing a Ph.D. truly takes a village. While I cannot possibly acknowledge all the people who shared their time, resources, and expertise throughout this project, I will try.

I would like first and foremost to thank my mentor, Dr. Mark Chiang. I joined the Chiang lab because I wanted to the opportunity to learn to think about science as he does, and I have not been disappointed. I've appreciated his endless mentoring, patience, and encouragement. I can attribute so much of my growth as a scientist and a person over the past five years to his teaching. I also want to thank members of the Chiang lab, past and present. It was such a pleasure learning from both Nancy and Rena; I was lucky to get to build this project upon such a solid foundation. I wish to thank Amparo for teaching me everything about mouse work; she is certainly missed. I learned so much from Cher, Angie, Yiran, Erin, Catherine, Ambre, Jennifer, Jahnavi and Noah, and thank them for all their contributions to this project. It's been wonderful to work with Alice for all these years; I'm grateful for her support and friendship. I'm so pleased that Ashley chose to join us, and I'm very excited to see what the future holds for her. I am confident that the Chiang lab is in good hands!

I want to thank my dissertation committee: Dr. Doug Engel, Dr. Beth Lawlor, Dr. Qing Li, and Dr. Ivan Maillard. Their questions and comments at dissertation committee meetings, hematopoiesis research group, and T-cell development club challenged me to think more deeply about this project and execute better experiments. Even when progress was difficult, their enthusiasm for my project was motivating. For this, I am so very grateful. I also want to thank

them for their support in my professional development; from grant applications to conferences, I've always appreciated their guidance, advice, and endorsement.

The incredible support I've received here at the University of Michigan has been so very appreciated. To the Ryan lab, my second home in the Cancer Center, I couldn't have asked for better collaborators and friends. I am so thankful for their teaching me everything about ChIP-seq and bioinformatics; this project simply would not have been possible without them. I want to thank Dr. Linda Samuelson and Theresa Keeley for generously sharing their time and expertise on the intestinal homeostasis project. I also want to thank Dr. Moshe Talpaz and Dr. Luke Petersen, for their support in the enhanced degradation studies. I've always appreciated Rork Kuick challenging us to ask better scientific questions and sending along fascinating images of mushrooms with his emails. It's been great getting to know Nick Kunnath this past year, and his efforts on the bioinformatics have been invaluable.

I also want to thank our external collaborators; their generosity with reagents, knowledge, and ideas made possible the large scope of this work. Dr. Michael Ostrowski sharing of the $Ets1^{f/f}$ mouse made so many more experiments possible. Dr. Andrew Weng supplied patient derived xenografts, T-ALL cell lines, and the invaluable know-how in working with both. Dr. Adolfo Ferrando and Dr. Guisy Della Gatta, brought amazing collaboration on the paper; their data and insights helped shape the publication into a much stronger piece.

I've received great support from the MSTP and CMB offices; I want to thank Dr. Ron Koenig, Justine Hein, Gretchen Aland, Liz Bowman, Dr. Robert Fuller, Pat Ocelnik, and Lauren Perl and past administrators Ellen Elkin, Laurie Koivupalo, Hilkka Ketola, and Margarita Bekiares, for their assistance in helping me to navigate graduate school. To my former mentors,

Dr. John Katzenellenbogen, Dr. Esmail Meisami, and Dr. Maria Morasso, I appreciate their encouraging me in research and demonstrating what it means to be a scientist.

Finally, I want to thank my friends and family, without whom I could not have completed this work. To my MSTP colleagues, particularly Bobby, Henry, and Sam, I am so thankful for their friendship, humor, and understanding through all the ups and downs of the past 7 years. I would like to thank my CMB cohort for the warm welcome. I also appreciate my "outside" friends for celebrating victories with me and cheering me up after defeats. I want to thank my family for all their support, past and present; I love them all. I'd like to especially acknowledge my uncle, Dr. Craig Mallak, for without his example and encouragement, I would never have pursued this path. Most of all, I want to thank my husband, Gillis; I'm so proud of the life we've built together, and I can't wait for the next chapter.

Table of Contents

List of Figures

Abstract

Notch is a signaling pathway involved in cellular growth and development. Aberrant activation of the Notch pathway is prevalent in cancer, including more than 60% of cases of T-cell acute lymphoblastic leukemia (T-ALL). Clinical trials using pan-Notch inhibitors to treat T-ALL patients have revealed excessive toxicities; Notch is required for tissue homeostasis in organs like the intestines. Intermittent dosing with pan-Notch inhibitors is tolerable but has weak anti-cancer effects. An alternative strategy for inhibiting Notch signaling in cancer would be to target tissue-specific cofactors required for Notch's transcriptional activity. Notch cannot activate response elements in the nucleus of the cell on its own; it requires a favorable nuclear context produced by transcriptional cofactors. Furthermore, Notch often utilizes tissue-specific enhancers to selectively drive transcription of its target genes in particular cell types; others have demonstrated that deletion of a T-cell specific Notch-dependent enhancer for the *MYC* oncogene impairs T-cell development and T-ALL proliferation without effects in other tissues. Targeting a cofactor required for Notch's function at T-cell specific enhancers might inhibit leukemic cell growth without the toxicities of pan-Notch inhibition.

One such tissue-specific cofactor might be Ets1, a hematopoietic transcription factor implicated in the pathogenesis of other cancers. Ets1 is an attractive candidate as a Notch cofactor in T-ALL since it is expressed primarily in lymphoid cells and binds to the majority of Notch1 response elements in a T-ALL cell line. To investigate the importance of Ets1 in T-cell development and T-ALL, I used a conditional *Ets1* knockout mouse and RNAi knockdown of

Ets1. Not only is Ets1 important for the same stages of T-cell development as Notch1, but deletion of Ets1 in Notch-driven T-ALL cells reduced leukemia cell burden and prolonged survival in mice. In order to identify the mechanism by which Ets1 inhibits the growth of T-ALL cells, I performed RNA-seq and ChIP-seq studies in a human T-ALL cell line. Ets1 co-regulates the expression of a subset of NOTCH1 target genes, including known T-ALL oncogenes. Ets1 is also important for Notch complex binding and activation of Notch-driven enhancers essential for T-cell development and T-ALL proliferation. Finally, silencing Ets1 sensitizes human T-ALL cell lines to pan-Notch inhibitors, suggesting that targeting both Ets1 and Notch might be an effective therapeutic strategy. This thesis work supports an emerging model in which transcription factors assist Notch in activating enhancers; exploiting this dependency might combat Notch activity in cancer with less toxicity than inhibiting Notch directly.

Chapter 1 Notch Signaling in T-Cell Acute Lymphoblastic Leukemia[1]

A need for targeted therapies for T-cell Acute Lymphoblastic Leukemia

T-cell acute lymphoblastic leukemia (T-ALL) is an aggressive lymphoid malignancy that arises from developing T-cells in the thymus or bone marrow. T-ALL accounts for 15% and 25% of childhood and adult ALL cases respectively, and is characterized by older age at onset, male sex predominance, and poor prognosis in comparison with B-cell acute lymphoblastic leukemia (Paganin and Ferrando 2011). T-ALL is highly curable in the pediatric population, with 85% of patients achieving long-term survival; however, survival rates in adults are far worse (35-40%)(Pui et al. 2009). Additionally, approximately 15% of children and 40% of adults do not respond to chemotherapy or subsequently relapse (Raetz and Teachey 2016). And since T-ALL patients are currently treated with aggressive multiagent chemotherapy, acute and long-term toxicities are common (Jacola et al. 2016). In order to reduce the sequalae associated with T-ALL treatment, it might be possible to harness the recent advancements made in the molecular characterization of T-ALL oncogenic drivers to develop targeted therapies.

T-ALL is genetically heterogenous, with multiple driver mutations and signaling pathways contributing to the pathogenesis of this disease. For example, the IL7R/JAK/STAT pathway is activated in 20-50% of patient T-ALLs, and TAL/LMO factors are dysregulated in almost 50% of cases ((Liu et al. 2017, Oliveira et al. 2019). However, the activating mutations in the Notch signaling pathway are the most common genetic perturbations found in T-ALL.

[1] Adapted and excerpted from McCarter AC, Wang Q, and Chiang MY. Notch in Leukemia. Adv Exp Med Biol. 1066:355-394, 2018.

The first evidence of aberrant activation of Notch in T-ALL was in the discovery of a t(7;9)(q34;q34.3) chromosomal translocation that places the Notch1 gene adjacent to the T-cell receptor locus, leading to the expression of a truncated, constitutively active Notch1(citation). After the initial discovery of acquired, recurrent, gain-of-function mutations of Notch1 in human pediatric T-ALLs, other large studies confirmed these findings and extended them to adult T-ALLs ((Weng et al. 2004, Mansour et al. 2009, Trinquand et al. 2013, Asnafi et al. 2009, Jenkinson et al. 2013, Clappier et al. 2010, Kox et al. 2010). The exception to this trend is early T-cell precursor ALL (ETP-ALL), where Notch1 mutations are less frequent than in conventional T-ALLs (11-30% of ETP-ALLs vs 50-62% of conventional T-ALL). ETP-ALL is a primitive form of T-ALL with stem cell and/or myeloid features (Coustan-Smith et al. 2009).

Activating Notch Mutations in T-ALL

Notch1 is one of the 4 paralogues of the Notch receptor, whose signaling governs cellular proliferation and fate decisions during development. Under physiological conditions, interaction between the extracellular domain of the Notch receptor with its ligand (JAGGED, DLL) on an adjacent cell triggers two proteolytic cleavage events. These liberate the intracellular portion of Notch (ICN), which then translocates to the nucleus. Through binding with canonical cofactors RBPJ and MAML, ICN then drives transcription of its target genes (Fig.1.1). NOTCH1 mutations in T-ALL cluster in two hotspots the lead to hyper-activation of the Notch pathway (Fig. 1.1). The first hotspot consists of single amino acid substitutions and in-frame insertions in the extracellular negative regulatory region (NRR mutations) and in-frame insertions in the juxta-membrane extracellular region (JME mutations). The NRR consists of the Lin12/Notch repeats (LNR, Exon 25) and the heterodimerization domain (HD, Exons 26 and 27). The NRR

locks the Notch receptor in the inactive conformation (Sanchez-Irizarry et al. 2004), burying the S2 cleavage site within a hydrophobic pocket, thus autoinhibiting S2 cleavage by a disintegrin and metalloproteinase domain-containing protein 10 [ADAM10,(Gordon et al. 2007, Gordon et al. 2009)]. LNR mutations (e.g. H1545P) disengage the LNR clamp from the HD domain possibly through loss of calcium binding [(Gordon et al. 2009), Fig. 1.2A]. HD class 1A mutations (e.g. L1601P) separate the extracellular domain from the trans-membrane domain (Malecki et al. 2006) while HD class 1B mutations (e.g. L1594P) cause con-formational changes. HD class 2 mutations (e.g. A1721_V1722InsARLGSLNIPYKIEA) or JME alleles (e.g. A1739_A1740InsQAVEPPPPA QLHFMYVA) insert short peptides that separate the NRR from the S2 site and/or membrane (Malecki et al. 2006, Sulis et al. 2008). All these ligand-independent changes, induced by mutations, expose the S2 cleavage site, leading to generation of the transcriptionally active form of Notch1, the intracellular Notch1 (ICN1).

The second hotspot of NOTCH1 mutations are nonsense mutations or short insertion/ deletions dispersed throughout the C-terminal PEST domain (Exon 34) (Fig.1.1, Fig. 1.2B). These mutations truncate the C-terminus through premature STOP codons. PEST truncations remove “degron” sites that are phosphorylated by serine/threonine kinases, such as the cyclin C-cyclin- dependent kinase 8 (CDK8)/cyclin-dependent kinase 19 (CDK19)/cyclin-dependent kinase 3 (CDK3) complexes and unknown kinases that phosphorylate a WSSSSP motif (Chiang et al. 2006, Fryer, White and Jones 2004, Li et al. 2014). Phosphorylated degrons are recognized and targeted for degradation by the E3 ubiquitin ligase f-box and WD repeat containing protein 7 (FBXW7) ((Thompson et al. 2007, O'Neil et al. 2007). Inactivating mutations in FBXW7 and

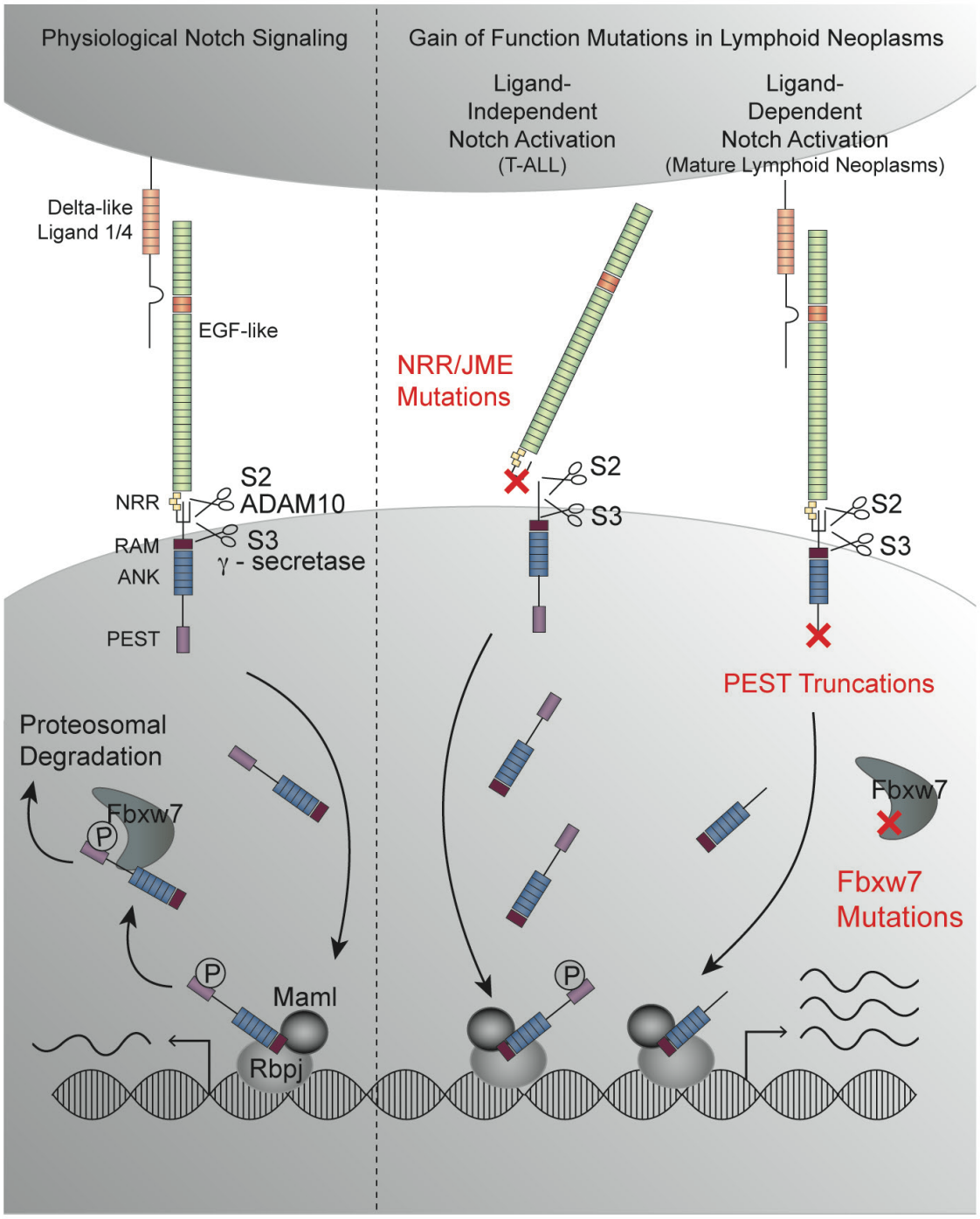

Figure 1.1 Oncogenic Notch Signaling in Lymphoid Neoplasms

(left) Physiological Notch signaling. (right) Ligand-independent cleavage triggered by NRR NOTCH1 mutations in T-ALL and ligand-dependent cleavage ofNOTCH1 in mature lymphoid neoplasms. Activation can be enhanced by PEST/FBXW7 mutations which increase half-life of intracellular Notch1 (ICN1).

CCNC (which encodes cyclin C) occur in ~14–24% and ~9% of patients, respectively (Thompson et al. 2007, O'Neil et al. 2007, Li et al. 2014). Thus, PEST, FBXW7 and CCNC mutations prolong ICN1 half-life. In ~20% of patients, NRR and PEST/FBXW7 mutations occur in cis, which cooperatively augments Notch signals (Weng et al. 2004). Altogether, NOTCH1 and/or FBXW7 mutations occur in ~54–74% of patients.

In the absence of rat sarcoma virus oncogene (RAS) and phosphatase and tensin homolog (PTEN) mutations, they are associated with favorable prognosis (Trinquand et al. 2013). Ligand interactions with unmutated receptors may trigger Notch activation in T-ALL. Mouse studies predict that circulating human T-ALL blasts will encounter the NOTCH1 ligand Delta-like 4 (DLL4) on thymic epithelial cells (Koch et al. 2008, Hozumi et al. 2008); fibroblastic reticular cells and follicular dendritic cells in LNs (Fasnacht et al. 2014, Chung et al. 2017); endothelial cells (Ramasamy et al. 2014); and bone-producing osteocalcin-expressing cells in the BM (Yu et al. 2015).

Although NRR-mutated Notch receptors activate Notch signaling constitutively, they also respond to ligands based on in vitro cell-based reporter assays (Malecki et al. 2006). Accordingly, patient-derived xenografts (PDX) with NRR-mutated or wildtype NOTCH1 receptors respond to ligand stimulation in proliferation and leukemia initiating assays (Armstrong et al. 2009). ~23% of NOTCH1 mutations are PEST mutations without an NRR mutation in cis (Weng et al. 2004). PEST mutations do not activate the Notch pathway per se. Thus, these receptors would require ligand to trigger activation (Malecki et al. 2006, Weng et al. 2004). If ligands are important, then Notch inhibitors might have antileukemic activity even when NOTCH1 mutations are absent or sub-clonal. Accordingly, PDX samples with wildtype receptors were inhibited by an anti-Dll4 antibody in mice (Minuzzo et al. 2015). In a clinical

trial, patients with wildtype receptors responded to GSI (Zweidler-McKay et al. 2014). These data suggest that ligand-receptor interactions might be important in T-ALL.

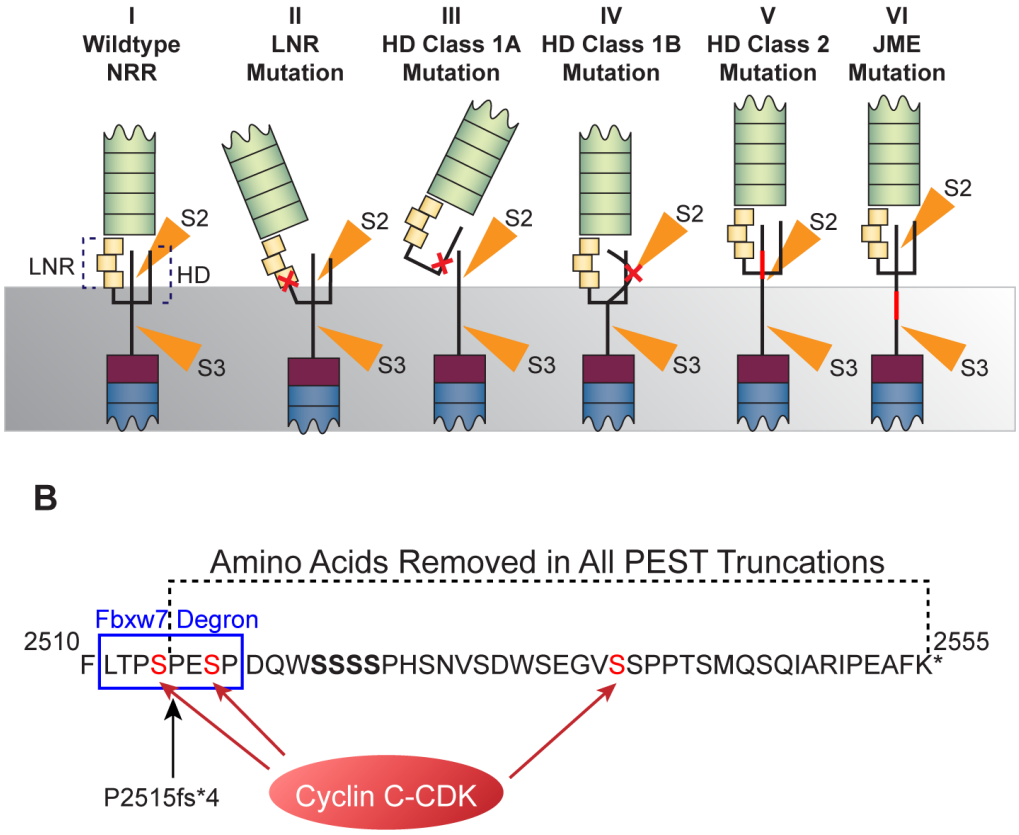

Figure 1.2 Mutational mechanisms of NOTCH1 gain-of-function

A) The S2 proteolytic cleavage site is exposed by (1) LNR mutations that disengage the LNR clamp from the HD domain; (2) class 1A HD mutations that dissociate the extracellular and transmembrane domains; (3) class 1B HD mutations that disturb the NOTCH1 conformation; (4) class 2 HD mutations that separate the NRR away from the S2 site; (5) juxta-membrane expansion (JME) mutations that separate the NRR and S2 site away from the membrane. B C-terminal protein sequence of human NOTCH1 (amino acids 2510-2555) that are lost upon PEST mutations. The most C-terminal truncation occurs at amino acid 2516. S (red), serine residues phosphorylated by CCNC-CDK; SSSS, serine residues phosphorylated by unknown kinase; P2515fs*4 represents ~70-80% of all PEST mutations in CLL and results in a frameshift (fs) starting at Proline #2515 with a shift frame of 4 including the stop codon (*); FBXW7 degron motif (box).

In ~43% of human T-ALL BM specimens, ICN1 cannot be detected by immunohistochemistry (Kluk et al. 2013). The authors concluded that these samples were unrelated to NOTCH1 activation; however, this study did not perform NOTCH1 mutational analysis, so the presence or absence of ICN1 for each sample was not linked to the presence or

absence of a NOTCH1 mutation. If some ICN1-negative samples had PEST mutations, it might be possible that Notch might have been activated by ligand in a different niche (e.g. thymus, spleen, or LN), or in an ancestral clone, or was activated by ligand at low levels below the sensitivity of the technique. Conversely, if some ICN1-positive samples lacked NRR mutations, it is possible that ligand was triggering cleavage.

Role of Notch Signaling in T-ALL Initiation, Progression, and Maintenance

NOTCH1 mutations can occur as an initiating event based on the detection of NRR mutations in peripheral blood cells at birth (Eguchi-Ishimae et al. 2008). These mutations occur prior to the acquisition of other oncogenic events and well in advance of the clinical appearance of childhood T-ALL. Further, the t(7;9) translocation occurs during normal T-cell development when the T-cell receptor β gene recombines at the pre-T-cell stage. Aberrant recombination creates the t(7;9) translocation, which juxtaposes the deoxyribonucleic acid (DNA) sequence encoding part of the transmembrane NOTCH1 subunit with the TCRB regulatory sequences. This rearrangement generates either ICN1 (Ellisen et al. 1991) or a membrane-tethered version of ICN1 (Palomero et al. 2006b). ICN1 is a potent initiator of T-ALL in mouse models (Pear et al. 1996, Aster et al. 2000, Deftos et al. 2000); however, t(7;9) is extremely rare compared to NRR mutations. Like ICN1 alleles, NRR mutant alleles can transactivate Notch reporters in vitro and induce ectopic T-cell development in the BM from hematopoietic stem cells (HSCs) in mouse models (Chiang et al. 2008). However, NRR alleles have much weaker effects than ICN1 alleles and are weak initiators of T-ALL. The NRR mutations are eventually lost from the HSCs and T-cell progenitor compartments because of excessive T-cell commitment (Chiang et al. 2013). Thus, Notch1 mutations can initiate T-ALL only in limited contexts.

The role of Notch during T-ALL progression is based on the finding that NOTCH1 mutations can be subclonal or occur at relapse but not at diagnosis (Mansour et al. 2007). By this measure, Notch activation frequently occurs during progression. A large sequencing study found that NOTCH1 mutations are subclonal in ~44% of the cases with NOTCH1 mutations (Liu et al. 2017). However, these data seem at odds with an IHC study showing that all cases of T-ALL (N=14) were diffusely positive for ICN1 [>80% of cells, (Kluk et al. 2013)]. Thus, NOTCH1 mutations but not NOTCH1 activation might be subclonal. To reconcile these data, it is possible that intra-tumoral heterogeneity can occur with some cells activating NOTCH1 through ligand-receptor interactions while other cells are also activating NOTCH1 through mutations. This possibility would be consistent with observations of several transgenic mouse lines that ectopically express oncogenes associated with human T-ALL (Aster, Pear and Blacklow 2008). In these mice, the transgenes initiate T-ALL in the thymus where Notch1 is activated by Dll4 expressed on stromal cells. Subsequently, Notch signals are raised during disease progression by the spontaneous acquisition of Notch1 mutations. In one of these models, developing T-ALL cells were forced to express a dominant-negative mastermind (DN-MAML) transgene that blocked Notch signals. In response, the cells deleted DN-MAML rather than finding alternatives for Notch signals (Chiang et al. 2016). Thus, Notch activation can be essential for progression. In established Notch1-activated T-ALL cells, Notch withdrawal frequently induces G1/S arrest and sometimes apoptosis (Weng et al. 2003, Weng et al. 2004, O'Neil et al. 2006). Notch inhibition also downregulates glycolysis and glutaminolysis and increases autophagy (Herranz et al. 2015). The target genes that are responsible for these effects are discussed in the next section. Would Notch inhibition have curative potential by targeting leukemia stem cells (LSCs)? LSCs are the subset of cells responsible for propagating the cancer. LSCs are measured by

transplanting leukemia cells at limiting dilution into recipient mice and estimating the number of leukemia- initiating cells (LICs) based on the fraction of mice that develop leukemia. Notch activation drives the development of LICs in mouse models of Notch-induced T-ALL (Chiang et al. 2013, Li et al. 2008). Inhibiting Notch signals with GSI decreases LICs in patient-derived xenograft models (Armstrong et al. 2009) and a T-cell acute lymphoblastic leukemia (Tal1)/Lim domain only 2 (Lmo2)-induced mouse model of T-ALL (Tatarek et al. 2011). DN-MAML also reduces LICs in the Kirsten rat sarcoma viral oncogene homolog (Kras)G12D-induced mouse model of T-ALL (Chiang et al. 2016). These data suggest that Notch inhibitors could contribute to curative therapy by targeting LSCs.

Oncogenic Direct Notch Target Genes and Pathways in T-ALL

Identifying direct Notch target genes with oncogenic functions is important given the on-target toxicities and primary resistance seen with pan-Notch inhibitors. Inhibiting important Notch target proteins rather than Notch itself might avoid toxicities and bypass resistance. We are mindful that Notch regulates target genes in a context-dependent manner, even within the confines of T-ALL transcriptomes. Of note, Notch likely regulates several important targets only indirectly, such as C-C chemokine receptor type 7 (CCR7) (Buonamici et al. 2009) immunoglobulin enhancer-binding factor E12/E47 protein (E2A, encoded by TCF3) (Nie et al. 2003), phosphatase of regenerating liver (PRL2) (Dong et al. 2012, Dong et al. 2014, Kobayashi et al. 2017) and tumor protein p53 (TP53) (Beverly, Felsher and Capobianco 2005).

To date, the direct NOTCH1 target genes that have been shown to maintain T-ALL proliferation are *MYC*, *HES1*, interleukin 7 receptor (*IL7R*), insulin like growth factor 1 Receptor (*IGF1R*), leukemia-associated non-coding IGF1R activator ribonucleic acid 1 (*LUNAR1*), cyclin

D3 (*CCND3*), and nuclear factor of kappa light polypeptide gene enhancer in B cells 2 (*NFκB2*)/relaxed B proto-oncogene (*RELB*). Less well understood are DEP domain containing MTOR interacting protein (*DEPTOR*) (Hu et al. 2017), tribbles pseudokinase 2 (*TRIB2*) (Sanda et al. 2012, Wouters et al. 2007) and *NOTCH3* (Bellavia et al. 2000, Wang et al. 2011). The evidence for each of these targets is summarized in Table 1. To show that these target genes were direct, earlier studies used chromatin immuno-precipitation (ChIP) assays at promoter regions. However, the promoter ChIP assay has been supplanted by ChIP-Seq, which has shown that ICN1 dynamically binds proximal and/or distal enhancers of target genes with greater frequency and often-greater affinity than the promoter region (Margolin et al. 2009, Wang et al. 2014a).

	BOX1: Assays testing direct regulation by NOTCH1				**BOX2**: Assays testing importance for Notch-activated T-ALL maintenance			
Direct NOTCH1 target gene	Location of major ICN1/RBPJ peak(s)[b]	GSI Wash-out Assay[c]	Luciferase Reporter Assay[d]	Induces T-ALL in GEMM	Human T-ALL cell lines (*in vitro*)	Rescues GSI-treated T-ALL cell lines (*in vitro*)[e]	Notch-activated GEMM (*in vivo*)	Primary human T-ALL[f]
MYC	+1.4Mb	x	x	x	x	x	x	both
HES1	promoter region	x	x	x	x		x	*in vitro*
IL7R	+27Kb; +43Kb	x	x	g	x	x		*in vitro*
IGF1R	intron 20 enhancer	x	x		x		x	*in vitro*
LUNAR1	intron 20, *IGFR1R*		x		x			
CCND3	intron 1 enhancer				x	x	x	*in vivo*
NFkB2	exon 14 enhancer				x		x	
RELB	promoter region				x		x	
DEPTOR	promoter region[h]				x			
TRIB2	intron 2 enhancer				x			
NOTCH3	intron 1 enhancer	x		x	x[i]			

Table 1 Oncogenic Direct NOTCH1 Target Genes in T-ALL

T-ALL, T-cell acute lymphoblastic leukemia/lymphoma; GEMM, Genetically engineered mouse model of T-ALL; GSI, γ-secretase inhibitor; ICN1, Intracellular Notch1 [a]defined as genes directly regulated by ICN1 binding (BOX1) and for which inhibition of encoded proteins (e.g. genetically or with pharmacological inhibitors, BOX2) reduces Notch-activated T-ALL proliferation; [b]Peak locations in CUTLL1 extracted from GSM1252936 (Wang et al. 2014a) relative to transcriptional start site (except for DEPTOR[h]); [c]details in (Bailis, Yashiro-Ohtani and Pear 2014), CUTLL1 expression data extracted from (Wang et al. 2011); [d]using genomic fragment containing the ICN1 peak(s) with adequate controls; [e]full or partial rescue of GSI-mediated growth inhibition when target gene is ectopically expressed; [f]in vitro, in vivo or both; gmature lymphoma; [h]by ChIP-qPCR not ChIP-Seq (Hu et al. 2017); [i]only the NOTCH3-mutated TALL-1 cell line (Bernasconi-Elias et al. 2016).

PI3K/AKT/mTOR

Notch1 was initially believed to activate the phosphatidylinositol 4,5-bisphosphate 3-kinase (PI3K)/Ak mouse transforming (AKT)/ mechanistic target of rapamycin (MTOR) pathway by inducing *MYC* (Chan et al. 2007). Subsequent reports showed that several other direct Notch1 target genes converge on this pathway – *HES1* (Palomero et al. 2007), *IGF1R* (Medyouf et al. 2010), *LUNAR1* (Trimarchi et al. 2014), *IL7R* (Gonzalez-Garcia et al. 2009), invariant preTα chain of the pre-T cell receptor (*PTCRA*) (Reizis and Leder 2002) and possibly *DEPTOR* (Hu et al. 2016). While these target genes have roles in PI3K/AKT-independent pathways, their regulation by Notch1 emphasizes the importance of PI3K/AKT as a downstream oncogenic mediator of converging Notch signals (Palomero et al. 2007, Cullion et al. 2009, Chiarini et al. 2009, Avellino et al. 2005, Herranz et al. 2015). HES1, a basic helix-loop-helix (bHLH) transcription factor, induces the PI3K/AKT pathway by suppressing the transcription of PTEN (Palomero et al. 2007). PTEN blocks PI3K signaling by dephosphorylating phosphatidylinositol (3,4,5)-trisphosphate P3 (PIP3) which inactivates AKT (Palomero et al. 2007). Notch inhibition with GSI has broad transcriptional effects on metabolic genes including those important for nucleic acid and amino acid bio-synthesis, protein translation and ribosome bio-synthesis; however, Pten inactivation largely reverses these effects in mouse models of Notch1-induced T-ALL (Herranz et al. 2015).

Direct Notch target genes that encode receptors presumably activate AKT through canonical receptor-ligand interactions [IL7R and IGF1R (Johnson et al. 2008)] or through tonic signals [PTCRA (Sade, Krishna and Sarin 2004)]. NOTCH1 binds a pair of distal enhancer sites 3' of the IL7R gene (Wang et al. 2014a). Enforced expression of IL7R rescues withdrawal of Notch signals in a human T-ALL cell line (Gonzalez-Garcia et al. 2009). High levels of IL7-IL7R interactions can also drive peripheral B and T-cell lymphomas in mice, although not T-ALL (Rich et al. 1993, Abraham et al. 2005). IL7 is required to grow primary human T-ALL cells in culture (Barata et al. 2004, Armstrong et al. 2009). The importance of IL7R is further highlighted by the discovery of ~10%of patients with activating IL7R mutations (Zenatti et al. 2011, Shochat et al. 2011). NOTCH1 directly binds an intronic enhancer in the human *IGF1R* gene to induce its transcription and genetic inactivation of mouse *Igf1r* inhibited LIC activity in a mouse model of Notch1-induced T-ALL (Medyouf et al. 2010). Antibodies or drugs that block IGF1R signals reduced the proliferation of human T-ALL cell lines and patient-derived xenograft cells. Interestingly, the intronic enhancer that regulates *IGF1R* also regulates *LUNAR1*, which encodes an enhancer-like long noncoding ribonucleic acid (RNA) that induces *IGF1R* transcription through long-range interactions (Trimarchi et al. 2014). Silencing *LUNAR1* inhibited the proliferation of human T-ALL cell lines in vitro and in vivo. Thus, NOTCH1 induces *IGF1R* directly and indirectly through *LUNAR1*. Pre-T cell receptor signals are important for leukemia initiation in mouse models of Notch-induced T-ALL (Allman et al. 2001, Campese et al. 2006, Bellavia et al. 2002). However, the relevance of these signals for human T-ALL maintenance is unclear.

MYC

MYC is a bHLH transcription factor regulating diverse target genes important for proliferation and metabolism (Palomero et al. 2006a). ICN1 binds strongly to the Notch-dependent and T-cell specific *Myc* enhancer ("N-ME" or "NDME") located at +1.4 MB downstream of the transcriptional start site (Herranz et al. 2014, Yashiro-Ohtani et al. 2014b). Notch may also stabilize MYC protein indirectly through activation of the PI3K/AKT pathway (Bonnet et al. 2011, Palomero et al. 2007). Ectopic expression of *Myc* drives T-ALL initiation in mice (Felsher and Bishop 1999) and zebrafish (Langenau et al. 2003). These leukemias lack *Notch1* mutations or cleaved ICN1. Retroviral insertional mutagenesis in mice showed mutual exclusivity of *Notch1* and *Myc* insertions in virtually all murine T-ALL tumors (Sharma et al. 2006, Uren et al. 2008). Similarly, human T-ALLs with *MYC* translocations are typically devoid of *NOTCH1* mutations (La Starza et al. 2014). Thus, MYC can substitute for ICN1 for leukemia initiation. MYC is also required for initiation as its genetic inactivation prevents the development of Notch1-induced murine T-ALL (Herranz et al. 2014, Li et al. 2008). In the KrasG12D-induced mouse model of T-ALL, spontaneous Notch1 mutations are acquired in >90% of tumors (Chiang et al. 2008). However, enforced expression of *Myc* relieves the selective pressure for Notch activation, leading to T-ALLs that lack *Notch1* mutations or cleaved ICN1 (Chiang et al. 2016). Thus, the MYC protein can replace activated Notch in T-ALL progression. In contrast, enforced expression of other Notch targets, such as *Hes1* (Dudley, Wang and Sun 2009) or *Akt1* in the transgenic *KrasG12D* mouse model (Chiang et al. 2016), leads to T-ALLs that retain Notch1 mutations or cleaved ICN1. In this regard, *MYC* appears to hold a unique role among Notch target genes during initiation and progression. However, the role of *MYC* during leukemia maintenance seems somewhat less prominent.

Genetic inactivation of the Notch-driven *Myc* enhancer in established murine Notch1-induced T-ALLs causes tumor regression (Herranz et al. 2014). Similarly, *MYC* transcription can be reduced through genetic or pharmacological inhibition of bromodomain containing 4 (BRD4). This inhibits proliferation and LIC activity in mouse models of Notch-induced T-ALL and patient-derived xenografts (King et al. 2013, Knoechel et al. 2014, Roderick et al. 2014, Loosveld et al. 2014). In contrast to its unique role during initiation and progression of T-ALL, MYC does not appear to be the dominant contribution of NOTCH1 during maintenance. For example, enforced expression of *MYC* only rescues a subset of human T-ALL cell lines from withdrawal of Notch signals (Weng et al. 2006, Palomero et al. 2006a). Similarly, enforced expression of *Myc* only rescues a subset of transgenic *KrasG12D*-induced murine T-ALL cell lines from Notch withdrawal (Chiang, unpublished observations). Overexpression of *Myc* in an ICN1-initiated mouse model cannot maintain T-ALL when ICN1 is withdrawn (Demarest, Dahmane and Capobianco 2011). Finally, a patient whose blasts overexpressed *MYC* independently of Notch nevertheless achieved a complete remission upon GSI treatment (Knoechel et al. 2015). Thus, MYC seems to be a dominant contributor for Notch-driven T-ALL maintenance in only some contexts.

NF-κB

The nuclear factor-κB (NF-κB) pathway can be blocked using bortezomib (Vilimas et al. 2007) or more specifically with a peptide inhibitor that disrupts the binding of NF-κB essential modulator (NEMO) to inhibitor of kappa-B kinase subunit beta (Ikkβ) (Espinosa et al. 2010). Both agents inhibit the proliferation of Notch-activated human T-ALL cell lines and maintenance of Notch1-induced T-ALL mouse models. NOTCH1 activates the NF-κB pathway by directly binding the *NFκB2* and *RELB* loci and inducing their transcription (Wang et al. 2014a, Vilimas

et al. 2007). NOTCH1 can also activate the NF-κB pathway indirectly by inducing HES1 protein expression, which represses the expression of ubiquitin carboxyl-terminal hydrolase (CYLD), which antagonizes inhibitor of kappa-B kinase (IKK). Elevated IKK then degrades IκBα, activating the NF-κB pathway (Espinosa et al. 2010). In activated murine T cells, ICN1 promotes the nuclear retention of NF-κB factors, possibly by directly binding and competing for inhibitor of nuclear factor kappa-B kinase subunit alpha (IκBα) (Shin et al. 2006). Thus, Notch promotes the NF-κB pathway through multiple mechanisms.

HES1

ICN1 binds directly to the promoter region of *HES1* in human T-ALL cell lines (Wang et al. 2014a). Enforced expression of *Hes1* induces T-ALL in mouse models (Dudley et al. 2009) and conversely, its genetic inactivation in mouse models of Notch-induced T-ALL impairs leukemia initiation and maintenance (Wendorff et al. 2010, Schnell et al. 2015). While HES1 promotes the PI3K/AKT and NF-κB pathways, it suppresses transcription of BCL-2 binding component 3 (Schnell et al. 2015). Given the diverse mechanisms by which HES1 drives T-ALL proliferation, there has been considerable interest in finding ways to therapeutically target HES1. Investigators identified drugs that phenocopy the gene expression changes induced by genetic deletion of Hes1 (Schnell et al. 2015). In detail, perhexiline, an inhibitor of mitochondrial carnitine palmitoyl-transferase-1, induces antileukemic effects on primary human T-ALL cells and in a mouse model of Notch-induced T-ALL. Perhexiline is better tolerated than GSI in clinical studies and it is being used to treat cardiac disease. While this is promising, the target of this drug within the HES1 pathway remains unknown.

Cell Cycle Regulators

Notch inhibition induces G1/S cycle arrest (Weng et al. 2004, Weng et al. 2003). In fact, it is known that Notch drives the G1/S transition by binding enhancers in the *CCND3* locus (Wang et al. 2014a) and inducing its transcription (Joshi et al. 2009) as well as by regulating *MYC* (Bretones, Delgado and Leon 2015). Additionally, Notch indirectly induces cyclin-dependent kinase 4 (*CDK4*) and cyclin- dependent kinase 6 (*CDK6*) and represses transcription of cyclin-dependent kinase inhibitors cyclin dependent kinase inhibitor 2d (*CDKN2D*) and cyclin dependent kinase inhibitor 1B (*CDKN1B*) presumably through indirect mechanisms (Rao et al. 2009). Inactivation of Ccnd3 impairs initiation and maintenance of Notch1- induced T-ALL in mouse models (Sicinska et al. 2003, Choi et al. 2012) while enforced expression of *CDK4* or *CDK6*, in combination with *CCND3*, partially rescues human T-ALL cell lines from Notch inhibition (Joshi et al. 2009). CDK4/6 inhibitors block the proliferation of human T-ALL cell lines and primary cells both in vitro and in vivo (Choi et al. 2012, Sawai et al. 2012, Rao et al. 2009, Pikman et al. 2017). Finally, MYC and Notch directly induce the transcription of S-phase kinase associated protein 2 (SKP2) in T-ALL and *Skp2* encodes an ubiquitin ligase that promotes cell cycle progression by targeting the Cdk inhibitor p27Kip1 for degradation (Dohda et al. 2007). Thus, Notch promotes cell cycle progression through multiple mechanisms.

Regulation of Notch1 Expression in T-ALL

It is important to understand the pathways and factors that regulate Notch1 expression in order to devise new strategies to downregulate the Notch pathway for therapeutic purposes. Since the regulators of Notch expression are frequently tissue-specific, such strategies might

have less toxicity compared to pan-Notch inhibitors. However, only a few studies have explored this possibility.

Direct Regulators of Notch1 Transcription in T-ALL

Notch1 directly auto-regulates its own transcription in conjunction with E2A transcription factors in murine thymocytes and T-ALL cell lines, and ectopic overexpression of inhibitor of DNA binding 3 HLH protein (*Id3*), an inhibitor of E2A, reduced Notch1 transcripts and inhibited the growth of murine T-ALL cell lines (Yashiro-Ohtani et al. 2009). Targeting E2A might seem attractive as E2A-deficient mice are generally healthy with defects limited to lymphoid development (Bain et al. 1997, Bain et al. 1994). However, chronic inhibition might be problematic as E2A-deficient mice frequently develop T-ALL. The homeobox transcription factor distal-less homeobox 5 (DLX5) binds an enhancer downstream of *Notch1* and an intronic enhancer in *Notch3* (Tan et al. 2017), inducing their transcription and driving T-ALL in transgenic mice. Targeting DLX5 might be challenging as Dlx5-deficient mice develop multiple cranio-facial abnormalities and do not survive post birth (Depew et al. 1999).

Post-Transcriptional Regulators of Notch1 Expression in T-ALL

RNA binding proteins zinc finger protein C3H type 36-like 1 (ZFP36L1) and zinc finger protein C3H type 36-like 1 (ZFP36L2) bind conserved AU-rich regulatory elements in the 3′UTR of Notch1 mRNA, impairing its stability and translation (Hodson et al. 2010). Mice deficient for these proteins develop T-ALL associated with Notch1 overexpression (Hodson et al. 2010). Similarly, MiR-101 binds the 3’ UTR of NOTCH1 and reduces NOTCH1 protein levels when overexpressed at high levels; since MiR-101 levels are relatively repressed in human T-ALL samples, this might help promote NOTCH1 over-expression (Qian et al. 2016). Given that enhancing Notch-depleting mechanisms such as the Ccnc/Fbxw7 pathway might be

challenging as a therapeutic strategy, one alternative approach would be to block the mechanisms that process or protect functional Notch receptors. For example, thapsigargin, a chemical inhibitor of sarco/endoplasmic reticulum calcium ATPase (SERCA), blocks the normal processing of wildtype and mutated Notch receptors in the endoplasmic reticulum and Golgi compartments, leading to depletion of ICN1, which then induces growth arrest of human T-ALL cell lines both in vitro and in vivo (Roti et al. 2013). In another example, the chaperone protein heat shock protein 90 (Hsp90) protects Notch proteins from E3 ligase STIP1 homology and U-box containing protein 1 (Stub1)-dependent degradation (Wang et al. 2017b). Inhibitors of SERCA or HSP90 had antileukemic effects in human T-ALL xenografts without major toxicity (Roti et al. 2013, Wang et al. 2017b) and similar effects would also be predicted for inhibitors of protein O-fucosyltransferase 1 (POFUT1), which is important for glycosylation of Notch receptors, as genetic inactivation of POFUT1 impaired leukemia-associated NOTCH1 mutant signaling (McMillan et al. 2017). Since SERCA and HSP90 inhibitors did not cause the major toxicities associated with pan-Notch inhibition, mutated Notch receptors might have an increased dependence compared to their wildtype counterparts on post-translational regulators.

Downstream Regulation of Notch1 Signals in T-ALL

In the nucleus, ICN1 engages mastermind-like protein (Maml) and recombination signal binding protein for immunoglobulin kappa J region (Rbpj) to form the core Notch transcriptional complex. Additional regulatory proteins bind the core complex to amplify Notch activity. Mass spectrometry screens of proteins pulled down by an anti-MAML1 antibody in human T-ALL cells (KOPT-K1) or streptavidin bead pulldown of biotin-tagged ICN1 in murine T-ALL cells (Beko) identified proteins that bind the core complex, such as DEAD-box RNA helicase 5 (DDX5/P68), an ATP-dependent RNA helicase (Lin et al. 2013, Jung et al. 2013). Knockdown

of DDX5 reduced Notch target gene transcription and proliferation of T-ALL cell lines both in vitro and in vivo (Lin et al. 2013, Jung et al. 2013). Another mass spectrometry study in a human T-ALL cell line (SUPT1) used an epitope-tagged ICN1 as bait (Yatim et al. 2012) and identified candidate interacting proteins such as histone demethylases [e.g. lysine (K)-specific demethylase 1A (LSD1) and PHD finger protein 8 (PHF8)], chromatin remodeling complexes [e.g. cohesin complex components and polybromo-associated BRG1- or HBRM-associated factors (PBAF) complex components – BRG1 and polybromo 1 (PB1)], co-activators [e.g. ALL1-fused gene from chromosome 4p12 protein (AF4p12)], histone acetylases [e.g. p300 and p300/CBP-associated factor (PCAF)], histone ubiquitinases [e.g. Bre1 subunit ring finger protein 40 (RNF40)] and transcription factors [e.g. B-cell CLL/lymphoma 11B (BCL11b), E2A/Hela E box-binding (HEB), runt related transcription factor 1 (RUNX1), NOTCH1, NOTCH2, and NOTCH3]. Apart from PBAF, these Notch- interacting proteins were previously discovered by other investigators in other cell types [for more comprehensive review see (Borggrefe and Liefke 2012)]. It is unclear whether these proteins bind NOTCH1 directly, but it is clear that BRG1, PB1, LSD1 and PHF8 are recruited by ICN1 to Notch binding sites. These cofactors catalyze chromatin changes, such as H3K9me1/2 demethylation and H3K27me2 demethylation and their genetic silencing leads to downregulation of oncogenic target genes (*IL7R*, *MYC*, and *HES1*) and slower proliferation of human T-ALL cell lines both in vitro and in vivo ((Yatim et al. 2012). Coactivator-associated arginine methyltransferase 1 (CARM1) binds directly to ICN1, is recruited by the Notch complex to enhancers, methylates five arginine residues within the Notch transcriptional activation domain and drives transcriptional activity at enhancers. Inhibiting the function of these cofactors, perhaps by disrupting their interaction with ICN1, might be an

effective therapeutic strategy with eventually fewer side effects compared to pan- Notch inhibition.

Context-Dependent Regulation

The Notch complex is not a "pioneer factor" that can activate enhancers by itself but requires cell type-specific nuclear contexts to transactivate and implement diverse functions (Bray 2016). ChIP-Seq analyses have identified several transcriptional regulators that might contribute to the nuclear context that promotes ICN1 activity in T-cell lineages. These factors frequently bind adjacent to ICN1 at enhancers and include GA binding protein transcription factor alpha Subunit (GABPA), E26 avian leukemia oncogene 1 (ETS1), RUNX1, HEB, E47, TAL1, GATA binding protein 3 (GATA3), zinc finger MIZ-type containing 1 (ZMIZ1) and IKAROS (Palii et al. 2011, Sanda et al. 2012, Wang et al. 2011, Wei et al. 2011, Pinnell et al. 2015b, Geimer Le Lay et al. 2014, Wang et al. 2014a). Like NOTCH1, several of them are important for normal T-cell development based on murine knockout studies (Barton et al. 1998, Muthusamy, Barton and Leiden 1995, Bories et al. 1995, Pinnell et al. 2015b, Yu et al. 2010, Egawa et al. 2007, Wang et al. 1996, Garcia-Ojeda et al. 2013, Xu et al. 2013, Scripture-Adams et al. 2014, Hattori et al. 1996, Hosoya et al. 2009). Thus, the combinatorial action of "ICN1-adjacent" transcriptional regulators might create the favorable nuclear context that promotes ICN1 activity in T-ALL cells.

The Notch-Dependent MYC Enhancer (NDME) in T-ALL

The prototypical, leukemia-relevant example of context-dependent regulation is the Notch-dependent *MYC*-enhancer NDME (also known as N-ME). This enhancer is active exclusively in T-cells. In fact, it is inactive in non-T-cells even if ICN is ectopically overexpressed (Herranz et al. 2014, Yashiro-Ohtani et al. 2014b). What are the cooperating

transcription factors than make this enhancer responsive to Notch signals? Several transcription factors bind the NDME, for example ETS1, RUNX1, HEB, E47, GABPA, TAL1, ZMIZ1, GATA3 AND IKAROS [(Palii et al. 2011, Sanda et al. 2012, Wang et al. 2011, Pinnell et al. 2015b, Wang et al. 2014a) Fig. 1.3]. Keeping with the notion that Notch is not a "pioneering" transcriptional activator, a recent study identified a role for transcription factor GATA3 in evicting nucleosomes from the NDME, activating *MYC* transcription (Belver et al. 2019). This function of GATA3 is required for *MYC* expression and the proliferation of Notch-induced T-ALLs (Belver et al. 2019).

In theory, one could disrupt NDME functions in order to target MYC specifically in T-cells, probably avoiding the intolerable effects of pan-Notch inhibition. To show proof-of-principle, tissue-wide deletion of the 1.1 Kb region encompassing the NDME in mice blocks *Myc* transcription and proliferation of T-ALL cells but has no effect on other cell types (Herranz et al. 2014). More precise clustered regularly interspaced short palindromic repeats (CRISPR)/CRISPR associated protein 9 (Cas9)-mediated excision of the NDME in a human T-ALL cell line reduced H3K27 acetylation, *MYC* transcription and cell proliferation (Pear et al. 2016). These studies suggest that targeting the transcriptional regulators that activate Notch responsive elements might be effective and safer than pan-Notch inhibition.

While some transcriptional regulators strengthen Notch signals, others weaken them. As discussed previously, CCNC/CDK associates with ICN1 leading to its degradation. ICN1 might also associate with transcriptional repressors such as retinoblasoma binding protein 4, chromatin remodeling factor (RBBP4), chromodomain helicase DNA binding protein 4 (CHD4), GATA zinc finger domain containing 2B (GATAD2B), and histone deacetylase 1 (HDAC1) which are

components of the nucleosome remodeling deacetylase (NuRD) complex (Yatim et al. 2012). It is unclear whether these repressors are selective for certain target genes or cell types.

IKAROS, encoded by Ikaros family zinc finger 1 (Ikzf1) gene, is a transcriptional repressor that binds ~60% of ICN1/Rbpj sites (including the NDME, Fig. 1.3) and suppresses a subset of Notch target genes in murine thymocytes and T-ALL (Geimer Le Lay et al. 2014, Chari and Winandy 2008). IKAROS orchestrates this regulation by competing with ICN1/Rbpj for shared binding sites (Beverly and Capobianco 2003, Kleinmann et al. 2008).

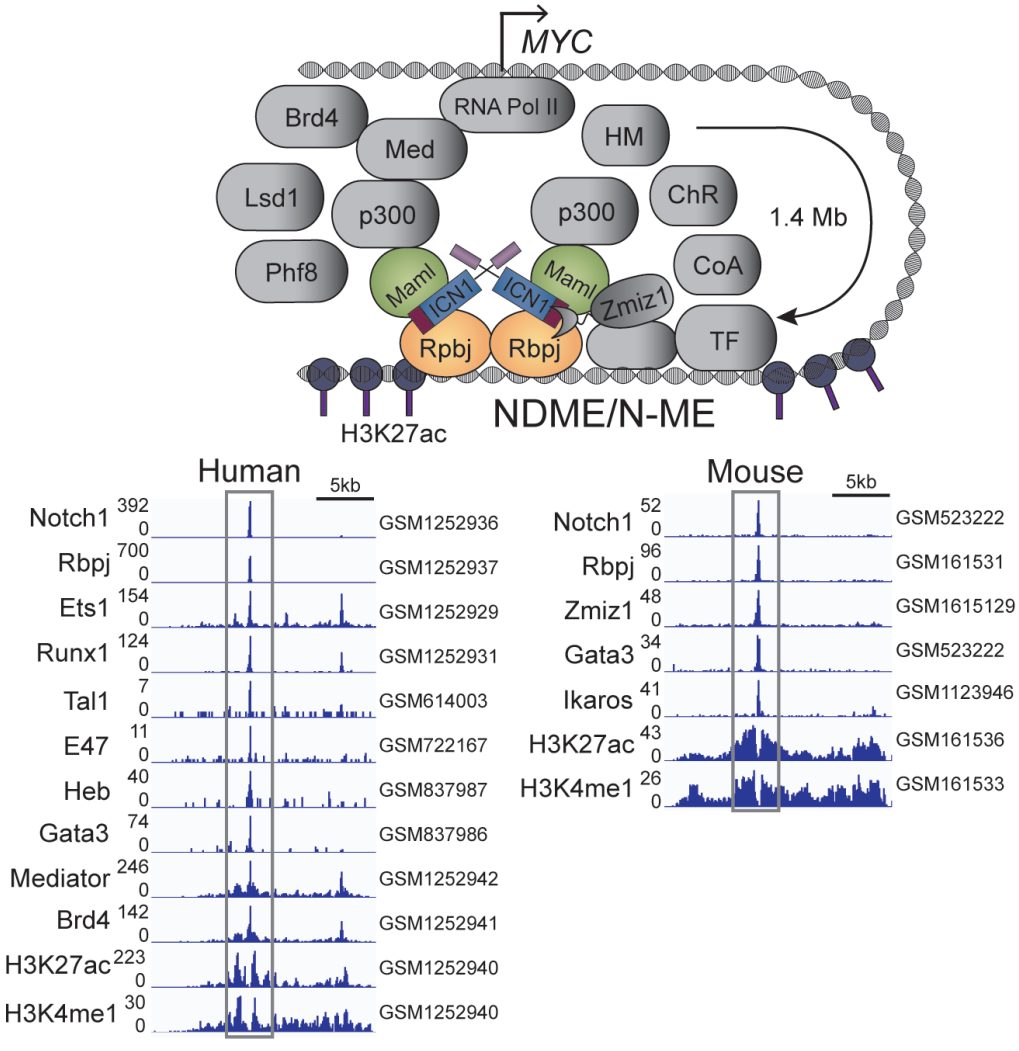

Figure 1.3 Notch cofactor binding at the Notch-dependent Myc Enhancer

Transcription factors (TF), chromatin remodelers (ChR), histone modifiers (HM) and coactivators (CoA) bind to a +1.4 MB MYC enhancer in a large complex around the core ICN1/RBPJ. These factors might create a favorable nuclear context in T-ALL cells, at this specific enhancer, that allows ICN1/RBPJ to transactivate the MYC promoter through long-range interactions.

Alternatively, IKAROS binds next to RBPJ and interferes with ICN1 function possibly through protein-protein interactions (Geimer Le Lay et al. 2014, Kathrein, Chari and Winandy 2008). The low frequency of inactivating IKZF1 mutations (<5%) in human T-ALL seems to argue against IKAROS having broad functional significance (Marcais et al. 2010).However, ICN1 represses IKZF1 transcription in human T-ALL (Witkowski et al. 2015) and induces dominant-negative isoforms of IKAROS in mouse models through alternative splicing (Bellavia et al. 2007). It must be noted that repression of *Pten* might also induce dominant-negative IKAROS isoforms (Yuan et al. 2017) and that restoring IKAROS levels induces tumor regression (Witkowski et al. 2015). Thus, it is intriguing to conceptualize therapeutic strategies that enhance IKAROS function, perhaps by interfering with its degradation (Song et al. 2015, Song et al. 2016).

Therapeutic Targeting of the Notch Signaling Pathway

With the extensive role Notch1 signaling plays in the pathogenesis of T-ALL, there is great interest in leveraging our understanding of the mechanisms of Notch regulation to develop targeted therapies. While pan-Notch inhibitors, like γ-secretase inhibitors, have progressed to clinical trials, the on-target toxicities of these agents provide rationale for agents that selectively inhibit Notch1 in T-ALL.

γ-secretase inhibitors

γ-secretase inhibitors (GSI) prevent proteolysis of all four Notch receptors thus blocking all Notch signals (mutant or wildtype) with the exception of the rare t(7;9) translocation that removes the S3 cleavage site. Unfortunately, GSIs have been disappointing in clinical trials. More than a dozen clinical trials tested GSIs in patients with mostly solid cancers showed responses seen in less than 5% of patients [reviewed in (Andersson and Lendahl 2014)]. These studies were generally hampered by dose- limiting gastrointestinal (GI) toxicity, which was attributed to on-target effects of pan-Notch inhibition on the intestinal epithelium (VanDussen et al. 2012, van Es et al. 2005). The first clinical trial testing GSIs (in particular MK-0752) in relapsed/refractory T-ALL was halted due to excessive diarrhea (Deangelo et al. 2006). However, 1 out of 7 patients had a 45% reduction in mediastinal mass. In a phase I trial of 8 relapsed/refractory adult T-ALL patients treated with the GSI PF-03084014, one patient achieved a complete remission for ~3 months (Papayannidis et al. 2015). In a preliminary report of an active Phase I trial, 25 relapsed/refractory pediatric T-ALL patients were treated with the GSI BMS- 906024 with or without corticosteroids (Zweidler-McKay et al. 2014). The response rate was particularly encouraging at 32% of patients, perhaps reflecting the synergy between GSI and corticosteroids. One of these patients was relapse-free for >19 months (Knoechel et al. 2015).

Ineffective Inhibition of Notch

Why have there been modest response rates of GSI in clinical trials, including the three mentioned above in T-ALL? One possibility is primary resistance. A second possibility is ineffective inhibition due to on-target toxicities. Because of these toxicities, GSI must be given intermittently, as infrequently as once or three times a week instead of daily. While intermittent

dosing is more tolerable, it fails to achieve continuous suppression of Notch signaling given the short half-life of the GSI molecules (Krop et al. 2012, Cullion et al. 2009). Intermittent dosing is predicted to be less effective for tumors with PEST or FBXW7 mutations. Since these mutations prolong the half-life of ICN1, the level of ICN1 after each dose of GSI administration decreases more slowly than in cells without these mutations. Unfortunately, there is no robust and comprehensive set of biomarkers to quantitatively determine whether sufficient GSI has been given to achieve cancer-killing levels. Preclinical studies in genetically engineered mouse models of T-ALL give clues to whether ineffective inhibition of Notch signals or primary resistance is the greater clinical problem (Cullion et al. 2009, Rakowski, Lehotzky and Chiang 2011). In these studies, an intermittent dosing schedule was used (three daily doses of GSI followed by 4 days off). Both studies showed disappointingly transient in vivo responses to GSI. However, tumor cells harvested from mice that succumbed to T-ALL despite treatment were highly sensitive to GSI inhibition ex vivo. Thus, the inability to raise Notch inhibition to cancer-killing levels might be an important clinical problem.

Other Pan-Notch Inhibitors

Besides GSI, other strategies that block all Notch signals are being developed and tested at the pre-clinical stage (Andersson and Lendahl 2014, Roti et al. 2013, Roti and Stegmaier 2014). These strategies include antibodies that target the γ-secretase complex (e.g. Nicastrin), inhibitors of ADAM protease, SERCA and HSP90 (Sect. 3.3) as well as MAM-like stapled peptides (SAHM) that disrupt the Notch transcriptional complex (Moellering et al. 2009). Since these strategies inhibit both normal and mutant Notch signals, it is possible that they might run into the same challenges that have plagued GSIs in clinical trials. However, there might be a therapeutic window not seen with GSI. For example, mice treated with SERCA inhibitors,

HSP90 inhibitors or SAHM peptides did not develop the gastrointestinal toxicities of pan-Notch inhibition at doses that were effective in inhibiting growth of T-ALL xenografts (Moellering et al. 2009, Roti et al. 2013). The reduced toxicity could indicate antileukemic, Notch-independent effects of these drugs or that mutated Notch proteins might be more dependent on the Notch pathway machinery than the wild-type Notch proteins performing essential physiological functions.

Selective Notch Inhibition

Antibodies that target specific receptors or ligands would be predicted to have less toxicity than pan-Notch inhibition. Biotech companies have developed blocking antibodies that clamp and stabilize the NRR even in the presence of a Class I NRR mutation (Wu et al. 2010, Aste-Amezaga et al. 2010, Agnusdei et al. 2014). In mouse studies, the GI toxicities of Notch1 anti- bodies were lower compared to GSIs or combined Notch1/Notch2 antibodies (Wu et al. 2010). However, the cost of lowered toxicity might be a reduced efficacy. Accordingly, signaling by Class II NRR and JME mutations are resistant to Notch1 antibodies (Wu et al. 2010, Aste-Amezaga et al. 2010). Further, the inhibitory effect of Notch1 antibodies in a variety of in vitro signaling assays is frequently inferior to GSI, including assays of human T-ALL cell line proliferation (Wu et al. 2010, Aste-Amezaga et al. 2010). Selective Notch inhibition is also being tested with antibodies that bind Notch ligands. Such antibodies are predicted to be less effective in cancers driven by NRR mutations (e.g. T-ALL) but more effective in cancers driven by ligands (e.g. CLL).

Resistance to Anti-Notch Agents

About two-thirds of human Notch-activated T-ALL cell lines are resistant to GSI (Weng et al. 2004) as well as about one-third of patient- derived xenografts tested ex vivo (Roderick et

al. 2014). Why do T-ALL cells develop resistance to Notch inhibitors without ever encountering Notch inhibitors? Investigators have speculated that Notch activation is an efficient mechanism for developing tumors to access multiple growth-promoting pathways simultaneously. It is possible that tumor cells undergo further selection to acquire additional mechanisms that amplify these pathways. In this way, the tumors become less dependent on the original Notch signals. Accordingly, the major mechanisms of resistance appear to be through Notch-independent activation of two Notch-driven pathways: PI3K/AKT and MYC. It is important to note that neither pathway is sufficient to confer resistance in all contexts; however, both might be sufficient. Accordingly, combined expression of Akt1 and Myc (but neither one alone) confers GSI resistance in 8 out of 8 *KrasG12D*-induced murine T-ALL cell lines (Chiang, unpublished observations).

Inactivating mutations or deletions of PTEN occur in 10-30% of T-ALL patients (Palomero et al. 2007, Mendes et al. 2014, Gutierrez et al. 2009, Zuurbier et al. 2012). Inactivation of PTEN was invariably associated with GSI resistance of T-ALL cell lines (Palomero et al. 2007) however, a subsequent study identified four cell lines with PTEN-inactivating mutations that retained sensitivity to GSI (Zuurbier et al. 2012). Thus, PTEN loss might promote resistance to Notch inhibitors but is not sufficient in all contexts. Accordingly, induction of genetic deletion of *Pten* confers in vivo GSI resistance to established murine Notch-induced T-ALL (Herranz et al. 2015). However, T-ALL cell lines generated by transducing activated Notch1 into *Pten*-deficient murine hematopoietic progenitors, which are then transplanted into mice, retain high sensitivity to GSI (Medyouf et al. 2010). To reconcile these data, it has been suggested that PI3K/AKT activation induces GSI resistance only when it is a late event during pathogenesis (Mendes et al. 2014). Consistent with this idea, we observed that

transduction of *Akt1* into *KrasG12D*-expressing murine hematopoietic progenitors (which eventually develop into tumors when transplanted into recipient mice) does not confer GSI resistance (Chiang et al. 2016). In contrast, transduction of Akt1 into some established *KrasG12D*-induced murine T-ALL cell lines confers GSI resistance (Chiang, unpublished observations). Similarly, CRISPR-Cas9- mediated *PTEN* inactivation in some human cell lines confers GSI resistance (Herranz et al. 2015). Thus, it is possible that PTEN inactivation/AKT activation can confer GSI resistance in the context of a late event.

In contrast to *Pten* loss, *Myc* activation seems to confer GSI resistance more often in the context of an early rather than late event. For example, enforced expression of *Myc* induces T-ALL in animal models that are GSI resistant (Felsher and Bishop 1999, Langenau et al. 2003, Chiang et al. 2016). However, enforced expression of *MYC* in established human T-ALL cell lines confers GSI resistance in only limited con-texts (Weng et al. 2006, Palomero et al. 2006a). In contrast to PI3K/AKT, which is frequently activated through mutations (Gutierrez et al. 2009), genetic lesions that induce MYC occur in only ~10% of human T-ALLs through t(8;14) translocation (Lange et al. 1992) or focal duplications of the NDME (Herranz et al. 2014). However, additional pathways that activate MYC likely remain to be discovered. For example, when GSI-sensitive human T-ALL cell lines are chronically treated with low doses of GSI, these cells develop GSI resistance by activating a Notch-independent, BRD4-dependent *MYC* enhancer (Knoechel et al. 2014). FBXW7 targets MYC protein for degradation, so it is not surprising that *MYC* is upregulated by FBXW7 mutations (O'Neil et al. 2007, Welcker et al. 2004, Yada et al. 2004, Thompson et al. 2007). In T-ALL cell lines, FBXW7 mutations correlate with GSI resistance (Thompson et al. 2007, O'Neil et al. 2007). Although suggestive, this study does not definitively implicate MYC as the resistance mechanism since FBXW7 degrades other

oncoproteins such as c-ju-nana (JUN), MCL1, MTOR, and cyclin E1 (CCNE1) (Mao et al. 2008, Koepp et al. 2001, Strohmaier et al. 2001, Wei et al. 2005, Wertz et al. 2011, Inuzuka et al. 2011).

Agents That Increase Sensitivity to Notch inhibitors

Given their relatively modest effects in clinical trials, GSIs are being tested in combination with other agents. Many of the agents discussed below inhibit known growth-promoting pathways downstream of Notch signals. The ability of these agents to enhance the effects of GSI is consistent with the notion that tumor cells have deepened their "addiction" to downstream Notch pathways by acquiring Notch-independent mechanisms to activate these pathways.

Activation of Notch1 confers resistance to glucocorticoids in murine cell lines and thymocytes (Deftos et al. 1998). Accordingly, inhibiting Notch promotes glucocorticoid sensitivity of human T-ALL cell lines (Real et al. 2009). Notch confers resistance in part through inducing HES1 protein, which directly suppresses the transcription of the glucocorticoid receptor (Real et al. 2009). Notch also activates AKT, which phosphorylates the glucocorticoid receptor preventing its nuclear translocation (Piovan et al. 2013). Conversely, glucocorticoids also promote GSI sensitivity. In fact, glucocorticoids scored frequently in a library screen for compounds that promote GSI-mediated inhibition of a human T-ALL cell line (Gutierrez et al. 2014). Glucocorticoids can also protect mice from the GI toxicities induced by pan-Notch inhibition (Real et al. 2009). These data provide rationale for combined therapies with GSI and glucocorticoids. Accordingly, preliminary results of a clinical trial testing GSI in combination with glucocorticoids showed relatively high efficacy and low toxicity (Zweidler-McKay et al. 2014).

In theory, MTOR inhibitors like rapamycin could help treating GSI-resistant T-ALLs by activating the PI3K pathway. Combining rapamycin with GSI synergistically enhances apoptosis and growth inhibition of Tal1/inhibitor of cyclin-dependent kinase 4 (Ink4)+/--induced murine T-ALLs and human T-ALL cell lines both in vitro and in vivo (Cullion et al. 2009, Chan et al. 2007). Combining the dual-specificity of PI3K/MTOR inhibitor PI-103 with GSI had additive antileukemic effects on KrasG12D-induced murine T-ALL cell lines (Dail et al. 2010). Phenothiazines (e.g. perphenazine) target PI3K and ribosomal protein S6 kinase beta-1 (p70S6K) by binding and activating the tumor suppressor human protein phosphatase 2A. Combining perphenazine with GSI synergistically inhibits T-ALL proliferation (Gutierrez et al. 2014). However, this study is challenging to interpret since phenothiazines inhibit other targets like extracellular signal-regulated kinase (ERK). ERK inhibitors also enhance the antileukemic effects of GSI on KrasG12D-induced murine T-ALL cell lines (Dail et al. 2010).

GSI and Inhibitors of Metabolism and Protein Synthesis

Since Notch has diverse metabolic effects (Herranz et al. 2015), it might seem unlikely that Notch-activated T-ALLs would be particularly dependent upon a single metabolic pathway. However, inhibiting glutaminolysis with the glutaminase inhibitor bis-2-(5- phenylacetamido-1,2,4-thiadiazol-2-yl)ethyl sulfide (BPTES) induced apoptosis of human T-ALL cell lines and PDX cells both in vitro and in vivo (Herranz et al. 2015). Further, combining BPTES with GSI had synergistic antileukemic effects. In a subsequent study, the same group identified associations between gene expression signatures given by various drugs and by GSI (Sanchez-Martin et al. 2017). Several of these drugs had strong synergistic effects in combination with GSI – withaferin A, rapamycin, vorinostat, parthenolide, wortmannin, astmizole, trifluoperazine and trichostatin A (Sanchez-Martin et al. 2017). Withaferin A is a steroidal lactone with multiple

cell-type specific effects. In T-ALL cells, it inhibits translation by targeting eukaryotic translation initiation factor 2a (EIF2A). Combining GSI with withaferin A or another translation inhibitor (e.g. silvestrol) had synergistic in vitro growth inhibitory effects on Notch-activated human T-ALL cell lines. Withaferin A also had synergistic in vivo effects on Notch-induced murine T-ALL and PDXs (Sanchez-Martin et al. 2017).

GSI and Cyclin/CDK Inhibitors

Since GSI inhibits cell cycle progression, there is rationale for combining GSI with cell cycle inhibitors. Accordingly, combining GSI with a cyclin D1 (CCND1)/CDK4 inhibitor (6-substituted indolocarbazole) enhanced retinoblastoma protein (RB) hypophosphorylation, G1/S arrest and apoptosis of Notch-activated human T-ALL cell lines (Rao et al. 2009). Another study found that combining GSI with the CDK4/6 inhibitor LEE011 synergistically inhibited proliferation of Notch1-activated T-ALL cell lines (Pikman et al. 2017). However, in both studies, these inhibitors had no effect on GSI-resistant T-ALL cell lines.

Targeting the Nuclear Context of ICN1 in T-ALL

How to target Notch responsive elements without pan-Notch inhibition? One option is to inhibit histone modifiers such as BRD4, a reader of acetylated histones that binds the NDME (Wang et al. 2014a, Yashiro-Ohtani et al. 2014b) or, alternatively, to target protein-protein interactions between ICN1 and its cofactors. Prior work from the Chiang lab showed that the protein inhibitor of activated STAT (PIAS)-like coactivator ZMIZ1 directly binds ICN1 through a tetratricopeptide repeat (TPR) domain (Pinnell et al. 2015b). ZMIZ1 recruits ICN1/RBPJ to the NDME resulting in elevated H3K27ac and *Myc* transcription (Pinnell et al. 2015b). In T-ALL, Zmiz1 regulates ~43% of Notch target genes and binds ~75% of overlapping ICN1/RBPJ sites, especially those enriched for Ets, Runx, Tal1/E2A and transcription factor 1 (Tcf1)/lymphoid

enhancer binding factor 1 (Lef1) motifs (Pinnell et al. 2015b). Genetic inactivation of *Zmiz1* or disruption of the NOTCH1-ZMIZ1 interaction using a dominant-negative TPR inhibitor, slowed leukemic proliferation or prolonged survival in Notch-induced T-ALL mouse models without significant toxicities (Pinnell et al. 2015b). Thus, targeting context-dependent direct cofactors of ICN1 might selectively disable the oncogenic functions of Notch while sparing its essential normal functions. Similarly, AF54p12 is a coactivator that is recruited by ICN1 to Notch1 binding sites (Yatim et al. 2012). By recruiting RNA polymerase II (RNAPII), AF54p12 drives the transcription of oncogenic genes like *IL7R* and *HES1* (Yatim et al. 2012). It also appears to be selective for some Notch target genes as it does not regulate or recruit RNAPII to the DTX1 locus. However, the mechanism for its context dependence is unclear. While these studies are promising, many of the cofactors that drive T-cell specific Notch activity are unknown. ETS1, a developmental transcription factor and established oncogene in carcinomas, is an attractive candidate. More about this transcription factor, its regulation, and its association with Notch are detailed below.

Ets1 as a potential T-cell specific Notch cofactor

ETS1 (ETS Proto-Oncogene 1) is the founder of the ETS family of transcription factors, whose members are involved in stem cell development, cell senescence, and tumorigenesis. ETS genes are conserved back to very primitive multicellular animals. Cells express multiple ETS proteins simultaneously, suggesting that there might be functional redundancies [reviewed in (Seth and Watson 2005)]. All 28 human genes share a winged helix-turn-helix DNA binding domain, called the ETS domain. The ETS domain binds GGAA/T motif. However, different family members exhibit preferences for particular sequences flanking the core motif (Hollenhorst

et al. 2007, Hollenhorst et al. 2009); for example, Ets1 prefers ACCGGAAGT (Wei et al. 2010). Additionally, ETS proteins also cooperate with different binding partners to enhance specificity of action (Hollenhorst, McIntosh and Graves 2011).

Ets1 was first identified in the E26 avian erythroblastosis virus, which carries a v-ets oncogene fused with v-myb (Leprince et al. 1983); a cellular form of Ets1 was later identified (Seth and Papas 1990). Mouse and human ETS1 are highly conserved (97% amino acid identity, 99% similarity). The high conservation of ETS1 across a variety of species indicates that there is strong selective pressure to maintain all domains of the protein, and that ETS1 has non-redundant roles with other members of the ETS family. It is expressed broadly during embryonic development, where it functions in cardiac neural crest development (Gao et al. 2010) and angiogenesis (Iwasaka et al. 1996, Wei et al. 2009). Postnatally, ETS1 is primarily expressed in hematopoietic lineage cells, and a detailed description of its role in lymphocyte development will be provided in the introduction of "Chapter 2: ETS1 is essential for Notch-dependent T-cell development, but dispensable for intestinal homeostasis". Like many other transcription factors involved in development, ETS1 is often hijacked by cancer cells to prevent differentiation and drive proliferation. More on ETS1 contribution to tumorigenesis and leukemogenesis will be covered in "Chapter 3: ETS1 is important for Notch-induced T-ALL maintenance and initiation". The mechanism by which ETS1 regulates Notch target genes in T-ALL will be explored in "Chapter 4: ETS1 promotes context-dependent recruitment of the Notch complex and Notch-induced gene expression in T-ALL". Strategies for targeting ETS1 in cancer will be discussed in the introduction of "Chapter 5: ETS1-targeted strategies for antileukemic therapies." Finally, last thoughts about the implications and future directions of this work will be detailed in "Chapter 6: Conclusions and Future Directions".

Chapter 2 ETS1 is Essential for Notch-Dependent T-Cell Development, but Dispensable for Intestinal Homeostasis[2]

Abstract

T-cell acute lymphoblastic leukemias primarily arise from the two phases of T-cell development that are Notch-signaling dependent, early thymic precursor (ETP) specification and the double negative-double positive (DN-DP) transition. If Ets1 collaborates with Notch1 in T-ALL, it may also function at these same Notch-dependent stages of T-ALL. Studies of mice with germline *Ets1* deletion have demonstrated the requirement for ETS1 in the normal development of lymphocytes. Utilizing a new murine inducible *Ets1* knockout allele, we deleted *Ets1* in hematopoietic stem cells and characterized the phenotypes of developing lymphoid and myeloid cells. *Ets1*-mutant mice have a profound loss of thymocytes and mature T-cells. Like NOTCH1, ETS1 is required for ETP specification and the DN-DP transition. Given these similarities, we were interested to know if *Ets1* deletion causes intestinal toxicity like Notch-inhibition. We used a tamoxifen inducible mouse model to delete *Ets1* in adult animals. Ubiquitous deletion of *Ets1* produces a mild Notch loss-of-function phenotype in the intestine, but it appears to be transient and less lethal than Notch-inhibition with gamma secretase inhibitors. These studies confirmed and expanded our understanding of the role of ETS1 in hematopoiesis, as well as provide rationale for ETS1 being a safer therapeutic target for T-ALL treatment.

[2] Adapted from McCarter, A. C., G. D. Gatta, A. Melnick, et al. (2020) Combinatorial ETS1-Dependent Control of Oncogenic NOTCH1 Enhancers in T-cell Leukemia. *Blood Cancer Discovery*.

Introduction: Known roles for ETS1 in hematopoiesis

Ets1 is expressed in many tissues during embryonic and early post-natal development (Bhat et al. 1987, Kola et al. 1993), but in adult mice, *Ets1* is mainly expressed at high levels in immune tissues (spleen, thymus, lymph nodes), especially T, B, NK, and NK T-cells (Kola et al. 1993). Thus, most of the work examining ETS1 in development has focused on lymphocytes, though there have been a few studies regarding other hematopoietic lineages that are detailed in "ETS1 in Erythroid and Megakaryocyte Development".

ETS1 in T-cell development

The best characterized role for ETS1 in hematopoiesis is during T-cell development. T-cells, as the cellular component of the adaptive immune system, carry out immune-mediated cell death and modulate B-cell responses through cytokine production and direct stimulation of B-cells. The role of ETS1 during T-cell development was previously studied in germline *Ets1*-mutant mouse models. These *Ets1*-deficient mice showed defects at multiple phases of T-cell development, including aberrant thymic differentiation, reduced peripheral T-cell numbers, and a skewing towards a memory/effector phenotype for mature T-cells (Bories et al. 1995, Muthusamy et al. 1995, Eyquem et al. 2004a).

During normal murine T-cell development, multipotent hematopoietic precursors from the bone marrow localize to the thymus [reviewed in (Koch and Radtke 2011)] . These early thymic progenitors (ETP) cells move through 4 stages of early thymic development, defined by the expression of cell surface markers: DN1 ($CD44^+CD25^-$), DN2 ($CD44^+CD25^+$), DN3 ($CD44^-CD25^+$), and DN4 ($CD44^-CD25^-$). As immature T-cells transition through the DN2 and DN3 stages, they commit to the T-cell lineage and rearrange their T-cell receptor (TCR) loci. Rearrangement of the TCRβ gene produces a TCRβ-chain, which is expressed at the thymocyte

cell surface as part of the pre-TCR. Signaling by the pre-TCR is essential to inhibit further rearrangements at the TCRβ locus, ensuring that each T cell expresses a unique β-chain in a process called allelic exclusion. After DN4, thymocytes begin expressing both the CD4 and CD8 surface markers (DP) before transitioning to mature single positive (SP) T-cells. This developmental pathway is summarized in Figure 2.1.

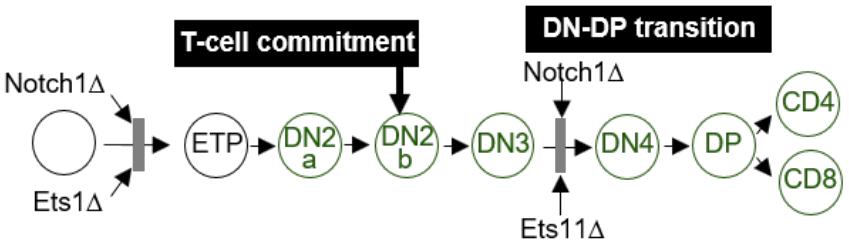

Figure 2.1 Notch and Ets1-dependent stages of thymic T-cell development

Schematic of T-cell development in the thymus, with Notch and Ets1-dependent stages indicated with arrows.

Consistently, the thymi of *Ets1*-deficient mice are hypocellular and the percentage of DP thymocytes is decreased, whereas the percentage of double negative (DN) thymocytes is increased (Muthusamy et al. 1995, Bories et al. 1995). Prior studies have primarily centered on the DN3-DP phases of T-cell development. *Ets1* expression is critical for pre-T cell receptor signaling, which is required the for development of αβT-cells (Eyquem et al. 2004a). This defective pre-T cell receptor signaling results in inefficient allelic exclusion at the TCRβ locus, with approximately 10% of cells expressing more than one TCRβ chain (Eyquem et al. 2004a). Studies done in the $Rag2^{-/-}$ complementation system demonstrated that T-cells lacking *Ets1* during the DN3 stage still expressed normal levels of the CD3 and TCR markers; however these *Ets1*-deprived DN cells failed to proliferate in response to pre-TCR signals and had increased rates of apoptosis (Muthusamy et al. 1995). Loss of *Ets1* impairs the DN3-DP transition, leading

to fewer mature T-cells in circulation. A recent study in murine T-cells demonstrated that ETS1 binds to nucleosome-occupied distal enhancers genome-wide in DN and may induce chromatin remodeling by displacing H3K4me1-marked nucleosomes (Cauchy et al. 2016). Furthermore, these changes are associated with T-cell lineage commitment by turning on T-cell specific gene expression programs (Cauchy et al. 2016). Thus, this work suggests ETS1 may possibly function as part of a "pioneering" transcription factor complex in developing T-cells.

Ets1 is expressed at high levels in CD4+ helper T-cells and regulatory T-cells (T-regs) (Bhat et al. 1989). T-regs are a subset of CD4+ T-cells that produce anti-inflammatory cytokines, including IL-10 and TGFβ, which limit the activation of other populations of immune cells. Accordingly, there are significant reductions in numbers of these populations in *Ets1*-deprived animals. ETS1 promotes the expression of IL7Ra (CD172) in peripheral T-cells, leading to defects in survival and expansion of CD4+ helper T-cells in a transplant setting (Grenningloh et al. 2011). *Ets1*-deficient mice also fail to develop adequate numbers of T-regs, due to ETS1 regulation of FoxP3, a transcription factor required for T-reg differentiation (Mouly et al. 2010, Polansky et al. 2010). Aberrant cytokine IL-2 production by *Ets1*-deficient CD4+ T-cells also promotes the development of Th17 γδT-cells over the development of T-regs (Boyman and Sprent 2012).

Ets1 is also expressed in CD8+ cytotoxic T-cells (Bhat et al. 1989), and mice lacking *Ets1* have marked reductions in CD8+ cells (Muthusamy et al. 1995). CD8+ T-cells deprived of *Ets1* display lower levels of the CD8 surface marker (Muthusamy et al. 1995). Studies performed using a mouse model with a hypomorphic allele of *Ets1* demonstrated defective positive selection of MHC class I-restricted DP thymocytes. Like in CD4+ helper T-cells, ETS1 also regulates IL7Rα in CD8+ cells; *Ets1*-deprived CD8+ cells express lower levels of *IL7R*α and

show impaired survival (Grenningloh et al. 2011) Although there are peripheral CD8+ T-cells present in *Ets1*-mutant mice, both CD4+ and CD8+ subsets contain an elevated proportion of cells with an effector-memory phenotype (Clements, John and Garrett-Sinha 2006).

There are far fewer T-cells in the spleens and lymph nodes of *Ets1* knockout mice. There is also reduced expression of CD5 and Thy1 on *Ets1*-mutant peripheral T-cells. Just as developing thymocytes deprived of *Ets1* are prone to apoptosis, peripheral T-cells from *Ets1*$^{-/-}$ mice exhibit increased cell death (Muthusamy et al. 1995, Barton et al. 1998, Bories et al. 1995). *Ets1*-mutant mice have decreased expression of many cytokines required immune cell differentiation, proliferation, and activation, including *IL-2, IFN-g, IL-4, IL-5, IL-13,TNF*α, and *CCL2* (Grenningloh, Bok and Ho 2005, Moisan et al. , Nagaleekar et al. 2008). Additionally, *IL-17*α and *IL-10*, cytokines involved in anti-inflammatory responses, are upregulated in *Ets1*-deficient mice (Moisan et al.).

ETS1 in B-cell development

B-lymphocytes are another part of the adaptive immune system, involved with humoral immunity and antigen presentation. B-cell development is also altered in Ets1-mutant mice; however, it is not clear which effects are B-cell autonomous, and which are secondary to the extensive T-cell defects of these mice. *Ets1* is highly expressed in naïve B-cells, but its expression diminishes after B-cell activation and terminal differentiation (John et al. 2008). The loss of *Ets1* does partially impair bone marrow B-cell development; in particular, there is inefficient transition from the pro-B to pre-B cell stages (Eyquem et al. 2004b). In the periphery, there are reduced numbers of marginal zone and transitional T-2 B-cells, but normal numbers of follicular B-cells (Eyquem et al. 2004a, Eyquem et al. 2004b). The most striking phenotype is the enhanced development of IgM and IgG-secreting plasma cells, which then accumulate in the

lymphoid organs and bone marrow (Barton et al. 1998, Bories et al. 1995). This is due to ETS1 suppression of the activity of Blimp-1, a transcription factor that promotes plasma cell formation (Wang et al. 2005, John et al. 2008). The mature B-cells in *Ets1*-mutant mice express increased levels of CD23, CD80, and CD86, suggesting an activated phenotype (Wang et al. 2005). They also express high levels of MHC class II (Wang et al. 2005). Recent studies using a B-cell specific Ets1 knockout mouse (*CD19-Cre Ets1*$^{f/f}$) suggest that while B-cell specific deletion of *Ets1* promotes abnormal B-cell activation and increased numbers of Ab-secreting plasma cells, the phenotype is much milder than conventional *Ets1* knockout mice(Sunshine et al. 2019). Thus, it appears that much of the effect of *Ets1* loss on B-cell development, particularly the phenotypes in peripheral B-cells, are driven by abnormal cytokine production by *Ets1*-deficient CD4+ helper T-cells.

ETS1 in NK-cell development

Just as *Ets1*-deficient mice show severe defects in T-cell development, they also have a marked decrease in natural killer (NK cells) and nature killer T-cells (NK-T cells). Natural killer cells are lymphoid cells with cytotoxic functions in the innate immune system. NK-T cells are a specific subset of T-cells with unique cell surface markers, restricted TCR repertoire, and particular effector functions upon activation. *Ets1*$^{-/-}$ mice have significant decreases in NK cells in the bone marrow, spleen, and lymph nodes, as measured by expression of CD49b or NK1.1 markers (Barton et al. 1998). *Ets1* is also important in the development of NK-T cells, with many fewer NK1.1+CD4+ cells found in the thymus and spleen of *Ets1*-knockout mice (Walunas et al. 2000).

ETS1 in Erythroid and Megakaryocyte Development

Myeloid cells, which include monocytes and granulocytes, are central players in the innate immune system; pathogen invasion activates them for phagocytosis and the secretion of inflammatory cytokines. Erythroid cells, better known as red blood cells, are responsible for oxygen and carbon dioxide transport in the blood. Megakaryocytes are large multinucleated cells in the bone marrow that produce platelets and other factors involved in the clotting cascade. In the *Ets1*$^{-/-}$ mice, there are no reported deficiencies or abnormalities in erythroid, megakaryocyte, or other myeloid lineages (Eyquem et al. 2004b, Mouly et al. 2010). However, because *Ets1* is expressed in hematopoietic stem cells and multipotent progenitors (Anderson et al. 1999), it would not be unexpected that ETS1 plays a role in hematopoiesis beyond lymphoid development.

Whether *ETS1* promotes or inhibits erythropoiesis remains contested in the field, with some publications claiming Ets1 activity increases the expression of erythroid markers in K562 and HEL cells (Clausen et al. 1997, Sieweke et al. 1996). Other studies suggest that loss of *Ets1* promotes erythroid development from hematopoietic progenitors transformed by the MYB-ETS protein encoded by the E26 acute avian leukemia virus (Rossi et al. 1996). One study, examining the impact of *ETS1* overexpression on erythroid cells, determined that *ETS1* expression normally declines during erythroid maturation, but overexpression in CD34+ progenitors blocks erythroid maturation at the polychromatophilic stage (Lulli et al. 2006). Additionally, enforced expression of *ETS1* increases GATA2 expression and decreases the expression of both GATA1 and erythropoietin receptor (Lulli et al. 2006). That same study showed that Ets1 overexpression promotes megakaryocyte differentiation and maturation, in part through direct upregulation of *GATA2* and megakaryocyte specific genes *GPIIb* and *PF4* (Lulli et al. 2006). While this work

does suggest that ETS1 plays some role in erythroid and megakaryocyte development, our understanding is limited by the need for *in vivo* studies to confirm and clarify these findings *in vitro*.

ETS1 in Innate Lymphoid Cell Development

Unsurprisingly, given its critical role in the development of lymphoid cells, ETS1 may also function in the development of innate lymphoid cells (ILCs). Innate lymphoid cells are immune cells that mirror the phenotypes and functions of T-cells. Like T-cells, they secrete cytokines and inflammatory mediators, but unlike T-cells, they do not express antigen receptors or undergo clonal selection [reviewed in (Eberl et al. 2015)]. Group 2 innate lymphoid cells (ILC2s) are a subset of ILCs that share properties with T-helper type 2 cells. In a murine model of IL7RaCre-induced *Ets1* deletion, *Ets1*-deprivation in lymphoid-primed bone marrow cells reduced ILC2 cells in the bone marrow and lymph nodes (Zook et al. 2016). Additionally, ETS1 is required for the IL-33-induced accumulation of ILC2s in the lung and their subsequent production of IL-5 and IL-13 (Zook et al. 2016). These phenotypes are in part due to ETS1 regulation of E protein transcription factor inhibitor ID2, a critical factor for ILC development (Zook et al. 2016).

Despite the significant body of work regarding ETS1 in lymphocyte development, there are limitations to our current understanding. Prior studies were limited either because ETS1 function was partly intact (Wang et al. 2005) or because complete ETS1 deficiency was lethal to neonatal mice (Eyquem et al. 2004), which required studying thymopoiesis using Rag-deficient blastocyst complementation (Bories et al. 1995, Muthusamy et al. 1995). Thus, the function of ETS1 in early hematopoietic precursors has not been explored. Furthermore, T cell-autonomous roles for ETS1 have not yet been explored though tissue-specific deletion of ETS1.

Results

ETS1 is highly expressed during Notch-dependent steps of early T-cell development.

A "Notch1-collaborating" transcription factor in T-ALL would be predicted to have overlapping functions with Notch1 in the normal thymic precursors from which T-ALL originates. As previously mentioned (see figure 2.1), T-cell development proceeds in the thymus through a series of stages from the early T-lineage progenitor (ETP), through the double-negative (DN) stages (DN2-DN4) to the immature single positive (ISP) and $CD4^+CD8^+$ double-positive (DP) stages, and then to the single-positive (SP) $CD4^+$ or $CD8^+$ stages. Notch1 is essential for two major stages of early T-cell development – ETP specification and the DN-to-DP transition (Rothenberg, Ungerback and Champhekar 2016). During thymocyte development, *Ets1* and Notch target genes are concurrently expressed (Fig. 2.2A). *ETS1* is also expressed in the corresponding stages in human thymocytes (Fig. 2.2B), which are susceptible to transformation to T-ALL (Tatarek et al. 2011, Berquam-Vrieze et al. 2011, Coustan-Smith et al. 2009). Thus, like *NOTCH1*, *ETS1* is expressed in T-cell precursors that can transform into T-ALL.

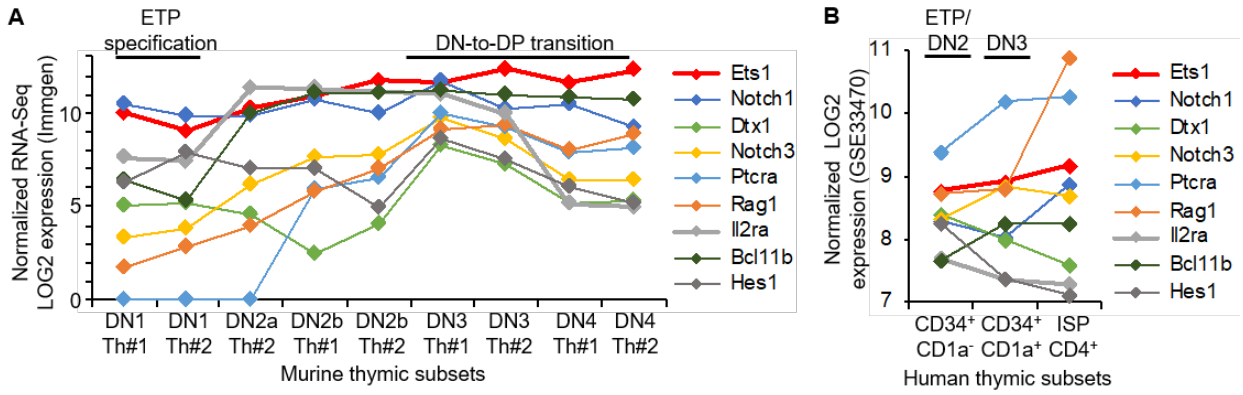

Figure 2.2 Ets1 is expressed during Notch-dependent stages of early T-cell development

A) Expression of *Ets1* (red line) and direct Notch target genes in murine early thymic subsets (Immgen, GSE109125). Notch-dependent stages (ETP specification and DN-to-DP transition) are highlighted. B) Expression of *Ets1* (red line) and human

analogs of Notch target genes in (A) in human early thymic subsets (GSE33470). Stages resembling murine ETP/DN2 and DN3 cells are indicated (Dik et al. 2005).

ETS1 is dispensable for the generation of pre-thymic bone marrow precursors.

The role of Ets1 during T-cell development was previously studied in germline *Ets1*-mutant mouse models. However, these early studies were hampered either because Ets1 function was partly intact (Wang et al. 2005) or because complete Ets1 deficiency was lethal to neonatal mice (Eyquem et al. 2004a), which required studying thymopoiesis using Rag-deficient blastocyst complementation (Bories et al. 1995, Muthusamy et al. 1995). This precluded analysis of ETP specification, a critical Notch-dependent stage of T-cell development. Thus, to better study early

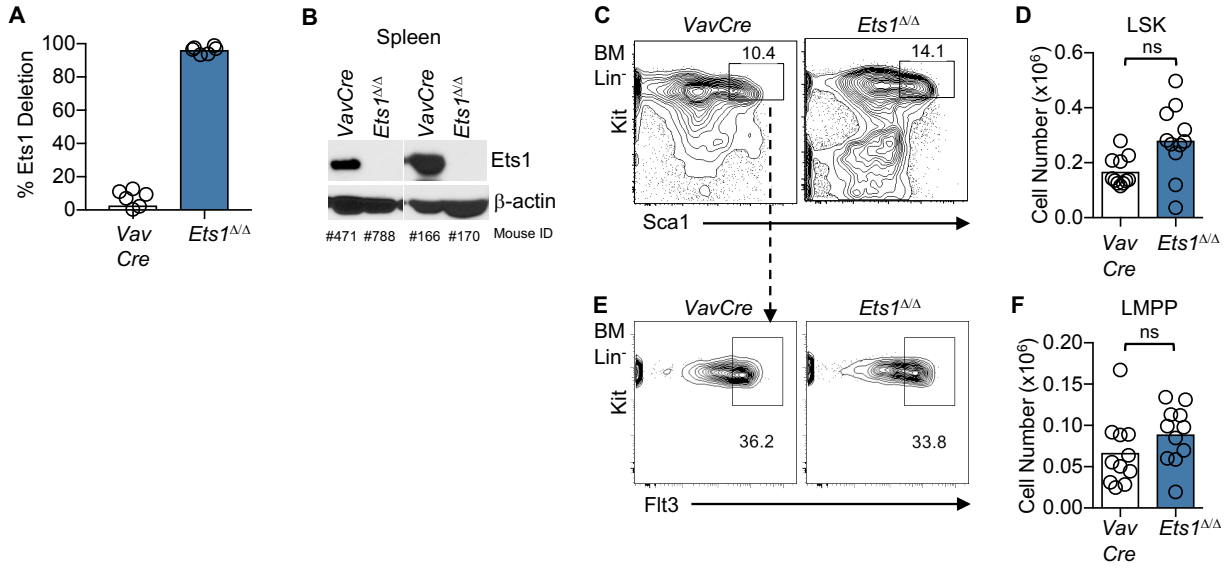

Figure 2.3 ETS1 is dispensable in pre-thymic bone marrow precursors.

A) QPCR assay showing *Ets1* deletion efficiency in spleen DNA from *VavCre* control (N=7) and $Ets1^{\Delta/\Delta}$ (N=6) mice. B) Western blot for Ets1 in spleen samples from *VavCre* control and $Ets1^{\Delta/\Delta}$ mice. C-F) Representative flow cytometric plots (C, E) and absolute numbers of LSK cells (D) and lymphoid-primed multipotent progenitor cells (LMPP, F) from bone marrow of *VavCre* control and $Ets1^{\Delta/\Delta}$ mice. LSK = Lineage$^-$Kit^{hi}Sca1^{hi}; LMPP=Lineage$^-$Kit^{hi}Sca1^{hi}Flt3^{hi}. ns=not significant.

thymopoiesis, we utilized *Ets1* knockout mice (*Ets1*$^{f/f}$) generated by our collaborators in the Ostrowski lab. In this model, loxP sites flanked the DNA-binding ETS domain such that Cre-mediated recombination create an *Ets1* null allele, similar to that of the germline *Ets1*$^{-/-}$ model (Bories et al. 1995).

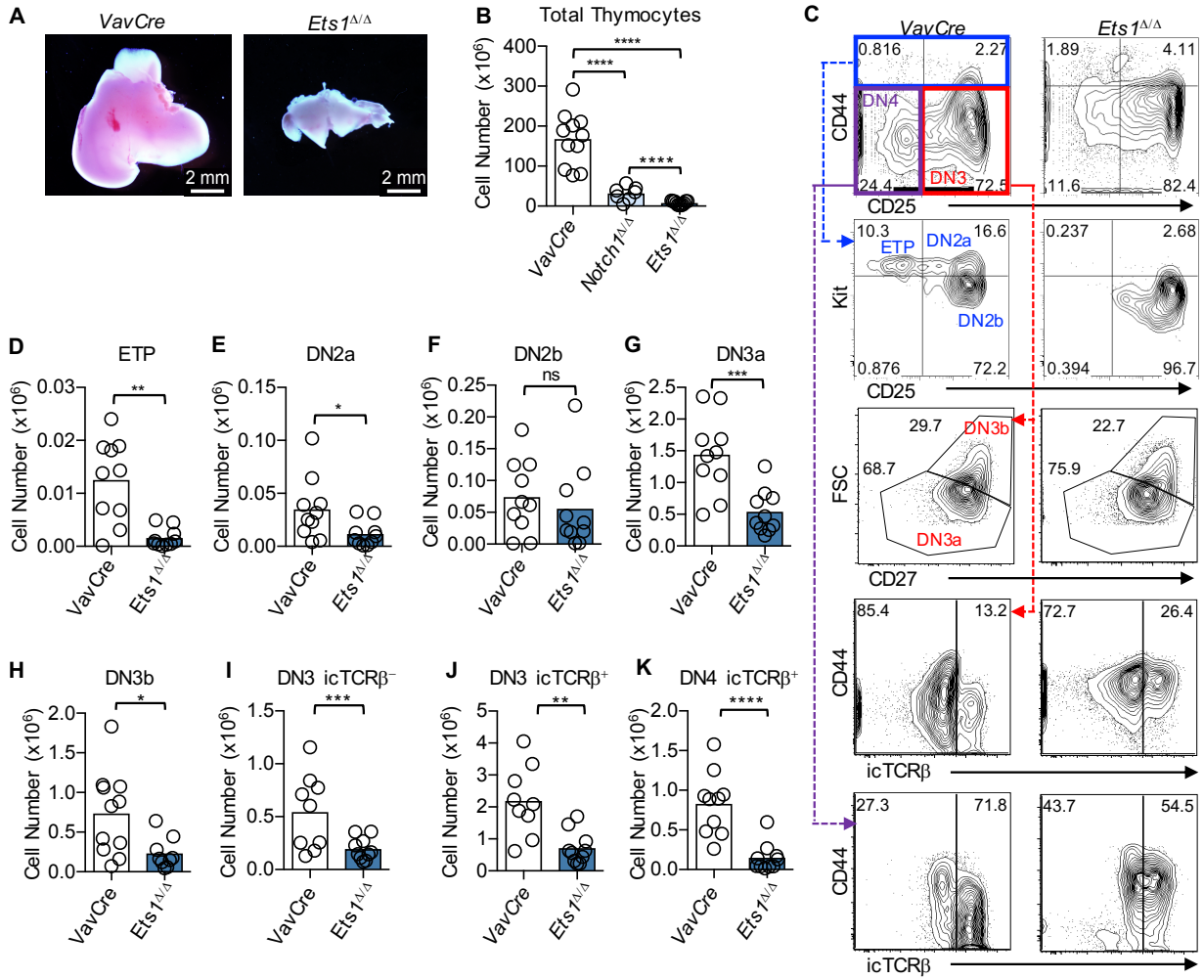

Figure 2.4 ETS1 is important for ETP specification and the DN3-DN4 transition

A) Representative images of thymuses of *VavCre* control and *Ets1*$^{\Delta/\Delta}$ mice. B) Absolute numbers of total thymocytes in *VavCre* control, *Notch1*$^{\Delta/\Delta}$, and *Ets1*$^{\Delta/\Delta}$ mice. C-K) Representative flow cytometric profiles of DN subsets (C); and absolute numbers of ETP (D), DN2a (E), DN2b (F), DN3a (G), DN3b (H), DN3 icTCRβ^{-} (I), DN3 icTCRβ^{+} (J) and DN4 (K) subsets in *VavCre* control and *Ets1*$^{\Delta/\Delta}$ mice. ETP=Lineage^{-}CD44^{+}CD25^{-}cKit^{hi}. DN2a=Lineage^{-}CD44^{+}CD25^{+}cKit^{hi}. DN2b=Lineage^{-}CD44^{+}CD25^{+}cKit^{lo}. DN3=Lineage^{-}CD44^{-}CD25^{+}. DN3a=Lineage^{-}CD44^{-}CD25^{+}FSC^{lo}CD27^{-}. DN3b=Lineage^{-}CD44^{-}CD25^{+}FSC^{hi}CD27^{+}. DN4 = Lineage^{-}CD44^{-}CD25^{-}.

To delete *ETS1* in hematopoietic cells we crossed *Ets1*$^{f/f}$ mice with *VavCre* mice generating *VavCre Ets1*$^{f/f}$ mice (*Ets1*$^{\Delta/\Delta}$). *Ets1*$^{\Delta/\Delta}$ mice showed >95% excision of the *Ets1* allele (Fig. 2.3A) and undetectable Ets1 protein in the spleen (Fig. 2.3B). Similar to Notch-deficient mice (Maillard et al. 2008), *Ets1*$^{\Delta/\Delta}$ mice showed normal numbers of bone marrow Lin^{-}Sca1^{hi}Kit^{hi} progenitors (LSKs, Fig. 2.3C-D) and lymphoid-primed multipotent progenitors (LMPP/MPP4, Fig. 2.3E-F), which are the major extrathymic precursors of ETPs (Allman et al. 2003, Bhandoola and Sambandam 2006, Ghaedi et al. 2016). In contrast, *Ets1*$^{\Delta/\Delta}$ mice showed profound depletion in total thymocyte number (~21-fold), which was more severe than seen in *VavCre Notch1*$^{f/f}$ mice (Fig. 2.4A-B). Like *VavCre Notch1*$^{f/f}$ mice (Wang et al. 2018), *Ets1*$^{\Delta/\Delta}$ mice showed defects in ETP specification (Fig. 2.4C-D) and loss of subsequent DN stages (Fig. 2.4C, E-K). These results support that, like Notch1, Ets1 is important for ETP specification in early T-cell development.

ETS1 is required for the DN-to-DP transition.

Notch1-deficient mice (Wolfer et al. 2002) show a defect in the DN-to-DP transition due to impaired TCRβ rearrangement and pre-TCR signaling (Wolfer et al. 2002). In contrast, *Ets1*$^{\Delta/\Delta}$ DN3 cells showed successful TCRβ rearrangement (Fig. 2.4C). Nevertheless, *Ets1*$^{\Delta/\Delta}$ cells were hindered in the DN-to-DP transition (Fig. 2.5A-C) and in their progression to the DN3b stage of development (Fig. 2.5D). This data is in agreement with defective pre-TCR signaling, as previously suggested in germline *Ets1* null thymocytes (Eyquem et al. 2004a). Consistent with the loss of the early T-cell subsets, subsequent T-cell stages in the thymus (Fig. 2.5A, E-H) and spleen (Fig. 2.5I-K) were suppressed in *Ets1*$^{\Delta/\Delta}$ mice. Thus, ETS1 has overlapping roles with NOTCH1 in promoting pre-TCR signaling and the DN-to-DP transition.

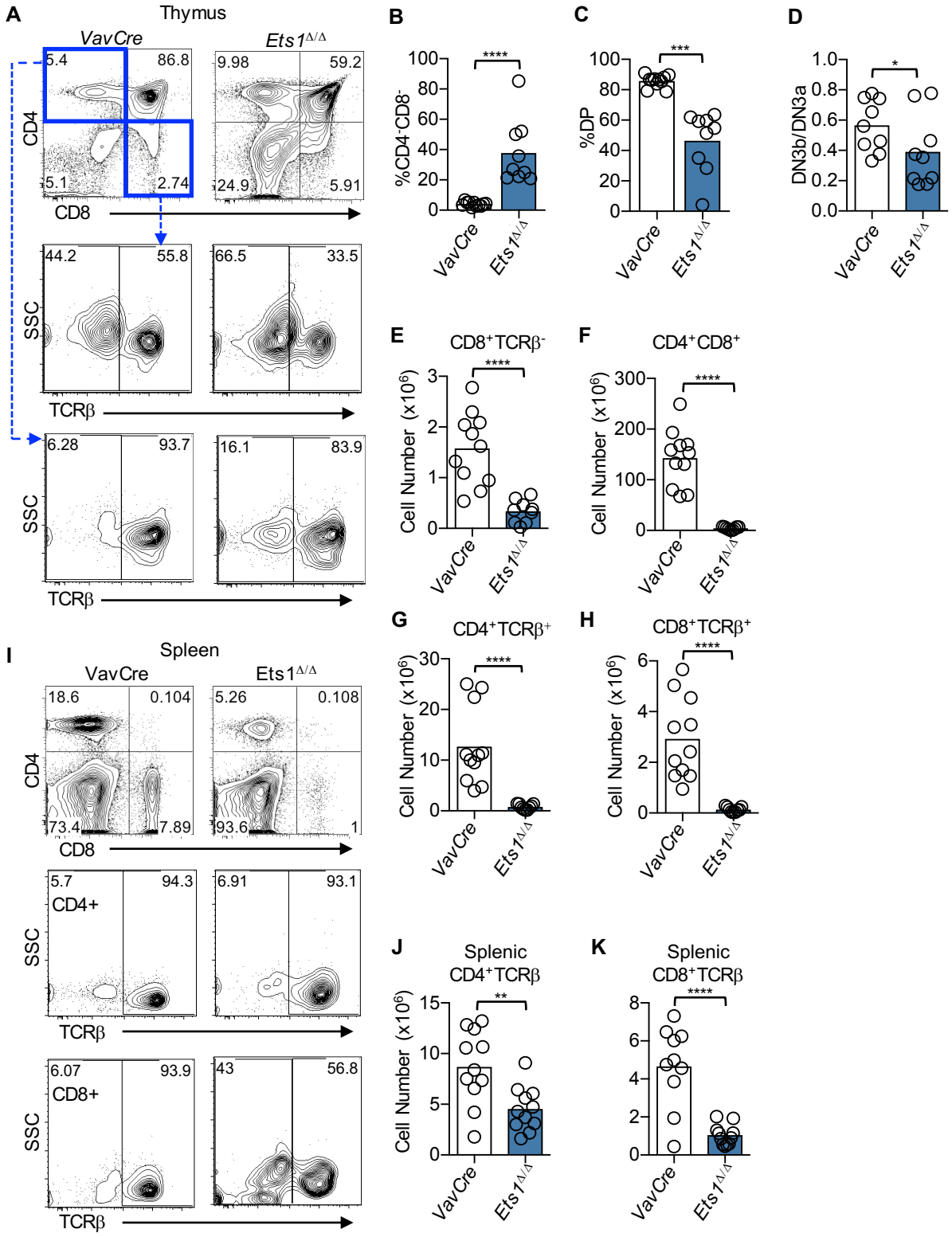

Figure 2.5 ETS1 is required for the DN-DP transition in the thymus and spleen

A-H) Representative flow cytometry profiles of CD4/CD8 thymic subsets (A); %DN (B); %DP (C); DN3b/DN3a ratio (D); and absolute numbers of ISP (E), DP (F), CD4 SP (G), and CD8 SP (H) thymic subsets in *VavCre* control and *Ets1*$^{\Delta/\Delta}$ mice. I-K) Representative flow cytometric plots (I) and absolute numbers of splenic CD4$^+$ (J) and CD8$^+$ (K) subsets from *VavCre* control and *Ets1*$^{\Delta/\Delta}$ mice. DP=CD4$^+$CD8$^+$. CD4 SP=CD4$^+$TCRβ$^+$. CD8 SP=CD8$^+$TCRβ$^+$. *P<0.05; **P<0.01; ***P<0.001; ****P<0.0001. Two-sided two-sample t-tests of non-transformed data were used for (B-D).

ETS1 deficiency alters the balance of T-cells, B-cells, and myeloid cells in the periphery.

As in the case of *Notch1*-deficient mice, *Ets1*-deficient animals did not show any general defects in B-cell numbers (Fig. 2.6A-B). Moreover, we observed a mild myeloproliferative phenotype in Ets1-deficient mice (Fig. 2.6C-E) that was reminiscent of that observed in *Notch1/Notch2*-deficient and Notch-signaling defective Nicastrin-deficient mice (Klinakis et al. 2011).

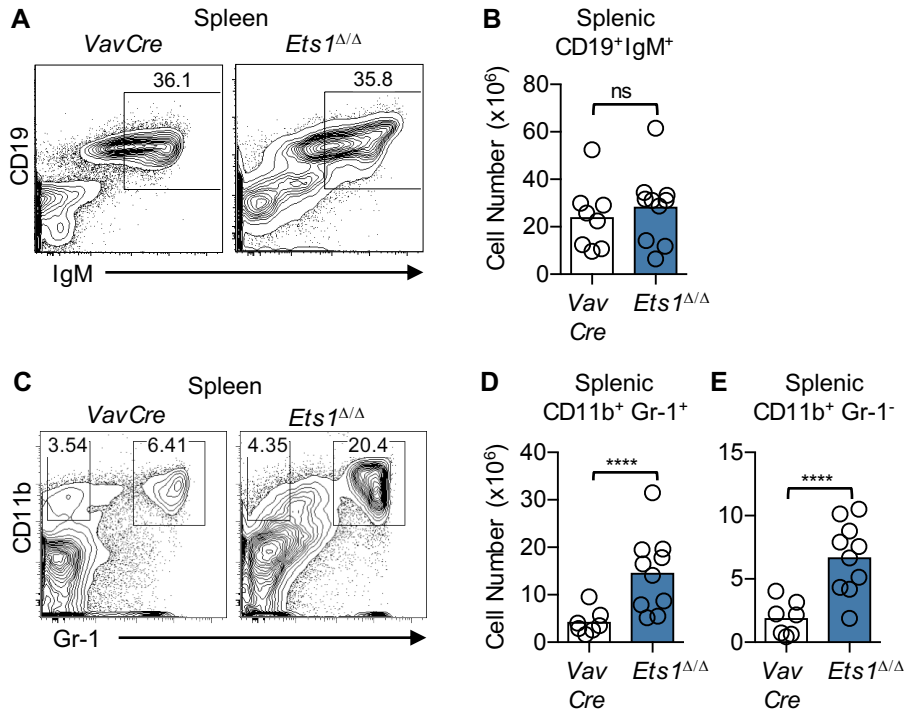

Figure 2.6 ETS1 deficient mice have normal B-cell numbers and increased myeloid cells in the spleen

A-E) Representative flow cytometric plots (A, C) and absolute numbers of splenic CD19$^+$IgM$^+$ (B), CD11b$^+$Gr-1$^+$ (D), and CD11b$^+$Gr-1$^-$ (E) subsets from *VavCre* control and *Ets1*$^{\Delta/\Delta}$ mice. ns=not significant; *P<0.05; ****P<0.0001.

ETS1 deficiency is less toxic than the pan-Notch inhibitor GSI.

Next, we explored the effects of Ets1 inactivation on overall health and in particular the intestine, which is the major organ affected by the toxicity of GSI in humans and mice (Real et al., 2009; VanDussen et al., 2012). We induced ubiquitous *Ets1* deletion in *Rosa26CreER^{T2} Ets1$^{f/f}$* mice via tamoxifen injection. In these experiments, *Ets1ΔRosa26CreER^{T2}* mice showed 70-90% *Ets1* deletion (Fig. 2.7A) and undetectable ETS1 protein in the intestine (Fig. 2.7B).

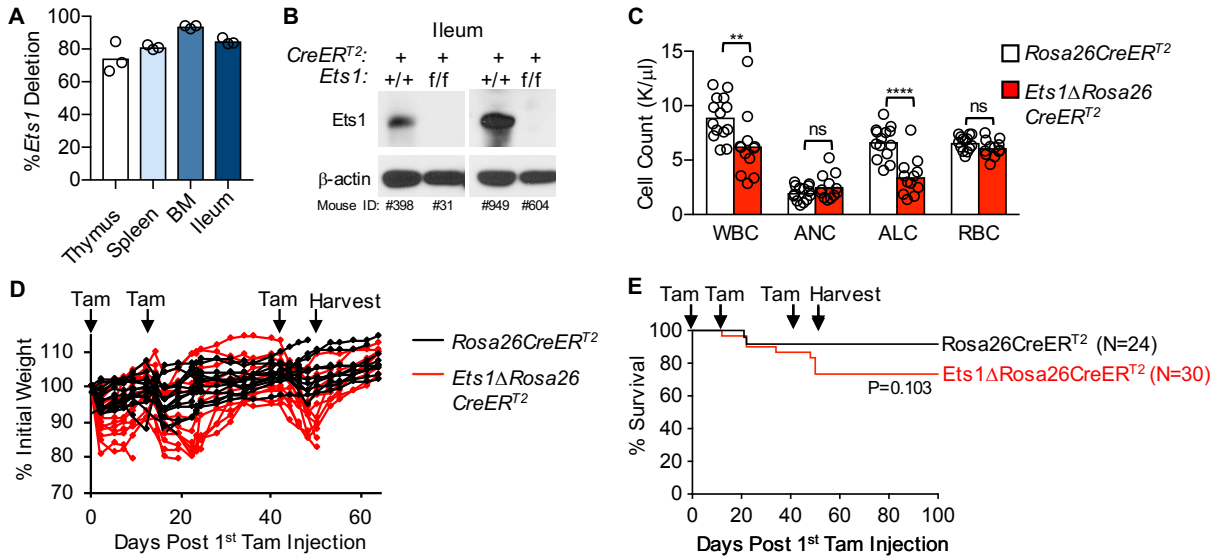

Figure 2.7 Ubiquitous deletion of Ets1 induces lymphopenia and transient weight loss

A) QPCR showing *Ets1* deletion efficiency in thymus, spleen, bone marrow, and intestine DNA of *Ets1ΔRosa26CreER^{T2}* mice after 3 doses of 150mg/kg tamoxifen. B) Western blot for Ets1 in *Rosa26CreER^{T2}* control and *Ets1ΔRosa26CreER^{T2}* intestine after the third dose of tamoxifen. C) Blood cell counts of mice in (D-E) on Day 24. WBC=white blood cell count. ANC=absolute neutrophil count. ALC=absolute lymphocyte count. RBC=red blood cell count. D) Weights of *Rosa26CreER^{T2}* control and *Ets1ΔRosa26CreER^{T2}* mice during treatment with 150mg/kg tamoxifen (Tam) on Days 0, 14, and 42. Per animal protocol, mice had to be sacrificed when weight dropped to 80% or less of starting weight. E) Survival curves of *Rosa26CreER^{T2}* control and *Ets1ΔRosa26CreER^{T2}* mice. ns=not significant; **P<0.01; ****P<0.0001.

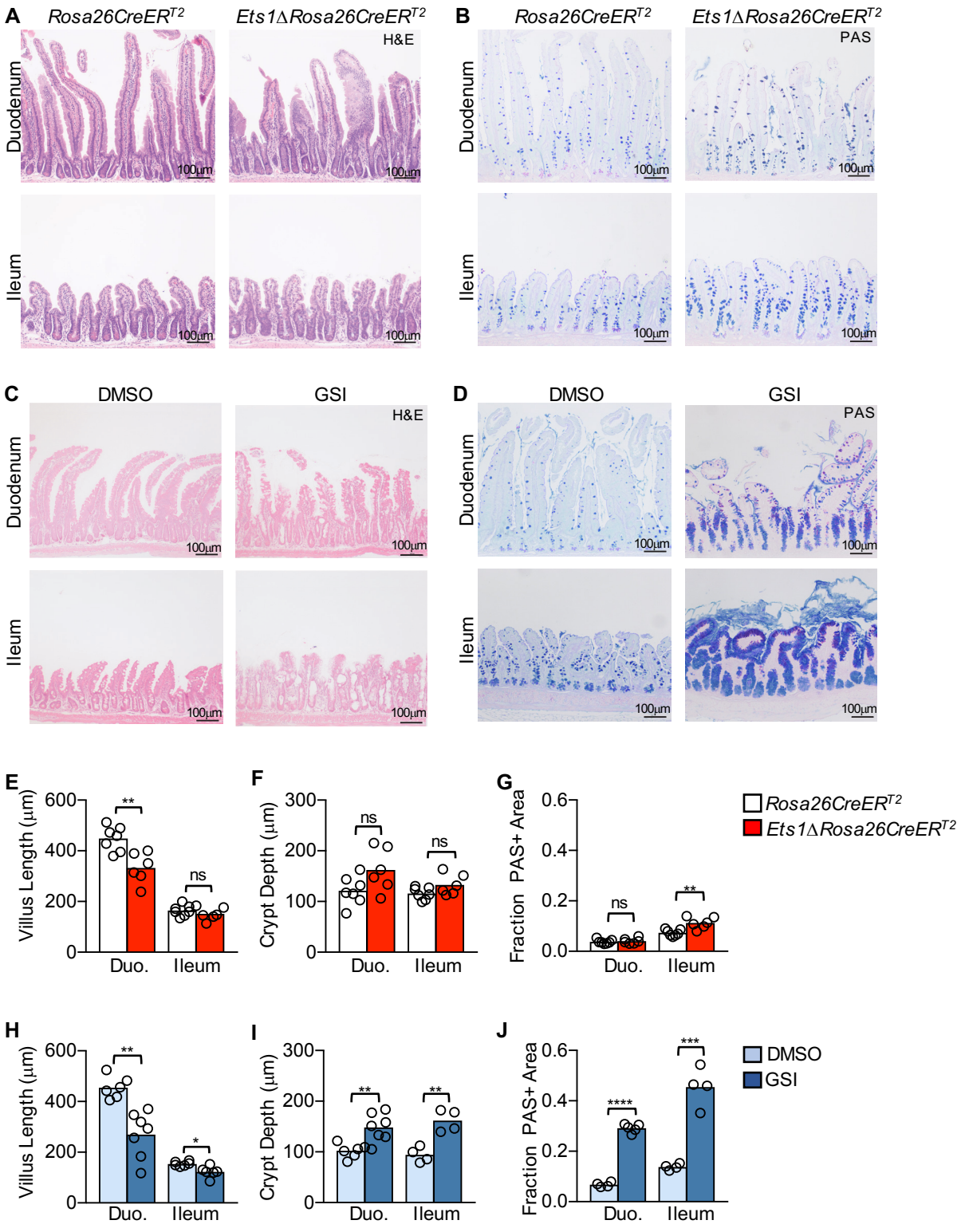

Figure 2.8 ETS1 deficiency is less toxic than pan-Notch inhibition with GSI

A-B) Representative H&E (A) and PAS/AB (B) images of duodenum and ileum from *Rosa26CreER^{T2}* control and *Ets1ΔRosa26CreER^{T2}* mice harvested 8 days after the third dose of 150mg/kg tamoxifen (see 2.7). C-D) Representative H&E (E)

and PAS/AB (F) images of duodenum and ileum harvested from mice one day after 5 consecutive days of injection with DMSO or 30μmol/kg GSI (DBZ). E-J) Quantitation of villus length (E,H), crypt depth (F,I) and fraction of PAS^+ area (G,J) from *Rosa26CreER^{T2}* control and *Ets1ΔRosa26CreER^{T2}* mice after the third dose of tamoxifen (E-G) or 5 days after 5 consecutive days of injection with DMSO/GSI (H-J). ns=not significant; *P<0.05; **P<0.01; ***P<0.001; ****P<0.0001.

To characterize the effects of *Ets1* deletion, we analyzed *Ets1ΔRosa26CreER^{T2}* mice after tamoxifen injection. At 24 days, *Ets1*-deleted mice showed unremarkable blood counts other than the expected lymphopenia (Fig. 2.7C). *Ets1ΔRosa26CreER^{T2}* mice showed no significant differences in weight (Fig. 2.7D) and survival compared to controls (Fig. 2.7E). At ~50 days from the first tamoxifen injection, histological examination of bone marrow, heart, liver, lungs, kidney, and muscle showed no apparent abnormalities (data not shown). Analysis of the intestinal tissues of *Ets1ΔRosa26CreER^{T2}* mice showed morphological changes that were similar, but less pronounced than those observed in mice after pan-Notch inactivation with GSI (Fig. 2.8A-D). Specifically, *Ets1ΔRosa26CreER^{T2}* mice showed modest reductions in duodenal villi length (Fig. 2.8E), a trend toward increased duodenal crypt depth (Fig. 2.8F), and modest ileal goblet cell metaplasia (Fig. 2.8G). Similar, but more pronounced changes were observed in GSI-treated mice (Fig. 2.8H-J).

The ETS1 intestinal phenotype may not be cell autonomous.

Further, we generated mice with intestinal-specific deletion using the *VilCreER^{T2}* transgene. *Ets1ΔVillinCreER^{T2}* mice showed 80-90% Ets1 deletion in intestinal crypt cells (Fig. 2.9A). In contrast to *Notch1ΔVillinCreER^{T2}* mice (Carulli et al., 2015), we did not observe any changes in villus morphology, goblet cell abundance, or weight (Figs. 2.9B-G). It is important to note that we did not achieve complete deletion of *Ets1* in the intestinal epithelium, which may explain the lack of phenotype in these mice. However, these data suggest that systemic ETS1

inhibition only partially recapitulates the phenotype of systemic Notch inhibition with GSIs and induces limited toxicity.

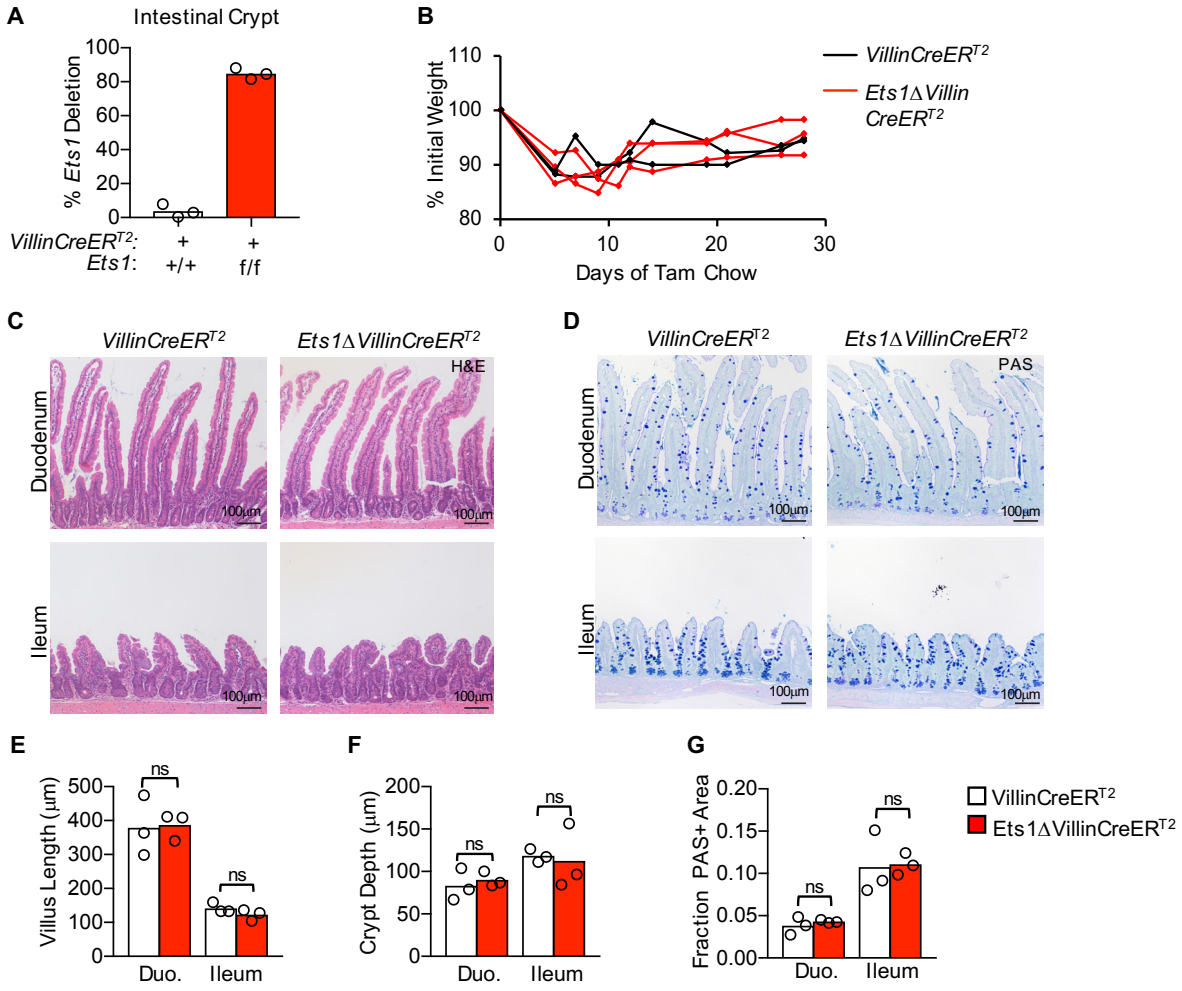

Figure 2.9 Crypt-specific Ets1 deletion does not impair intestinal homeostasis

A-F) *VillinCreER^{T2}* control (n=3) and *Ets1ΔVillinCreER^{T2}* (n=3) mice were injected with five daily doses of 100mg/kg tamoxifen and then harvested the next day for QPCR analysis of *Ets1* deletion efficiency in intestinal crypt cells (A); representative H&E images of duodenum and ileum (B); PAS/AB images of duodenum and ileum (C); and quantitation of villus length (D), crypt depth (E), and fraction of PAS^{+} area (F). G) Weights of *VillinCreER^{T2}* (n=2) and *Ets1ΔVillinCreER^{T2}* (n=3) mice during continuous treatment with 40mg/kg tamoxifen chow (Tam Chow). ns=not significant; **P<0.01; ****P<0.0001.

Discussion

T-ALL cells hijack the transcriptional programs from physiological T-cell development in order to prevent maturation and drive proliferation. If ETS1 is indeed a Notch-cofactor that promotes expression of Notch target genes in T-cell development and T-ALL, one would expect it to be co-expressed with NOTCH1 and essential for the same stages of T-cell development. Accordingly, we saw *Ets1* co-expression and requirement for ETP specification and the DN-DP transition, both stages of T-cell development dependent on Notch signaling. These studies affirm the large body of work that demonstrated a profound loss of thymocytes and impaired DN3-DN4 transition in *Ets1*$^{-/-}$ mice (Bories et al. 1995, Eyquem et al. 2004b, Barton et al. 1998, Muthusamy et al. 1995).

Additionally, we were able to expand upon these studies using our *VavCre* conditional deletion mice to look at the influence of ETS1 on the earliest phases of hematopoiesis. ETS1 appears to be dispensable for the generation of LSK and LMPPs, lymphoid progenitors that give rise to ETPs, though further studies would be needed to ensure their multipotency and regenerative potential was intact. Like NOTCH1, ETS1 is necessary for ETP specification in the thymus. Also like NOTCH1, ETS1 is needed for facile differentiation from DN3a-DN4 cells, the subsequent DN-to-DP transition, and ultimately the generation of mature SP CD4 and CD8 T-cells in the periphery. *Ets1*-deficient animals have an overabundance of myeloid cells accumulating in the spleen. While one prior study suggested that the splenomegaly observed in *Ets1*$^{-/-}$ mice was the result of T-reg deficiencies (Mouly et al. 2010), the accumulation of myeloid cells has not been reported, and additional experiments are needed to determine if these mice are prone to myeloproliferative disease. Another avenue for further study would be to identify T-cell

development stage-specific Ets1 target genes and pathways. In all, these findings provide strong rationale for ETS1 as a co-regulator of Notch1 in T-cell development.

The similarities in function of ETS1 and NOTCH1 extend to the intestine, where ubiquitous *Ets1* deletion produces a mild Notch loss-of-function phenotype. Fortunately, this *Ets1*-loss phenotype lacks the severity and mortality of the Notch-inhibition phenotype. While members of the ETS family are known to govern intestinal development, these studies identify a novel role for ETS1 in intestinal homeostasis. Further studies, with greater mouse numbers and a variety of Cre-drivers, would be necessary to fully elucidate the function of Ets1 in intestinal homeostasis. Our data suggests that this role may not be entirely cell autonomous. While we would anticipate that the lymphopenia and intestinal phenotype from our global *Ets1* deletion mice would occur in human patients, we are cognizant that there might be additional effects of ETS1 depletion in humans unforeseen from our mouse studies. Regardless, our data suggest that ETS1 blockade would be less toxic than pan-Notch inhibitors.

Chapter 3 ETS1 is Important for Notch-Induced T-ALL Maintenance and Initiation[3]

Abstract

Despite the importance of ETS1 for the development of T-cells and in the pathogenesis of solid tumors, its role in T-ALL is poorly understood. Furthermore, no function for ETS1 has been established in the initiation or maintenance Notch-mutated T-ALLs. Here we present evidence from that ETS1 is important for the both the initiation and maintenance of murine Notch-driven T-ALLs *in vivo*. Acute deletion of *Ets1* in maintenance models of leukemia promotes apoptosis, leading to reduced leukemic blasts in circulation and enhanced survival of the mice. Additionally, ETS1 is required for the proliferation of most human T-ALL cell lines *in vitro* and patient-derived xenografts *in vivo*. These studies indicate a novel role for ETS1 in the proliferation of T-ALL cells, providing rationale for the development targeted therapies inhibiting Ets1.

Introduction: ETS1 function in hematologic malignancies

ETS1 overexpression has been observed in many invasive and metastatic cancers, including breast, lung, colon, pancreatic, and thyroid cancers (Lu et al. 2014, Dittmer 2015, Potu et al. 2017, Rothhammer et al. 2004). In carcinomas, ETS1 drives gene expression programs involved with cellular differentiation, migration, proliferation, survival and angiogenesis;

[3] A Adapted from McCarter, A. C., G. D. Gatta, A. Melnick, et al. (2020) Combinatorial ETS1-Dependent Control of Oncogenic NOTCH1 Enhancers in T-cell Leukemia. *Blood Cancer Discovery*.

high *ETS1* expression is associated with higher grading, poorer differentiation, and increased invasiveness (Yamaguchi et al. 2007, Takanami, Takeuchi and Karuke 2001, Nakayama et al. 1996, Saeki et al. 2000, Takai et al. 2000, Puzovic et al. 2014). For example, overexpression of *ETS1* in stratified squamous epithelial cells is capable of blocking terminal differentiation and inducing the secretion of matrix metalloproteases, epidermal growth factor ligands, and inflammatory signals (Nagarajan et al. 2010) While ETS1 has been extensively studied in the context of solid tumors [reviewed in (Dittmer 2015)], much less is known about the function of ETS1 in hematological malignancies.

As discussed in the introduction to this thesis (Chapter 1), ETS1 was originally identified as part of an oncogenic ETS-MYB fusion protein encoded by the E26 chicken leukemia retrovirus, which is capable of inducing mixed myeloid/erythroid leukemias (Leprince et al. 1983). Additionally, another leukemia retrovirus, the Moloney murine leukemia virus (MoMuLV) shows recurrent integrations at the *Ets1* promoter region, suggesting a role for ETS1 in the T-cell lymphoma tumor progress that is induced by MoMuLV (Bellacosa et al. 1994).

The best evidence for the role of ETS1 in leukemia and lymphoma are amplifications in *ETS1* copy-number in patient samples of marginal zone B-cell lymphomas (Flossbach et al. 2013), diffuse large B-cell lymphomas (Pasqualucci et al. 2011, Morin et al. 2011), and pediatric acute myeloid leukemias (Radtke et al. 2009). In these cases, high *ETS1* expression level is associated with aggressive large cell variants of these diseases and poor prognosis for patients. Though promising, these data do not demonstrate a mechanism for ETS1 function in hematologic malignancy. A recent publication suggests ETS1 may promote the pathogenesis of MLL/EB1-driven myeloid leukemias (Fu et al. 2019). *Ets1* is a direct target gene of both the MLL and MLL/AF9 fusion proteins and is upregulated in the context of MLL/EB1

overexpression (Fu et al. 2019). Using a murine bone marrow transplantation model, the authors demonstrated that silencing *Ets1* with shRNAs reduced the expression of leukemic markers and the incidence of leukemia, as well as prolonged survival in the mice (Fu et al. 2019).

Given the substantial role for ETS1 in T-cell development and tumorigenesis, there have been surprisingly few studies examining ETS1 in T-cell acute lymphoblastic leukemia. ETS1 has been shown to bind to oncogenic driver TLX1, repressing TCRα rearrangement and blocking differentiation of immature T-cells (Dadi et al. 2012); this contributes to the development of T-cell neoplasms in TLX-1 overexpression models (Della Gatta et al. 2012). A recent study of human T-ALL cell lines and patient samples identified intronic mutations in the *LMO2* oncogene that produced de novo ETS1 binding sites (Rahman et al. 2017). ETS family binding motifs are enriched at the enhancers of T-ALL oncogenes, often in conjunction with TAL1, a well-known T-ALL oncogenic transcription factor (Vanden Bempt et al. 2018). In vitro studies looking at drivers of DHX15, a RNA helicase highly expressed in T-ALL and B-ALL cell lines, showed that ETS1 and SP1 bind to the *DHX15* promoter and drive its expression (Chen et al. 2018). However, despite all these studies, a direct purpose for ETS1 in T-cell leukemia, including its functional relevance and target genes, remains poorly understood.

Results

ETS1 is important for Notch-induced T-ALL maintenance

We wondered whether the ETS1-dependence of T-cell precursors would be conserved after they transform to leukemia. To test this possibility, we used a well-established murine model of Notch-induced T-ALL (Aster et al. 2000, Pear et al. 1996). We transduced bone marrow stem and progenitor cells of *Rosa26CreER*^{T2}, *Rosa26CreER*^{T2} *Ets1*$^{f/+}$, or *Rosa26CreER*^{T2} *Ets1*$^{f/f}$ mice with an activated *Notch1* allele (*ΔE/Notch1*) (Weng et al. 2003, Schroeter, Kisslinger and Kopan 1998).

We transplanted these cells into recipient mice to generate primary tumors (Fig. 3.1A-B). To test the effect of *Ets1* deletion on T-ALL maintenance, we transferred primary tumors into secondary recipients, which were then injected with tamoxifen to induce *Ets1* deletion. In this setting, homozygous deletion of *Ets1* alleles caused ~32-fold loss of circulating leukemic cells and prolonged median survival by >100% compared to vehicle treatment controls (Fig. 3.2A-B). In contrast, heterozygous *Ets1* deletion had no effect on tumor progression and survival. We confirmed the survival benefit of homozygous *Ets1* deletion compared to control/heterozygous deletion with additional independent *Rosa26CreER*^{T2} (Fig. 3.2C), *Rosa26CreER*^{T2} *Ets1*$^{f/+}$ (Fig. 3.2D), and *Rosa26CreER*^{T2} *Ets1*$^{f/f}$ (Fig. 3.2E) tumors. In these experiments, Cre activation induced mild or negligible effects in survival of control *Ets1*$^{+/+}$ or *Ets1*$^{f/+}$ T-ALL mice. In contrast, tamoxifen treatment conferred a marked and significant survival benefit of ~125% compared to vehicle treatment in the *Ets1*$^{f/f}$ T-ALL group (Fig. 3.2F).

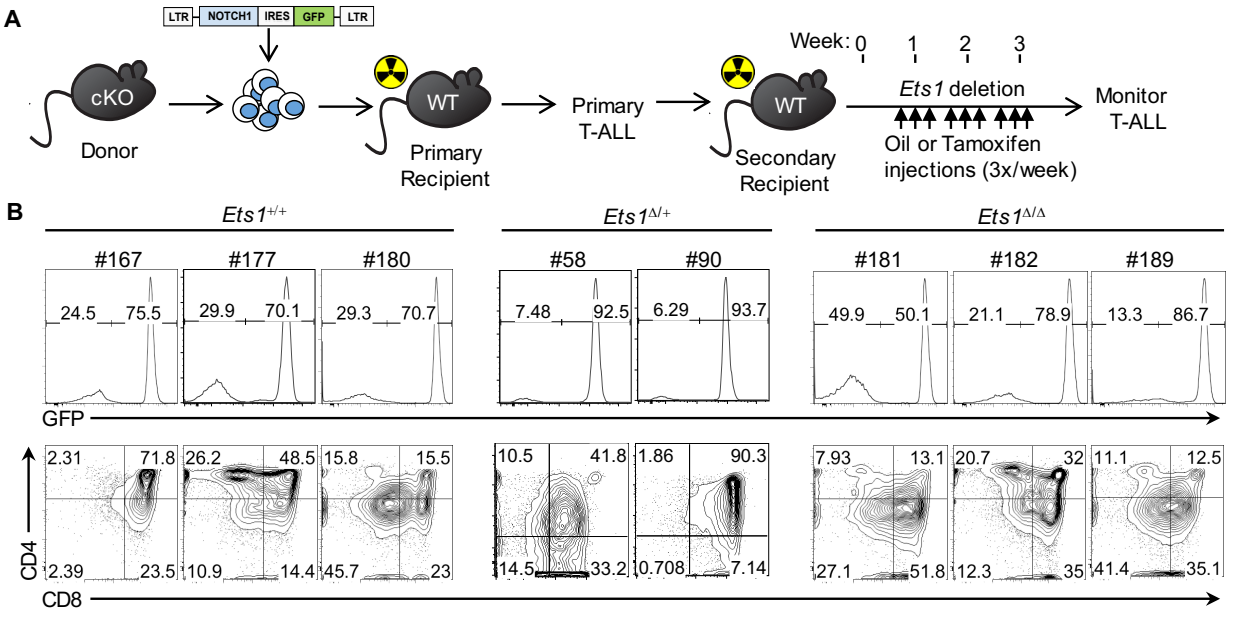

Figure 3.1 Generation of Notch-induced murine T-ALLs

A) Experimental strategy to study maintenance of murine ΔE/Notch1-induced T-ALL. Tam=25mg/kg tamoxifen. B) Representative flow cytometric GFP/CD4/CD8 profiles of Rosa26CreERT2 Ets1$^{+/+}$, Rosa26CreERT2 Ets1$^{f/+}$, and Rosa26CreERT2 Ets1$^{f/f}$ primary splenic tumors used in secondary transplant studies described in (A).

The robust growth of *Ets1*$^{\Delta/+}$ tumors suggested that T-ALLs can thrive with only a single *Ets1* allele. Accordingly, the deletion efficiency of secondary splenic *Ets1*$^{\Delta/\Delta}$ tumors from morbid mice was only ~50%, which matched the ~50% deletion efficiency of *Ets1*$^{\Delta/+}$ tumors (Fig. 3.3G). To investigate this further, we transplanted secondary *Ets1*$^{\Delta/\Delta}$ tumors into tertiary recipients. The deletion efficiency of tertiary tumors extracted from terminally diseased mice was also ~50% (Fig. 3.2H). These results suggest that partial recombination resulting in deletion of only one *Ets1* allele is sufficient to support leukemia cell growth and drive genetic escape.

To further test the requirement of Ets1 in Notch-induced T-ALL maintenance, we acutely deleted *Ets1* in T-ALLs generated with a second conditional Ets1-deficient mouse model (Zook et al. 2016) and a different *Rosa26CreER*^{T2} strain with high deletion efficiency (Guo et al. 2007). To avoid confusion with the previous mouse model, we have labeled these mice as "*Ets1*$^{f/f\text{-}alt}$" and "*Rosa26CreER*$^{T2\text{-}alt}$" respectively. We deleted *Ets1* when GFP^{+} *Rosa26CreER*$^{T2\text{-}alt}$ *Ets1*$^{f/f\text{-}alt}$ T-ALL blasts comprised 50-60% of circulating white blood cells in secondary recipients using a dose of tamoxifen that does not induce toxicity in *Rosa26CreER*$^{T2\text{-}alt}$ control tumors (Schnell et al. 2015, Herranz et al. 2014) and then harvested splenic tumors 48 hours later. Compared to controls, deletion of *Ets1* in *Ets1*$^{\Delta/\Delta-alt}$ tumors reduced spleen size (Fig. 3.3A-B) and increased apoptosis in T-ALL blasts (Fig. 3.3C) with modest effects on cell cycle (Fig. 3.3D). In all, complementary experiments using two independently derived genetic mouse models show that Ets1 is important for maintenance of Notch-induced T-ALL.

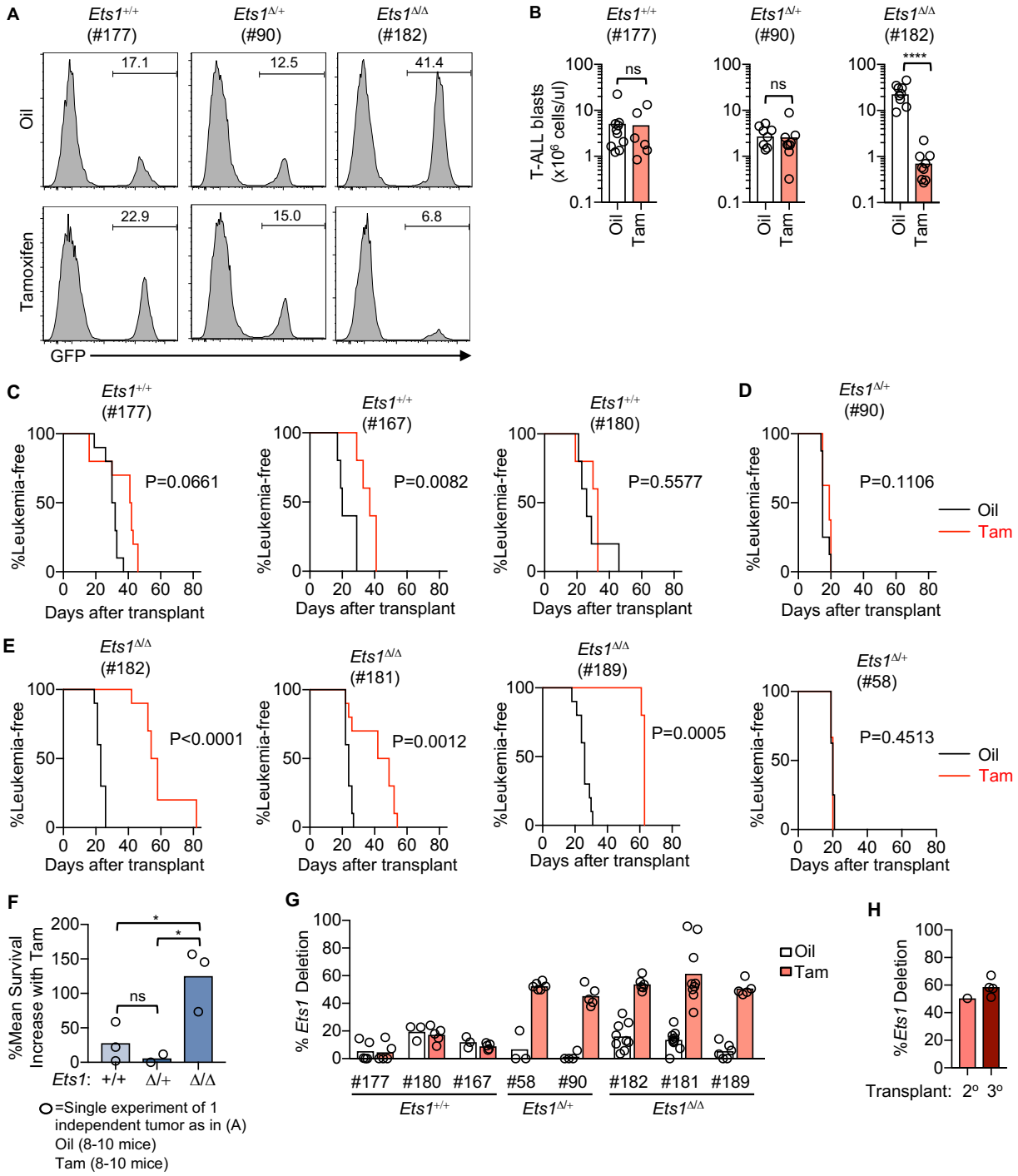

Figure 3.2 ETS1 is important for the maintenance of murine Notch-driven T-ALLs

A-B) Representative flow cytometric plots (A) and peripheral blood GFP$^+$ T-ALL cell counts (B) at 2.5 weeks post-transplant; and survival curves of mice transplanted with *Rosa26CreER^{T2}*, *Rosa26CreER^{T2} Ets1$^{f/+}$*, or *Rosa26CreER^{T2} Ets1$^{f/f}$* T-ALL tumors. C-F) Survival curves of mice transplanted *with Rosa26CreER^{T2} Ets1$^{+/+}$* (C), *Rosa26CreER^{T2} Ets1$^{f/+}$* (D), and *Rosa26CreER^{T2} Ets1$^{f/f}$* (E) primary ΔE/Notch1-induced T-ALL tumors. 9 doses (3x/week) of 25mg/kg tamoxifen or corn vehicle control. Tumor ID# shown in parentheses. Mean %survival increase comparing median survivals after tamoxifen versus vehicle injection of secondary recipient mice that were transplanted with 2-3 independent *Ets1$^{+/+}$*, *Ets1$^{f/+}$*, or *Ets1$^{f/f}$* tumors (F). G) QPCR assay showing *Ets1* deletion efficiency in splenic tumor cells harvested from terminally diseased mice in (C-E) H) Tumor #182 (*Ets1$^{f/f}$*)

from a secondary recipient mouse (2º) was injected into four tertiary recipients (3º). QPCR assay showing *Ets1* deletion efficiency in splenic tumor cell DNA prior to injection into tertiary recipient mice and harvested from terminally diseased tertiary recipient mice at time of morbidity. ns=not significant; *P<0.05; **P<0.01; ***P<0.001; ****P<0.0001.

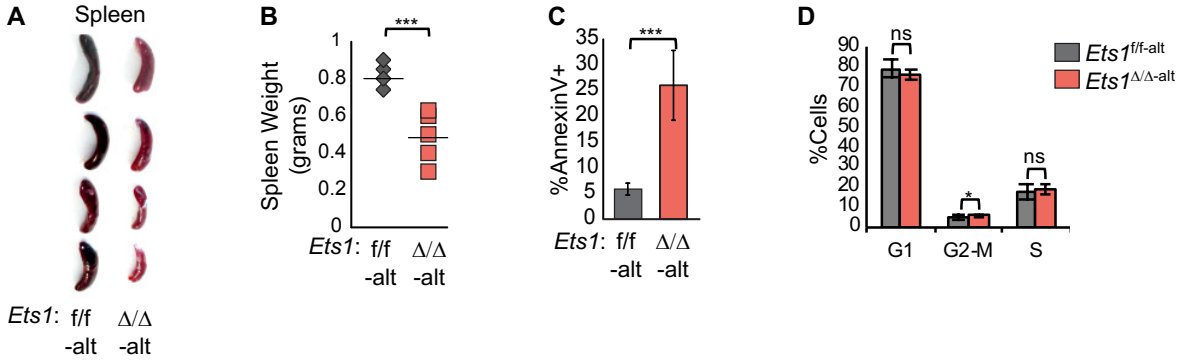

Figure 3.3 Acute deletion of Ets1 promotes apoptosis of murine Notch-driven T-ALLs

A-D) Images (A), weights (B), AnnexinV analysis (C), and cell cycle analysis (D) of splenic tumors from an alternative ("alt") Notch-induced T-ALL mouse model that were generated using the same experimental strategy as shown in Fig. 3.1, but were harvested from secondary recipients at 48 hours after injection with 300mg/kg tamoxifen. ns=not significant; *P<0.05; **P<0.01; ***P<0.001; ****P<0.0001. (A-D conducted by G. Della Gatta, Ferrando lab).

ETS1 is important for initiation of Notch-induced T-ALL

To determine the effect of *Ets1* deletion on initiation of Notch-induced T-ALL, we used a previously described "*Ets1*$^{p/p}$" mouse, which produces a hypo-morphic Ets1 protein lacking the N-terminal PNT domain (Wang et al. 2005). These mice show a weak Ets1 loss-of-function phenotype with a ~2.8-fold loss of thymocytes (Barton et al. 1998). We transduced bone marrow stem and progenitor cells from *Ets1*$^{+/+}$, *Ets1*$^{+/p}$, or *Ets1*$^{p/p}$ mice with ΔE/Notch1 and transplanted these into isogenic recipient mice (Fig. 3.4A). Most mice injected with *Ets1*$^{+/+}$ cells died of leukemia by 90 days after transplant. In contrast, 6% and 0% of mice transplanted with *Ets1*$^{+/p}$ and *Ets1*$^{p/p}$ cells respectively died of T-ALL (Fig. 3.4B). These data demonstrate a strict requirement of Ets1 function for *in vivo* initiation of Notch-induced T-ALL.

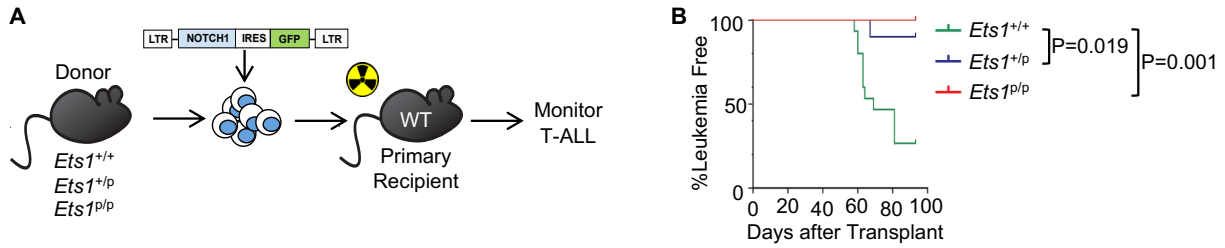

Figure 3.4 ETS1 is important for the initiation of murine Notch-induced T-ALL

A) Experimental strategy to study initiation of murine ΔE/Notch1-induced T-ALL. (B) Survival curves of mice transplanted with *Ets1*$^{+/+}$, *Ets1*$^{p/+}$, or *Ets1*$^{p/p}$ bone marrow progenitors transduced with ΔE/Notch1. (A-B conducted by G. Della Gatta, Ferrando lab).

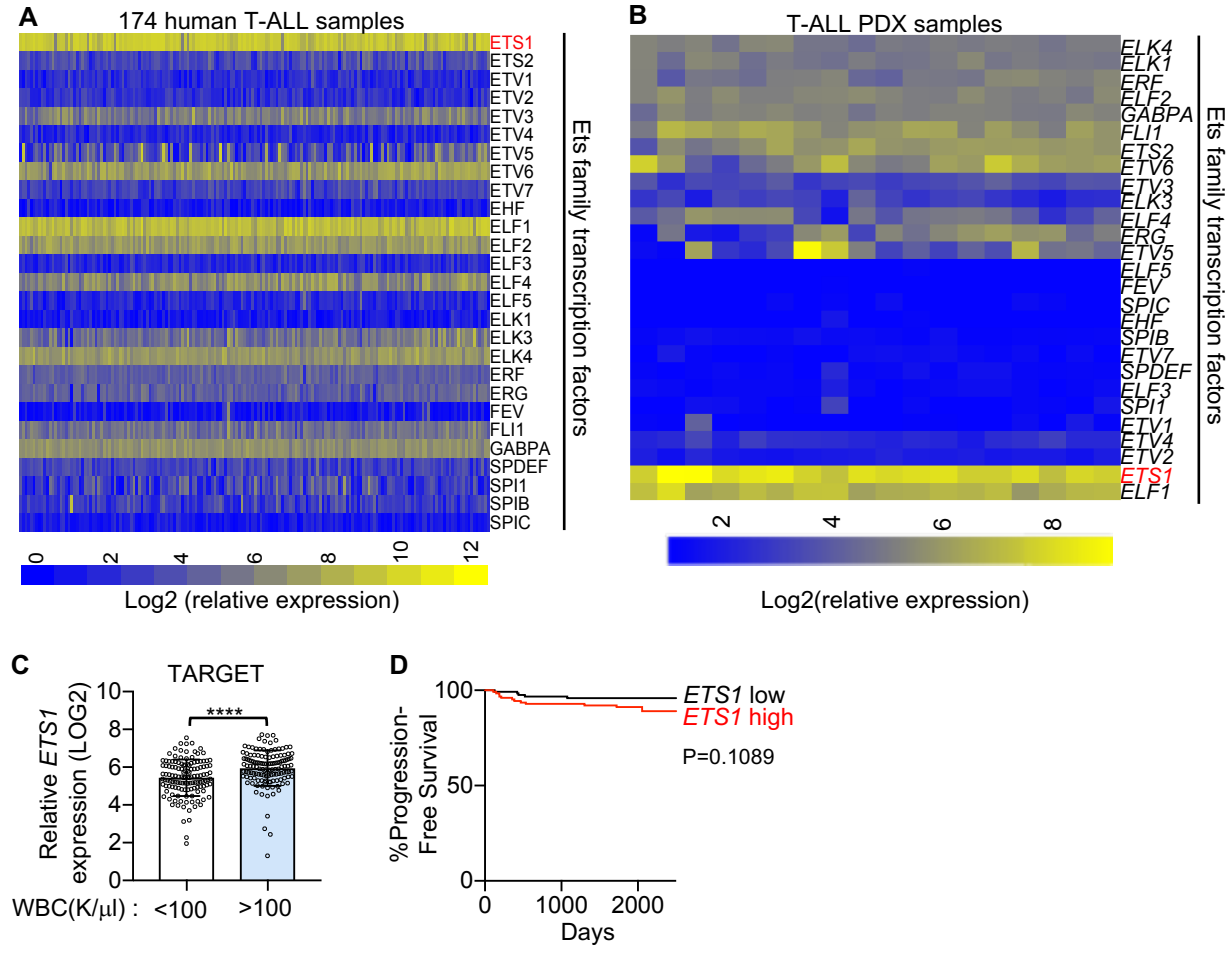

Figure 3.5 ETS1 is highly expressed in patient T-ALL samples and is associated with worse prognosis

A) Heatmap of Ets family member mRNA in primary human T-ALL samples (GSE13159). B) Heatmap of Ets family member expression in patient derived xenograft (PDX) samples (ProXe) (Townsend et al. 2016). C) *ETS1* expression level in pediatric T-ALL patient samples as a function of WBC at time of diagnosis (unpublished TARGET ALL study, see Experimental Procedures) D) Survival curves of T-ALL patients stratified by *ETS1* expression ("high" and "low" are the 50% above and below the mean respectively; TARGET).

Ets1 important for propagation of human T-ALL cells in vitro and in vivo

ETS1 was one of the most highly and consistently expressed Ets transcription factor genes in primary human T-ALL samples (Fig. 3.5A) and patient-derived xenografts (PDXs, Fig. 3.5B). In a clinically annotated cohort of pediatric T-ALL, high *ETS1* expression was associated with hyperleukocytosis (white blood cell count >100K, Fig. 3.5C), an adverse prognosis factor in survival (Rowe et al. 2005). Accordingly, high *ETS1* expression trended toward worse progression-free survival (Fig. 3.5D).

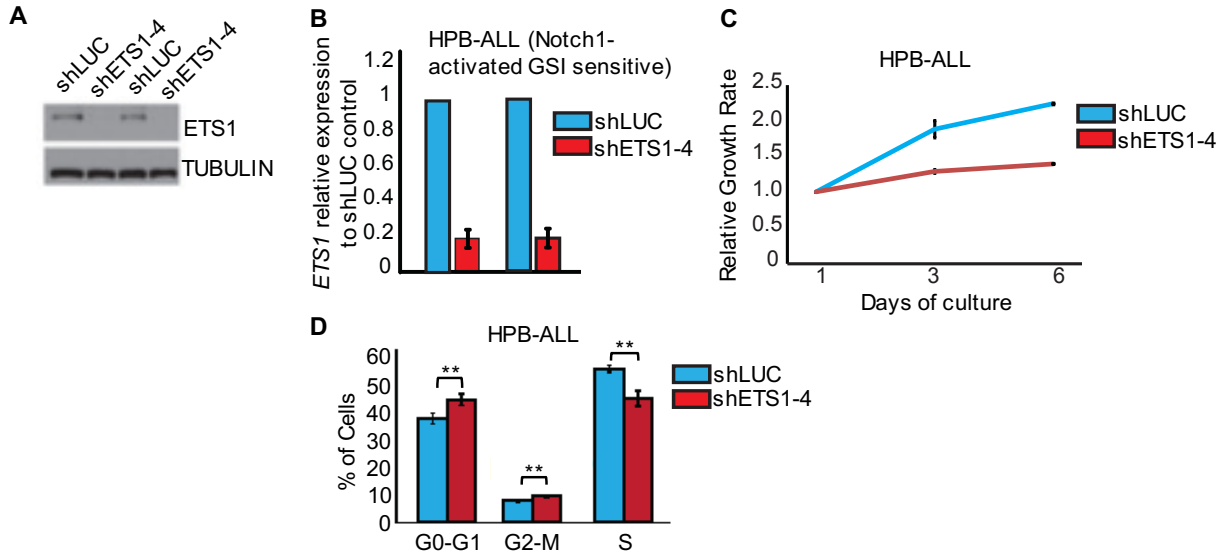

Figure 3.6 ETS1 knockdown reduces proliferation of HPB-ALL cells

A-D) Western blot of Ets1 (A); qRT-PCR analysis of *ETS1* mRNA (B); growth curves through MTT assay (C); and cell cycle analysis (D) of the NOTCH1-activated GSI-sensitive HPB-ALL cell line transduced with shETS1-4. ns=not significant; **P<0.01 (A-D conducted by G. Della Gatta, Ferrando lab).

To test the functional importance of ETS1 in human T-ALL, we transduced *ETS1* shRNAs into T-ALL cell lines. In depth analysis of *ETS1* knockdown in HPB-ALL cells showed effective suppression of ETS1 protein and mRNA levels (Fig. 3.6A-B), reduced proliferation (Fig. 3.6C), and delayed G1/S transition (Fig. 3.6D). Similarly, *ETS1* knockdown reduced proliferation of 6/8 additional cell lines tested (CEM, THP-6, DND-41, SUP-T1, MOLT4, and DU.528; Fig. 3.7A-I).

To test the anti-tumor effects of *ETS1* inactivation in non-immortalized human T-ALL cells *in vivo*, we took advantage of the success of shRNA protocols in knocking down gene expression in patient-derived xenograft (PDX) cells (Giambra et al. 2012, Benyoucef et al. 2016). In these experiments, we transduced PDX3 cells, which expressed high levels of ETS1 and NOTCH1 (Fig. 3.8A) with shETS1/YFP and transplanted them into immunodeficient NSG mice (Fig. 3.8B). Knockdown cells were viable as they could expand for several more days *in vitro* (Fig. 3.8C-D). However, ETS1 inactivation markedly blunted disease progression, reducing circulating T-ALL blasts by 44-fold at 8 weeks post-transplant (Fig. 3.8E-F), and improved survival (Fig. 3.8G). Moreover, PDX cells that were recovered from terminally diseased mice showed reduced levels of YFP (Fig. 3.8H) and restored *ETS1* expression (Fig. 3.8I), consistent with positive selection of cells that escaped ETS1 knockdown. Taken together, these results demonstrate a strong and highly prevalent ETS1-dependency in human T-ALL.

Discussion

Despite the significant body of work examining the role of ETS1 in many solid tumors, there was little evidence of a role for ETS1 in hematologic malignancies. Using a murine model of Notch-driven T-ALL, we determined the requirement of ETS1 for the initiation and maintenance of T-ALL *in vivo*. We also utilized *ETS1* knockdown with shRNA to confirm the importance of ETS1 in human T-ALL proliferation in vitro and in vivo. Acute deletion of *ETS1* induced apoptosis in a human T-ALL cell line and altered the cell cycle regulation of these cells. Here, we present evidence that Ets1 is broadly important for the proliferation of leukemia cells, providing strong rationale for targeting Ets1 therapeutically.

A single Ets1 allele appears sufficient to maintain Notch-driven T-ALLs in maintenance, but the leukemia initiation studies executed by our collaborators suggest that haploinsufficiency

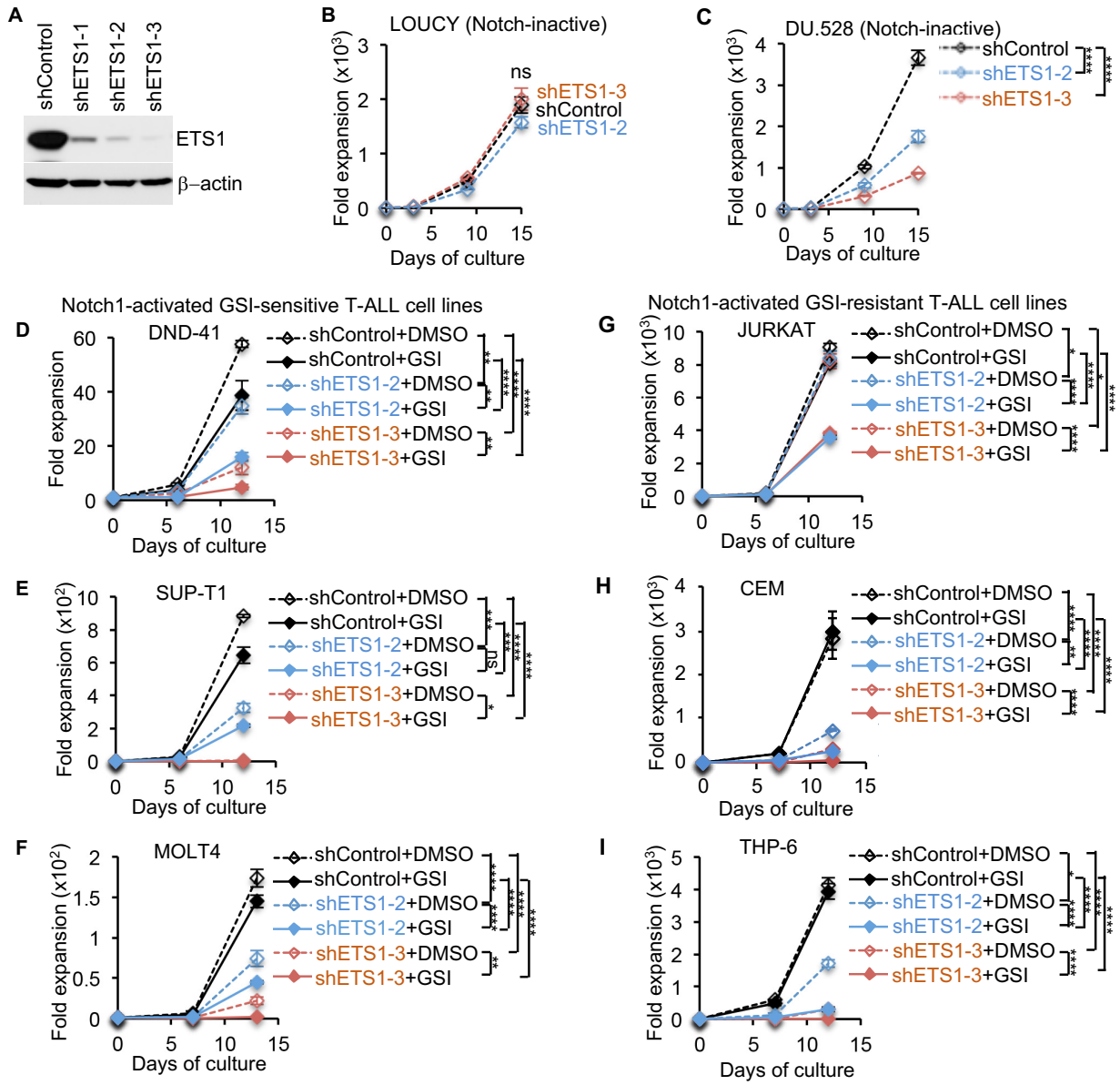

Figure 3.7 ETS1 is important for the proliferation of human T-ALL cell lines

A) Western blot of ETS1 in CEM cells transduced with shETS1. B-I) Growth curves of LOUCY (B), DU.528 (C), DND-41 (D), SUP-T1 (E), MOLT4 (F), JURKAT (G), CEM (H), and THP-6 (I) T-ALL cells transduced with shETS1. GSI=200nM DBZ. Fold expansion=cell count divided by cell count on Day 0. "NOTCH1-activated" is defined by detection of cleaved ICN1 by Western blot or presence of *NOTCH1* mutation. "Notch-inactive" is defined by lack of cleaved ICN1 by Western blot or *NOTCH1* mutation. *P<0.05; **P<0.01; ***P<0.001; ****P<0.0001.

in Ets1 prevents the initiation of Notch-driven T-ALL. An important caveat in this discrepancy lies in the different mouse models used for these experiments. While both the Chiang and Ferrando labs utilized the same ΔE Notch allele to drive leukemogenesis from hematopoietic stem cells, the

Chiang lab experiments utilized an *Ets1*^{flox} allele in which the loxP sites flank the DNA-binding ETS domain of *Ets1*. This allele has been demonstrated to be a true null allele in multiple publications (Bories et al. 1995, Eyquem et al. 2004a, Mouly et al. 2010). In contrast, the *Ets1*^{P} allele used in the Ferrando lab leukemogenesis experiment has loxP sites surrounding the pointed (PNT) domain of *Ets1*. This allele has been demonstrated to produce a truncated ETS1 protein (Wang et al. 2005). It is possible that this ETS protein, lacking the PNT domain needed for many protein-protein interactions, might serve as a dominant-negative regulator in T-ALL initiation, therefore preventing leukemogenesis in the *Ets1*$^{P/+}$ cells.

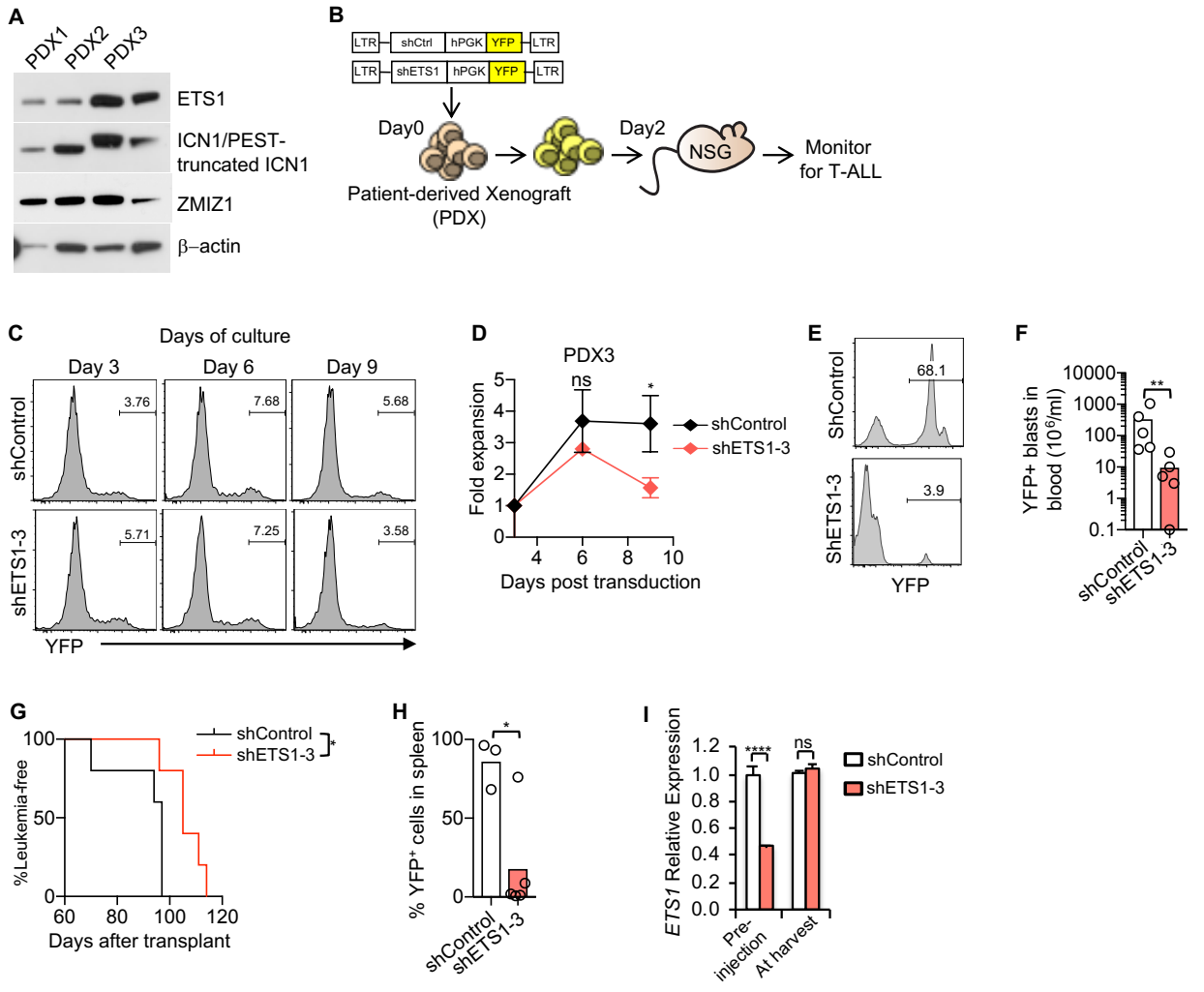

Figure 3.8 ETS1 is important for the propagation of human T-ALL cells

A) Western blot of ETS1, cleaved NOTCH1 (ICN1), and ZMIZ1 in patient-derived xenograft (PDX) samples. B-I) Experimental strategy testing maintenance of PDX cells transduced with shETS1-3/YFP after transplantation into NSG mice (B). Flow cytometric plots (C) and growth curves (D) of PDX cells transduced on Day 0, sorted on Day 2, and co-cultured with OP9-DLL4 cells. N=3 transduced bioreplicates per group. Representative flow cytometric plots (E) and peripheral blood T-ALL counts (F) at 8 weeks post-transplant; survival curves (G); and %YFP (H) and *ETS1* transcripts normalized to respective controls (I) of splenic tumors harvested from terminally diseased mice compared to cells prior to injection into NSG mice. ns=not significant, *P<0.05, **P<0.01, ***P<0.001, ****P<0.0001.

Further inquiry into the need for one or more *Ets1* alleles in other models of murine T-ALL leukemogenesis, such as the *LMO2*-driven model (Smith et al. 2014), might shed light on whether this requirement is Notch-dependent. Additionally, while most of the human T-ALL cell lines could not proliferate after *ETS1* knockdown, two of the human T-ALL cell lines that we examined did not respond. Another avenue of potential exploration are the factors that govern ETS-dependency in T-ALL cells. What distinguishes ETS1-inhibition responsive T-ALLs from those that are not responsive?

These studies establish a novel role for ETS1 in the proliferation of T-ALL cells. As striking as the T-ALL apoptotic and growth arrest phenotypes might be, these studies do not elucidate the mechanism by which Ets1 contributes to the growth of these cells. In Chapter 4, we will identify ETS1 target genes in T-ALL cell lines and explore the function of ETS1 in Notch complex recruitment and enhancer activation at enhancers genome-wide.

Chapter 4 ETS1 Promotes Context-Dependent Recruitment of the Notch Complex and Notch-Induced Gene Expression in T-ALL[4]

Abstract

Notch1 drives transcription of its target genes in T-ALL through T-cell specific enhancers. However, Notch1 requires other transcription factors, chromatin modifiers, and co-activators to create a favorable chromatin context for Notch to function at these enhancers. These studies propose that Ets1 is an important cofactor at a subset of enhancers for Notch-driven T-ALL oncogenes. Through RNA-seq and microarray studies in human T-ALL cell lines, we determined that Ets1 co-regulates a portion of Notch target genes, including important pathways like Myc and mTOR. Additionally, we identified direct Ets1 target genes and characterized "dynamic" Ets1 peaks through comparative ChIP-seq studies in human T-ALL cell lines with Ets1 knockdown. "Dynamic" Ets1 peaks showed reduced recruitment of Notch complex members and H3K27ac with Ets1 deprivation, as well as enrichment in GATA3 binding. This paired with co-immunoprecipitation studies that showed interaction between Ets1 and the Notch complex support the notion that Ets1, perhaps in conjunction with GATA3, recruits the Notch complex to a subset of enhancers. These enhancers include T-cell development and leukemia-associated genes such as Myc, Myb, Hes1, Notch3, and Dtx1. In all, these studies provide evidence that Ets1 participates as a part of T-cell specific Notch enhancers, making Ets1 a potential therapeutic target for T-ALL treatment.

[4] Adapted from McCarter, A. C., G. D. Gatta, A. Melnick, et al. (2020) Combinatorial ETS1-Dependent Control of Oncogenic NOTCH1 Enhancers in T-cell Leukemia. *Blood Cancer Discovery*.

Introduction: Notch1 functions at T-cell specific enhancers in T-ALL

NOTCH1 requires protein-protein interactions in order to function. Accordingly, breaking the NOTCH1-MAML interaction inhibits T-ALL proliferation (Moellering et al. 2009). Unfortunately, this results in pan-Notch inhibition. In order to develop Notch-directed therapies with less toxicity than pan-Notch inhibitors we can exploit recent insights that ICN cannot activate enhancers by itself (Bray 2016). An important example is *MYC*. *MYC* is a critical direct NOTCH1 target gene (King et al. 2013, Weng et al. 2006, Palomero et al. 2006a) that can substitute for oncogenic Notch functions (Chiang et al. 2016). In T-ALL, *MYC* expression is controlled by the NOTCH1-dependent T-cell specific 3' *MYC* enhancer (Herranz et al. 2014, Yashiro-Ohtani et al. 2014a, Yashiro-Ohtani et al. 2014b). This enhancer is inactive in non-T cells even if ICN is ectopically overexpressed (Herranz et al. 2014). That is because NOTCH1 requires a T-cell specific "oncogenic nuclear context" consisting of groups of cooperating transcription factors. Thus, one might avoid the intolerable effects of pan-Notch inhibition by specifically targeting the "oncogenic nuclear context" that drives target genes like *MYC*. Prior work in our lab showed that this might be possible with the discovery that the PIAS-like coactivator ZMIZ1 is a direct and context-dependent cofactor of NOTCH1 (Pinnell et al. 2015b). Accordingly, inactivation of ZMIZ1 causes T-ALL regression, but no toxicities linked to pan-Notch inhibition (Pinnell et al. 2015a).

Like ZMIZ1, ETS1 might also be an important cofactor at T-cell specific Notch enhancers. As discussed in Chapter 3, ETS1 drives proliferation of T-ALL cell lines and primary cells and promotes GSI resistance. Further evidence raising the importance of ETS1 is the recent identification of mutations that create neomorphic ETS1 binding sites that induce oncogenes in

T-ALL (Rahman et al. 2017). ETS1 has been proposed as a NOTCH1 coregulator as ETS1 binding at chromatin associates with NOTCH1 and RUNX1 sites (Wang et al. 2014a, Choi et al. 2017). Consistently, ETS motifs are highly enriched in T-ALL-associated enhancers (Rahman et al. 2017, Sanda et al. 2012, Palii et al. 2011, Vanden Bempt et al. 2018). While these correlative observations are suggestive of a functional and clinically relevant interaction between ETS1 and NOTCH1 in early T cell leukemogenesis, this notion remains to be tested.

Results

ETS1 promotes NOTCH1-driven oncogenic pathways

We sought to understand the underlying mechanism of the ETS1 requirement for NOTCH1-induced T-ALL initiation and maintenance. Towards this goal, we performed RNA-Seq in THP-6 T-ALL cells following ETS1 knockdown and NOTCH1 inhibition using GSI. These analyses revealed broadly overlapping signatures between ETS1 and NOTCH1 deprivation. About 33% of ETS1-regulated genes were also controlled by NOTCH1 (Fig. 4.1A). Conversely, about 22% of NOTCH1-controlled genes were also regulated by ETS1. Of the 467 ETS1-NOTCH1 coregulated genes, 290 (62%) were regulated in the same direction. Interestingly, pathway analyses showed Myc target genes as the most prominent Hallmark signature enriched in ETS1-induced and NOTCH1-induced genes (ETS1 NES=-5.81, FDR<0.0001; NOTCH1 NES -6.15, FDR<0.0001; Fig. 4.1B-C). Consistently, pathway analyses showed that the list of genes containing at least one Myc binding motif (CACGTG) and the C6 oncogenic signature of Myc-induced genes were among the topmost enriched in ETS1-induced and NOTCH1-induced genes (FDR<0.0001; Fig. 4.1D-E). In addition, pathway analyses showed that the C6 oncogenic signature of mTOR-induced genes and the mTOR-related Rapamycin_Response and

Leucine_Deprivation gene sets were highly enriched in ETS1-induced and NOTCH1-induced genes (FDR<0.01; Fig. 4.1D-E). These results reinforce the well-established roles for Myc and mTOR as major oncogenic effector pathways in Notch1-induced T-ALL (McCarter, Wang and Chiang 2018). To test the importance of MYC and mTOR as downstream effectors of the ETS1-driven oncogenic/dependency programs, we expressed MYC or myr-AKT in THP-6 cells (Fig. 4.1F) and CEM cells (Fig. 4.1G) using previously described constructs (Chiang et al. 2016). Enforced expression of MYC or myr-AKT was sufficient for partial rescue from the anti-proliferative effects of ETS1 deprivation.

These data support the prominent role of MYC and mTOR signaling in ETS1 programs convergent with NOTCH1 in the control of T-ALL proliferation. Moreover, it did not escape our attention that several known direct NOTCH1 target genes were downregulated by ETS1 knockdown, including *MYC*, *NOTCH3*, *HES1*, *DTX1*, *SHQ1*, *NOTCH1*, and *IL7R* (Q<0.05, Fig. 4.1H-K).

In experiments independently performed by our collaborators in the Ferrando lab, ETS1-regulated genes in HPB-ALL cells (data not shown) were significantly enriched in a core set of NOTCH1-regulated genes shared among seven T-ALL cell lines (Palomero et al. 2006a) (P<0.001, Fig. 4.2A-B). Moreover, corner gene analysis showed markedly concordant effects of ETS1 deprivation between THP-6 and HPB-ALL (P=1E-190, Fig. 4.2C-D). Of the top 28 NOTCH1-controlled genes most downregulated by shETS1-4 in HPB-ALL cells, 23 were also downregulated by shETS1-3 in THP-6 cells (P=9.0E-14, Fig. 4.2B), including well-established NOTCH1-induced target genes like *MYC*, *DTX1*, *HES1,* and *NOTCH3* (Fig. 4.2B,D). In all, the results show that ETS1 and NOTCH1 co-induce shared target genes and oncogenic pathways across multiple T-ALL cell lines.

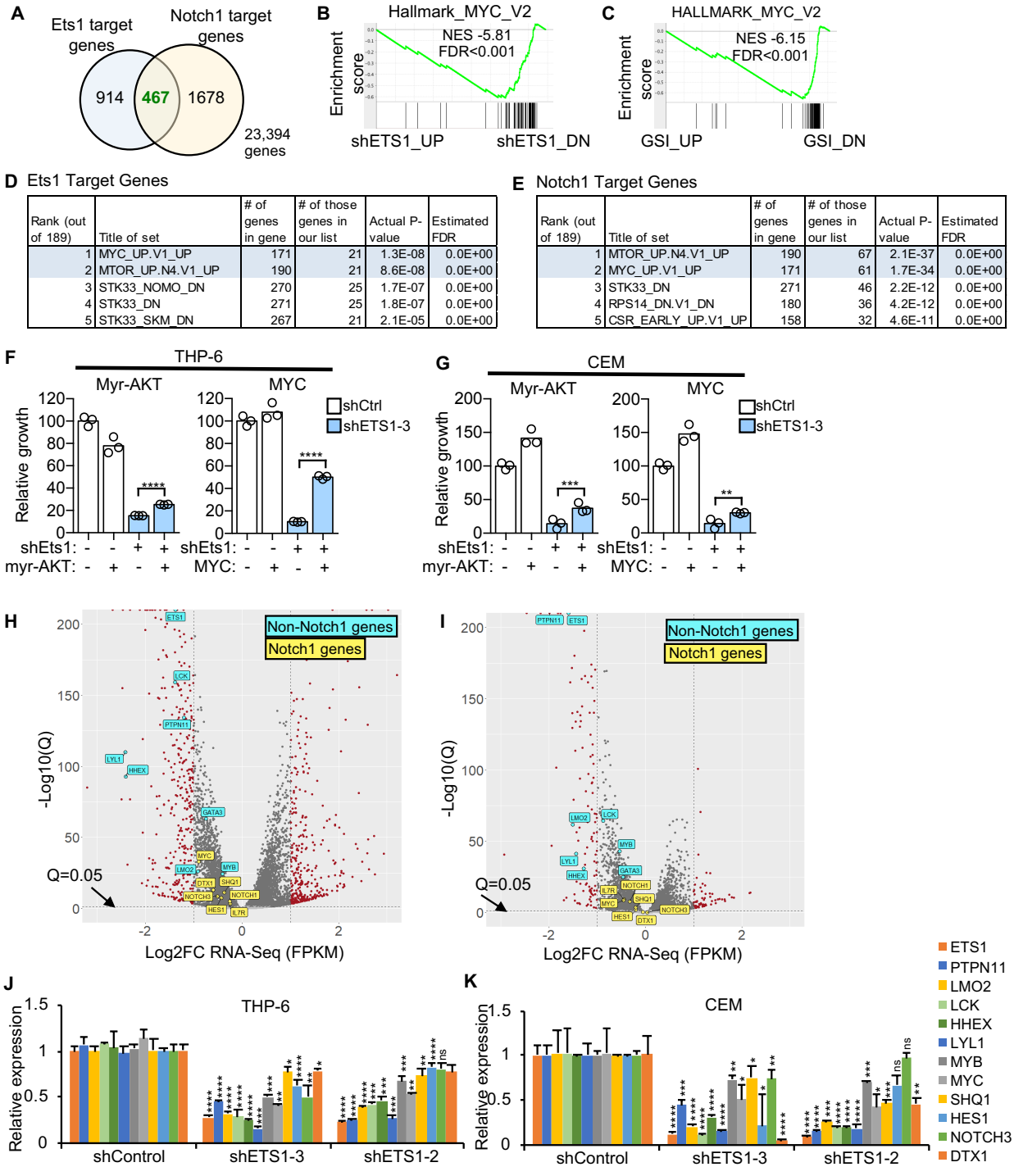

Rank (out of 189)	Title of set	# of genes in gene	# of those genes in our list	Actual P-value	Estimated FDR
1	MYC_UP.V1_UP	171	21	1.3E-08	0.0E+00
2	MTOR_UP.N4.V1_UP	190	21	8.6E-08	0.0E+00
3	STK33_NOMO_DN	270	25	1.7E-07	0.0E+00
4	STK33_DN	271	25	1.8E-07	0.0E+00
5	STK33_SKM_DN	267	21	2.1E-05	0.0E+00

Rank (out of 189)	Title of set	# of genes in gene	# of those genes in our list	Actual P-value	Estimated FDR
1	MTOR_UP.N4.V1_UP	190	67	2.1E-37	0.0E+00
2	MYC_UP.V1_UP	171	61	1.7E-34	0.0E+00
3	STK33_DN	271	46	2.2E-12	0.0E+00
4	RPS14_DN.V1_DN	180	36	4.2E-12	0.0E+00
5	CSR_EARLY_UP.V1_UP	158	32	4.6E-11	0.0E+00

Figure 4.1 ETS1 promotes Notch-driven oncogenic pathways in T-ALL

A) Venn diagram showing ETS1 and NOTCH1 target genes in THP-6 cells. ETS1 target genes= P<.01 and fold-change (FC)>1.2 for the comparison of shControl vs both shETS1 (3/2). NOTCH1 target genes=P<.01 and FC>1.2 for the DMSO vs GSI comparison. B-C) Gene set enrichment analysis (GSEA) using the MSigDB HALLMARK_MYC_V2 list for the shControl vs shETS1-3/2 (B) and DMSO vs GSI (C) comparisons. D-E) Pathway analyses of 189 gene lists (MSigDB Oncogenic Signatures,

C6) showing the enriched pathways with lowest P-values for ETS1 (D) and NOTCH1 (E) target genes in THP-6 cells (defined in Fig. 4.1A) F-G) Rescue experiments showing relative growth of THP-6 (F) or CEM (G) cells co-transduced with shETS1-3 and myr-AKT or Myc. H-I) Volcano plots of RNA-Seq Log2FC data showing the shControl vs shETS1-3 (H) or shETS1-2 (I) comparison and selected ETS1 (yellow) and NOTCH1 (blue) target genes. J-K) QRT-PCR validation of RNA-Seq data showing expression of selected ETS1 target genes (*PTPN11, LMO2, LCK, HHEX, LYL1, MYB*) and ETS1/NOTCH1 target genes (*MYC*, *SHQ1, HES1*, *DTX1*) in THP-6 cells (J) and CEM cells (K) with two independent shETS1 (3/2). Non-transformed ANOVA was performed for *HES1*.

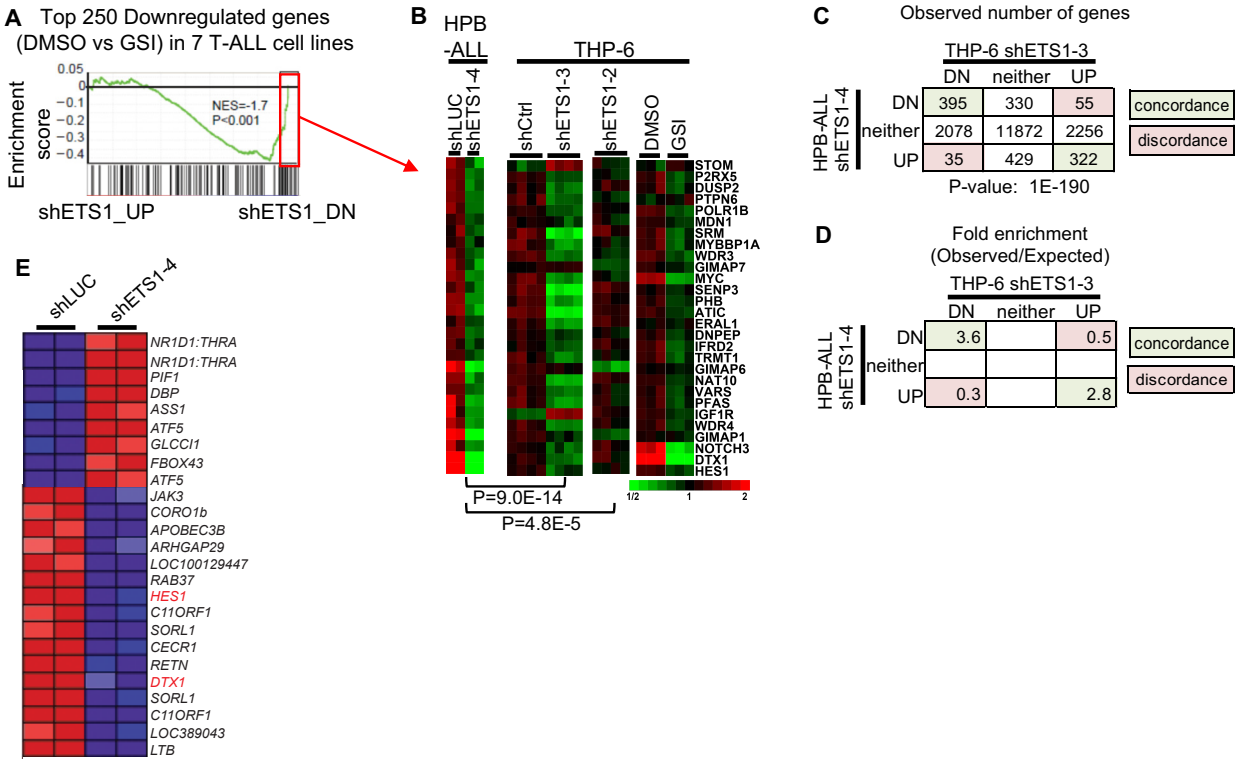

Figure 4.2 ETS1-NOTCH1 shared target genes are conserved between THP-6 and HPB-ALL cell lines

A-B) GSEA using list of shared NOTCH1 target genes in T-ALL (Palomero et al. 2006a) for the shLUC vs shETS1-4 comparison in HPB-ALL cells (A); and heatmaps of the top 28 down-regulated genes (red box in A) in HPB-ALL cells merged with the corresponding genes for the shControl vs shETS1-3/2 comparison and the DMSO vs GSI comparison in THP-6 cells (B). P-values represent Mantel-Haenszel Chi-Square tests of association of the indicated comparisons between HPB-ALL cells and THP-6 cells. C-D) Corner gene analysis with 3 by 3 tables that showed observed (C) and fold enrichment (D) of differentially increased expression ("UP"; P<0.01; FC>1.2) or differentially decreased expression ("DN"; P<0.01; FC<0.83), or no change ("neither") upon shETS1 transduction in THP-6 cells and HPB-ALL cells. Concordance (i.e. shETS1 regulates genes in the same direction in the two cell lines) is indicated in green. Discordance (i.e. shETS1 regulates genes in opposing directions in the two cell lines) is indicated in red. P-value=Mantel-Haenszel Chi-square test for association. E) Heatmap showing microarray data for the top 25 ETS1 target genes in HPB-ALL cells with the lowest P-values for the shLUC vs shETS1-4 comparison. Colors represent Log2FC from the mean. NOTCH1 target genes *HES1* and *DTX1* are highlighted in red. (A, B, E have contributions from G. Della Gatta, Ferrando lab).

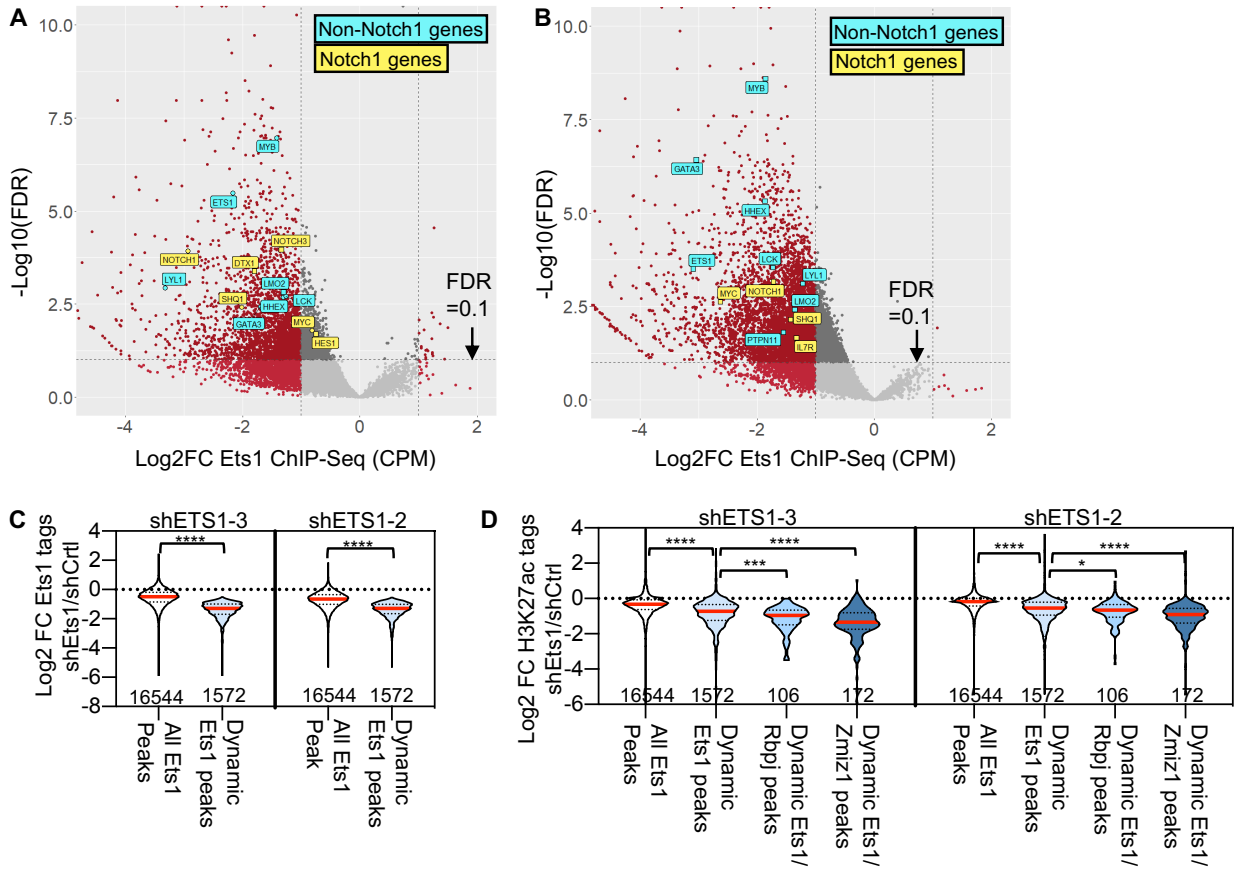

E

De Novo Motif analysis of 801 dynamic Ets1 peaks with FDR<0.1 for H3K27ac tags comparing shCtrl vs shETS1			
Rank	De Novo Motif	P-value	%sites
1	ETS	1E-446	60%
2	GATA	1E-67	28%
3	RUNX	1E-48	39%
4	HMG	1E-27	53%
5	Zf	1E-15	12%

Known Motif analysis (N=801) (FDR<0.1)[1]		Known Motif analysis (N=771) (FDR>0.1)[2]	
P-value	%sites	P-value	%sites
1E-418	77%	1E-348	73%
1E-66	26%	1E-24	16%
1E-58	30%	1E-54	29%
1E-13	28%	1E-03	20%
1E-04	5%	-	-

Figure 4.3 ETS1 activates the enhancers of a subset of Notch target genes

A-B) Volcano plot of ETS1 ChIP-Seq Log2FC in THP-6 cells showing the shControl vs shETS1-3 (A) or shETS1-2 (B) comparison and target genes in Fig. 4.1 that are located within the same TAD (GSM3967126, (Kloetgen et al. 2019)) as the ETS1 peaks. C) Violin plots showing the ETS1 ChIP-Seq Log2FC in THP-6 cells of all ETS1 peaks and dynamic ETS1 peaks. #peaks of each type are indicated. Dynamic ETS1 peaks=union intervals with Log2FC<0 and FDR<0.1 for both shControl vs shETS1-3/2 comparisons. Red line=median. D) Violin plots showing the H3K27ac ChIP-Seq Log2FC at all ETS1 peaks, dynamic ETS1 peaks, and ETS1 peaks that co-bind RBPJ peaks or ZMIZ1 peaks that decrease (FDR<0.1) with both shETS1 (3/2). L) HOMER de novo motif analysis of 801 dynamic ETS1 peaks with overlapping H3K27ac read counts that decrease (FDR<0.1) with two independent shETS1 (3/2). Dynamic ETS1 peak=FDR<0.1 for both shControl vs shETS1-3/2 comparisons. The top 5 motifs with the lowest P-values are shown. For these motifs, HOMER known motif analysis was also performed comparing dynamic ETS1 peaks associated with H3K27ac read counts that decrease (FDR<0.1[1] for both shETS1 comparisons) with dynamic ETS1 peaks associated with H3K27ac read counts that do not decrease (FDR>0.1[2] for at least one shETS1 comparison) using two independent shETS1 (3/2). ***P<0.001; ****P<0.0001.

Dynamic ETS1 binding increases H3K27ac at GATA-associated response elements

To define the genomic landscape of ETS1 direct target genes, we performed ETS1 ChIP-Seq in THP-6 cells following ETS1 knockdown. We defined "dynamic ETS1 peaks" as those with differential ChIP-Seq read count FDR<0.1 for two independent ETS1 shRNA knockdowns compared with controls. Using these parameters, we identified 3,697 dynamic ETS1 peaks (data not shown) in which ETS1 knockdown significantly reduced ETS1 occupancies compared to all ETS1 binding sites (Fig. 4.3C).

Only ~15% of ETS1 peaks met criteria as dynamic ETS1 peaks. Moreover, transcription factor motif analysis showed that 70% of dynamic ETS1 peaks contained the HOMER Ets1 motif compared with only 35% of non-dynamic ETS1 peaks, indicating that dynamic ETS1 peaks could signify a class of high confidence ETS1 binding sites. Next, we identified dynamic ETS1 peaks located within the same topologically associating domain (TAD) of 1,739 genes differentially expressed after ETS1 knockdown (DEGs, Q<0.05 for both shETS1) and designated these loci as "high confidence direct ETS1 target genes" (Fig. 4.3A-B, data not shown). Among these, 1,011 genes showed chromatin looping linking promoter regulatory sequences with a distal dynamic ETS1 peak based on H3K27ac Hi-ChIP (data not shown). Of these genes, 430 (43%) were also NOTCH1 target genes at Q<0.05.

To evaluate the functional role of ETS1 in enhancer regulation, we performed H3K27ac ChIP-Seq in THP-6 cells in basal conditions and following ETS1 knockdown. In these experiments, ETS1 deprivation reduced H3K27ac read counts at dynamic ETS1 peaks compared to all ETS1 peaks (Fig. 4.3E). Mean Log2FC differences were -0.479 and -0.412 for shETS1-3 and shETS1-2 compared with controls, respectively, in line with the known interaction of ETS1 with P300/CBP acetyl transferases (Hollenhorst et al. 2011). However, only ~51% of dynamic

ETS1 peaks were associated with differential H3K27ac read counts. To better understand the regulatory logic by which ETS1 facilitates activation of response elements, we performed de novo HOMER motif analysis of dynamic ETS1 peaks associated with differential H3K27ac read counts following ETS1 knockdown (Fig. 4.3E). These analyses recovered an Ets family motif as the top hit and a sequence closely matching GATA family motifs as the second most frequent element associated with dynamic ETS1 peaks linked to H3K27ac regulation compared to all other dynamic ETS1 peaks (26% vs 16%; P=1E-8). These findings support a cooperating role for ETS1 and GATA factors in enhancer regulation.

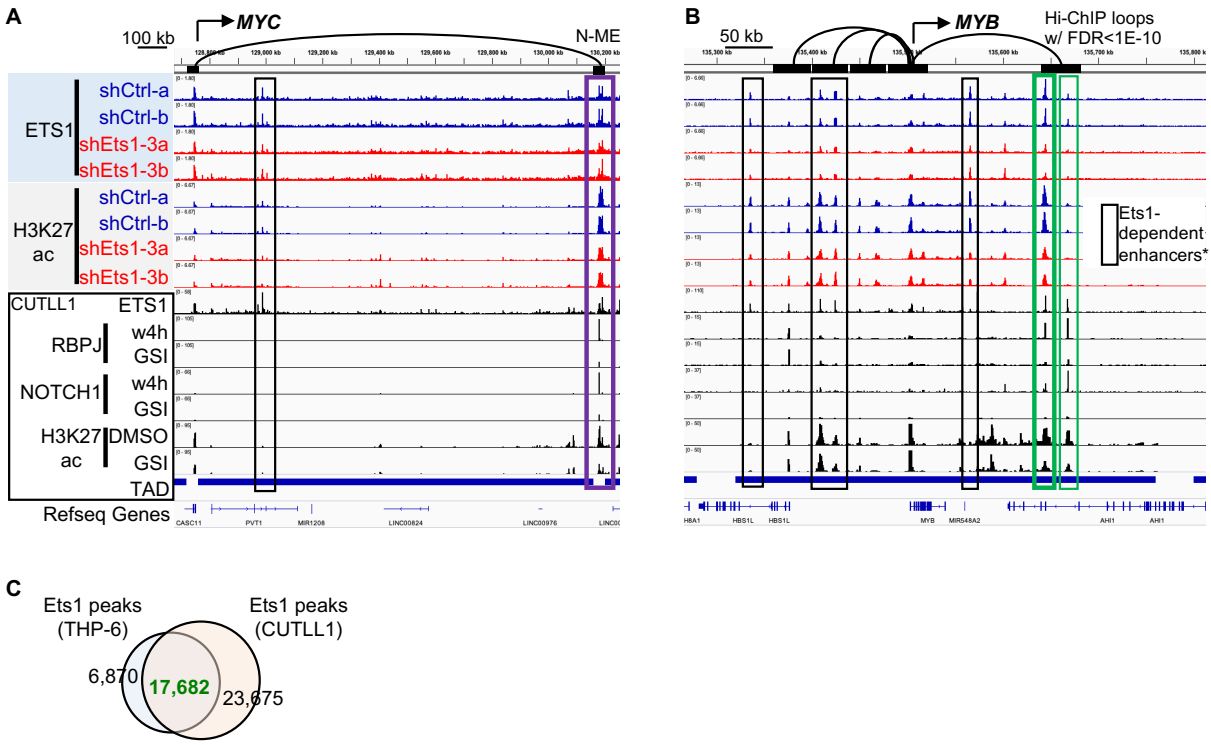

Figure 4.4 ETS1 regulates enhancers for the Myc and Myb oncogenes

A-B) ETS1 and H3K27ac ChIP-Seq tracks in THP-6 cells transduced with shETS1-3 at the TADs encompassing the *MYC* (A) and *MYB* (B) genomic loci. *ETS1-dependent enhancers=sites of dynamic ETS1 peaks where H3K27ac decreases with FDR<0.1. "a" and "b" are biological replicates. CUTLL1 ChIP-Seq (GSE51800) (Wang et al. 2014a), H3K27ac Hi-ChIP (GSM3967135) (Kloetgen et al. 2019), and Hi-C TAD (GSM3967126) (Kloetgen et al. 2019) datasets are shown. W4h=4 hours after GSI washout. C) Venn diagram showing overlap of ETS1 ChIP-Seq peaks in THP-6 and CUTLL1 cells (GSM1252929) (Wang et al. 2014a).

To better understand the impact of ETS1 control of oncogenic programs in T-ALL, we examined the effect of ETS1 deprivation on enhancers located in the same TADs containing *MYC* (Fig. 4.4A) and *MYB* (Fig. 4.4B), two major T-ALL oncogenes. H3K27ac Hi-ChIP data identified the N-ME (purple box, Fig. 4.4A) as the only enhancer associated with the *MYC* promoter in CUTLL1 cells at FDR<1E-10. In contrast, multiple enhancers were associated with the *MYB* promoter (Fig. 4.4B). Two *MYB* enhancers showed dynamic NOTCH1/RBPJ binding associated with differential H3K27ac signals (Fig. 4.4B). In this context, ETS1 deprivation reduced ETS1 and H3K27ac read counts at the NDME and multiple *MYB*-associated enhancers, including the Notch-bound *MYB* distal regulatory sites. Importantly, we observed convergent and largely overlapping ETS1 and H3K27ac peaks associated with *MYC* and *MYB* in THP-6 and CUTLL1 cells supporting a common regulatory logic across T-ALL tumors. Overall, 72% of ETS1 peaks identified in THP-6 cells were detected in CUTLL1 cells (Fig. 4.4C). These data suggest that dynamic ETS1 binding might promote oncogene expression by facilitating H3K27ac deposition at enhancers.

ETS1 interacts with NOTCH1 and co-occupies most ICN1/RBPJ binding sites

Given the strong genetic interaction between Notch signaling and Ets1, we hypothesized that ETS1 could physically bind the Notch transcriptional complex. Accordingly, co-immunoprecipitation experiments in THP-6 and HPB-ALL cells showed interactions between endogenous ETS1 and activated intracellular NOTCH1 proteins (Fig. 4.5A-B). In addition, we verified interactions between ETS1 and ZMIZ1, a context-dependent direct transcriptional cofactor of Notch1 (Pinnell et al. 2015b, Wang et al. 2018).

To define the genomic locations of ETS1-NOTCH1 and ETS1-ZMIZ1 complexes, we performed ICN1, RBPJ, and ZMIZ1 ChIP-Seq in control and shETS1-transduced THP-6 cells. These analyses identified 971 sites where ETS1, ZMIZ1, ICN1, and RBPJ peaks overlapped (Fig 4.5C). Remarkably, 94% of overlapping ICN1 and RBPJ peaks contained an overlapping ZMIZ1 peak. Moreover, 35% and 28% of ETS1 peaks were co-bound by RBPJ and ZMIZ1, respectively. In contrast, 77%, 73%, and 85% of ICN1 peaks were co-bound by ETS1, RBPJ, and ZMIZ1, respectively. Moreover, analysis of the 24,552 THP-6 ETS1 binding sites with ETS1, NOTCH1, RBPJ, and H3K27ac peaks in CUTLL1 and JURKAT cells revealed largely overlapping signals (Fig. 4.5D-E). These results support that ETS1 binds to and potentially coregulates a large fraction of NOTCH1 target genes consistent with our gene expression results and mouse genetic interaction analyses.

ETS1 facilitates recruitment of Notch complex members and H3K27ac deposition at response elements enriched for GATA factor binding motifs

Given the physical interaction between ETS1 and NOTCH1, we proposed that ETS1 could facilitate the recruitment of Notch complex members to chromatin. To test this possibility, we investigated if ETS1 deprivation could reduce RBPJ occupancy at sites where RBPJ peaks overlap with dynamic ETS1 peaks. Accordingly, ETS1 deprivation reduced read counts of RBPJ peaks that overlapped with dynamic ETS1 peaks compared to all RBPJ peaks (Fig. 4.6A). Mean RBPJ ChIP-Seq Log2FC differences were -0.517 and -0.436 by shETS1-3 and shETS1-2 compared with controls, respectively. Similarly, ETS1 deprivation reduced read counts of ICN1 and ZMIZ1 peaks that overlapped with dynamic ETS1 peaks compared to all ICN1 and ZMIZ1 peaks with mean Log2FC differences of -0.895 and -0.665 for ICN1 (Fig. 4.6B) and -0.921 and -0.780 for ZMIZ1 (Fig. 4.6C) by shETS1-3 and shETS1-2 compared with controls, respectively. Consistently,

metagene plots showed that ETS1 deprivation reduced average read counts of RBPJ and ICN1 peaks that overlapped with dynamic ETS1 peaks (Fig. 4.6E) compared to all RBPJ and ICN1 binding sites (Fig. 4.6D).

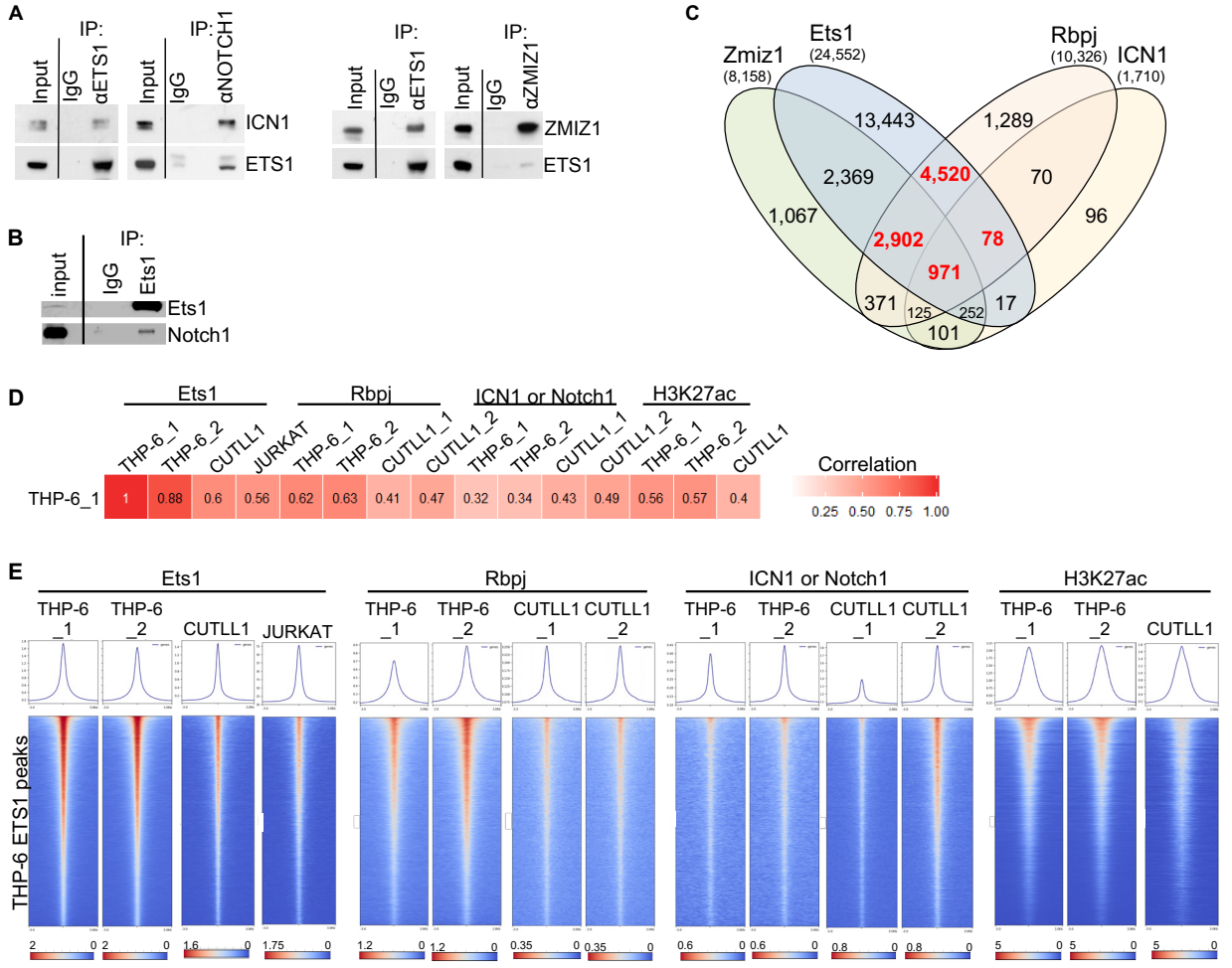

Figure 4.5 ETS1 co-binds the members of the Notch complex

A) Endogenous co-immunoprecipitation assays showing interactions between ETS1, cleaved NOTCH1 (ICN1), and ZMIZ1 in THP-6 cells. B) Endogenous coimmunoprecipitation assay showing interactions between ETS1 and NOTCH1 in nuclear extracts from HPB-ALL cells (performed by G. Della Gatta of Ferrando lab). C) Venn diagram showing overlaps between ETS1, RBPJ, ICN1, and ZMIZ1 ChIP-Seq peaks in control THP-6 cells. D-E) Spearman correlation coefficients (D) and metagene plots and heatmaps (E) of ChIP-Seq signal intensities of indicated datasets at the 24,552 ETS1 peaks in THP-6 cells ranked from the strongest ETS1_THP-6_1 signal (top) to weakest ETS1_THP-6_1 ETS1 signal (bottom). Heatmaps were not sorted separately from each other. Heatmaps were only normalized to each other if they were bioreplicates (i.e. "_1" and "_2"). JURKAT ETS1 ChIP-Seq -- GSM449525 (Hollenhorst et al. 2007). CUTLL1 ETS1, NOTCH1, and RBPJ ChIP-Seq -- GSE51800 (Wang et al. 2014a).

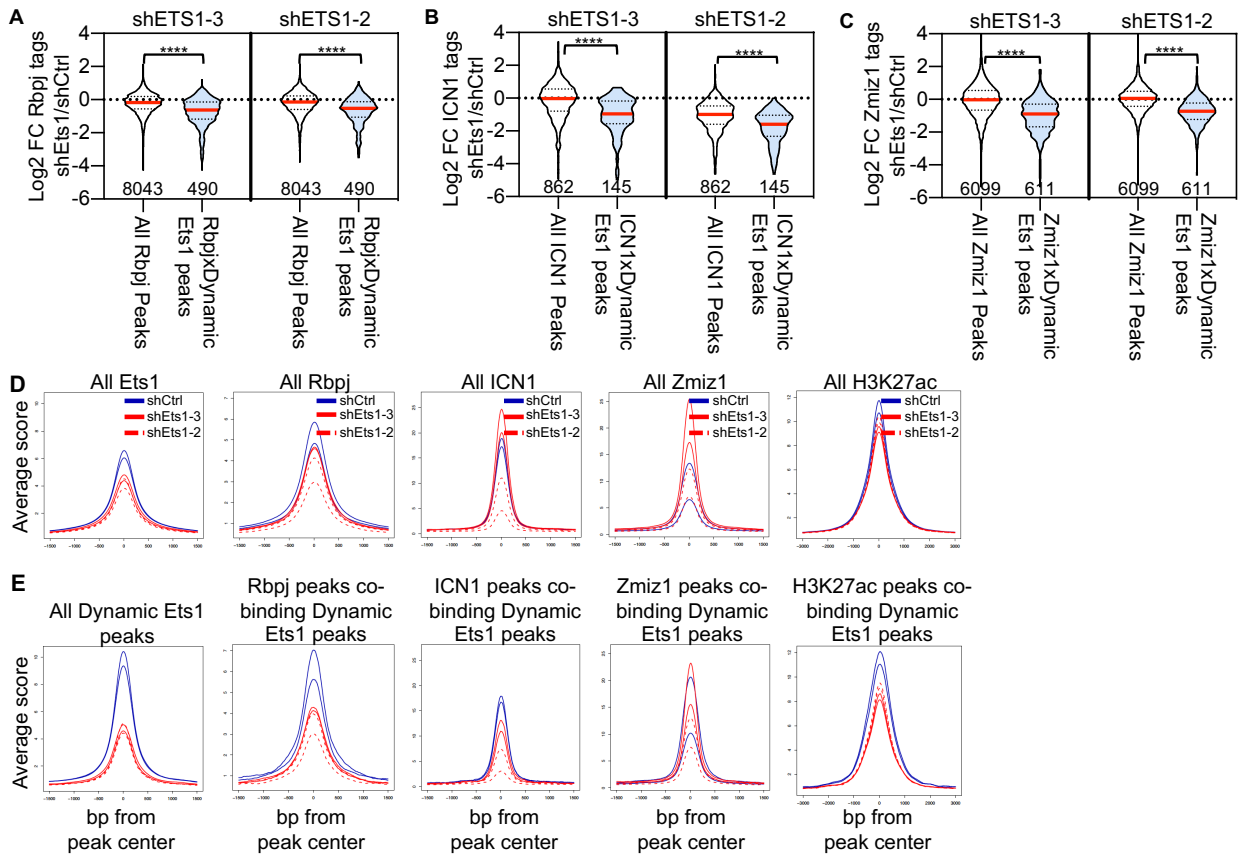

Figure 4.6 ETS1 recruits RBPJ, ICN1, and ZMIZ1 genome-wide

A) Violin plots showing the RBPJ ChIP-Seq Log2FC of all RBPJ peaks and RBPJ peaks that overlap with dynamic ETS1 peaks. B) Violin plots showing the ICN1 ChIP-Seq Log2FC for all ICN1 peaks and ICN1 peaks that overlap with dynamic ETS1 peaks. C) Violin plots showing the ZMIZ1 ChIP-Seq Log2FC of all ZMIZ1 peaks or ZMIZ1 peaks that overlap with dynamic ETS1 peaks. D-E) Metagene plots of averaged ETS1, RBPJ, ICN1, ZMIZ1, and H3K27ac ChIP-Seq binding intensities in THP-6 cells transduced with shControl (2 bioreplicate solid blue lines), shETS1-3 (2 bioreplicate solid red lines), or shETS1-2 (2 bioreplicate dotted red lines) of all peaks (D) or only those peaks that overlap with dynamic ETS1 peaks (E). Dynamic ETS1 peak=FDR<0.1 for both shControl vs shETS1-3/2 comparisons. Metagene plot windows were +/- 1.5kb (or +/- 3kb for H3K27ac). "All H3K27ac" represents averaged H3K27ac signals centered on all ETS1, RBPJ, ICN1, and ZMIZ1 peaks. ****P<0.0001.

To better understand the mechanisms by which ETS1 facilitates recruitment of RBPJ to chromatin, we first defined "dynamic RBPJ peaks" as sites with differential RBPJ read counts following ETS1 knockdown (FDR<0.1). Next, we performed motif analysis on dynamic ETS1 peaks that overlapped with dynamic RBPJ peaks. Similar to what we found for dynamic ETS1 peaks associated with differential H3K27ac signals (Fig. 4.3E), a GATA family motif was the top-ranked non-ETS motif present in these locations. Interestingly, this GATA family motif was more

closely associated with dynamic ETS1 peaks that overlapped with dynamic RBPJ peaks than dynamic ETS1 peaks that overlapped with non-dynamic RBPJ peaks (43% vs 17%; P=1E-3; Fig. 4.7A). Similarly, a GATA family motif was the top-ranked non-ETS motif for dynamic ETS1 peaks that overlapped with dynamic ICN1 peaks (90% vs 53%; P=1E-2; Fig. 4.7B) and for dynamic ETS1 peaks that overlapped with dynamic ZMIZ1 peaks (92% vs 16%; P=1E-10; Fig. 4.7C). Comparing our H3K27ac, Ets1, Rbpj, ICN1, and Zmiz1 ChIP-seq data with previously published GATA3 ChIP-seq in CEM and JURKAT human T-ALL cell lines, we observed enrichment of GATA3 binding at H3K27Ac, Rbpj, ICN1, and Zmiz1 peaks dynamically regulated by Ets1, compared with non-dynamic peaks (Fig. 4.7E-F). These data suggest that ETS1 facilitates the recruitment of RBPJ, ICN1, and ZMIZ1 to response elements in cooperation with GATA-site associated transcription factors.

Since the Notch complex is known to facilitate H3K27ac deposition, we wondered whether ETS1 deprivation would weaken H3K27ac signals at dynamic ETS1 sites where RBPJ binding was reduced. In support of this hypothesis, ETS1 knockdown significantly reduced H3K27ac read counts at dynamic ETS1 peaks that overlap with dynamic RBPJ peaks compared to all dynamic ETS1 sites (Fig. 4.3D). H3K27ac ChIP-Seq mean Log2FC differences were -0.292 and -0.152 for shETS1-3 and shETS1-2 compared with controls, respectively. Further, ETS1 knockdown also significantly reduced H3K27ac read counts at dynamic ETS1 peaks that overlap with dynamic ZMIZ1 peaks compared to all dynamic ETS1 peaks (Fig. 4.3D) with mean Log2FC differences of -0.529 and -0.400 for shETS1-3 and shETS1-2 respectively. Taken together, these data suggest that ETS1 might facilitate recruitment of RBPJ, ICN1, and ZMIZ1 to promote H3K27ac deposition at GATA-associated response elements.

A

De Novo Motif analysis of 65 Rbpj Peaks that co-bind dynamic Ets1 peaks and change with FDR<0.1 for shCtrl vs shETS1				Known Motif analysis (N=65) (FDR<0.1)[1]		Known Motif analysis (N=425) (FDR>0.1)[2]	
Rank	De Novo Motif	P-value	%sites	P-value	%sites	P-value	%sites
1	ETS	1E-31	40%	1E-21	40%	1E-48	20%
2	GATA	1E-22	52%	1E-17	43%	1E-25	17%
3	ETS-RUNX	1E-19	24%	1E-23	31%	1E-19	23%
4	bHLH	1E-11	38%	1E-05	35%	1E-05	17%
5	RBPJ	1E-10	54%	1E-02	29%	1E-02	20%

B

De Novo Motif analysis of 20 ICN1 Peaks that co-bind dynamic Ets1 peaks and give FDR<0.1 for shCtrl vs shETS1				Known Motif analysis (N=20) (FDR<0.1)[1]		Known Motif analysis (N=125) (FDR>0.1)[2]	
Rank	De Novo Motif	P-value	%sites	P-value	%sites	P-value	%sites
1	GATA	1E-15	39%	1E-11	90%	1E-25	53%
2	ETS	1E-15	50%	1E-11	75%	1E-50	68%
3	Forkhead	1E-13	20%	-	-	-	-
4	GATA	1E-12	60%	1E-06	50%	1E-33	43%
5	bHLH	1E-11	25%	-	-	-	-

C

De Novo Motif analysis of 138 Zmiz1 Peaks that co-bind dynamic Ets1 peaks and give FDR<0.1 for shCtrl vs shETS1				Known Motif analysis (N=138) (FDR<0.1)[1]		Known Motif analysis (N=295) (FDR>0.1)[2]	
Rank	De Novo Motif	P-value	%sites	P-value	%sites	P-value	%sites
1	GATA	1E-63	65%	1E-58	92%	1E-06	6%
2	ETS-RUNX	1E-61	28%	1E-52	44%	1E-99	29%
3	Homeobox	1E-28	7%	-	-	-	-
4	ETS	1E-24	41%	1E-22	52%	1E-56	38%
5	Zf	1E-23	8%	1E-10	31%	-	-

D

CEM

ChIP-Seq target	%GATA3 overlap: Dynamic peaks	%GATA3 overlap: Non-dynamic peaks
H3K27ac	11%	5%
RBPJ	28%	9%
ICN1	35%	34%
ZMIZ1	24%	8%

E

JURKAT

ChIP-Seq target	%GATA3 overlap: Dynamic peaks	%GATA3 overlap: Non-dynamic peaks
H3K27ac	24%	13%
RBPJ	46%	22%
ICN1	75%	59%
ZMIZ1	57%	22%

F

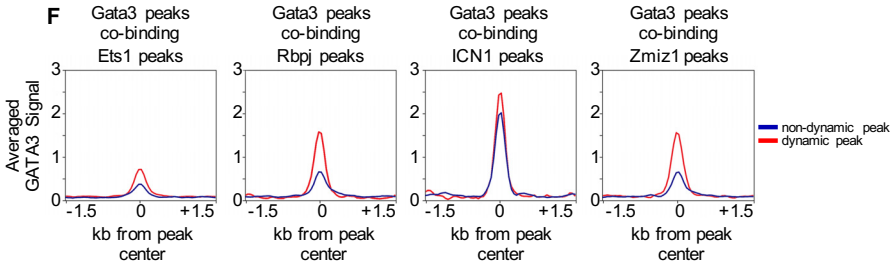

G

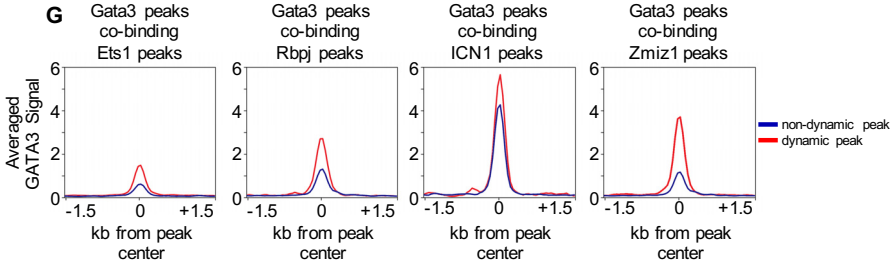

Figure 4.7 GATA3 binding is enriched at ETS1-regulated Notch complexes

A) HOMER de novo motif analysis of RBPJ peaks that co-bind dynamic ETS1 peaks and decrease upon ETS1 deprivation. The top 5 motifs with the lowest P-values are shown with subsequent known motif analysis comparing RBPJ peaks overlapping with dynamic ETS1 peaks that decrease with FDR<0.1[1] or do not decrease with FDR<0.1[2] for two shETS1 (3/2). B) HOMER de novo motif analysis of 20 ICN1 peaks that overlap with dynamic ETS1 peaks and that decrease (FDR<0.1) for both independent shETS1 (3/2). The top 5 motifs with the lowest P-values are shown with subsequent known motif analysis comparing ICN1 peaks overlapping with dynamic ETS1 peaks that decrease (FDR<0.1[1] for both shETS1 comparisons) or do not decrease (FDR>0.1[2] for at least one shETS1 comparison). C) HOMER de novo motif analysis of 138 ZMIZ1 peaks that overlap with dynamic ETS1

peaks and that decrease (FDR<0.1) for both independent shETS1 (3/2). The top 5 motifs with the lowest P-values are shown with subsequent known motif analysis comparing ZMIZ1 peaks overlapping with dynamic ETS1 peaks that decrease (FDR<0.1[1] for both shETS1 comparisons) or do not decrease (FDR>0.1[2] for at least one shETS1 comparison). D-E) Table percentage of overlap of GATA3 ChIP-Seq peaks in CEM (D) or JURKAT (E) cells with ETS1, RBPJ, ICN1, and ZMIZ1 ChIP-Seq peaks in THP-6 cells that are dynamically regulated by Ets1 (FDR<0.1 for shControl vs shETS1-3/2) vs non-dynamic (FDR>0.1 for shControl vs shETS1-3/2). F-G) Metagene plots of averaged GATA3 ChIP-Seq binding intensities in CEM (F) or JURKAT (G) cells for peaks that overlap with Ets1, Rbpj, ICN1, or Zmiz1 ChIP-seq in THP-6 cells that are dynamically regulated by Ets1 (blue lines, FDR<0.1 for shControl vs shETS1-3/2) vs non-dynamic (red lines, FDR>0.1 for shControl vs shETS1-3/2). Metagene plot windows were +/- 1.5kb. CEM GATA3 ChIP-seq -- GSM837986 (Sanda et al. 2012). JURKAT GATA3 ChIP-seq -- GSM722168 (Sanda et al. 2012).

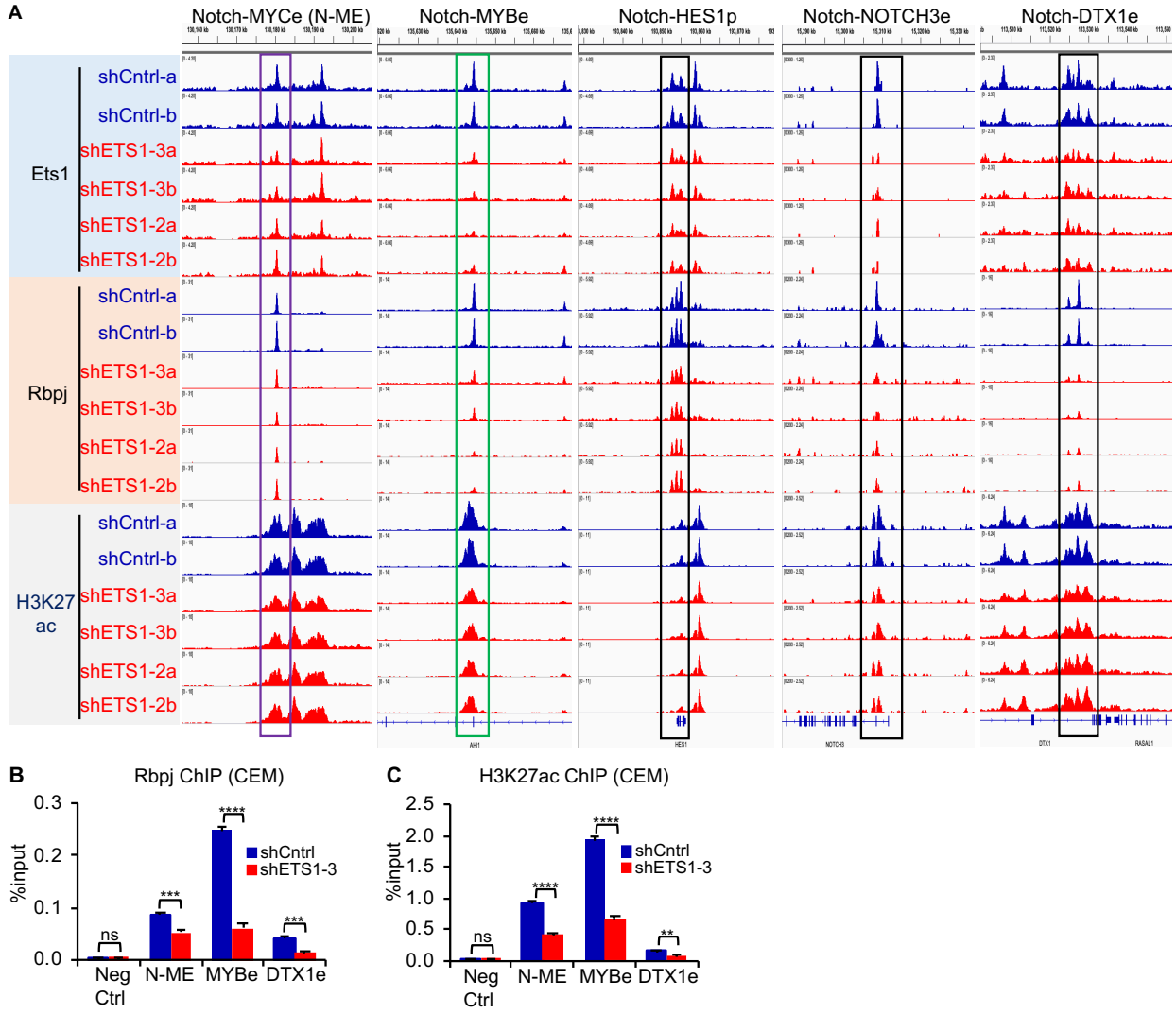

Figure 4.8 ETS1 regulates the enhancers of Notch target genes

A) ETS1, RBPJ, and H3K27ac ChIP-Seq tracks at the Notch-*MYC* enhancer (N-ME; also see purple box in Fig. 4.4A), Notch-*MYB* enhancer; also see thick green box in Fig. 4.4B), Notch-*HES1* promoter, Notch-*NOTCH3* enhancer, and the Notch-*DTX1* enhancer. RBPJ peaks within black and green boxes gave P<0.05 for both shETS1 comparisons. "a" and "b" are biological replicates. B-C) RBPJ (B) and H3K27ac (C) ChIP-qPCR in CEM cells transduced with shControl or shETS1-3 with negative control primers (located 2kb upstream of the N-ME) or at the N-ME, the Notch-*MYB* enhancer (MYBe), or the Notch-*DTX1* enhancer (DTX1e). ns=not significant; *P<0.05; **P<0.01; ***P<0.001; ****P<0.0001. (B-C performed by A. Melnick).

We next considered the possibility that ETS1 recruits Notch to response elements that regulate shared NOTCH1/ETS1 target genes (Fig. 4.1H-K). To test this possibility, we examined ETS1, RBPJ and H3K27ac ChIP-Seq tracks at Notch-bound response elements of *MYC* (N-ME), *MYB* (Notch-MYBe), *HES1* (Notch-HES1p), *NOTCH3* (Notch-NOTCH3e), and *DTX1* (Notch-DTX1e) (Fig. 4.8A). ETS1 knockdown in THP-6 cells reduced RBPJ and H3K27ac read counts at the Notch-MYBe, Notch-HES1p, Notch-NOTCH3e, and Notch-DTX1e enhancers, but not N-ME. In contrast, ETS1 knockdown significantly reduced RBPJ signals at the N-ME in CEM cells (Fig. 4.8B-C). Thus, ETS1 facilitates recruitment of RBPJ to known Notch-regulated response elements.

Discussion

The greatest challenge in the development of targeted therapies against Notch signaling in cancer is the toxicity of pan-Notch inhibitors. Continuous dosing with gamma secretase inhibitors results in intolerable intestinal harm, leading to reduced efficacy of these drugs. Alternative methods for modulating notch signaling, including blocking antibodies for the Notch receptor and the SAHM1 stapled peptide which prevents the formation of the Notch-RBPJ-MAML complex in the nucleus, are still expected to recapitulate the limitations of pan-Notch inhibition (Moellering et al. 2009, Tran et al. 2013). A safer strategy to inhibiting Notch signaling in cancer lies in targeting cofactors essential for Notch's function in T-cell leukemia and development but dispensable for its function in gut homeostasis. We previously determined that the PIAS-like coactivator Zmiz1 is a direct cofactor of Notch1 that selectively promotes Notch1 activity at the T-cell specific Myc enhancer (Pinnell et al. 2015b). However, it was uncertain which other factors were also promoting context dependent Notch1 activity.

We found that ETS1 coregulates a subset of NOTCH1 target genes, including the *MYC* and *MYB* oncogenes. Many of these target genes were conserved across multiple human T-ALL cell lines, suggesting that ETS1 may function similarly in a wide array of oncogenomic subtypes of T-ALL. This finding is consistent with our work in Chapter 3, in which most of the T-ALL cell lines responded to ETS1 silencing. The fact that Notch-independent ETS1 targets include characterized T-ALL oncogenes like *LMO2* and *LYL1* increases the likelihood that targeting ETS1 will have antileukemic effects independently of Notch mutations. However, further studies in a broader set of oncogenomic subtypes of T-ALL would be needed to explore this possibility.

ETS1 deprivation also reduced Notch complex formation and H3K27 acetylation at critical enhancers for T-cell development and T-ALL genes. These studies demonstrate that ETS1 recruits the Notch complex to a subset of Notch-driven enhancers and subsequent transcription of these target genes. We don't know what factors distinguish between Notch-driven enhancers that are co-regulated by ETS1 and those that are not. Our motif analyses and comparisons to others' GATA3 ChIP-seq suggest that GATA3 might function in ETS1-regulated Notch complexes. GATA factors have been shown to recruit chromatin remodelers, and our collaborators in the Ferrando lab recently demonstrated that GATA3 binding at the Notch-dependent *MYC* enhancer is necessary for nucleosome invasion and chromosome accessibility at this enhancer (Takaku et al. 2016, Belver et al. 2019). Future studies examining the purpose of GATA proteins in ETS1-dependent Notch complexes may provide greater insight into the composition of these complexes and yield new therapeutic targets. More on our proposed model on GATA function in the ETS1-dependent Notch complex and experiments to test this model will be discussed in Chapter 6.

Our findings delineate a novel role for ETS1 in the pathogenesis of Notch-driven T-ALLs. ETS1 cooperates with NOTCH to regulate a subset of key oncogenes in T-ALL, and the disruption of this collaboration has significant impact on enhancer activation, gene expression, and leukemia cell proliferation. The removal of the Notch complex from the chromatin of a select set of Notch-driven enhancers with ETS1 withdrawal presents a new method of modulating Notch signaling in cancer. This discovery suggests that targeting Notch cofactors, rather than Notch itself, might be a therapeutic approach with greater efficacy and less toxicity that pan-Notch inhibition.

Chapter 5 ETS1-Targeted Strategies for Antileukemic Therapies[5]

Abstract

Targeting transcription factors has long proved to be a challenge in developing cancer therapies. New advancements in strategy, namely enhanced degradation and protein-protein interaction inhibitors, have made it possible to degrade or prevent the activity of transcription factors in cancer. There are several clinical trials currently underway using such methods. While no targeted therapy has been developed yet for ETS1, we can expand our understanding of the regulation of ETS1 transcription, post-translational modification, and binding partners to inform future drug development efforts. To demonstrate the efficacy of combinatory ETS1-NOTCH1 inhibition in leukemia, we coupled *Ets1* deletion with low-dose pan-Notch inhibition in a murine model of Notch-driven leukemia maintenance to reduced blast counts and extend survival far beyond either intervention alone. We also demonstrated that enhancing Ets1 degradation by pharmacological inhibition of ETS1-deubiquitinase USP9X prevents the growth of leukemia cells. Finally, we identified that the N-terminal domains of ETS1 are important for the interaction of Ets1 with members of the Notch complex. These studies provide evidence that ETS1 is a valuable and feasible target for antileukemia therapy development.

[5] Adapted from McCarter, A. C., G. D. Gatta, A. Melnick, et al. (2020) Combinatorial ETS1-Dependent Control of Oncogenic NOTCH1 Enhancers in T-cell Leukemia. *Blood Cancer Discovery*.

Introduction: Targeting ETS1 in cancer

In order to devise potential therapeutics targeting ETS1, is imperative to understand the mechanisms of ETS1 regulation. Most of the work exploring the regulation of ETS1 has been conducted in the context of solid tumors; however, these findings might still yield valuable insights applicable to T-ALL.

Regulators of ETS1 Transcription

The human ETS1 promoter contains binding sites for ETS1, AP-1, AP-2, SP1, and OCT (Jorcyk et al. 1991). Thus, ETS1 can enhance its own transcription (Seth and Papas 1990), and binds in conjunction with AP-1 to amplify its expression and that of other ETS factors (Plotnik et al. 2014, Majérus et al. 1992). Such ETS/AP-1 composite binding sites are found at promoters genome-wide, and can mediate responsiveness of promoters to the Ras/Raf/MEK/ERK1/2 pathways (Plotnik et al. 2014). The ability of ETS1 to drive its own transcription is the mechanism by which many signaling pathways increase ETS1 expression. Signaling cascades, which lead to Ets1 post-translational modification, stabilize and activate the ETS1 protein, allowing for greater transcription of additional *ETS1* mRNA. In this way, *ETS1* transcription is responsive to growth factor signaling. *ETS1* mRNA is upregulated by this pathway in downstream of hepatocyte growth factor (Ozaki et al. 2002), basic fibroblast growth factor(Hahne et al. 2011), and vascular endothelial growth factor signaling (Watanabe et al. 2004). Similarly, *ETS1* transcription is also increased by endothelial growth factor induction of the PI3K/AKT pathway in endothelial and lung cancer cells (Lavenburg et al. 2003, Phuchareon et al. 2015). Like ERK1/2, AKT activity has proven necessary to maintain ETS1 activity in lung cancer models (Phuchareon et al. 2015).

The *ETS1* promoter contains a hypoxia-responsive element and antioxidant-responsive element, and accordingly, *ETS1* mRNA is induced by HIF-1 and reactive oxygen species respectively (Wilson et al. 2005, Oikawa et al. 2001). The tumor microenvironment is often hypoxic, which could drive the increased levels of ETS1 observed in carcinomas. Given the role of hypoxia in promoting the formation of cancer stem cells [reviewed in (Saito et al. 2015)], it is possible that ETS1 activity is part of the hypoxia-response that contributes to the stemness of cancer cells. Transforming growth factor β (TGFβ), a cytokine associated with cancer initiation and progression, also regulates *ETS1* expression in a multitude of cell types, though this is likely indirect through upregulation of the Smad family of transcription factors, Ras/Raf/MEK/ERK1/2, AP-1, or p38 [reviewed in (Leivonen and Kähäri 2007)].

Post-transcriptional Regulation of ETS1

The eight exons of the ETS1 gene encode a 54 kDa protein (sometimes referred to as p51). The full length ETS1 protein is comprised of 441 amino acids. In addition to the ETS1 DNA-binding domain signature to the ETS family (amino acids 331-415), ETS1 contains a pointed domain (amino acids 54-134), a transactivation domain (amino acids 135-242), and a set of autoinhibitory domains (amino acids 301-330 and amino acids 416-441). The autoinhibitory domains flank the ETS domain, preventing binding to the DNA. This autoinhibition of the ETS1 protein allows for its activity to be finely tuned by post-translational modifications and protein-protein interactions.

There is a second isoform of ETS1, which lacks exon VII, called p42. As exon VII encodes part of the autoinhibitory domain, the p42 isoform more readily binds to DNA. This isoform makes up about 10% of the ETS1 in lymphocytes, and the balance between the p54 and p42 isoforms is thought to be important for lymphocyte development (Higuchi et al. 2007). A

third isoform of ETS1, the p27 isoform, is expressed in human spleen, thymus, placenta, and ovaries. The p27 isoform lacks the pointed domain and transactivation domains, but maintains the autoinhibitory and ETS DNA binding domains; as such, it serves as a dominant-negative inhibitor of full-length ETS1 (Laitem et al. 2009).

ETS1 is often modified by phosphorylation, in which the addition of a phosphate functional group to an amino acid to alters ETS1 activity. As previously mentioned, the Ras/Raf/MEK/ERK1/2 pathway regulates Ets1 at the post-translational level; this pathway results in the phosphorylation of ETS1 at threonine-38, leading to enhanced transactivation activity (Yang et al. 1996). ERK2 has been extensively studied to clarify the mechanism by which ERK1/2 mediate ETS1 phosphorylation (Callaway et al. 2010); ERK2 binds to two docking sites in flexible N-terminal (amino acids 1-52) and pointed domains, and phosphorylates threonine 38, which in turn recruits CBP (cAMP-responsive element binding protein-CREB-binding protein) or p300 (Foulds et al. 2004, Yang et al. 1998). CMB and p300 are co-activators that acetylate histones and recruit additional transcription machinery. Thus, phosphorylation of the N-terminus of ETS1 by the Ras/Raf/MEK/ERK1/2 “superactivates” ETS1 and enhances transcription of its target genes.

A study in developing thymocytes suggests that ETS1 might by phosphorylated at serines 251, 257, 282, and 285 due to an increase in intracellular calcium (Pognonec et al. 1988). This phosphorylation, which may be catalyzed by calmodulin-dependent protein kinase II, located in exon VII adjacent to the autoinhibitory domain, promotes ETS1 autoinhibition, reduces DNA binding, and decreases ETS1 transcriptional activation (Rabault and Ghysdael 1994). Additionally, phosphorylation of serines 276 and 282 have been show to increase the recruitment of COP1, an E3 ubiquitin ligase, which ultimately induces ETS1 protein ubiquitination and

degradation (Lu et al. 2014). Interestingly, phosphorylation of the adjacent tyrosine 283 prevents this COP1 recruitment, belying the complexity of ETS1 regulation via phosphorylation (Lu et al. 2014). Finally, DNA-PK (DNA-dependent protein kinase) phosphorylates ETS1 and diminishes its activity in vitro (Choul-li, Drobecq and Aumercier 2009).

Another means of post-translationally influencing ETS1 activity is through the addition of acetyl and ADP-ribose units to lysines in ETS1. TGFβ promotes the acetylation of ETS1 by activating AKT, which in turn phosphorylated histone acetyltransferase p300 (Kato et al. 2013). In some contexts, it appears that acetylation of ETS1 removes it from the promoter miR-192 (a microRNA involved in diabetic nephropathy), allowing for TGFβ effector Smad3 to drive expression of miR-192 (Kato et al. 2013). It is unclear whether other signaling pathways alter ETS1 activity via acetylation.

The C-terminus of ETS1 can also be PARylated by poly(ADP-ribose) polymerase-1 (PARP1) in breast cancer cell lines, leading to reduced *ETS1* levels and transcription of target genes (Legrand et al. 2013). Inhibition of the catalytic activity of PARP1 enhances ETS1 transcriptional activity and causes accumulation of ETS1 protein in the cell nuclei, resulting in increased DNA damage and cell death (Legrand et al. 2013). Given these effects, PARP-inhibitors have been proposed as a method to treating cancers driven by ETS-fusion genes [Reviewed in (Feng et al. 2014)].

Ubiquitination and SUMOylation are post-translation modifications in which ubiquitin and SUMO functional groups are added to alter protein stability and activity. Ubc9 SUMOylates ETS1 at lysine 15, which increases ETS1 transcriptional activity by providing an alternative protein-protein interaction site (Macauley et al. 2006). Ubc9 also SUMOylates ETS1 at lysine 227, which has no impact on ETS1 protein stability, but does decrease its activity (Ji et al. 2007).

Ets1 can also be SUMOylated by PIASγ, which increases the stability, yet reduces the DNA-binding affinity, of polyubiquitinylated Ets1 protein. It is believed that this prevents proteasomal degradation of Ets1, thus also preventing the exchange of polyubiquitinylated Ets1 for non-ubiquitinylated Ets1 (Nishida, Terashima and Fukami 2006). In prostate cancer and melanoma cell lines, ETS1 is ubiquitinated at lysine 388, within the ETS domain, which promotes the proteasomal degradation of the protein (Wang et al. 2014b, Potu et al. 2017). ETS1 is deubiquitinated by ubiquitin specific peptidase 9, x-linked (USP9X), the overexpression of which has been linked to tumor cell signaling and survival (Potu et al. 2017, Schwickart et al. 2010). ETS1 deubiquitination blocks its proteasomal degradation, increasing cellular levels and tumorigenicity in melanoma (Potu et al. 2017). Pharmacologic inhibition of deubiquitination is a possible route for enhancing Ets1 degradation in cancer. Whether USP9X is the deubiquitinase of ETS1 in T-ALL had not yet been explored; this data will be discussed in the results section of this chapter.

Protein-Protein interactions that modulate ETS1 activity

The autoinhibitory domains that flank the ETS DNA binding domain prevent the association of ETS1 with DNA. However, association with other transcription factors and co-activators are able to alleviate this autoinhibition, allowing for context dependent ETS1 transcriptional activation. Established interacting partners to ETS1 are summarized in Figure 5.1.

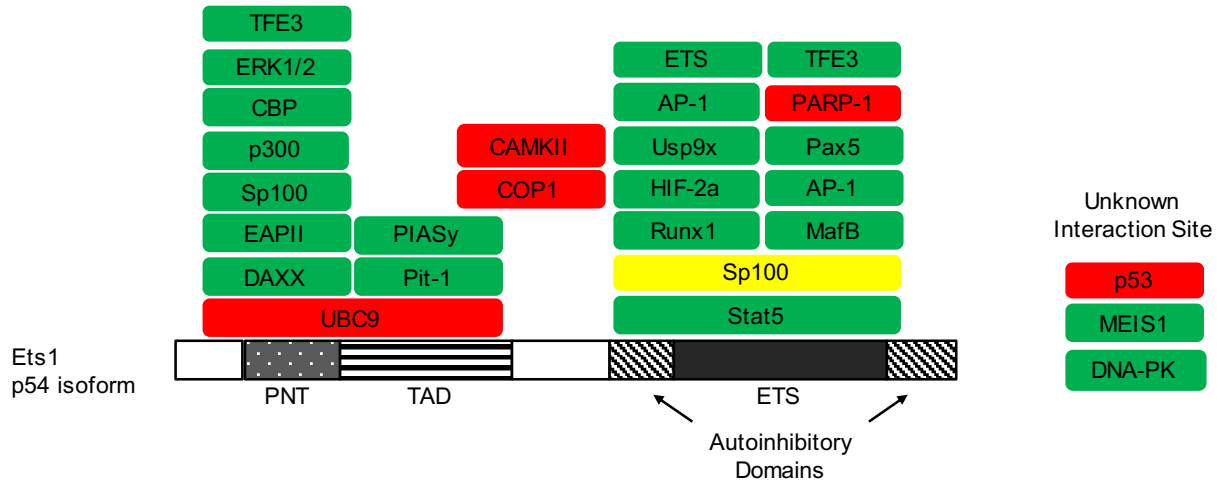

Figure 5.1 Protein-protein interactions that influence ETS1 activity

Domain map of the Ets1 p54 isoform, showing the protein-protein interactions that modulate Ets1's transcriptional activity. Interactions that increase Ets1's activity are shown in green, interactions that decrease Ets1's activity are shown in red, and interactions for which the evidence is mixed are in yellow.

The best characterized binding partner to ETS1 is RUNX1 (runt related transcription factor 1). By mutually blocking their autoinhibitory domains, RUNX1 and ETS1 cooperatively bind to composite RUNX1/ETS1 sites and induce transcription (Shrivastava et al. 2014). In particular, T-cell specific genes harbor RUNX1/ETS1 binding elements and show co-occupation of these sites by ETS1, RUNX1 and the co-activator CBP in vivo (Shiina et al. 2014). Interaction with RUNX1 allows ETS1 to bind to the TCRA promoter, even if ETS1 has been deactivated through CAMKII-mediated phosphorylation (Shrivastava et al. 2014, Shiina et al. 2015). AP-1, previously discussed as a driver of *ETS1* transcription in through interaction with ETS1 itself, also alleviates ETS1 autoinhibition at other ETS11/AP-1 binding sites genome-wide in developing T-cells (Bassuk and Leiden 1995).

HIF2α is another transcription factor that binds to ETS1 adjacent to the autoinhibitory domain to counteract autoinhibition (Le Bras et al. 2007). It cooperates with ETS1 to regulate VEGF receptor 2 in endothelial cells (Le Bras et al. 2007). Unlike HIF2α, the related protein

HIF1α shows only weak binding to ETS1. The transcription factor PAX5 (paired box binding factor 5) overrides Ets1 autoinhibition by binding to its DNA binding domain and altering the interaction of tyrosine 395 with the ETS domain. However, unlike RUNX1, association with PAX5 is unable to alleviate Ets1 deactivation via CAMKII-mediated phosphorylation (Shrivastava et al. 2014). STAT5 (signal transducer and activators of transcription 5), which is often activated in T-cell leukemias, lymphomas, and breast cancers, also interacts with Ets1 by binding to the Ets1 protein between amino acids 238 and 441. In mature T-cells, IL2 signaling is shown to generate a STAT5/ETS1/ETS2 complex, which in turn activates a proliferative cellular program (Rameil et al. 2000). PIT-1 (POU domain transcription factor) binds to the transactivating domain of ETS1, and together they regulate the prolactin promoter (Augustijn et al. 2002). Finally, TFE3, a member of the basic helix-loop-helix protein family, through interactions with both the N- and C-terminal portions of ETS1, enhances ETS1 binding at the immunoglobulin mu heavy-chain enhancer (Tian et al. 1999).

Tumor suppressor p53 inhibits ETS1-dependent transcription at *MDR1* and *TXSA* genes (Sampath et al. 2001, Kim et al. 2003). Additionally, AP-1-like protein MAFB also represses ETS1 activity by binding the ETS domain of ETS1 directly (Sieweke et al. 1996). Proteins that localize to the pro-myelocytic leukemia (PML) nuclear bodies, SP100 (Wasylyk et al. 2002, Yordy et al. 2004), DAXX/EAP1 (Pei et al. 2003, Li et al. 2000), and TDP2/TRAPP (Vilotti et al. 2012) also interact with ETS1. These associations are thought to be anti-oncogenic, repressing ETS1-dependent transcription at the *MMP1* and *uPA* promoters and inhibiting invasion of breast cancer cells (Yordy et al. 2004). However, SP100 has also been reported to activate ETS1 function at the stromolysin promoter, suggesting that there might be context-dependency to the nuclear-body with ETS1 interaction story (Wasylyk et al. 2002).

Current methods for targeting transcription factors in cancer treatment

Despite the lack of a "druggable" active site on most transcription factors, there are several strategies that have been successfully demonstrated in other transcription factors which could potentially be utilized for ETS1. The first option is to modulate the expression of the transcription factor. An excellent example of this is the use of BRD4 inhibitors to prevent the transcription of the *MYC* oncogene. JQ1, a small molecule inhibitor of the BET family of chromatin adaptors, uncouples BRD4 from the chromatin and prevents the transcription of *MYC*, with efficacy in some cancer types (Fowler et al. 2014, Mertz et al. 2011).

Another avenue for targeting transcription factors is to enhance their degradation. By depleting the quantity of the transcription factor in the cell, activation of its target genes can also be prevented. Recently developed compounds capable of achieving this are PROTACs (for PROteolysis TArgeting Chimeric molecules), which degrades target proteins via ubiquitination. Examples of PROTACs include Cmp 8 that associates the SMAD3 with the HIF1 recognition motif of the VHL E3 ubiquitin ligase (Wang et al. 2016) or CM11 Homo-PROTAC dimer that induces VHL E3 ubiquitin ligase dimerization and sub-sequent self-degradation (Maniaci et al. 2017). Recently, a PROTAC that targets the androgen receptor proceeded to phase I/II clinical trials (Mullard 2019).

A third option is to interrupt a protein-protein interaction critical for the function of the transcription factor. This is typically achieved by slipping a small molecular into the interface between the two proteins. A relevant example to Ets1 is the series of small molecule inhibitors to the association of RUNX1 and its co-factor CBF in AML cells (Gorczynski et al. 2007, Cunningham et al. 2012, Illendula et al. 2015). A drug that is currently in clinical trials is a small

molecule inhibitor of the MLL-menin interaction in acute leukemias (Borkin et al. 2015, Grembecka et al. 2012).

Finally, it is possible to target the DNA binding domain of a transcription factor, preventing its interaction with its binding motif at target genes. This strategy has been employed in targeting other members of the ETS family with some success. DB1255, a small molecule, inhibits the interaction of ETS transcription factor family member ERG with DNA (Nhili et al. 2013). A similar effect is achieved with a peptidomimetic compound that also targets the ERG-DNA binding interface (Wang et al. 2017a). Another recent publication announced the generation of a small molecule that prevents the association of ETS family member PU.1 from interacting with the promoters of its target genes in AML cells (Antony-Debré et al. 2017). While there is not yet a small molecule or peptide that specifically targets the ETS1 ETS domain, these ERG and PU.1 inhibitors provide proofs-of-principle that such a strategy might be viable in targeting ETS1.

Results

ETS1 deprivation sensitizes leukemic cells to Notch inhibition.

One strategy to circumvent the toxicity of full strength GSI is to combine partial strength GSI with other agents to inhibit downstream effectors (Sanchez-Martin et al. 2017). This combination strategy might also help overcome resistance to GSI, which occurs in roughly two-thirds of T-ALL cell lines (Weng et al. 2004).The MYC and mTOR pathways are major pathways downstream of Notch, but also confer resistance to GSI (Herranz et al. 2015, Weng et al. 2006). Since our data shows that ETS1 promotes MYC and mTOR (Fig. 4.1D, F, G), we

wondered whether suppressing ETS1 signals might confer sensitivity to low doses of GSI. To test this possibility, we transduced human T-ALL cell lines with shETS1-3/2 and cultured them in the presence of low doses of GSI (0.2 μM). *ETS1* deprivation sensitized three GSI-resistant T-ALL cell lines to GSI-induced growth inhibition (Fig. 3.7G-I). Further, ETS1 deprivation increased the anti-proliferative effects of low dose GSI on three GSI-sensitive T-ALL cell lines (Fig. 3.7D-F). In light of these effects, we wondered if combined ETS1 and NOTCH1 deprivation would cooperatively suppress Notch target gene expression. The combination cooperatively reduced *MYC* expression in THP-6 cells (Fig. 5.3A). Moreover, *Ets1* deletion and Notch inhibition with a GSI in Notch-induced *Rosa26CreER*^{T2} *Ets1*$^{f/f}$ murine T-ALL cells cooperatively downregulated *Myb* and *Dtx1* expression (Fig. 5.3B-D).

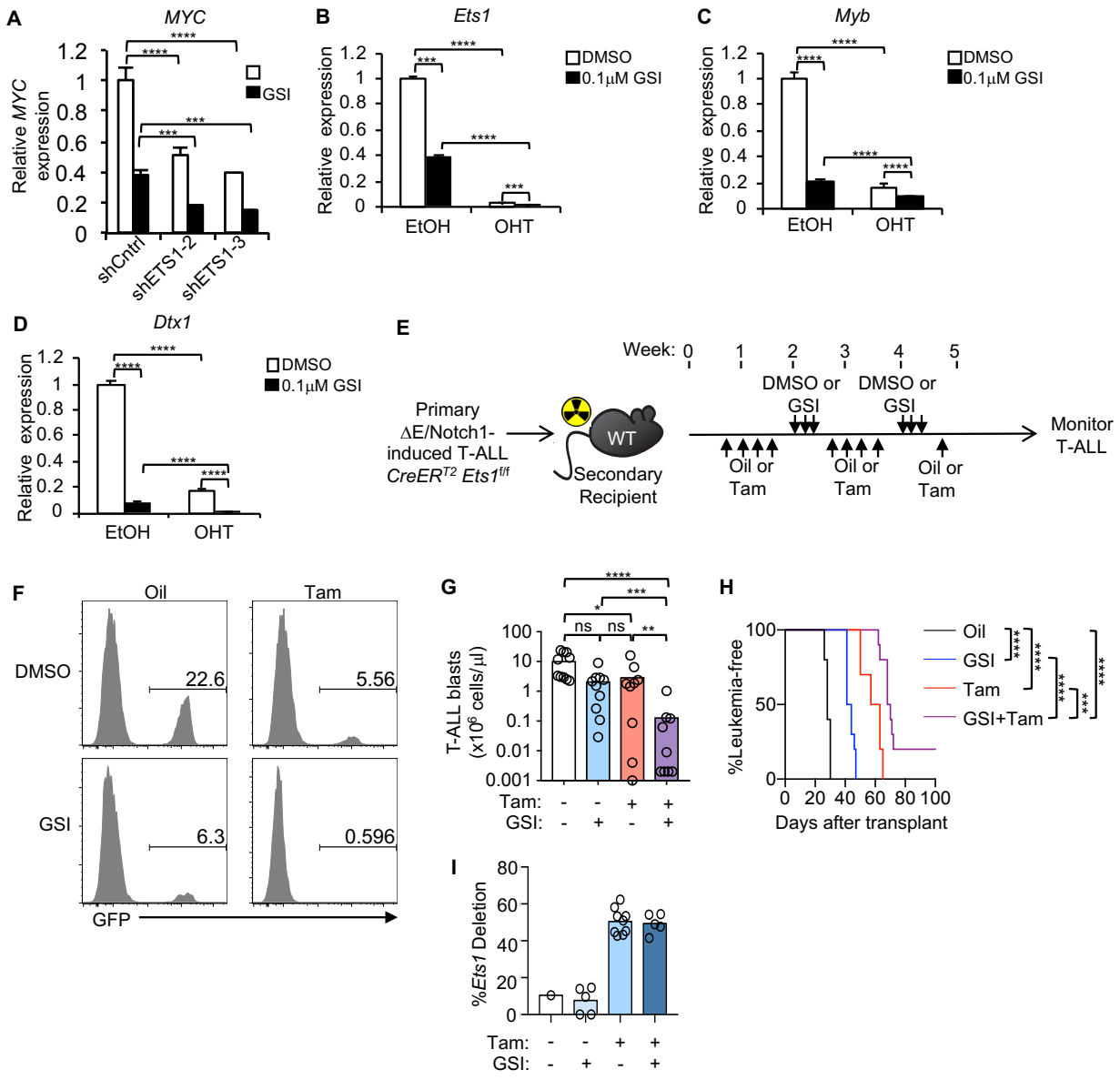

Figure 5.2 Ets1 deprivation sensitizes Notch-activated T-ALLs to the pan-Notch inhibitor GSI

A) Relative *MYC* expression in THP-6 cells transduced with shETS1 for four days and treated with GSI (DBZ, 1μM) one day prior to harvest. B-E) Expression of *Ets1* (B), *Myb* (C), and *Dtx1* (D) in murine *Rosa26CreER^{T2} Ets1$^{f/f}$* cells (#643) treated with 12nM OHT to induce *Ets1* deletion for 42 hours +/- low dose GSI for 18 hours (DBZ, 0.1μM). E-H) Experimental strategy to study effects of combinatorial effects of Ets1/Notch deprivation on in vivo maintenance of murine ΔE/Notch1-induced T-ALL (#182) (E). Tam=25mg/kg tamoxifen. GSI=10μmol/kg DBZ. Representative flow cytometric plots (F) and peripheral blood GFP$^+$ T-ALL cell counts (G) at 26 days post-transplant; survival curves (H); *Ets1* deletion efficiency in splenic tumor DNA harvested from terminally diseased mice after treatment with tamoxifen (Tam) or GSI (I). ns=not significant, *P<0.05, **P<0.01, ***P<0.001, ****P<0.0001.

In addition, and of therapeutic relevance, *in vivo* deletion of *Ets1* by tamoxifen treatment in this a Notch-induced leukemia maintenance model enhanced the antileukemic effects of

intermittent GSI dosing resulting in reduced peripheral blood T-ALL blasts and increased survival compared to controls (Fig. 5.3E-H). Consistent with our prior studies (Fig. 3.2G-H), leukemic blasts harvested at time of morbidity showed ~50% *Ets1* deletion (Fig. 5.3I). These studies suggest that ETS1 inhibitors might enhance the antileukemic effects of tolerable doses of GSI. These results support a therapeutic role for ETS1 inhibition in combination with anti-NOTCH1 therapies for the treatment of T-ALL. Considering the prior discussion of possible means of inhibiting transcription factors for therapeutic effect, we explored enhanced degradation and protein-protein interaction inhibition as methods to block ETS1 activity as a targeted therapy in T-ALL.

Enhanced degradation of ETS1 to impair growth is possible.

Targeting transcription factors with small molecules has been stymied by the lack of "druggable" active sites. However, agents that enhance degradation of target proteins by exploiting the ubiquitin-proteasome system is a promising new approach (Winter et al. 2015). In order to investigate if targeted degradation might be an effective antileukemic strategy, we treated ETS1-dependent T-ALLs with G9, a small molecule inhibitor of USP9x. As mentioned in the introduction, USP9x is the deubiquitinase of Ets1 (Potu et al. 2017) (Fig. 5.4A). In contrast to continuous GSI treatment, continuous G9 treatment is tolerated by mice as anti-cancer therapy (Pal et al. 2018, Peterson et al. 2015). Greater levels of ETS1 protein degradation (Fig. 5.4B) roughly correlated with stronger growth inhibition (Fig. 5.4C). G9 treatment of T-ALL cells inhibited viability with sub-micromolar GI50s (Fig. 5.4D). However, cells resistant to *ETS1* withdrawal (e.g. LOUCY) or resistant to ETS1 degradation (e.g. CEM) were still sensitive to G9. Thus, G9 likely has substantial ETS1-independent effects. Accordingly, partial or full restoration of ETS1 expression (Fig. 5.4E) only modestly (if at all) rescued the proliferation of G9-treated cells (Fig. 5.4F). Nevertheless, these data suggest that the proteasome pathways that degrade

ETS1 are likely intact in many T-ALLs. Therefore, other strategies that enhance the degradation of proteins (i.e. PROTAC), might prove useful in inhibiting ETS1 in T-ALL.

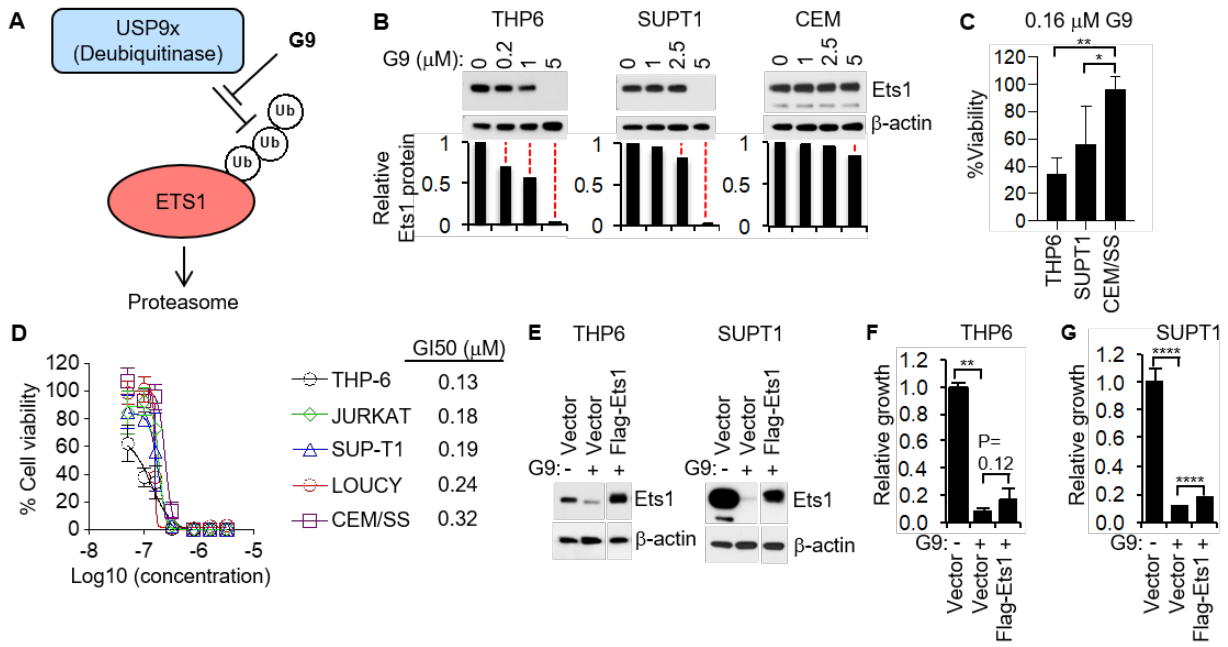

Figure 5.3 ETS1 can be targeted for protein degradation

A) Schematic showing degradation of Ets1 by G9, a selective small molecule inhibitor of USP9x, the Ets1 deubiquitinase. B-C) Western blots and ImageJ quantification showing dose-dependent effect of G9 on Ets1 protein expression in three T-ALL cell lines with increasing levels of resistance to G9 based on %viability at 0.16μM (C). D) Dose response curves for 5 human T-ALL cell lines treated with increasing doses of G9 in a 9-day in vitro culture assay. Viability was assessed by PI-staining flow cytometry. E-G) Western blot (E) and rescue experiments were performed showing relative growth of THP-6 (F) or SUP-T1 (G) cells transduced with Flag-ETS1 in the presence of 0.16μM G9. Split western blot images were taken from the different locations of the same gel. (B-C performed by J. Jiminez, D performed by C. Chang, E-F performed by E. Kim).

Multiple domains mediate ETS1 interaction with the Notch complex in T-ALL

One could exploit the context-dependency of Notch transcriptional complexes by slipping a small molecule into the interface of a protein-protein interaction necessary for complex activity. In Chapter 4, we demonstrated that silencing *ETS1* reduced the recruitment of ICN1, RBPJ, and ZMIZ1, and diminished H3K27ac at oncogenic enhancers. Thus, targeting the interaction of ETS1 with members of the Notch complex might be a potential therapeutic

strategy. However, it is first necessary to identify the domains and residues required for the ETS1-NOTCH1 or ETS1-RBPJ interactions. Using the guidance of Phyre2 to predict secondary structure within the Ets1 protein (Kelley et al.), we first generated a series of truncated Flag-tagged ETS1 proteins containing either the unstructured N-terminal domain (amino acids 1-41), the pointed (PNT; amino acids 1-136), the transactivation domain (TAD; amino acids 136-276) or the autoinhibitory domains and ETS DNA binding domain (amino acids 276-441) (Fig. 5.5A). We utilized Flag co-immunoprecipitation, probing for endogenous ICN1 and RBPJ, to determine which domains are necessary for ETS1 interaction with these proteins (Fig. 5.5B-C). While these studies clearly demonstrate that the PNT-TAD domains are needed for interaction with ICN1 and RBPJ (1-276; Fig. 5.5B-C), the contributions of the PNT and TAD domains individually have proven difficult to reproduce across multiple individual experiments (Fig 5.5B). Further work is necessary to clarify if the PNT alone is sufficient for ETS1 interaction with the NOTCH1 complex, or if the TAD participates in stabilizing binding.

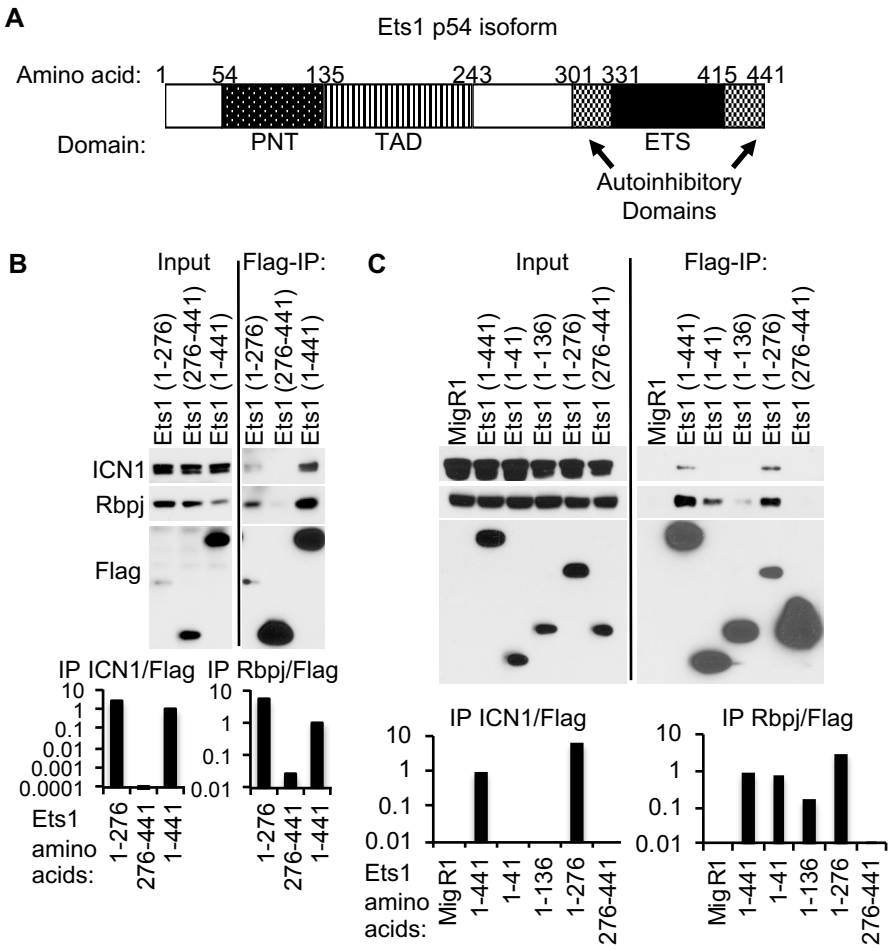

Figure 5.4 ETS1 interacts with NOTCH1 and RBPJ through the N-terminal PNT-TAD domains

A) Domain structure of Ets1, showing the amino-acid numbers demarking the PNT, TAD, Autoinhibitory, and ETS domains. PNT = pointed; TAD = transactivation; ETS; Ets DNA binding domain. B) Flag co-immunoprecipitation in THP-6 cells using full length Flagged Ets1 (1-441), Ets1 (1-276; PNT-TAD domains), Ets1 (276-441; Autoinhibitory-Ets domains) to detect pull-down of endogenous ICN1 and Rbpj, and Image J quantification of IP ICN1 or Rbpj normalized to IP Flag bait. C) Flag co-immunoprecipitation in THP-6 cells using full length Flagged Ets1 (1-441), Ets1 (1-41; unstructured N-terminus), Ets1 (1-136; PNT domain), Ets1 (1-276; PNT-TAD domains), Ets1 (276-441; Autoinhibitory-Ets domains) to detect pull-down of endogenous ICN1 and Rbpj, and Image J quantification of IP ICN1 or Rbpj normalized to IP Flag bait. (C performed by C. Sha).

Discussion

Targeting transcription factors with small molecule inhibitors has historically proven more challenging than blocking enzyme catalytic or allosteric sites. However, the recent development of enhanced protein degraders and protein-protein interaction inhibitors have overturned the narrative of transcription factors as “undruggable”. Here, we present data showing

that a combinatorial regiment with ETS1-deletion and Notch-inhibitors has strong antileukemic effects, both *in vitro* and *in vivo*. Our studies in cell lines and mice suggest synergy between ETS1 and NOTCH1 in promoting the proliferation of Notch-driven T-ALLs.

Additionally, we demonstrated the potential efficacy of an enhanced-degradation strategy for targeting ETS1. G9, the inhibitor of ETS1 deubiquitinase USP9x, reduced ETS1 protein levels and the halt of cellular proliferation in a panel of human T-ALL cell lines. And while we have not yet identified the residues of ETS1 essential for its interaction with members of the Notch complex, we narrowed the probable domains to the N-terminal portion of the ETS1 protein. We also acknowledge there is much about these ETS1-dependent Notch complexes that remains to be elucidated. We do not yet know whether the interaction between ETS1 and NOTCH1 is direct, or if there are other cofactors involved. Additional in-vitro assays would be necessary to determine if there is a druggable interface between these two proteins. More thoughts about future directions for this project will be discussed in Chapter 6.

There are other strategies for targeting ETS1 that have not yet been tested. Since c-Src or YES1 phosphorylation of ETS1 at tyrosine 283 reverses CAMKII-dependent destabilization of ETS1 protein (Lu et al. 2014), Src inhibitors such as dasatinib and saracatinib may accelerate rapid turnover of ETS1 protein and might prevent transactivation of ETS1 target genes. Blocking the ETS-DNA interaction with a small molecule or stapled peptide, as has been developed for ERG (Nhili et al. 2013, Wang et al. 2017a), might prove effective in inhibiting ETS1 activity in T-ALL. Regardless, these findings provide strong rationale for a therapeutic approach combining ETS1-degradation and low-dose Notch inhibitors, albeit with a more specific ETS1-degradation strategy.

Chapter 6 Conclusions and Future Directions[6]

Conclusions

During T-ALL transformation, Notch1 can become supraphysiologically activated or "hijacked", leading to widespread expression of cleaved intracellular Notch1 (Kluk et al. 2013). Current models support that Notch in turn hijacks its normal cellular partners including the co-binding transcription factors that it normally relies upon to promote T-cell development. In this context, such "Notch-collaborating" transcription factors might comprise new vulnerabilities in Notch-dependent cancers like T-ALL. These concepts are clinically relevant as continuous pan-Notch inhibition with GSI is poorly tolerated (Real et al. 2009).

This thesis work presents evidence that Ets1 is a Notch-collaborating transcription factor and a potential therapeutic target in T-ALL. Using mouse models, we show that *Ets1* inactivation resembled the Notch1 inhibition phenotype by impairing ETP specification and the DN-to-DP transition, which are the two major Notch-dependent steps during early T-cell development. *Ets1* inactivation also impaired leukemic proliferation and Notch-induced gene expression in complementary mouse and human models of Notch-activated T-ALL. Accordingly, ChIP-Seq analyses of T-ALL cells showed that ~80% of ICN1/RBPJ sites were co-occupied by ETS1. Compared to Notch inhibition, the effects of *Ets1* inactivation were strong in T-cell precursors or T-ALL cells, but relatively weak in the intestine. Thus, Ets1 might have more substantial Notch-collaborating functions in the context of T-cell development and leukemogenesis than in the

[6] Adapted from McCarter, A. C., G. D. Gatta, A. Melnick, et al. (2020) Combinatorial ETS1-Dependent Control of Oncogenic NOTCH1 Enhancers in T-cell Leukemia. *Blood Cancer Discovery*.

context of intestine stem cell differentiation.

Functional analysis of ETS1 binding to chromatin sites in T-ALL revealed that only a minority of ETS1 peaks were suppressed upon ETS1 knockdown (dynamic ETS1 peaks). This finding is reminiscent of an earlier study showing that fewer than 10% of NOTCH1 peaks in CUTLL1 cells were dynamic when switching between Notch-on and Notch-off states (Wang et al. 2014a). Like dynamic ETS1 peaks, dynamic NOTCH1 peaks were associated with differential H3K27ac read counts (Wang et al. 2014a). For ETS1, our motif analyses suggest that dynamic peaks might signify a class of high confidence binding sites that are highly sensitive to ETS1 dose reduction. In contrast to the high percentage of ICN1/RBPJ peaks that are co-occupied by ETS1, a much smaller percentage of ETS1 peaks were co-occupied by ICN1/RBPJ. Consistently, we identified several ETS1 target genes that, to our knowledge, have not been linked to dynamic NOTCH1 peaks or implicated as direct NOTCH1 target genes in publicly available T-ALL gene expression screens. Many of these genes, such as *GATA3*, *LYL1*, *PTPN11*, *LMO2*, *LCK*, and *HHEX* have prominent roles in early T-cell development and leukemia transformation.

ETS1 loss often reduced H3K27ac read counts without affecting ICN1/RBPJ binding. However, we observed a small subgroup of ETS1 sites containing GATA motifs where ETS1 knockdown reduced ICN1/RBPJ binding and strongly reduced H3K27ac tags. Of note, this is a discrete feature suggestive of a strong functional interaction as GATA motifs were uncommonly associated with ETS1 peaks (~15% of total). Combined with our observations of protein-protein interactions between ETS1 and NOTCH1 in two T-ALL cell lines, these data suggest the possibility of context-dependent transcriptional complexes that stabilize NOTCH1 complex interactions with chromatin. GATA3 is the predominant GATA family member expressed in T-ALL cells and is the only GATA family member expressed in the cell line we analyzed by ChIP-

Seq. It is possible that GATA3 might act as a scaffold linking ETS1 to the NOTCH1 complex. GATA3 pioneering factor activity can facilitate nucleosome eviction at the N-ME to promote transcription factor binding (Belver et al. 2019). Thus, GATA3-driven chromatin remodeling might help other proteins "connect" ETS1 to the Notch complex. Accordingly, our motif analysis suggests that transcription factors other than GATA3 are associated with dynamic changes of Notch factors and H3K27ac upon ETS1 knockdown. Moreover, since *GATA3* is an ETS1-induced gene, ETS1 might indirectly promote Notch complex recruitment and H3K27ac deposition through *GATA3* induction.

Future Directions

What other functions does ETS1 serve in hematopoiesis?

There remain many unanswered questions about ETS1 function in normal hematopoiesis and leukemogenesis. Our inducible *Ets1*$^{f/f}$ mouse model can be leveraged to gain a much greater understanding of ETS1-controlled steps of early and late hematopoiesis. While their absolute numbers were similar to controls, the *Ets1*-deprived LSK (Lineage^{-}Kit^{hi}Sca1^{hi}) and LMPP (Lineage^{-} Kit^{hi}Sca1^{hi}Flt3^{hi}) precursors in the bone marrow of *VavCreEts1*$^{f/f}$ mice may not have full differentiation potential. It might be possible to interrogate their multipotency by transplanting sorted CD45.2+ LSK or LMPP cells from *VavCreEts1*$^{f/f}$ mice, mixed 1:1 with sorted *VavCre* control CD45.1+ LSK or LMPP cells respectively, into irradiated CD45.1+ SJL recipients [similar to (de Pooter et al. 2019)] . Subsequent analysis of bone marrow and peripheral populations might reveal defects in bone marrow reconstitution by the CD45.2+ *Ets1*-deficient progenitors not observed in steady state hematopoiesis.

The apparent increase in myeloid cells accumulating in the spleens of *VavCreEts1$^{f/f}$* mice is also an interesting point of further inquiry. The mild myeloproliferative phenotype in *Ets1*-deficient mice was reminiscent of that observed in mice with Notch-signaling defective Nicastrin-deficient hematopoietic stem cells (Klinakis et al. 2011). These Nicastrin-deficient mice had an increase in the LSK CD150+CD48+ subset in the bone marrow (Klinakis et al. 2011), which are known to have a myeloid commitment bias (Challen et al. 2010); these effects were largely attributed to the repression of Hes1 in these animals. We identified *HES1* as a shared ETS1-NOTCH1 target gene in human T-ALL cell lines. An interesting extension of our studies would be to examine hematopoietic precursors in *VavCreEts1$^{f/f}$* mice to determine if the myeloproliferation in our mice is also due to reductions in *Hes1* expression.

Is there a therapeutic window for ETS1 inhibition in leukemia?

The acute sensitivity of T-cells and leukemia cells to ETS1 loss, in contrast with the relatively mild intestinal phenotype observed in Ets1-deficient animals, suggests there may be. The ETS family has been implicated in intestinal development [reviewed in (Jedlicka and Gutierrez-Hartmann 2008)]. However, a direct role for Ets1 in intestinal homeostasis has not been established. As mentioned in the discussion section of Chapter 2, further studies using tissue-restricted Cre-mediated *Ets1* deletion would be necessary to clarify the role of ETS1 in intestinal maintenance. If ETS1 is indeed serving similar function to Notch in intestinal stem cells, there is concern that Ets1 loss might exacerbate the toxicity of pan-Notch inhibition. A critical experiment is currently underway to examine the effect of combining *Ets1* deletion with low dose pan-Notch inhibitors. If *Ets1*-deprivation heightens the sensitivity of intestinal stem cells to Notch inhibitors, as it does in T-ALL cells, we would anticipate increased goblet cell metaplasia and villi malformation in the context of dual inhibition. If the intestinal phenotype

induced in our *Rosa26CreER^{T2} Ets1$^{f/f}$* mice is not caused by *Ets1* loss in the intestinal stem cells, but rather mediated via a different cell population in mucosa or immune cell subsets, there may be no increased toxicity with dual inhibition of ETS1 and NOTCH1.

Is ETS1 required for the proliferation of other oncogenomic subsets of T-ALL?

While *Ets1*-deprivation halted the proliferation of a majority of human T-ALL cell lines, two cell lines, JURKAT and LOUCY, remained unaffected. We largely restricted our examination of ETS1 in T-ALL to Notch-driven leukemias. However, the Notch-driven murine T-ALL model employed in these studies, while broadly used (Aster et al. 2000, Chiang et al. 2013, Chiang et al. 2008, Pajcini et al. 2017, Herranz et al. 2014), does not represent the array of subtypes of patient T-ALLs. Deletion of *Ets1* in additional murine models, such as the *CD2-LMO2* model (Smith et al. 2014), might yield valuable insights into the broader role in ETS1 in T-ALL.

What else is ETS1 doing as a part of the complex at Notch-driven enhancers?

This thesis work demonstrated that ETS1 recruits Notch cofactors to enhancers, results in H3K27ac and subsequent transcription (Chapter 4). Future work in the Chiang lab will explore additional functions of ETS1 as part of the Notch complex. ETS1, upon phosphorylation in the PNT domain, recruits transcriptional co-activators CBP/P300 (Foulds et al. 2004, Tetsu and McCormick 2017, Yang et al. 1998). We want to know if ETS1 recruits any additional co-activators that might enhance transcription of ETS -NOTCH1 shared target genes. We have preliminary data showing that Ets1 interacts with polymerase associated factor complex (PAFc) member CDC73. Deletion of *Cdc73* in a murine Notch-driven T-ALL maintenance model sharply reduces leukemic blast counts and increases disease-free survival. CDC73 co-binds the majority of Notch-driven enhancers in THP-6 cells, and CDC73 recruitment to these enhancers is reduced

in the absence of Ets1 (data not shown). Future studies will examine the role of CDC73 in T-cell development and the CD2-LMO2 model of T-ALL leukemogenesis. The Chiang lab will identify CDC73 target genes in T-ALL, interrogate the effect of CDC73 loss on Notch complex recruitment, enhancer activation, and enhancer-promoter chromatin looping.

What role does GATA3 play in ETS1-regulated Notch complexes?

In the Conclusions section, we proposed two potential roles for GATA3 in Notch complexes co-regulated by ETS1; that of a "scaffolding" protein mediating the recruitment of additional co-activators or that of a chromatin remodeler displacing nucleosomes to make space for transcription factor binding (Fig. 6.1).

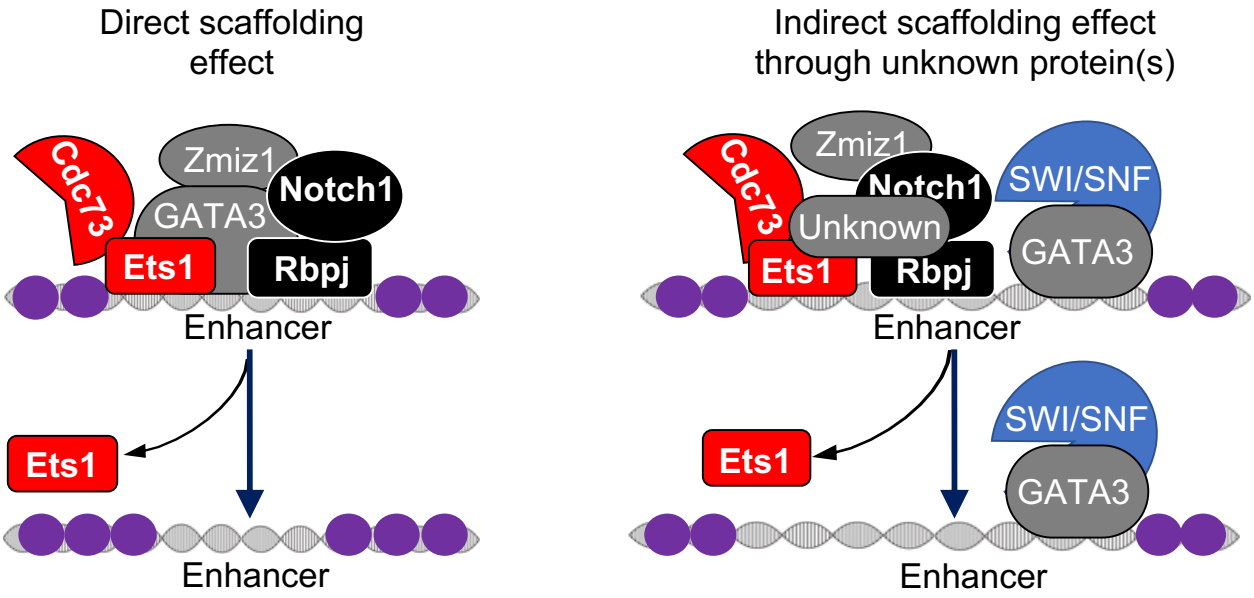

Figure 6.1 Model: Direct actions of GATA factors or indirect actions through chromatin remodeling

Model figure demonstrating two possible means through which GATA3 might be contributing to the activity of Ets1-dependent Notch-driven enhancers.

Future studies in the lab will directly test this model. In order to distinguish between these two potential functions for GATA3, we can perform ChIP-seq in human T-ALL cells transduced with

shETS1-2/3. If GATA3 serves in a scaffolding capacity as a part of the larger Notch complex, we would anticipate that loss of ETS1 would diminish GATA3 recruitment, just as it did for other complex members RBPJ, ICN1, and ZMIZ1. However, if GATA3 is independently working to evict nucleosomes from the DNA, GATA3 binding should be preserved despite ETS1 loss. We are mindful that the role for GATA3 might be more complex than our model belies, and plan to follow up these experiments with additional studies examining the effect of GATA3-inhibition on Notch complex recruitment and enhancer activation genome-wide.

Summary

Therapeutically, our study suggests that it is possible to disengage Notch from many of its chromatin or gene expression functions in cancer cells without resorting to toxic, continuous dosing of GSI. Further, our results rationalize the testing of combination strategies with anti-ETS1 and anti-Notch agents. Finally, our study supports a model in which Notch-collaborating partner transcription factors like Ets1 create a favorable chromatin context for NOTCH1 to activate a subset of response elements. This evolutionary conserved principle already present in *Drosophila* (Falo-Sanjuan and Bray 2019) can be relevant to human disease as context dependence could be exploited to oppose parts of the Notch downstream pathway in cancer with less toxicity than pan-Notch inhibitors. Moreover, given emerging data supporting a role for ETS1 in tumors such as breast, ovarian and colon cancer (Dittmer 2015) that are Notch-dependent (Miele and Artavanis-Tsakonas 2018), our findings raise the possibility that ETS1 could be hijacked along with Notch as a driver of transformation in a diverse number of human cancers.

Chapter 7 Materials and Methods[7]

Mice

C57BL/6 mice ranging from 4-weeks to 8-weeks of age were obtained from Taconic for bone marrow transplantation experiments. *Rosa26CreER^{T2} Ets1*$^{f/f}$ mice were generated by crossing *Ets1*$^{f/f}$ mice (a gift from M. Ostrowski, manuscript in preparation) with *Rosa26CreER^{T2}* mice (Jackson). *Rosa26CreER$^{Tz2\text{-alt}}$ Ets1*$^{f/f\text{-alt}}$ mice were generated by crossing *Ets1*$^{f/f\text{-alt}}$ mice (Zook et al. 2016) with *Rosa26CreER$^{T2\text{-alt}}$* mice (Guo et al. 2007). The "alt" term was used to avoid confusion with the Jackson/Ostrowski *Rosa26CreER^{T2}Ets1*$^{f/f}$ mouse model described above. In *Ets1*$^{f/f}$ and *Ets1*$^{f/f\text{-alt}}$ mice, the *Ets1* conditional allele was constructed by flanking exons 7 and 8 with loxP sites. *Ets1*$^{p/p}$ mice, a gift from Dr. Garrett-Sinha (University at Buffalo), were previously described (Barton et al. 1998). In these mice, the exons 3 and 4 of *Ets1* (containing the PNT domain) were deleted, thus creating a hypomorphic "p" allele (Wang et al. 2005). *Notch1*$^{f/f}$ and *VavCre* (also known as "*Vav1-iCre*") mice were obtained from The Jackson Laboratory. *VillinCreER^{T2}* mice were obtained from S. Robin (el Marjou et al. 2004). Mice used for T-cell developmental studies were 5-8 weeks of age. Mice used for *Rosa26-CreER^{T2}* and *VillinCreER^{T2}* experiments were 8-12 weeks old. Per animal protocol, mice were sacrificed when weight dropped to 80% or less of starting weight. All mouse experiments were performed according to National Institutes of Health guidelines with approved protocols from the institutional animal care and use committees at the University of Michigan and Columbia University Medical Center.

[7] Excerpted from methods section of McCarter AC, Della Gatta G, Melnick A, et al. Disrupting the combinatorial control of oncogenic NOTCH1 enhancers in T-cell leukemia. Submitted to Immunity.

Mouse Strain	Short Name	Source/Reference
B6.Cg-Commd10Tg(Vav1-icre)A2Kio/J	*VavCre*	Jackson, #008610
B6.129-Gt(ROSA)26Sor$^{tm1(cre/ERT2)Tyj}$/J	*Rosa26CreER^{T2}*	Jackson, #008463
ROSA26$^{Cre-ERT2/+}$	*Rosa26CreER^{T2}*-alt	(Guo et al. 2007)
B6.Cg-Tg(Vil1-cre/ERT2)23Syr/J	*VillinCreER^{T2}*	S. Robin; Jackson, #020282
Ets1$^{f/f}$	*Ets1$^{f/f}$*	M. Ostrowski
Ets1$^{f/f}$	*Ets1$^{f/f}$*-alt	(Zook et al. 2016)
Notch1tm2Rko/GridJ	*Notch1$^{f/f}$*	Jackson, #006951
Ets1$^{p/p}$	*Ets1$^{p/p}$*	(Wang et al. 2005, Barton et al. 1998)

Transduction and bone marrow transplantation

For experiments depicted in Figure 3A-E, Figure S3A-F, Figure 7F-I, and Figure S7H, retroviral transduction of bone marrow cells and transfer into lethally irradiated recipients was performed as described (Aster et al. 2000, Chiang et al. 2008, Pui et al. 1999). Briefly, bone marrow cells were collected from the femurs and tibias of 4-8 week old *Rosa26-CreER^{T2}* control or *Rosa26-CreER^{T2} Ets1$^{f/f}$* mice 4 days after intraperitoneal administration of 5-fluorouracil (5FU, 250mg/kg). The cells were cultured overnight in the presence of IL-3 (6ng/ml), IL-6 (5-10ng/ml), and SCF (100ng/ml). The cells were then washed, resuspended in retroviral supernatant containing MSCV-ΔE/Notch1-IRES-GFP retrovirus. Each condition was normalized to retroviral titers based on GFP expression. The cells were placed in the same cytokine cocktail with the addition of polybrene (4μg/ml) and centrifuged at 1290 x g for 90 minutes. A second round of "spinoculation" was performed the following morning. After washing with PBS, 4-5x10^5 cells were injected

intravenously into lethally irradiated (950rads) syngeneic recipients. Mice were maintained on antibiotics in drinking water for two weeks after bone marrow transplantation. Flow cytometry measured circulating Notch-induced $CD4^+CD8^+$ (DP) T cells. Mice were bled every 2-3 weeks to monitor blood counts. T-ALL was defined as WBC>50K/µl or morbidity with splenomegaly (>200mg) or lymphadenopathy (>200mg). Primary tumors were harvested from morbid mice and live frozen in 10% DMSO/FBS for injection into secondary recipients. For secondary transplants, 2-10x10^4 GFP^+ leukemia cells were injected intravenously into sub-lethally irradiated (450rads) syngeneic recipients. For maintenance studies, 9 doses of 25mg/kg tamoxifen were administered intraperitoneally 5, 7, 9, 12, 14, 16, 19, 21, and 23 days after injection of the leukemia cells. This dosing strategy was empirically determined after we observed that single doses of varying strengths (up to 250mg/kg) were unable to efficiently induce *Ets1* deletion. For cross-sectional studies of Notch-induced T-ALLs generated using *Rosa26-CreER*$^{T2\text{-alt}}$ *Ets1*$^{f/f\text{-alt}}$ mice (Fig. 2F-I), 0.3mg/g of body weight of 4-hydroxytamoxifen was injected intraperitoneally after disease appearance. This dose of tamoxifen was previously shown not to induce toxicity in *Rosa26CreER*$^{T2\text{-}alt}$ control tumors (Schnell et al. 2015, Herranz et al. 2014).The major organs were collected at 48 hours after 4-hydroxytamoxifen injection and used for further analyses. For studies shown in Fig. 2J-K, bone marrow from 8-week-old *Ets1*$^{+/+}$, *Ets1*$^{+/p}$ *and Ets1*$^{p/p}$ mice was harvested from freshly dissected femurs and tibias. Cells were spun for 2.5 min at 200 x *g* and red blood cells were lysed for 3 min at 25 °C with ammonium chloride–potassium bicarbonate lysis buffer. Cells were then washed in 2% (vol/vol) FBS in PBS and were spun. Then the cells were passed through a cell strainer, counted and lineage depleted using the Mouse Lineage Cell Depletion Kit (Miltenyl). Lin^- progenitor cells were subjected to 2 rounds of infection with MigR1-ΔE-Notch1 retroviral particles. 50,000 Lin^-Sca1^+–infected cells were transplanted into irradiated C57BL/6

recipients via intravenous injection. Transplanted animals were monitored for leukemia development by flow cytometric analysis of green fluorescent protein (GFP) and CD4/CD8 expression in peripheral blood.

Complete Blood Count (CBC)

CBC was measured at the University of Michigan Unit for Laboratory Animal Medicine pathology core using a Hemavet 950 Hematology System.

Histological Analysis

Paraffin sections (5μm) were stained with periodic acid-Schiff (PAS)/Alcian Blue (Newcomer Supply, Middleton, WI, USA) to assess mucin-containing goblet cells. PAS/AB stained images from mouse intestines were quantified for proportion of blue staining (blue stained region in μm/total villus region in μm) using ImageJ software (NIH) as previously described (Kvidera et al. 2017). Villi length and crypt depth was traced and analyzed using the Measure tool. All quantitative analyses of the intestinal histology were performed by an observer who was blinded to the genotypes and treatment of the mice.

Cell lines

Jurkat cells were provided by Jon Aster (Harvard University). CEM cells were CEM/SS (a subclone of CCRF-CEM), which were provided by Katherine Collins (University of Michigan). THP-6, DU.528, MOLT4, DND-41, and SUP-T1 cells were provided by Andrew Weng (Terry

Fox Laboratory). THP-6 is a GSI-resistant LYL1/LMO2-type T-ALL that expresses ICN1 (Pinnell et al. 2015b, Wang et al. 2018, Kawamura et al. 1999). HPB-ALL cells were obtained from DSMZ. LOUCY cells were obtained from ATCC. OP9-DL4 cells were provided by J.C. Zuniga-Pflucker (University of Toronto). 643 cells were established from a primary *Rosa26-Cre^{ERT2} Ets1$^{f/f}$* splenic tumor. In these cells, *Ets1* can be deleted in vitro via the administration of 4-hydroxytamoxifen. All human cell lines were authenticated using STR analysis (Genetica Corporation).

Cell culture conditions

T-ALL cell lines were grown in RPMI 1640 (Invitrogen) supplemented with 10% fetal bovine serum (Hyclone or Gibco), 2mM L-glutamine, 2-mercaptoethanol (0.0005% (v/v), Sigma), penicillin and streptomycin. 293T cells were maintained in Dulbecco's modified Eagle medium (DMEM, Invitrogen) with the same supplements except 2-mercaptoethanol. Cells were grown at 37°C under 5% CO2. All cell lines were cultured less than three months after resuscitation and tested for contaminants using MycoAlert (Lonza) every 1-3 months to ensure they were free of mycoplasma contamination. Retroviral and lentiviral transduction of T-ALL cells, and sorting or selection, were performed as previously described (Rakowski et al. 2013). DBZ (GSI) was obtained from EMD chemicals (for *in vitro* studies) or Syncom (for *in vivo* studies). 4-hydroxytamoxifen was obtained from Sigma. For knockdown experiments, puromycin (Sigma) was added to transduced cell cultures 48 hours after transduction.

Constructs and viral production

Previously described constructs include: MSCV-IRES-GFP (MigR1) and MSCV-IRES-NGFR

(NGFR), MSCV-Myr-AKT-IRES-NGFR, and MSCV-Myc-IRES-NGFR (Chiang et al. 2016). Flag-ETS1 was cloned into MSCV-IRES-GFP from pCDNA3-ETS1 (Origene) using standard PCR cloning methods. ShRNA constructs were obtained from Sigma Aldrich -- shControl (SHC002 control plasmid), shETS1-1 (TRCN0000231915), shETS1-2 (TRCN0000231916), shETS1-3 (TRCN0000005591), or from Invitrogen. Methods for retroviral supernatant production and titering have been previously described (Pui et al. 1999, Luo et al. 2005). Briefly, shControl, shETS1-2 and shETS1-3 viral particles were produced in triplicate in HEK293T cells by cotransfection with gag-pol and V-SVG–expressing vectors using the Fugene HD transfection reagent (Promega). Concentrated lentivirus was prepared using Lenti-X (Takara) according to manufacturer's instructions. Lentiviruses were tittered by transducing CEM cells with increasing volumes of virus, culturing for 48 hours and then measuring YFP^+/GFP^+ cells by flow cytometry or culturing for an additional 24 hours in the presence of 10□g/ml puromycin and then measuring %puromycin resistant cells. pLKO-shLUC and pLKO-shETS1-4 viral particles were produced HEK293T cells cotransfection with gag-pol and VSVG–expressing vectors using the JetPEI transfection reagent (Polyplus). Viral supernatants were collected after 48 hours filtered and used for infecting HPBALL cell lines by spinoculation in the presence of retronectin (Takara Bio, Inc). Equal viral titers were used for each condition for an experiment.

Co-Immunoprecipitation

THP-6 cells were washed with TBS and lysed in IP buffer (10% Glycerol, 150mM NaCl, 50mM HEPES, pH 8.0, 2mM EDTA, 0.1% NP-40) with protease and phosphatase inhibitors. Lysates were pre-cleared with 55µl prewashed Protein A/G beads (Santa Cruz) and then incubated with antibody (IgG control, ETS1 or NOTCH1) overnight at 4°C. IPs were incubated with 55ul of

prewashed protein A or G beads for 2 hours at 4°C. Beads were washed and proteins eluted at 95°C for 5 minutes. 6x sample buffer was added, input samples and immunoprecipitation elutes were electrophoresed on a 4-12% gradient gel (Thermo Fisher), and transferred to PVDF membranes. Ponceau S staining was used to confirm equal loading and transfer of proteins. All membranes were blocked in 5% milk. Primary and secondary antibodies were diluted in 1% milk with TBST. Antibody binding was visualized by HRP, using Pico and Femto reagents (Thermo Fisher). Membranes were stripped between antibodies with Restore Western Blot Stripping Buffer (Thermo Fisher) and checked with the secondary antibody for the next primary antibody. HPB-ALL cells were washed with TBS and lysed in IP buffer (Tris-HCl 50mM pH=7.4, NaCl 150mM, MgCl2 5mM, Glycerol 10%, Triton 1%) with protease and phosphatase inhibitors. Lysates were pre-cleared with 50µl prewashed Protein A/G beads for 30 minutes at 4C, and then incubated with antibody (IgG control, ETS1 from Santa Cruz, Table S5) overnight at 4°C. IPs were then incubated with 60ul of prewashed protein A or G beads for 2 hours at 4°C. The IP-beads complex was washed with IP buffer. After the final wash, the IP-beads complex was pulled down by centrifugation and eluted in IP and 6x sample buffer. The samples were boiled at 95°C for 10 minutes. Input samples and immunoprecipitation eluates were electrophoresed on a 4-12% gradient gel (Thermo Fisher) and transferred to PVDF membranes. Ponceau S staining was used to confirm equal loading and transfer of proteins. All membranes were blocked in 5% milk. Primary and secondary antibodies were diluted in 2% milk with TBST. Antibody binding was visualized by HRP, using Pico and Femto reagents (Thermo Fisher). Membranes were stripped between antibodies with Restore Western Blot Stripping Buffer (Thermo Fisher) and checked with the secondary antibody for the next primary antibody

Western Blot

25 million cells from human patient derived xenografts, murine splenocytes, or human T-ALL cell lines were washed with ice cold TBS (50mM Tris, pH8.0, 150 mM NaCl) and lysed in 250 µl NTEN buffer (50 mM Tris, pH 8.0, 1 mM EDTA, 150 mM NaCl and 1% (v/v) NP-40, Sigma I3021) supplemented with the protease and phosphatase inhibitors on ice for 20 min, followed by centrifugation to remove cell debris (20min, 16,000 x g). For western blot of murine ileum samples, 20mg of snap-frozen tissue was lysed in 500ul RIPA buffer with protease inhibitors on ice for 15 minutes, homogenized via a Branson 250 sonifier (10 pulses at 35% power), and centrifuged to remove cell debris. Cell lysates were quantified using Bradford (Biorad) or BCA (Pierce) assays, denatured, electrophoresed on a 4-12% gradient gel (Thermo Fisher), and transferred to PVDF membranes. Ponceau S staining was used to confirm equal loading and transfer of proteins. All membranes were blocked in 5% milk. Primary and secondary antibodies were diluted in 1% milk with TBST. Antibody binding was visualized by HRP, using Pico and Femto reagents (Thermo Fisher). Membranes were stripped between antibodies with Restore Western Blot Stripping Buffer (Thermo Fisher) and checked with the secondary antibody for the next primary antibody.

Flow cytometry

Cells were stained on ice in PBS containing 2% fetal bovine serum, 10mM Hepes and 0.02% NaN3 after blocking with rat and mouse IgG (Sigma). Flow cytometry antibodies were obtained from Biolegend or eBioscience (Table S5). Samples were analyzed on an LSR Fortessa flow cytometer

or sorted using a FACSAria II (BD Biosciences). Dead cells were excluded using 7-aminoactinomycin D (7-AAD) or 4′,6-diamidino-2-phenylindole (DAPI). Intracellular staining was performed using the BD Cell Fixation/Permeablization Kit (BD Cat# 554714). Data were analyzed using FlowJo (Tree Star). Cell cycle analysis was performed by administering 1mL of propidium iodide stain solution (PI, 20µg/ml and DNase free RNase A, 100µg/ml) to the freshly collected cells from primary tissues and analyzed by FACS within 30 minutes.

AnnexinV/7-AAD staining was performed on fresh cells according to manufacturer's specifications (BD Bioscience) for apoptosis and cell death analysis. Each experimental condition was run in triplicate. The values displayed are representative of three biological replicates. All data acquisition was performed on BD-FACS Canto and analyzed using FlowJo analysis software (Tree Star).

Cell proliferation assay

Relative cell growth was determined in triplicates by measurement of metabolic reduction of the tetrazolium salt MTT using Cell Proliferation Kit I (Roche) according to the manufacturer's instructions.

Human patient/patient-derived xenografts (PDX) Expression Data

The human patient data in Figures S4B-C were based upon data generated by the Therapeutically Applicable Research to Generate Effective Treatments (TARGET) (https://ocg.cancer.gov/programs/target) initiative, phs000218. The ALL project team was headed by Stephen P. Hunger, M.D. at the University of Colorado Cancer Center, Denver, CO, USA. The

dbGaP Sub-study ID was phs000463/phs000464. The data used for this analysis are available at https://portal.gdc.cancer.gov/projects. Heatmap of Ets family member expression was generated in the ProXe database app (https://proxe.shinyapps.io/PRoXe/) using only the T-ALL PDXs available in the database.

PDX experiments

PDXs (IDs: M71, BCAT17802-V2, and BCAT82114-V1 were obtained from Andrew Weng and were previously described (Townsend et al. 2016, Giambra et al. 2015, Giambra et al. 2012). De-identified human samples were obtained and used with appropriate institutional approval (University of Michigan Institutional Review Board, UBC/BCCA Research Ethics Board, Institutional Review Board of the Institut Universitaire d'Hématologie/Université Paris Diderot) and informed consent under guidelines established by the Declaration of Helsinki. PDXs were expanded by injecting them into non-irradiated NOD-*scid*-IL2Rgamma^{null} (NSG) mice and then harvesting spleens at time of morbidity. Human-specific antibodies against CD45 and CD7 were used to discern human T-ALL lymphoblasts and differentiated from mouse cells with antibodies against murine CD45. Live-frozen PDX aliquots were thawed and co-cultured on irradiated OP9-DL4 stromal cells in IMDM media (Invitrogen) supplemented with human stem cell factor (hSCF, Peprotech, #300-07, 50ng/ml), human insulin-like growth factor (hIGF, Peprotech, #100-11, 10ng/ml), human IL-2 (hIL2, Peprotech, #200-02, 10ng/ml), murine IL-7 (mIL7, Peprotech, #217-17, 10ng/ml), and SR-1 (Cayman, 0.57□M). PDXs were transduced with concentrated lentivirus and plated on irradiated OP9-DL4 cells for in vitro growth assay. Cells were analyzed via FACs for YFP and replated on freshly irradiated OP9-DL4 cells every 3 days, "YFP^{hi}" cells were defined as DAPI^{-}, hCD45^{+}, and top 25% of YFP expression. Transduced YFP^{hi} PDXs cells sorted and

injected (20K cells/mouse) into NSG mice for leukemia initiation studies. The development of leukemia was monitored by flow cytometry (hCD45, YFP). Once the mice were moribund, spleen cells were harvested and analyzed by flow cytometry and qRT-PCR.

Quantitative PCR

The DNA-based qPCR assay to assess *Ets1* deletion efficiency used the following deletion primers that bind Intron 5 between the loxP sequences – Forward: 5'-TCCCGGATCGAACAGAGAAG-3' Reverse: 5'-TCTTGCAGCCTCACCAGATG-3' And the following control primers that bind Intron 33 outside the loxP sequences: Forward: 5'-CTGCGTGTGCGACCTATGAT-3' Reverse: 5'-GATGCACAGAGCGCAGGGACTA-3'. QPCR was quantified using standard curve constructed from serial dilutions of spleen DNA of an $Ets1^{f/f}$ mouse, thus containing decreasing amounts of *Ets1* floxed DNA. For qRT-PCR, total RNA was prepared using the RNeasy Plus Mini kit (Qiagen) according to the manufacturer's protocol. Random-primed total RNAs (0.5 µg) were reverse-transcribed with SuperScript II (Invitrogen). Transcripts were amplified with either TaqMan Universal PCR Master Mix or Power Sybr Green PCR Master Mix (Applied Biosystems) on the Applied Biosystems StepOnePlus (Applied Biosystems). Relative expression of target genes compared to the control was calculated using the delta-delta cycle threshold method with the expression of EF1A or 18S as an internal reference. See Table S5 for sequences of primers that were used or validated primer/probe sets from TaqMan® Gene Expression Assays (Invitrogen).

RNA-Seq

THP-6 cells were transduced with equal titers of concentrated lentivirus in biological quadruplicates with shControl (SHC002, Sigma) or shETS1 (TRCN00005591 or TRCN00001916, Sigma) lentivirus, treated at 48 hours with puromycin (10□g/ml), and harvested after an additional 24 hours. Other THP-6 cells were treated in triplicate with either DMSO or GSI (DBZ from EMD, 1□g/ml) for 24 hours before harvest. Total mRNA was isolated (Qiagen RNeasy), quantified via Nanodrop, and quality measured by Bioanalyzer. At the University of Michigan Sequencing Core, RNA samples with RINs of 8 or greater were prepped with the Illumina TruSeq mRNA Sample Prep v2 kit (Catalog #s RS-122-2001, RS-122-2002) (Illumina). Final libraries were sequenced with 50 cycle single end on a HiSeq 4000 (Illumina) according to manufacturer's protocols. The UM Bioinformatics Core downloaded the reads files from the Sequencing Core's storage, and concatenated those into a single .fastq file for each sample. The quality of the raw reads data was checked for each sample using FastQC (version v0.11.3) to identify features of the data that may indicate quality problems (e.g. low quality scores, over-represented sequences, inappropriate GC content). The Bioinformatics Core used the Tuxedo Suite software package for alignment, differential expression analysis, and post-analysis diagnostics (Langmead et al. 2009, Trapnell et al. 2013, Draghici et al. 2007). Briefly, they aligned reads to the reference genome including both mRNAs and lncRNAs (UCSC hg19) using TopHat (version 2.0.13) and Bowtie2 (version 2.2.1.). They used default parameter settings for alignment, with the exception of: "--b2-very-sensitive" telling the software to spend extra time searching for valid alignments. They used FastQC for a second round of quality control (post-alignment), to ensure that only high quality data would be input to expression quantitation and differential expression analysis. They ran two different

popular techniques for differential expression analysis: Cufflinks/CuffDiff and HTSeq/DESeq2, using UCSC hg19.fa as the reference genome sequence. For Cufflinks/Cuffdiff (version 2.1.1) for expression quantitation, normalization, and differential expression analysis, the Bioinformatics Core used parameter settings: "--multi-read-correct" to adjust expression calculations for reads that map in more than one locus, as well as "--compatible-hits-norm" and "--upper-quartile–norm" for normalization of expression values. For HTSeq (version 0.6.1) /DESeq2 (version 1.14.1), expression quantitation was performed with HTSeq, to count non-ambiguously mapped reads only. Data were pre-filtered to remove genes with 0 counts in all samples. Normalization and differential expression was performed with DESeq2, using a negative binomial generalized linear model. Plots were generated using variations or alternative representations of native DESeq2 plotting functions, ggplot2, plotly, and other packages within the R environment. Volcano Plots for differential gene expression were generated using R Version 3.6.1, with packages: tidyverse(1.3.0), ggrepel(0.8.1), extrafont(0.17), stringr(1.4.0). For consistency with previous data, Cufflinks/CuffDiff was used for all RNA-Seq data analyses with the exception of volcano plots, which were generated using DESeq2 because of the larger dynamic range of the Q-values. A selection of target genes was validated via qRT-PCR in THP-6 and CEM cell lines. Primers used in this validation are included in Table S5.

Microarray

HPB-ALL cells were transduced with lentivirus encoding shLuciferase (shLUC) or shETS1-4. After transduction, the cells were selected for 5 days in puromycin and live cells were isolated via ficoll gradient the day before experiments. The level of knockdown was verified by qRT-PCR for RNA and by Western blot. Total RNA was extracted using the RNeasy Micro Kit (Qiagen)

according to the manufacturer's protocol. 10ng of RNA from each sample was amplified using the Ovation PicoSL WTA System (NuGen), labeled by the Encore BiotinIL Module (NuGen). Following fragmentation, cDNA was hybridized for 20 hr at 48C to Affymetrix Human Genome U133 Plus 2.0 arrays (with 54,673 probe-sets). Arrays were scanned using the Affymetrix Gene Atlas system. Log2 RNA abundances estimated using gcRMA algorithms (Wu et al. 2004) as implemented in the Affy package of the R statistical computing environment. Two samples each of shETS1-4 and shLUC were compared using two-sample T-tests on the log-transformed data, and fold-changes were computed as the anti-logarithms of the differences in means of the log-transformed data. Gene set enrichment analysis (GSEA) was performed using a previously published list of 250 target genes that were differentially regulated by GSI treatment and were shared among seven human T-ALL cell lines (Palomero et al. 2006a). The top 28 leading edge genes with the lowest fold change ratio (shETS1-4/shLUC) were identified in Fig. 5E (red box). We plotted the RNA-Seq Cufflinks/CuffDiff data for the shControl vs shETS1-3/2 using log2(FPKM +0.1) for each gene, where FPKM is the fragments per kilobase of transcript per million reads. For heatmaps, the "ratio" shown is based on the difference of the log-transformed data for each sample from the midpoint of the two means of the log-transformed data for the controls and the treated conditions in that experiment. The color legend to the heatmaps shows the anti-logs of the differences.

ChIP qPCR

THP-6 or CEM cells were transduced with shControl (SHC002, Sigma), shETS1-3 (TRCN00005591, Sigma), or shETS1-2 (TRCN00001916, Sigma) lentivirus, treated at 48 hours with puromycin (10ug/ml), and harvested after an additional 48 hours. Crosslinking was performed

with either formaldehyde alone (for NOTCH1 (ICN1), ZMIZ1, RBPJ, and H3K27Ac ChIPs) or a DSG and formaldehyde method (ETS1 ChIP). In the formaldehyde-alone method, 10 million cells were resuspended in 10ml of 2% FBS DPBS, at either 25°C (H3K27Ac) or 37°C (ICN1, ZMIZ1, RBPJ). Formaldehyde (1%, Thermo-Fisher) was added to the solution, and the samples were incubated with shaking for 10 minutes at either 25°C (H3K27Ac) or 37°C (ICN1, ZMIZ1, RBPJ). Crosslinking was quenched with glycine buffer (125mM) with shaking for 10 minutes. Samples were washed 2x in ice cold DPBS and snap frozen. In the DSG and formaldehyde method, 10 million cells were resuspended in 10 ml 2% FBS DPBS at 25°C. Crosslinking was performed in a 0.6mM DSG (Thermo Scientific) solution with shaking at 25°C for 30 minutes. Formaldehyde (1%, Thermo-Fisher) was added to the solution with shaking for 10 minutes at 25°C. Crosslinking was quenched with glycine buffer (125mM) with shaking for 10 minutes. Samples were washed 2x with ice cold DPBS and snap frozen. Frozen cell pellets were thawed for 15 minutes on ice before lysis with 1ml of cytoplasmic lysis buffer + protease inhibitors (20 mM Tris-HCl ph8.0, 85 mM KCl, 0.5% NP40) for 10 minutes on ice. Nuclei were pelleted via centrifugation for 5 minutes at 3000 x g and resuspended in 150ul of 0.6% SDS lysis buffer + protease inhibitors (0.6% SDS, 10mM EDTA, 50mM Tris-HCl, pH 8.1). Samples were lysed on ice for 10 minutes, diluted to 0.3% SDS with 150ul lysis buffer (10mM EDTA, 50mM Tris-HCl, pH 8.1), homogenized by 27 gauge needle two times, and chromatin sheared via Q800 sonicator (Qsonica) with 70% amplitude, 30 second pulse, 20 minutes of active time (for ICN1, ZMIZ1, RBPJ, and ETS1 ChIPs) or 50% amplitude, 30 second pulse, 10 minutes of active time (for H3K27Ac), with a water bath set to 8°C. Samples were centrifuged at 17,000xg for 8 minutes to remove debris, diluted with 700ul of dilution buffer (0.01% SDS, 1.1% Triton X-100, 1.2mM EDTA, 16.7mM Tris-HCl, pH 8.1, 167mM NaCl), and incubated with antibody overnight at 4°C with rotation. Dynabeads Protein G

(Invitrogen, 10003D) were washed with RIPA buffer (0.1% DOC, 0.1% SDS, 1% Triton x-100, 10mM Tris-HCl pH 8.0, 1mM EDTA, 140 Mm NaCl), added to samples (40 µl), and incubated for 4hr at 4°C with rotation. Samples were then washed 6x in RIPA buffer (0.1% DOC, 0.1% SDS, 1% Triton x-100, 10mM Tris-HCl pH 8.0, 1mM EDTA, 140 Mm NaCl), 2x with high salt RIPA buffer (0.1% DOC, 0.1% SDS, 1% Triton x-100, 10mM Tris-HCl pH 8.0, 1mM EDTA, 360 mM NaCl), 2x with LiCl Wash Buffer (250mM LiCl, 0.5% NP40, 0.5% deoxycholate, 1mM EDTA, 10mM Tris-HCl, pH 8.0), and 2x with TE Buffer (10mM Tris-HCl pH 8.0, 1mM EDTA). Elution and reverse crosslinking were performed by incubating the beads at 65°C for 6 hr with low SDS elution buffer (10mM Tris-HCl pH 8.0, 1 mM EDTA, 300mM NaCl, 0.1% SDS) with 5mM DTT (Sigma). Samples were treated with RNAse (Roche Cat #11119915001), followed Proteinase K (0.3125ng/ul Thermo Cat#AM2546) treatment, and DNA was isolated by SPRI purification (AmpureXP, Beckman Coulter). Concentration was measured using the Quant-IT dsDNA HS assay kit (Promega). Input ladders (1%, 0.1%, and 0.01%) were prepared from input chromatin pulled prior to immunoprecipitation. Eluted ChIP DNA was diluted 1:1. 2ul was added to each qRT-PCR reaction. Target regions were amplified with POWER SybrGreen PCR Master Mix (Applied Biosystems) on the Applied Biosystems StepOnePlus (Applied Biosystems). The primers used are in Table S5.

ChIP-Seq library preparation and sequencing

ChIP chromatin was prepared from as described above from THP-6 cells in biological duplicates with shControl (SHC002, Sigma), shETS1-3 (TRCN00005591, Sigma), or shETS1-2 (TRCN00001916, Sigma), treated at 48 hours with puromycin and harvested after an additional 48 hours. ChIP-Seq libraries were prepared as previously described(Ryan et al. 2015). Briefly,

ChIP DNA was end-repaired (End-It, Epicentre), A-tailed (Klenow fragment 3'-->5' exo-, New England Biolabs), and ligated to barcoded Illumina adaptors (Quick T4 DNA ligase, NEB; adaptors produced by KAPA). Each reaction was followed by clean-up with SPRI beads (AmpureXP, Beckman Coulter). Ligation products were amplified by 14 cycles of PCR with Illumina indexing primers and PFU Ultra II HS PCR mix (Agilent). Library size selection for 300-600 bp chromatin was performed using two-step SPRI bead selection (AmpureXP, Beckman Coulter). Library size was confirmed via Tapestation D1000 (Agilent). Final libraries were sequenced with 75 cycle paired end (38bp x 2) on a Nextseq (Illumina) according to manufacturer's protocols.

ChIP-Seq alignment, filtering, track generation, peak calling, and overlaps

Reads were aligned to the hg19 genome assembly using bwa-aln (bwa version 0.7.12). Data were filtered to remove PCR duplicates and reads mapping to >2 genomic sites. All peak sets were also post-filtered for known ENCODE blacklist regions (available at http://hgdownload.cse.ucsc.edu/goldenpath/hg19/encodeDCC/wgEncodeMapability/ wgEncodeDacMapabilityConsensusExcludable.bed.gz). Filtered bam files were marked as "pruned bam files". Next, bigwig display files were generated with igvtools count and deepTools bamCoverage. Bed peak files were generated with HOMER findPeaks ("style -factor" for transcription factors) (Heinz et al. 2010, Robinson et al. 2011, Ramírez et al. 2016). Scaling for all ChIP-Seq tracks in the figures is equal to local paired-end fragment coverage x (1,000,000 / totalCount). To determine overlaps between ETS1, NOTCH1, ZMIZ1, and RBPJ peaks, we first concatenated the two shControl bioreplicates for each transcription factor, using mergeBed in BEDTools (Quinlan and Hall 2010). We then identified the total number of peaks for each

transcription factor as well as the overlaps between the transcription factors using intersectBed in BEDTools. These data were then plotted in a Venn diagram using Microsoft Excel.

Identification of high confidence ETS1 direct target genes

To identify high confidence ETS1 direct target genes, we concatenated peaks from the two shControl ETS1 ChIP-Seq biological replicates and merged overlapping ones using mergeBed in BEDTools (Quinlan and Hall 2010). We performed differential binding analysis comparing shETS1-3 or shETS1-2 versus shControl, using DiffBind (2.14.0) (http://bioconductor.org/packages/release/bioc/vignettes/DiffBind/inst/doc/DiffBind.pdf) (Ross-Innes et al. 2012). Since DiffBind can use either DESeq2 or edgeR to do normalization and differential tests, it was run twice to generate results from both methods. The DESeq2 method was used as it identified more differentially regulated peaks than edgeR. We defined "Dynamic ETS1 Peaks" as ETS1 peaks that gave FDR<0.1 for the shControl versus shETS1-3 comparison and the shControl versus shETS1-2 comparison. Next, we extracted from the RNA-Seq data in THP-6 cells (above) the differentially expressed genes (DEGs) that were shared between the shControl vs shETS1-3 and shControl vs shETS1-2 comparisons requiring Q<0.05 in both and the changing direction to be the same. We extracted topologically associating domains (TADs) based on Hi-C data in CUTLL1 cells (GSE134761) (Kloetgen et al. 2019). For each dynamic ETS1 peak, we found the TAD(s) it intersected with and the DEGs that intersected with the same TAD(s) using intersectBed in BEDTools. TAD boundaries were first extended to cover the flanking gaps. These DEGs were designated as high-confidence direct NOTCH1 target genes as they were linked to at least one ETS1 dynamic peak within the same TAD as the DEG. Dynamic ETS1 peaks that overlapped with two adjacent TADs were assigned to both TADs. DEGs that overlapped with two

adjacent TADs were assigned to both TADs. We also extracted H3K27ac Hi-ChIP intervals in CUTLL1 cells (GSE134761) (Kloetgen et al. 2019). We filtered the DEGs to only include those DEGs with TSS within Hi-ChIP intervals that were linked to another Hi-ChIP interval that contained at least one dynamic ETS1 peaks using R version 3.6.1 with tidyverse(1.3.0). The DEGs linked to dynamic ETS1 peaks within the same TAD and the filtered DEGs that were additionally linked to dynamic ETS1 peaks through H3K27ac Hi-ChIP were listed in separate tabs in Table S4.

Comparative ChIP-Seq analysis

To determine differential binding of Notch complex members and differential H3K27ac signals, we created a set of union intervals by merging the bed files for the ETS1, NOTCH1, RBPJ, and ZMIZ1 peaks. Narrow windows for transcription factors were 200bp, centered on the union interval peak. Broad windows for H3K27Ac were 2000bp, centered on the union interval peak. For each of the union intervals, we found the intersection counts and overlap fraction from each factor's peak sets, using annotateBed in BEDTools (Quinlan and Hall 2010). We used annotatedPeaks.pl in HOMER to calculate normalized tag count distribution surrounding the interval centers. DiffBind (2.14.0) was run twice to generate results using both DESeq2 and edgeR methods. DESeq2 was used for ETS1 and H3K27Ac ChIP-Seq data. edgeR was used for ICN1, RBPJ, and ZMIZ1 ChIP-Seq data. Binding/H3K27ac quantitation and differential binding/H3K27ac analysis were then obtained (Ross-Innes et al. 2012). For violin plot analyses, we defined transcription factor peaks as union intervals that intersected with at least one peak of that transcription factor in at least one control bioreplicate. Unless otherwise indicated, we defined "dynamic ETS1 peaks" as union intervals that intersected with at least one ETS1 peak in at least one control bioreplicate and that gave FDR<0.1 for the shControl versus shETS1-3 comparison

and the shControl versus shETS1-2 comparison. Likewise, we defined dynamic ICN1, RBPJ, and ZMIZ1 peaks as union intervals that intersected at least one peak of that factor in at least one control bioreplicate and gave FDR<0.1 for the shControl versus shETS1-3 comparison and the shControl versus shETS1-2 comparison. To generate metagene plots, two interval sets were selected: (a) "All Peaks" = intervals that intersect with at least one peak of that factor in all of the shETS1 bioreplicates (shETS1-3 and shETS1-2) or intersect with at least one peak of that factor in both shControl replicates; (b) intervals from (a) that intersect with at least one dynamic ETS1 peak. To generate metagene plots in Fig. S6D-E, we used annotatedPeaks.pl in HOMER to calculate normalized tag count distribution surrounding the interval centers for each of the two groups (a and b) above, and plotted them using R. We also calculated the normalized tag count distribution for (c) the broader H3K27ac intervals that intersected with at least one ETS1 peak in all of the shETS1 bioreplicates (shETS1-3 and shETS1-2) or intersected at least one ETS1 peak in both shControl replicates; (d) broad intervals from (c) that intersected with at least one dynamic ETS1 peak. Volcano plots for ETS1 ChIP-Seq differential binding were generated using R Version 3.6.1, with packages: tidyverse(1.3.0), ggrepel(0.8.1), extrafont(0.17), stringr(1.4.0). De novo DNA motif enrichment analysis was performed with HOMER findMotifs, using findMotifsGenome.pl with a setting of -size 200. The background peakset was HOMER-generated and GC content normalized. Known motif analysis was performed with the HOMER motif library version 4.10.4, using two sets of peaks: (1) peaks identified as differentially bound by the given transcription factor in both the shETS1-3 and shETS1-2 treated cells (vs shControl, FDR<0.1); (2) peaks that were NOT identified as differentially bound by the given transcription factor in either the shETS1-3 or shETS1-2 comparison (vs shControl, FDR>0.1). To obtain P-values for the enrichment of the GATA family motif in the first peakset versus the second peakset, we inputted

the first peakset as the “target” peaks and the second peakset as the “background” peaks and the known motif Gata4(Zf)/Heart-Gata4-ChIP-Seq(GSE35151) into the HOMER findMotifsGenome.pl command. The HOMER (v4.10.4) annotatePeaks program was used to find tag intensities for both the CEM and Jurkat GATA3 peaks. Using bedtools (v2.26.0) intersect, peaks from each transcription factor that overlap with a CEM or Jurkat GATA3 peak were found. This data was merged in R (v3.6.1) using the tidyverse (v1.3.0) package, associating a GATA3 peak tag intensity with each transcription factor tag. In Galaxy v20.01, the GATA3 bigwigs were used with the coordinating TF peak data beds to create correlation matrices using deepTools computeMatrix, v 3.3.0. From there, the correlation matrices were turned into metagene plots using deepTools plotHeatmap, v3.3.0.

Signal-to-noise calculations

Using Galaxy Version 1.9, samtools Version 1.9, and bedtools v2.29.0, we constructed the following workflow to determine signal-to-noise for all control transcription factor ChIP-Seq data. Step 1: Create the signal bam using samtools view (input: pruned bam file and bed file containing the control transcription factor peaks). Step 2: Convert the pruned bam file to a bed file using bedtools BAM to BED (input: pruned bam file). Step 3: Create the noise bed using bedtools subtract (input: Step 2 output and bed file containing the control transcription factor peaks). Step 4: Create the noise bam using bedtools BED to BAM (input: Step 3 output). Step 5: Count the pruned merged bam file using samtools view (input: pruned bam file). Step 6: Count the signal bam using samtools view (input: Step 1 output). Step 7: Count the noise bam using samtools view (input: Step 4 output). We then divided the signal bam counts by the noise bam counts to derive the following signal-to-noise ratios for the control transcription factor ChIP-Seq data:

ETS1_shControl-a 0.0408; ETS1_shControl-b 0.0363; ICN1_shControl-a 0.00458; ICN1_shControl-b .00597; RBPJ _shControl-a 0.00976; RBPJ _shControl-b 0.0150; ZMIZ1_shControl-a 0.0152; ZMIZ1_shControl-b 0.0258. “a” and “b” represent bioreplicates.

Correlating ChIP-Seq data with publicly available ChIP-Seq data

For apples-to-apples comparisons, we re-analyzed previously published ETS1, NOTCH1, RBPJ, and H3K27ac ChIP-Seq data from CUTLL1 cells (GSE51800 and GSE29600) and ETS1 ChIP-Seq data from Jurkat cells (GSE17954) to compare against our THP-6 ChIP-Seq data, using the same pipeline described above for the THP-6 ChIP-Seq data. We compared our shControl ETS1 merged peakset (see above) with the CUTLL1 ETS1 peakset, using intersectBed in BEDTools. This data was then plotted in a Venn diagram in Microsoft Excel. Metagene plots and heatmaps at the 24,552 ETS1 intervals were generated using Galaxy version 19.09, with use of computeMatrix 3.30 and plotHeatmap 3.30, both from deepTools. We used the coolwarm colormap, and the sort was based on the decreasing mean value per region from the ETS1 THP-6_1 file. To obtain correlation coefficients, we used deepTools to obtain raw read scores using the multiBigwigSummary function at the 24,552 ETS1 intervals and used the plotCorrelation function to produce pairwise correlations of the ETS1 THP6_1 file to the other files using the Spearman correlation methods. The correlation heatmap was created with ggplot and R 3.6.1 with tidyverse 1.3.0 and reshape2 1.4.3.

Deposition of sequences

The high-throughput sequencing and microarray data were deposited in the Gene Expression Omnibus database with accession GSE138660 for the SuperSeries. SubSeries include GSE138516 (ChIP-Seq), GSE138659 (RNA-Seq), and GSE138803 (microarray), The data is accessible to reviewers using the following token: gnspeuckxhwtvur.

Additional statistical information

Unless otherwise indicated, P-values were derived from two-sided two-sample t-tests of Log2-transformed data for comparisons in experiments involving two groups and 1-way ANOVA of Log2-transformed data for pairwise contrasts in experiments with more than two groups. Unless otherwise stated, horizontal lines are means and values are shown as mean $\pm$ standard deviation. Survival curves (or time to event data) was tested with log-rank tests comparing pairs of groups. For enrichment analysis using MSigDB (Liberzon et al. 2011), P-values were one-sided Fisher exact tests of the intersection of two gene lists. False discovery rates (FDRs) were computed based on 100 data sets in which the gene labels were randomly permuted. For Cuffdiff2, the linear fold change was the ratio of the average FPKMs for the two groups and the Benjamini–Hochberg procedure was used to calculate FDR or adjusted P-value (Q). Fold change for the "NOTCH1 dataset" is the FPKM read count ratio of GSI-treated THP-6 cells divided by DMSO-treated THP-6 cells. Fold change for the "ETS1 dataset" is the FPKM read count ratio of shETS1-2 or shETS1-3-transduced THP-6 cells divided by shControl-transduced THP-6 cells. For microarray analysis,

we picked the probe-set of each gene that gave the small p-value for comparisons. Fold change for the HPB-ALL microarray dataset was ratio of the geometric means for shETS1-4 and shLUC.

Bibliography

Abraham, N., M. C. Ma, J. W. Snow, M. J. Miners, B. G. Herndier & M. A. Goldsmith (2005) Haploinsufficiency identifies STAT5 as a modifier of IL-7-induced lymphomas. *Oncogene,* 24**,** 5252-7.

Agnusdei, V., S. Minuzzo, C. Frasson, A. Grassi, F. Axelrod, S. Satyal, A. Gurney, T. Hoey, E. Seganfreddo, G. Basso, S. Valtorta, R. M. Moresco, A. Amadori & S. Indraccolo (2014) Therapeutic antibody targeting of Notch1 in T-acute lymphoblastic leukemia xenografts. *Leukemia,* 28**,** 278-88.

Allman, D., F. G. Karnell, J. A. Punt, S. Bakkour, L. Xu, P. Myung, G. A. Koretzky, J. C. Pui, J. C. Aster & W. S. Pear (2001) Separation of Notch1 promoted lineage commitment and expansion/transformation in developing T cells. *J Exp Med,* 194**,** 99-106.

Allman, D., A. Sambandam, S. Kim, J. P. Miller, A. Pagan, D. Well, A. Meraz & A. Bhandoola (2003) Thymopoiesis independent of common lymphoid progenitors. *Nat Immunol,* 4**,** 168-74.

Anderson, M. K., G. Hernandez-Hoyos, R. A. Diamond & E. V. Rothenberg (1999) Precise developmental regulation of Ets family transcription factors during specification and commitment to the T cell lineage. *Development,* 126**,** 3131-48.

Andersson, E. R. & U. Lendahl (2014) Therapeutic modulation of Notch signalling--are we there yet? *Nat Rev Drug Discov,* 13**,** 357-78.

Antony-Debré, I., A. Paul, J. Leite, K. Mitchell, H. M. Kim, L. A. Carvajal, T. I. Todorova, K. Huang, A. Kumar, A. A. Farahat, B. Bartholdy, S.-R. Narayanagari, J. Chen, A. Ambesi-Impiombato, A. A. Ferrando, I. Mantzaris, E. Gavathiotis, A. Verma, B. Will, D. W. Boykin, W. D. Wilson, G. M. K. Poon & U. Steidl (2017) Pharmacological inhibition of the transcription factor PU.1 in leukemia. *The Journal of Clinical Investigation,* 127**,** 4297-4313.

Armstrong, F., P. Brunet de la Grange, B. Gerby, M. C. Rouyez, J. Calvo, M. Fontenay, N. Boissel, H. Dombret, A. Baruchel, J. Landman-Parker, P. H. Romeo, P. Ballerini & F. Pflumio (2009) NOTCH is a key regulator of human T-cell acute leukemia initiating cell activity. *Blood,* 113**,** 1730-40.

Asnafi, V., A. Buzyn, S. Le Noir, F. Baleydier, A. Simon, K. Beldjord, O. Reman, F. Witz, T. Fagot, E. Tavernier, P. Turlure, T. Leguay, F. Huguet, J. P. Vernant, F. Daniel, M. C. Bene, N. Ifrah, X. Thomas, H. Dombret & E. Macintyre (2009) NOTCH1/FBXW7 mutation identifies a large subgroup with favorable outcome in adult T-cell acute lymphoblastic leukemia (T-ALL): a Group for Research on Adult Acute Lymphoblastic Leukemia (GRAALL) study. *Blood,* 113**,** 3918-24.

Aste-Amezaga, M., N. Zhang, J. E. Lineberger, B. A. Arnold, T. J. Toner, M. Gu, L. Huang, S. Vitelli, K. T. Vo, P. Haytko, J. Z. Zhao, F. Baleydier, S. L'Heureux, H. Wang, W. R. Gordon, E. Thoryk, M. B. Andrawes, K. Tiyanont, K. Stegmaier, G. Roti, K. N. Ross, L. L. Franlin, F. Wang, M. Chastain, A. J. Bett, L. P. Audoly, J. C. Aster, S. C. Blacklow & H. E. Huber (2010) Characterization of Notch1 antibodies that inhibit signaling of both normal and mutated Notch1 receptors. *PLoS One,* 5**,** e9094.

Aster, J. C., W. S. Pear & S. C. Blacklow (2008) Notch signaling in leukemia. *Annu Rev Pathol,* 3**,** 587-613.

Aster, J. C., L. Xu, F. G. Karnell, V. Patriub, J. C. Pui & W. S. Pear (2000) Essential roles for ankyrin repeat and transactivation domains in induction of T-cell leukemia by notch1. *Mol Cell Biol,* 20**,** 7505-15.

Augustijn, K. D., D. L. Duval, R. Wechselberger, R. Kaptein, A. Gutierrez-Hartmann & P. C. van der Vliet (2002) Structural characterization of the PIT-1/ETS-1 interaction: PIT-1 phosphorylation regulates PIT-1/ETS-1 binding. *Proceedings of the National Academy of Sciences of the United States of America,* 99**,** 12657-12662.

Avellino, R., S. Romano, R. Parasole, R. Bisogni, A. Lamberti, V. Poggi, S. Venuta & M. F. Romano (2005) Rapamycin stimulates apoptosis of childhood acute lymphoblastic leukemia cells. *Blood,* 106**,** 1400-6.

Bailis, W., Y. Yashiro-Ohtani & W. S. Pear (2014) Identifying direct Notch transcriptional targets using the GSI-washout assay. *Methods Mol Biol,* 1187**,** 247-54.

Bain, G., I. Engel, E. C. Robanus Maandag, H. P. te Riele, J. R. Voland, L. L. Sharp, J. Chun, B. Huey, D. Pinkel & C. Murre (1997) E2A deficiency leads to abnormalities in alphabeta T-cell development and to rapid development of T-cell lymphomas. *Mol Cell Biol,* 17**,** 4782-91.

Bain, G., E. C. Maandag, D. J. Izon, D. Amsen, A. M. Kruisbeek, B. C. Weintraub, I. Krop, M. S. Schlissel, A. J. Feeney, M. van Roon & et al. (1994) E2A proteins are required for proper B cell development and initiation of immunoglobulin gene rearrangements. *Cell,* 79**,** 885-92.

Barata, J. T., T. D. Keenan, A. Silva, L. M. Nadler, V. A. Boussiotis & A. A. Cardoso (2004) Common gamma chain-signaling cytokines promote proliferation of T-cell acute lymphoblastic leukemia. *Haematologica,* 89**,** 1459-67.

Barton, K., N. Muthusamy, C. Fischer, C. N. Ting, T. L. Walunas, L. L. Lanier & J. M. Leiden (1998) The Ets-1 transcription factor is required for the development of natural killer cells in mice. *Immunity,* 9**,** 555-63.

Bassuk, A. G. & J. M. Leiden (1995) A direct physical association between ETS and AP-1 transcription factors in normal human T cells. *Immunity,* 3**,** 223-37.

Bellacosa, A., K. Datta, S. E. Bear, C. Patriotis, P. A. Lazo, N. G. Copeland, N. A. Jenkins & P. N. Tsichlis (1994) Effects of provirus integration in the Tpl-1/Ets-1 locus in Moloney murine leukemia virus-induced rat T-cell lymphomas: levels of expression, polyadenylation, transcriptional initiation, and differential splicing of the Ets-1 mRNA. *J Virol,* 68**,** 2320-30.

Bellavia, D., A. F. Campese, E. Alesse, A. Vacca, M. P. Felli, A. Balestri, A. Stoppacciaro, C. Tiveron, L. Tatangelo, M. Giovarelli, C. Gaetano, L. Ruco, E. S. Hoffman, A. C. Hayday, U. Lendahl, L. Frati, A. Gulino & I. Screpanti (2000) Constitutive activation of NF-kappaB and T-cell leukemia/lymphoma in Notch3 transgenic mice. *Embo j,* 19**,** 3337-48.

Bellavia, D., A. F. Campese, S. Checquolo, A. Balestri, A. Biondi, G. Cazzaniga, U. Lendahl, H. J. Fehling, A. C. Hayday, L. Frati, H. von Boehmer, A. Gulino & I. Screpanti (2002) Combined expression of pTalpha and Notch3 in T cell leukemia identifies the requirement of preTCR for leukemogenesis. *Proc Natl Acad Sci U S A,* 99**,** 3788-93.

Bellavia, D., M. Mecarozzi, A. F. Campese, P. Grazioli, C. Talora, L. Frati, A. Gulino & I. Screpanti (2007) Notch3 and the Notch3-upregulated RNA-binding protein HuD regulate Ikaros alternative splicing. *Embo j,* 26**,** 1670-80.

Belver, L., A. Y. Yang, R. Albero, D. Herranz, F. G. Brundu, S. A. Quinn, P. Perez-Duran, S. Alvarez, F. Gianni, M. Rashkovan, D. Gurung, P. P. Rocha, R. Raviram, C. Reglero, J. R.

Cortes, A. J. Cooke, A. A. Wendorff, V. Cordo, J. P. Meijerink, R. Rabadan & A. A. Ferrando (2019) Gata3-controlled nucleosome eviction drives Myc enhancer activity in T-cell development and leukemia. *Cancer Discov*.

Benyoucef, A., C. G. Palii, C. Wang, C. J. Porter, A. Chu, F. Dai, V. Tremblay, P. Rakopoulos, K. Singh, S. Huang, F. Pflumio, J. Hebert, J. F. Couture, T. J. Perkins, K. Ge, F. J. Dilworth & M. Brand (2016) UTX inhibition as selective epigenetic therapy against TAL1-driven T-cell acute lymphoblastic leukemia. *Genes Dev,* 30**,** 508-21.

Bernasconi-Elias, P., T. Hu, D. Jenkins, B. Firestone, S. Gans, E. Kurth, P. Capodieci, J. Deplazes-Lauber, K. Petropoulos, P. Thiel, D. Ponsel, S. Hee Choi, P. LeMotte, A. London, M. Goetcshkes, E. Nolin, M. D. Jones, K. Slocum, M. J. Kluk, D. M. Weinstock, A. Christodoulou, O. Weinberg, J. Jaehrling, S. A. Ettenberg, A. Buckler, S. C. Blacklow, J. C. Aster & C. J. Fryer (2016) Characterization of activating mutations of NOTCH3 in T-cell acute lymphoblastic leukemia and anti-leukemic activity of NOTCH3 inhibitory antibodies. *Oncogene,* 35**,** 6077-6086.

Berquam-Vrieze, K. E., K. Nannapaneni, B. T. Brett, L. Holmfeldt, J. Ma, O. Zagorodna, N. A. Jenkins, N. G. Copeland, D. K. Meyerholz, C. M. Knudson, C. G. Mullighan, T. E. Scheetz & A. J. Dupuy (2011) Cell of origin strongly influences genetic selection in a mouse model of T-ALL. *Blood,* 118**,** 4646-56.

Beverly, L. J. & A. J. Capobianco (2003) Perturbation of Ikaros isoform selection by MLV integration is a cooperative event in Notch(IC)-induced T cell leukemogenesis. *Cancer Cell,* 3**,** 551-64.

Beverly, L. J., D. W. Felsher & A. J. Capobianco (2005) Suppression of p53 by Notch in lymphomagenesis: implications for initiation and regression. *Cancer Res,* 65**,** 7159-68.

Bhandoola, A. & A. Sambandam (2006) From stem cell to T cell: one route or many? *Nat Rev Immunol,* 6**,** 117-26.

Bhat, N. K., R. J. Fisher, S. Fujiwara, R. Ascione & T. S. Papas (1987) Temporal and tissue-specific expression of mouse ets genes. *Proc Natl Acad Sci U S A,* 84**,** 3161-5.

Bhat, N. K., K. L. Komschlies, S. Fujiwara, R. J. Fisher, B. J. Mathieson, T. A. Gregorio, H. A. Young, J. W. Kasik, K. Ozato & T. S. Papas (1989) Expression of ets genes in mouse thymocyte subsets and T cells. *J Immunol,* 142**,** 672-8.

Bonnet, M., M. Loosveld, B. Montpellier, J. M. Navarro, B. Quilichini, C. Picard, J. Di Cristofaro, C. Bagnis, C. Fossat, L. Hernandez, E. Mamessier, S. Roulland, E. Morgado, C. Formisano-Treziny, W. A. Dik, A. W. Langerak, T. Prebet, N. Vey, G. Michel, J. Gabert, J. Soulier, E. A. Macintyre, V. Asnafi, D. Payet-Bornet & B. Nadel (2011) Posttranscriptional deregulation of MYC via PTEN constitutes a major alternative pathway of MYC activation in T-cell acute lymphoblastic leukemia. *Blood,* 117**,** 6650-9.

Borggrefe, T. & R. Liefke (2012) Fine-tuning of the intracellular canonical Notch signaling pathway. *Cell Cycle,* 11**,** 264-76.

Bories, J. C., D. M. Willerford, D. Grevin, L. Davidson, A. Camus, P. Martin, D. Stehelin & F. W. Alt (1995) Increased T-cell apoptosis and terminal B-cell differentiation induced by inactivation of the Ets-1 proto-oncogene. *Nature,* 377**,** 635-8.

Borkin, D., S. He, H. Miao, K. Kempinska, J. Pollock, J. Chase, T. Purohit, B. Malik, T. Zhao, J. Wang, B. Wen, H. Zong, M. Jones, G. Danet-Desnoyers, M. L. Guzman, M. Talpaz, D. L. Bixby, D. Sun, J. L. Hess, A. G. Muntean, I. Maillard, T. Cierpicki & J. Grembecka (2015) Pharmacologic inhibition of the menin-MLL interaction blocks progression of MLL leukemia invivo. *Cancer Cell,* 27**,** 589-602.

Boyman, O. & J. Sprent (2012) The role of interleukin-2 during homeostasis and activation of the immune system. *Nat Rev Immunol,* 12**,** 180-90.
Bray, S. J. (2016) Notch signalling in context. *Nat Rev Mol Cell Biol,* 17**,** 722-735.
Bretones, G., M. D. Delgado & J. Leon (2015) Myc and cell cycle control. *Biochim Biophys Acta,* 1849**,** 506-16.
Buonamici, S., T. Trimarchi, M. G. Ruocco, L. Reavie, S. Cathelin, B. G. Mar, A. Klinakis, Y. Lukyanov, J. C. Tseng, F. Sen, E. Gehrie, M. Li, E. Newcomb, J. Zavadil, D. Meruelo, M. Lipp, S. Ibrahim, A. Efstratiadis, D. Zagzag, J. S. Bromberg, M. L. Dustin & I. Aifantis (2009) CCR7 signalling as an essential regulator of CNS infiltration in T-cell leukaemia. *Nature,* 459**,** 1000-4.
Callaway, K., W. F. Waas, M. A. Rainey, P. Ren & K. N. Dalby (2010) Phosphorylation of the transcription factor ets-1 by ERK2: Rapid dissociation of ADP and phospho-ets-1. *Biochemistry,* 49**,** 3619-3630.
Campese, A. F., A. I. Garbe, F. Zhang, F. Grassi, I. Screpanti & H. von Boehmer (2006) Notch1-dependent lymphomagenesis is assisted by but does not essentially require pre-TCR signaling. *Blood,* 108**,** 305-10.
Cauchy, P., M. A. Maqbool, J. Zacarias-Cabeza, L. Vanhille, F. Koch, R. Fenouil, M. Gut, I. Gut, M. A. Santana, A. Griffon, J. Imbert, C. Moraes-Cabe, J. C. Bories, P. Ferrier, S. Spicuglia & J. C. Andrau (2016) Dynamic recruitment of Ets1 to both nucleosome-occupied and -depleted enhancer regions mediates a transcriptional program switch during early T-cell differentiation. *Nucleic Acids Res,* 44**,** 3567-85.
Challen, G. A., N. C. Boles, S. M. Chambers & M. A. Goodell (2010) Distinct Hematopoietic Stem Cell Subtypes Are Differentially Regulated by TGF-β1. *Cell Stem Cell,* 6**,** 265-278.
Chan, S. M., A. P. Weng, R. Tibshirani, J. C. Aster & P. J. Utz (2007) Notch signals positively regulate activity of the mTOR pathway in T-cell acute lymphoblastic leukemia. *Blood,* 110**,** 278-86.
Chari, S. & S. Winandy (2008) Ikaros regulates Notch target gene expression in developing thymocytes. *J Immunol,* 181**,** 6265-74.
Chen, X. L., Y. H. Cai, Q. Liu, L. L. Pan, S. L. Shi, X. L. Liu, Y. Chen, J. G. Li, J. Wang, Y. Li, X. F. Li & S. Y. Wang (2018) ETS1 and SP1 drive DHX15 expression in acute lymphoblastic leukaemia. *J Cell Mol Med,* 22**,** 2612-2621.
Chiang, M. Y., O. Shestova, L. Xu, J. C. Aster & W. S. Pear (2013) Divergent effects of supraphysiologic Notch signals on leukemia stem cells and hematopoietic stem cells. *Blood,* 121**,** 905-17.
Chiang, M. Y., Q. Wang, A. C. Gormley, S. J. Stein, L. Xu, O. Shestova, J. C. Aster & W. S. Pear (2016) High selective pressure for Notch1 mutations that induce Myc in T-cell acute lymphoblastic leukemia. *Blood,* 128**,** 2229-2240.
Chiang, M. Y., L. Xu, O. Shestova, G. Histen, S. L'Heureux, C. Romany, M. E. Childs, P. A. Gimotty, J. C. Aster & W. S. Pear (2008) Leukemia-associated NOTCH1 alleles are weak tumor initiators but accelerate K-ras-initiated leukemia. *J Clin Invest,* 118**,** 3181-94.
Chiang, M. Y., M. L. Xu, G. Histen, O. Shestova, M. Roy, Y. Nam, S. C. Blacklow, D. B. Sacks, W. S. Pear & J. C. Aster (2006) Identification of a conserved negative regulatory sequence that influences the leukemogenic activity of NOTCH1. *Mol Cell Biol,* 26**,** 6261-71.
Chiarini, F., F. Fala, P. L. Tazzari, F. Ricci, A. Astolfi, A. Pession, P. Pagliaro, J. A. McCubrey & A. M. Martelli (2009) Dual inhibition of class IA phosphatidylinositol 3-kinase and

mammalian target of rapamycin as a new therapeutic option for T-cell acute lymphoblastic leukemia. *Cancer Res,* 69**,** 3520-8.

Choi, A., A. Illendula, J. A. Pulikkan, J. E. Roderick, J. Tesell, J. Yu, N. Hermance, L. J. Zhu, L. H. Castilla, J. H. Bushweller & M. A. Kelliher (2017) RUNX1 is required for oncogenic Myb and Myc enhancer activity in T-cell acute lymphoblastic leukemia. *Blood,* 130**,** 1722-1733.

Choi, Y. J., X. Li, P. Hydbring, T. Sanda, J. Stefano, A. L. Christie, S. Signoretti, A. T. Look, A. L. Kung, H. von Boehmer & P. Sicinski (2012) The requirement for cyclin D function in tumor maintenance. *Cancer Cell,* 22**,** 438-51.

Choul-li, S., H. Drobecq & M. Aumercier (2009) DNA-dependent protein kinase is a novel interaction partner for Ets-1 isoforms. *Biochemical and Biophysical Research Communications,* 390**,** 839-844.

Chung, J., C. L. Ebens, E. Perkey, V. Radojcic, U. Koch, L. Scarpellino, A. Tong, F. Allen, S. Wood, J. Feng, A. Friedman, D. Granadier, I. T. Tran, Q. Chai, L. Onder, M. Yan, P. Reddy, B. R. Blazar, A. Y. Huang, T. V. Brennan, D. K. Bishop, B. Ludewig, C. W. Siebel, F. Radtke, S. A. Luther & I. Maillard (2017) Fibroblastic niches prime T cell alloimmunity through Delta-like Notch ligands. *J Clin Invest,* 127**,** 1574-1588.

Clappier, E., S. Collette, N. Grardel, S. Girard, L. Suarez, G. Brunie, S. Kaltenbach, K. Yakouben, F. Mazingue, A. Robert, P. Boutard, D. Plantaz, P. Rohrlich, P. van Vlierberghe, C. Preudhomme, J. Otten, F. Speleman, N. Dastugue, S. Suciu, Y. Benoit, Y. Bertrand & H. Cave (2010) NOTCH1 and FBXW7 mutations have a favorable impact on early response to treatment, but not on outcome, in children with T-cell acute lymphoblastic leukemia (T-ALL) treated on EORTC trials 58881 and 58951. *Leukemia,* 24**,** 2023-31.

Clausen, P. A., M. Athanasiou, Z. Chen, K. J. Dunn, Q. Zhang, J. A. Lautenberger, G. Mavrothalassitis & D. G. Blair (1997) ETS-1 induces increased expression of erythroid markers in the pluripotent erythroleukemic cell lines K562 and HEL. *Leukemia,* 11**,** 1224-1233.

Clements, J. L., S. A. John & L. A. Garrett-Sinha (2006) Impaired generation of CD8+ thymocytes in Ets-1-deficient mice. *J Immunol,* 177**,** 905-12.

Coustan-Smith, E., C. G. Mullighan, M. Onciu, F. G. Behm, S. C. Raimondi, D. Pei, C. Cheng, X. Su, J. E. Rubnitz, G. Basso, A. Biondi, C. H. Pui, J. R. Downing & D. Campana (2009) Early T-cell precursor leukaemia: a subtype of very high-risk acute lymphoblastic leukaemia. *Lancet Oncol,* 10**,** 147-56.

Cullion, K., K. M. Draheim, N. Hermance, J. Tammam, V. M. Sharma, C. Ware, G. Nikov, V. Krishnamoorthy, P. K. Majumder & M. A. Kelliher (2009) Targeting the Notch1 and mTOR pathways in a mouse T-ALL model. *Blood,* 113**,** 6172-81.

Cunningham, L., S. Finckbeiner, R. K. Hyde, N. Southall, J. Marugan, V. R. Yedavalli, S. J. Dehdashti, W. C. Reinhold, L. Alemu, L. Zhao, J. R. Yeh, R. Sood, Y. Pommier, C. P. Austin, K. T. Jeang, W. Zheng & P. Liu (2012) Identification of benzodiazepine Ro5-3335 as an inhibitor of CBF leukemia through quantitative high throughput screen against RUNX1-CBFbeta interaction. *Proc Natl Acad Sci U S A,* 109**,** 14592-7.

Dadi, S., S. Le Noir, D. Payet-Bornet, L. Lhermitte, J. Zacarias-Cabeza, J. Bergeron, P. Villarese, E. Vachez, W. A. Dik, C. Millien, I. Radford, E. Verhoeyen, F. L. Cosset, A. Petit, N. Ifrah, H. Dombret, O. Hermine, S. Spicuglia, A. W. Langerak, E. A. Macintyre, B. Nadel, P. Ferrier & V. Asnafi (2012) TLX homeodomain oncogenes mediate T cell

maturation arrest in T-ALL via interaction with ETS1 and suppression of TCRalpha gene expression. *Cancer Cell,* 21**,** 563-76.

Dail, M., Q. Li, A. McDaniel, J. Wong, K. Akagi, B. Huang, H. C. Kang, S. C. Kogan, K. Shokat, L. Wolff, B. S. Braun & K. Shannon (2010) Mutant Ikzf1, KrasG12D, and Notch1 cooperate in T lineage leukemogenesis and modulate responses to targeted agents. *Proc Natl Acad Sci U S A,* 107**,** 5106-11.

de Pooter, R. F., S. Dias, M. Chowdhury, E. T. Bartom, M. K. Okoreeh, M. Sigvardsson & B. L. Kee (2019) Cutting Edge: Lymphomyeloid-Primed Progenitor Cell Fates Are Controlled by the Transcription Factor Tal1. *The Journal of Immunology***,** ji1801220.

Deangelo, D. J., R. M. Stone, L. B. Silverman, W. Stock, E. C. Attar, I. Fearen, A. Dallob, C. Matthews, J. Stone, F. S. J. & J. Aster (2006) A phase I clinical trial of the notch inhibitor MK-0752 in patients with T-cell acute lymphoblastic leukemia/lymphoma (T-ALL) and other leukemias. *Journal of Clinical Oncology, 2006 ASCO Annual Meeting Proceedings,* 24**,** 6585.

Deftos, M. L., Y. W. He, E. W. Ojala & M. J. Bevan (1998) Correlating notch signaling with thymocyte maturation. *Immunity,* 9**,** 777-86.

Deftos, M. L., E. Huang, E. W. Ojala, K. A. Forbush & M. J. Bevan (2000) Notch1 signaling promotes the maturation of CD4 and CD8 SP thymocytes. *Immunity,* 13**,** 73-84.

Della Gatta, G., T. Palomero, A. Perez-Garcia, A. Ambesi-Impiombato, M. Bansal, Z. W. Carpenter, K. De Keersmaecker, X. Sole, L. Xu, E. Paietta, J. Racevskis, P. H. Wiernik, J. M. Rowe, J. P. Meijerink, A. Califano & A. A. Ferrando (2012) Reverse engineering of TLX oncogenic transcriptional networks identifies RUNX1 as tumor suppressor in T-ALL. *Nat Med,* 18**,** 436-40.

Demarest, R. M., N. Dahmane & A. J. Capobianco (2011) Notch is oncogenic dominant in T-cell acute lymphoblastic leukemia. *Blood,* 117**,** 2901-9.

Depew, M. J., J. K. Liu, J. E. Long, R. Presley, J. J. Meneses, R. A. Pedersen & J. L. Rubenstein (1999) Dlx5 regulates regional development of the branchial arches and sensory capsules. *Development,* 126**,** 3831-46.

Dik, W. A., K. Pike-Overzet, F. Weerkamp, D. de Ridder, E. F. de Haas, M. R. Baert, P. van der Spek, E. E. Koster, M. J. Reinders, J. J. van Dongen, A. W. Langerak & F. J. Staal (2005) New insights on human T cell development by quantitative T cell receptor gene rearrangement studies and gene expression profiling. *J Exp Med,* 201**,** 1715-23.

Dittmer, J. (2015) The role of the transcription factor Ets1 in carcinoma. *Semin Cancer Biol,* 35**,** 20-38.

Dohda, T., A. Maljukova, L. Liu, M. Heyman, D. Grander, D. Brodin, O. Sangfelt & U. Lendahl (2007) Notch signaling induces SKP2 expression and promotes reduction of p27Kip1 in T-cell acute lymphoblastic leukemia cell lines. *Exp Cell Res,* 313**,** 3141-52.

Dong, Y., L. Zhang, Y. Bai, H. M. Zhou, A. M. Campbell, H. Chen, W. Yong, W. Zhang, Q. Zeng, W. Shou & Z. Y. Zhang (2014) Phosphatase of regenerating liver 2 (PRL2) deficiency impairs Kit signaling and spermatogenesis. *J Biol Chem,* 289**,** 3799-810.

Dong, Y., L. Zhang, S. Zhang, Y. Bai, H. Chen, X. Sun, W. Yong, W. Li, S. C. Colvin, S. J. Rhodes, W. Shou & Z. Y. Zhang (2012) Phosphatase of regenerating liver 2 (PRL2) is essential for placental development by down-regulating PTEN (Phosphatase and Tensin Homologue Deleted on Chromosome 10) and activating Akt protein. *J Biol Chem,* 287**,** 32172-9.

Draghici, S., P. Khatri, A. L. Tarca, K. Amin, A. Done, C. Voichita, C. Georgescu & R. Romero (2007) A systems biology approach for pathway level analysis. *Genome research,* 17**,** 1537-1545.

Dudley, D. D., H. C. Wang & X. H. Sun (2009) Hes1 potentiates T cell lymphomagenesis by up-regulating a subset of notch target genes. *PLoS One,* 4**,** e6678.

Eberl, G., M. Colonna, J. P. Di Santo & A. N. J. McKenzie (2015) Innate lymphoid cells: A new paradigm in immunology. *Science,* 348**,** aaa6566.

Egawa, T., R. E. Tillman, Y. Naoe, I. Taniuchi & D. R. Littman (2007) The role of the Runx transcription factors in thymocyte differentiation and in homeostasis of naive T cells. *J Exp Med,* 204**,** 1945-57.

Eguchi-Ishimae, M., M. Eguchi, H. Kempski & M. Greaves (2008) NOTCH1 mutation can be an early, prenatal genetic event in T-ALL. *Blood,* 111**,** 376-8.

el Marjou, F., K. P. Janssen, B. H. Chang, M. Li, V. Hindie, L. Chan, D. Louvard, P. Chambon, D. Metzger & S. Robine (2004) Tissue-specific and inducible Cre-mediated recombination in the gut epithelium. *Genesis,* 39**,** 186-93.

Ellisen, L. W., J. Bird, D. C. West, A. L. Soreng, T. C. Reynolds, S. D. Smith & J. Sklar (1991) TAN-1, the human homolog of the Drosophila notch gene, is broken by chromosomal translocations in T lymphoblastic neoplasms. *Cell,* 66**,** 649-61.

Espinosa, L., S. Cathelin, T. D'Altri, T. Trimarchi, A. Statnikov, J. Guiu, V. Rodilla, J. Ingles-Esteve, J. Nomdedeu, B. Bellosillo, C. Besses, O. Abdel-Wahab, N. Kucine, S. C. Sun, G. Song, C. C. Mullighan, R. L. Levine, K. Rajewsky, I. Aifantis & A. Bigas (2010) The Notch/Hes1 pathway sustains NF-kappaB activation through CYLD repression in T cell leukemia. *Cancer Cell,* 18**,** 268-81.

Eyquem, S., K. Chemin, M. Fasseu & J. C. Bories (2004a) The Ets-1 transcription factor is required for complete pre-T cell receptor function and allelic exclusion at the T cell receptor beta locus. *Proc Natl Acad Sci U S A,* 101**,** 15712-7.

Eyquem, S., K. Chemin, M. Fasseu, M. Chopin, F. Sigaux, A. Cumano & J. C. Bories (2004b) The development of early and mature B cells is impaired in mice deficient for the Ets-1 transcription factor. *Eur J Immunol,* 34**,** 3187-96.

Falo-Sanjuan, J. & S. J. Bray (2019) Decoding the Notch signal. *Dev Growth Differ*.

Fasnacht, N., H. Y. Huang, U. Koch, S. Favre, F. Auderset, Q. Chai, L. Onder, S. Kallert, D. D. Pinschewer, H. R. MacDonald, F. Tacchini-Cottier, B. Ludewig, S. A. Luther & F. Radtke (2014) Specific fibroblastic niches in secondary lymphoid organs orchestrate distinct Notch-regulated immune responses. *J Exp Med,* 211**,** 2265-79.

Felsher, D. W. & J. M. Bishop (1999) Reversible tumorigenesis by MYC in hematopoietic lineages. *Mol Cell,* 4**,** 199-207.

Feng, F. Y., J. C. Brenner, M. Hussain & A. M. Chinnaiyan (2014) Molecular pathways: targeting ETS gene fusions in cancer. *Clinical cancer research : an official journal of the American Association for Cancer Research,* 20**,** 4442-4448.

Flossbach, L., K. Holzmann, T. Mattfeldt, M. Buck, K. Lanz, M. Held, P. Moller & T. F. Barth (2013) High-resolution genomic profiling reveals clonal evolution and competition in gastrointestinal marginal zone B-cell lymphoma and its large cell variant. *Int J Cancer,* 132**,** E116-27.

Foulds, C. E., M. L. Nelson, A. G. Blaszczak & B. J. Graves (2004) Ras/mitogen-activated protein kinase signaling activates Ets-1 and Ets-2 by CBP/p300 recruitment. *Molecular and Cellular Biology,* 24**,** 10954-10964.

Fowler, T., P. Ghatak, D. H. Price, R. Conaway, J. Conaway, C. M. Chiang, J. E. Bradner, A. Shilatifard & A. L. Roy (2014) Regulation of MYC expression and differential JQ1 sensitivity in cancer cells. *PLoS One,* 9**,** e87003.

Fryer, C. J., J. B. White & K. A. Jones (2004) Mastermind recruits CycC:CDK8 to phosphorylate the Notch ICD and coordinate activation with turnover. *Mol Cell,* 16**,** 509-20.

Fu, J.-F., T.-H. Yen, Y.-J. Huang & L.-Y. Shih (2019) Ets1 Plays a Critical Role in MLL/EB1-Mediated Leukemic Transformation in a Mouse Bone Marrow Transplantation Model. *Neoplasia (New York, N.Y.),* 21**,** 469-481.

Gao, Z., G. H. Kim, A. C. Mackinnon, A. E. Flagg, B. Bassett, J. U. Earley & E. C. Svensson (2010) Ets1 is required for proper migration and differentiation of the cardiac neural crest. *Development,* 137**,** 1543-51.

Garcia-Ojeda, M. E., R. G. Klein Wolterink, F. Lemaitre, O. Richard-Le Goff, M. Hasan, R. W. Hendriks, A. Cumano & J. P. Di Santo (2013) GATA-3 promotes T-cell specification by repressing B-cell potential in pro-T cells in mice. *Blood,* 121**,** 1749-59.

Geimer Le Lay, A. S., A. Oravecz, J. Mastio, C. Jung, P. Marchal, C. Ebel, D. Dembele, B. Jost, S. Le Gras, C. Thibault, T. Borggrefe, P. Kastner & S. Chan (2014) The tumor suppressor Ikaros shapes the repertoire of notch target genes in T cells. *Sci Signal,* 7**,** ra28.

Ghaedi, M., C. A. Steer, I. Martinez-Gonzalez, T. Y. F. Halim, N. Abraham & F. Takei (2016) Common-Lymphoid-Progenitor-Independent Pathways of Innate and T Lymphocyte Development. *Cell Rep,* 15**,** 471-480.

Giambra, V., C. E. Jenkins, S. H. Lam, C. Hoofd, M. Belmonte, X. Wang, S. Gusscott, D. Gracias & A. P. Weng (2015) Leukemia stem cells in T-ALL require active Hif1α and Wnt signaling. *Blood,* 125**,** 3917-3927.

Giambra, V., C. R. Jenkins, H. Wang, S. H. Lam, O. O. Shevchuk, O. Nemirovsky, C. Wai, S. Gusscott, M. Y. Chiang, J. C. Aster, R. K. Humphries, C. Eaves & A. P. Weng (2012) NOTCH1 promotes T cell leukemia-initiating activity by RUNX-mediated regulation of PKC-theta and reactive oxygen species. *Nat Med,* 18**,** 1693-8.

Gonzalez-Garcia, S., M. Garcia-Peydro, E. Martin-Gayo, E. Ballestar, M. Esteller, R. Bornstein, J. L. de la Pompa, A. A. Ferrando & M. L. Toribio (2009) CSL-MAML-dependent Notch1 signaling controls T lineage-specific IL-7R{alpha} gene expression in early human thymopoiesis and leukemia. *J Exp Med,* 206**,** 779-91.

Gorczynski, M. J., J. Grembecka, Y. Zhou, Y. Kong, L. Roudaia, M. G. Douvas, M. Newman, I. Bielnicka, G. Baber, T. Corpora, J. Shi, M. Sridharan, R. Lilien, B. R. Donald, N. A. Speck, M. L. Brown & J. H. Bushweller (2007) Allosteric inhibition of the protein-protein interaction between the leukemia-associated proteins Runx1 and CBFbeta. *Chem Biol,* 14**,** 1186-97.

Gordon, W. R., M. Roy, D. Vardar-Ulu, M. Garfinkel, M. R. Mansour, J. C. Aster & S. C. Blacklow (2009) Structure of the Notch1-negative regulatory region: implications for normal activation and pathogenic signaling in T-ALL. *Blood,* 113**,** 4381-90.

Gordon, W. R., D. Vardar-Ulu, G. Histen, C. Sanchez-Irizarry, J. C. Aster & S. C. Blacklow (2007) Structural basis for autoinhibition of Notch. *Nat Struct Mol Biol,* 14**,** 295-300.

Grembecka, J., S. He, A. Shi, T. Purohit, A. G. Muntean, R. J. Sorenson, H. D. Showalter, M. J. Murai, A. M. Belcher, T. Hartley, J. L. Hess & T. Cierpicki (2012) Menin-MLL inhibitors reverse oncogenic activity of MLL fusion proteins in leukemia. *Nature Chemical Biology,* 8**,** 277-284.

Grenningloh, R., Y. K. Bok & I. C. Ho (2005) Ets-1, a functional cofactor of T-bet, is essential for Th1 inflammatory responses. *Journal of Experimental Medicine,* 201**,** 615-626.

Grenningloh, R., T. S. Tai, N. Frahm, T. C. Hongo, A. T. Chicoine, C. Brander, D. E. Kaufmann & I. C. Ho (2011) Ets-1 maintains IL-7 receptor expression in peripheral T cells. *J Immunol,* 186**,** 969-76.

Guo, K., J. E. McMinn, T. Ludwig, Y. H. Yu, G. Yang, L. Chen, D. Loh, C. Li, S. Chua, Jr. & Y. Zhang (2007) Disruption of peripheral leptin signaling in mice results in hyperleptinemia without associated metabolic abnormalities. *Endocrinology,* 148**,** 3987-97.

Gutierrez, A., L. Pan, R. W. Groen, F. Baleydier, A. Kentsis, J. Marineau, R. Grebliunaite, E. Kozakewich, C. Reed, F. Pflumio, S. Poglio, B. Uzan, P. Clemons, L. VerPlank, F. An, J. Burbank, S. Norton, N. Tolliday, H. Steen, A. P. Weng, H. Yuan, J. E. Bradner, C. Mitsiades, A. T. Look & J. C. Aster (2014) Phenothiazines induce PP2A-mediated apoptosis in T cell acute lymphoblastic leukemia. *J Clin Invest,* 124**,** 644-55.

Gutierrez, A., T. Sanda, R. Grebliunaite, A. Carracedo, L. Salmena, Y. Ahn, S. Dahlberg, D. Neuberg, L. A. Moreau, S. S. Winter, R. Larson, J. Zhang, A. Protopopov, L. Chin, P. P. Pandolfi, L. B. Silverman, S. P. Hunger, S. E. Sallan & A. T. Look (2009) High frequency of PTEN, PI3K, and AKT abnormalities in T-cell acute lymphoblastic leukemia. *Blood,* 114**,** 647-50.

Hahne, J. C., A. F. Okuducu, T. Fuchs, A. Florin & N. Wernert (2011) Identification of ETS-1 target genes in human fibroblasts. *International Journal of Oncology,* 38**,** 1645-1652.

Hattori, N., H. Kawamoto, S. Fujimoto, K. Kuno & Y. Katsura (1996) Involvement of transcription factors TCF-1 and GATA-3 in the initiation of the earliest step of T cell development in the thymus. *J Exp Med,* 184**,** 1137-47.

Heinz, S., C. Benner, N. Spann, E. Bertolino, Y. C. Lin, P. Laslo, J. X. Cheng, C. Murre, H. Singh & C. K. Glass (2010) Simple combinations of lineage-determining transcription factors prime cis-regulatory elements required for macrophage and B cell identities. *Mol Cell,* 38**,** 576-89.

Herranz, D., A. Ambesi-Impiombato, T. Palomero, S. A. Schnell, L. Belver, A. A. Wendorff, L. Xu, M. Castillo-Martin, D. Llobet-Navas, C. Cordon-Cardo, E. Clappier, J. Soulier & A. A. Ferrando (2014) A NOTCH1-driven MYC enhancer promotes T cell development, transformation and acute lymphoblastic leukemia. *Nat Med,* 20**,** 1130-7.

Herranz, D., A. Ambesi-Impiombato, J. Sudderth, M. Sanchez-Martin, L. Belver, V. Tosello, L. Xu, A. A. Wendorff, M. Castillo, J. E. Haydu, J. Marquez, J. M. Mates, A. L. Kung, S. Rayport, C. Cordon-Cardo, R. J. DeBerardinis & A. A. Ferrando (2015) Metabolic reprogramming induces resistance to anti-NOTCH1 therapies in T cell acute lymphoblastic leukemia. *Nat Med,* 21**,** 1182-9.

Higuchi, T., F. O. Bartel, M. Masuya, T. Deguchi, K. W. Henderson, R. Li, R. C. Muise-Helmericks, M. J. Kern, D. K. Watson & D. D. Spyropoulos (2007) Thymomegaly, Microsplenia, and Defective Homeostatic Proliferation of Peripheral Lymphocytes in p51-Ets1 Isoform-Specific Null Mice. *Molecular and Cellular Biology,* 27**,** 3353.

Hodson, D. J., M. L. Janas, A. Galloway, S. E. Bell, S. Andrews, C. M. Li, R. Pannell, C. W. Siebel, H. R. MacDonald, K. De Keersmaecker, A. A. Ferrando, G. Grutz & M. Turner (2010) Deletion of the RNA-binding proteins ZFP36L1 and ZFP36L2 leads to perturbed thymic development and T lymphoblastic leukemia. *Nat Immunol,* 11**,** 717-24.

Hollenhorst, P. C., K. J. Chandler, R. L. Poulsen, W. E. Johnson, N. A. Speck & B. J. Graves (2009) DNA specificity determinants associate with distinct transcription factor functions. *PLoS Genet,* 5**,** e1000778.

Hollenhorst, P. C., L. P. McIntosh & B. J. Graves (2011) Genomic and biochemical insights into the specificity of ETS transcription factors. *Annu Rev Biochem,* 80**,** 437-71.

Hollenhorst, P. C., A. A. Shah, C. Hopkins & B. J. Graves (2007) Genome-wide analyses reveal properties of redundant and specific promoter occupancy within the ETS gene family. *Genes Dev,* 21**,** 1882-94.

Hosoya, T., T. Kuroha, T. Moriguchi, D. Cummings, I. Maillard, K. C. Lim & J. D. Engel (2009) GATA-3 is required for early T lineage progenitor development. *J Exp Med,* 206**,** 2987-3000.

Hozumi, K., C. Mailhos, N. Negishi, K. Hirano, T. Yahata, K. Ando, S. Zuklys, G. A. Hollander, D. T. Shima & S. Habu (2008) Delta-like 4 is indispensable in thymic environment specific for T cell development. *J Exp Med,* 205**,** 2507-13.

Hu, Y., H. Su, C. Liu, Z. Wang, L. Huang, Q. Wang, S. Liu, S. Chen, J. Zhou, P. Li, Z. Chen, H. Liu & G. Qing (2017) DEPTOR is a direct NOTCH1 target that promotes cell proliferation and survival in T-cell leukemia. *Oncogene,* 36**,** 1038-1047.

Illendula, A., J. A. Pulikkan, H. Zong, J. Grembecka, L. Xue, S. Sen, Y. Zhou, A. Boulton, A. Kuntimaddi, Y. Gao, R. A. Rajewski, M. L. Guzman, L. H. Castilla & J. H. Bushweller (2015) Chemical biology. A small-molecule inhibitor of the aberrant transcription factor CBFbeta-SMMHC delays leukemia in mice. *Science,* 347**,** 779-84.

Inuzuka, H., S. Shaik, I. Onoyama, D. Gao, A. Tseng, R. S. Maser, B. Zhai, L. Wan, A. Gutierrez, A. W. Lau, Y. Xiao, A. L. Christie, J. Aster, J. Settleman, S. P. Gygi, A. L. Kung, T. Look, K. I. Nakayama, R. A. DePinho & W. Wei (2011) SCF(FBW7) regulates cellular apoptosis by targeting MCL1 for ubiquitylation and destruction. *Nature,* 471**,** 104-9.

Iwasaka, C., K. Tanaka, M. Abe & Y. Sato (1996) Ets-1 regulates angiogenesis by inducing the expression of urokinase-type plasminogen activator and matrix metalloproteinase-1 and the migration of vascular endothelial cells. *J Cell Physiol,* 169**,** 522-31.

Jacola, L. M., K. Edelstein, W. Liu, C. H. Pui, R. Hayashi, N. S. Kadan-Lottick, D. Srivastava, T. Henderson, W. Leisenring, L. L. Robison, G. T. Armstrong & K. R. Krull (2016) Cognitive, behaviour, and academic functioning in adolescent and young adult survivors of childhood acute lymphoblastic leukaemia: a report from the Childhood Cancer Survivor Study. *Lancet Psychiatry,* 3**,** 965-972.

Jedlicka, P. & A. Gutierrez-Hartmann (2008) Ets transcription factors in intestinal morphogenesis, homeostasis and disease. *Histology and histopathology,* 23**,** 1417-1424.

Jenkinson, S., K. Koo, M. R. Mansour, N. Goulden, A. Vora, C. Mitchell, R. Wade, S. Richards, J. Hancock, A. V. Moorman, D. C. Linch & R. E. Gale (2013) Impact of NOTCH1/FBXW7 mutations on outcome in pediatric T-cell acute lymphoblastic leukemia patients treated on the MRC UKALL 2003 trial. *Leukemia,* 27**,** 41-7.

Ji, Z., C. Degerny, N. Vintonenko, J. Deheuninck, B. Foveau, C. Leroy, J. Coll, D. Tulasne, J. L. Baert & V. Fafeur (2007) Regulation of the Ets-1 transcription factor by sumoylation and ubiquitinylation. *Oncogene,* 26**,** 395-406.

John, S. A., J. L. Clements, L. M. Russell & L. A. Garrett-Sinha (2008) Ets-1 regulates plasma cell differentiation by interfering with the activity of the transcription factor blimp-1. *Journal of Biological Chemistry,* 283**,** 951-962.

Johnson, K., T. Hashimshony, C. M. Sawai, J. M. Pongubala, J. A. Skok, I. Aifantis & H. Singh (2008) Regulation of immunoglobulin light-chain recombination by the transcription factor IRF-4 and the attenuation of interleukin-7 signaling. *Immunity,* 28**,** 335-45.

Jorcyk, C. L., D. K. Watson, G. J. Mavrothalassitis & T. S. Papas (1991) The human ETS1 gene: genomic structure, promoter characterization and alternative splicing. *Oncogene,* 6**,** 523-532.

Joshi, I., L. M. Minter, J. Telfer, R. M. Demarest, A. J. Capobianco, J. C. Aster, P. Sicinski, A. Fauq, T. E. Golde & B. A. Osborne (2009) Notch signaling mediates G1/S cell-cycle progression in T cells via cyclin D3 and its dependent kinases. *Blood,* 113**,** 1689-98.

Jung, C., G. Mittler, F. Oswald & T. Borggrefe (2013) RNA helicase Ddx5 and the noncoding RNA SRA act as coactivators in the Notch signaling pathway. *Biochim Biophys Acta,* 1833**,** 1180-9.

Kathrein, K. L., S. Chari & S. Winandy (2008) Ikaros directly represses the notch target gene Hes1 in a leukemia T cell line: implications for CD4 regulation. *J Biol Chem,* 283**,** 10476-84.

Kato, M., V. Dang, M. Wang, J. T. Park, S. Deshpande, S. Kadam, A. Mardiros, Y. Zhan, P. Oettgen, S. Putta, H. Yuan, L. Lanting & R. Natarajan (2013) TGF-β Induces Acetylation of Chromatin and of Ets-1 to Alleviate Repression of miR-192 in Diabetic Nephropathy. *Science Signaling,* 6**,** ra43.

Kawamura, M., H. Ohnishi, S. X. Guo, X. M. Sheng, M. Minegishi, R. Hanada, K. Horibe, T. Hongo, Y. Kaneko, F. Bessho, M. Yanagisawa, T. Sekiya & Y. Hayashi (1999) Alterations of the p53, p21, p16, p15 and RAS genes in childhood T-cell acute lymphoblastic leukemia. *Leuk Res,* 23**,** 115-26.

Kelley, L. A., S. Mezulis, C. M. Yates, M. N. Wass & M. J. E. Sternberg The Phyre2 web portal for protein modeling, prediction and analysis.

Kim, E., W. Günther, K. Yoshizato, H. Meissner, S. Zapf, R. M. Nüsing, H. Yamamoto, E. G. Van Meir, W. Deppert & A. Giese (2003) Tumor suppressor p53 inhibits transcriptional activation of invasion gene thromboxane synthase mediated by the proto-oncogenic factor ets-1. *Oncogene,* 22**,** 7716-7727.

King, B., T. Trimarchi, L. Reavie, L. Xu, J. Mullenders, P. Ntziachristos, B. Aranda-Orgilles, A. Perez-Garcia, J. Shi, C. Vakoc, P. Sandy, S. S. Shen, A. Ferrando & I. Aifantis (2013) The Ubiquitin Ligase FBXW7 Modulates Leukemia-Initiating Cell Activity by Regulating MYC Stability. *Cell,* 153**,** 1552-66.

Kleinmann, E., A. S. Geimer Le Lay, M. Sellars, P. Kastner & S. Chan (2008) Ikaros represses the transcriptional response to Notch signaling in T-cell development. *Mol Cell Biol,* 28**,** 7465-75.

Klinakis, A., C. Lobry, O. Abdel-Wahab, P. Oh, H. Haeno, S. Buonamici, I. van De Walle, S. Cathelin, T. Trimarchi, E. Araldi, C. Liu, S. Ibrahim, M. Beran, J. Zavadil, A. Efstratiadis, T. Taghon, F. Michor, R. L. Levine & I. Aifantis (2011) A novel tumour-suppressor function for the Notch pathway in myeloid leukaemia. *Nature,* 473**,** 230-3.

Kloetgen, A., P. Thandapani, P. Ntziachristos, Y. Ghebrechristos, S. Nomikou, C. Lazaris, X. Chen, H. Hu, S. Bakogianni & J. Wang (2019) Dynamic 3D chromosomal landscapes in acute leukemia. *bioRxiv***,** 724427.

Kluk, M. J., T. Ashworth, H. Wang, B. Knoechel, E. F. Mason, E. A. Morgan, D. Dorfman, G. Pinkus, O. Weigert, J. L. Hornick, L. R. Chirieac, M. Hirsch, D. J. Oh, A. P. South, I. M. Leigh, C. Pourreyron, A. J. Cassidy, D. J. Deangelo, D. M. Weinstock, I. E. Krop, D.

Dillon, J. E. Brock, A. J. Lazar, M. Peto, R. J. Cho, A. Stoeck, B. B. Haines, S. Sathayanrayanan, S. Rodig & J. C. Aster (2013) Gauging NOTCH1 Activation in Cancer Using Immunohistochemistry. *PLoS One,* 8**,** e67306.

Knoechel, B., A. Bhatt, L. Pan, C. S. Pedamallu, E. Severson, A. Gutierrez, D. M. Dorfman, F. C. Kuo, M. Kluk, A. L. Kung, P. Zweidler-McKay, M. Meyerson, S. C. Blacklow, D. J. DeAngelo & J. C. Aster (2015) Complete hematologic response of early T-cell progenitor acute lymphoblastic leukemia to the gamma-secretase inhibitor BMS-906024: genetic and epigenetic findings in an outlier case. *Cold Spring Harb Mol Case Stud,* 1**,** a000539.

Knoechel, B., J. E. Roderick, K. E. Williamson, J. Zhu, J. G. Lohr, M. J. Cotton, S. M. Gillespie, D. Fernandez, M. Ku, H. Wang, F. Piccioni, S. J. Silver, M. Jain, D. Pearson, M. J. Kluk, C. J. Ott, L. D. Shultz, M. A. Brehm, D. L. Greiner, A. Gutierrez, K. Stegmaier, A. L. Kung, D. E. Root, J. E. Bradner, J. C. Aster, M. A. Kelliher & B. E. Bernstein (2014) An epigenetic mechanism of resistance to targeted therapy in T cell acute lymphoblastic leukemia. *Nat Genet,* 46**,** 364-70.

Kobayashi, M., Y. Bai, S. Chen, R. Gao, C. Yao, W. Cai, A. A. Cardoso, J. Croop, Z. Y. Zhang & Y. Liu (2017) Phosphatase PRL2 promotes oncogenic NOTCH1-Induced T-cell leukemia. *Leukemia,* 31**,** 751-754.

Koch, U., E. Fiorini, R. Benedito, V. Besseyrias, K. Schuster-Gossler, M. Pierres, N. R. Manley, A. Duarte, H. R. Macdonald & F. Radtke (2008) Delta-like 4 is the essential, nonredundant ligand for Notch1 during thymic T cell lineage commitment. *J Exp Med,* 205**,** 2515-23.

Koch, U. & F. Radtke (2011) Mechanisms of T Cell Development and Transformation. *Annual Review of Cell and Developmental Biology,* 27**,** 539-562.

Koepp, D. M., L. K. Schaefer, X. Ye, K. Keyomarsi, C. Chu, J. W. Harper & S. J. Elledge (2001) Phosphorylation-dependent ubiquitination of cyclin E by the SCFFbw7 ubiquitin ligase. *Science,* 294**,** 173-7.

Kola, I., S. Brookes, A. R. Green, R. Garber, M. Tymms, T. S. Papas & A. Seth (1993) The Ets1 transcription factor is widely expressed during murine embryo development and is associated with mesodermal cells involved in morphogenetic processes such as organ formation. *Proceedings of the National Academy of Sciences of the United States of America,* 90**,** 7588-7592.

Kox, C., M. Zimmermann, M. Stanulla, S. Leible, M. Schrappe, W. D. Ludwig, R. Koehler, G. Tolle, O. R. Bandapalli, S. Breit, M. U. Muckenthaler & A. E. Kulozik (2010) The favorable effect of activating NOTCH1 receptor mutations on long-term outcome in T-ALL patients treated on the ALL-BFM 2000 protocol can be separated from FBXW7 loss of function. *Leukemia,* 24**,** 2005-13.

Krop, I., T. Demuth, T. Guthrie, P. Y. Wen, W. P. Mason, P. Chinnaiyan, N. Butowski, M. D. Groves, S. Kesari, S. J. Freedman, S. Blackman, J. Watters, A. Loboda, A. Podtelezhnikov, J. Lunceford, C. Chen, M. Giannotti, J. Hing, R. Beckman & P. Lorusso (2012) Phase I pharmacologic and pharmacodynamic study of the gamma secretase (Notch) inhibitor MK-0752 in adult patients with advanced solid tumors. *J Clin Oncol,* 30**,** 2307-13.

Kvidera, S. K., M. J. Dickson, M. Abuajamieh, D. B. Snider, M. V. S. Fernandez, J. S. Johnson, A. F. Keating, P. J. Gorden, H. B. Green, K. M. Schoenberg & L. H. Baumgard (2017) Intentionally induced intestinal barrier dysfunction causes inflammation, affects

metabolism, and reduces productivity in lactating Holstein cows. *J Dairy Sci,* 100**,** 4113-4127.

La Starza, R., C. Borga, G. Barba, V. Pierini, C. Schwab, C. Matteucci, A. G. Lema Fernandez, A. Leszl, G. Cazzaniga, S. Chiaretti, G. Basso, C. J. Harrison, G. Te Kronnie & C. Mecucci (2014) Genetic profile of T-cell acute lymphoblastic leukemias with MYC translocations. *Blood,* 124**,** 3577-82.

Laitem, C., G. Leprivier, S. Choul-Li, A. Begue, D. Monte, D. Larsimont, P. Dumont, M. Duterque-Coquillaud & M. Aumercier (2009) Ets-1 p27: a novel Ets-1 isoform with dominant-negative effects on the transcriptional properties and the subcellular localization of Ets-1 p51. *Oncogene,* 28**,** 2087-99.

Lange, B. J., S. C. Raimondi, N. Heerema, P. C. Nowell, J. Minowada, P. E. Steinherz, E. B. Arenson, R. O'Connor & D. Santoli (1992) Pediatric leukemia/lymphoma with t(8;14)(q24;q11). *Leukemia,* 6**,** 613-8.

Langenau, D. M., D. Traver, A. A. Ferrando, J. L. Kutok, J. C. Aster, J. P. Kanki, S. Lin, E. Prochownik, N. S. Trede, L. I. Zon & A. T. Look (2003) Myc-induced T cell leukemia in transgenic zebrafish. *Science,* 299**,** 887-90.

Langmead, B., C. Trapnell, M. Pop & S. L. Salzberg (2009) Ultrafast and memory-efficient alignment of short DNA sequences to the human genome. *Genome Biology,* 10**,** R25.

Lavenburg, K. R., J. Ivey, T. Hsu & R. C. Muise-Helmericks (2003) Coordinated functions of Akt/PKB and ETS1 in tubule formation. *FASEB Journal,* 17**,** 2278-2280.

Le Bras, A., F. Lionneton, V. Mattot, E. Lelievre, B. Caetano, N. Spruyt & F. Soncin (2007) HIF-2alpha specifically activates the VE-cadherin promoter independently of hypoxia and in synergy with Ets-1 through two essential ETS-binding sites. *Oncogene,* 26**,** 7480-9.

Legrand, A. J., S. Choul-Li, C. Spriet, T. Idziorek, D. Vicogne, H. Drobecq, F. Dantzer, V. Villeret & M. Aumercier (2013) The level of Ets-1 protein is regulated by poly(ADP-ribose) polymerase-1 (PARP-1) in cancer cells to prevent DNA damage. *PloS one,* 8**,** e55883-e55883.

Leivonen, S. K. & V. M. Kähäri (2007) Transforming growth factor-β signaling in cancer invasion and metastasis. *International Journal of Cancer,* 121**,** 2119-2124.

Leprince, D., A. Gegonne, J. Coll, C. De Taisne, A. Schneeberger, C. Lagrou & D. Stehelin (1983) A putative second cell-derived oncogene of the avian leukaemia retrovirus E26. *Nature,* 306**,** 395-397.

Li, N., A. Fassl, J. Chick, H. Inuzuka, X. Li, M. R. Mansour, L. Liu, H. Wang, B. King, S. Shaik, A. Gutierrez, A. Ordureau, T. Otto, T. Kreslavsky, L. Baitsch, L. Bury, C. A. Meyer, N. Ke, K. A. Mulry, M. J. Kluk, M. Roy, S. Kim, X. Zhang, Y. Geng, A. Zagozdzon, S. Jenkinson, R. E. Gale, D. C. Linch, J. J. Zhao, C. G. Mullighan, J. W. Harper, J. C. Aster, I. Aifantis, H. von Boehmer, S. P. Gygi, W. Wei, A. T. Look & P. Sicinski (2014) Cyclin C is a haploinsufficient tumour suppressor. *Nat Cell Biol,* 16**,** 1080-91.

Li, R., H. Pei, D. K. Watson & T. S. Papas (2000) EAP1/Daxx interacts with ETS1 and represses transcriptional activation of ETS1 target genes. *Oncogene,* 19**,** 745-753.

Li, X., F. Gounari, A. Protopopov, K. Khazaie & H. von Boehmer (2008) Oncogenesis of T-ALL and nonmalignant consequences of overexpressing intracellular NOTCH1. *J Exp Med,* 205**,** 2851-61.

Liberzon, A., A. Subramanian, R. Pinchback, H. Thorvaldsdottir, P. Tamayo & J. P. Mesirov (2011) Molecular signatures database (MSigDB) 3.0. *Bioinformatics,* 27**,** 1739-40.

Lin, S., L. Tian, H. Shen, Y. Gu, J. L. Li, Z. Chen, X. Sun, M. J. You & L. Wu (2013) DDX5 is a positive regulator of oncogenic NOTCH1 signaling in T cell acute lymphoblastic leukemia. *Oncogene,* 32**,** 4845-53.

Liu, Y., J. Easton, Y. Shao, J. Maciaszek, Z. Wang, M. R. Wilkinson, K. McCastlain, M. Edmonson, S. B. Pounds, L. Shi, X. Zhou, X. Ma, E. Sioson, Y. Li, M. Rusch, P. Gupta, D. Pei, C. Cheng, M. A. Smith, J. G. Auvil, D. S. Gerhard, M. V. Relling, N. J. Winick, A. J. Carroll, N. A. Heerema, E. Raetz, M. Devidas, C. L. Willman, R. C. Harvey, W. L. Carroll, K. P. Dunsmore, S. S. Winter, B. L. Wood, B. P. Sorrentino, J. R. Downing, M. L. Loh, S. P. Hunger, J. Zhang & C. G. Mullighan (2017) The genomic landscape of pediatric and young adult T-lineage acute lymphoblastic leukemia. *Nature Genetics,* 49**,** 1211-1218.

Loosveld, M., R. Castellano, S. Gon, A. Goubard, T. Crouzet, L. Pouyet, T. Prebet, N. Vey, B. Nadel, Y. Collette & D. Payet-Bornet (2014) Therapeutic targeting of c-Myc in T-cell acute lymphoblastic leukemia, T-ALL. *Oncotarget,* 5**,** 3168-72.

Lu, G., Q. Zhang, Y. Huang, J. Song, R. Tomaino, T. Ehrenberger, E. Lim, W. Liu, R. T. Bronson, M. Bowden, J. Brock, I. E. Krop, D. A. Dillon, S. P. Gygi, G. B. Mills, A. L. Richardson, S. Signoretti, M. B. Yaffe & W. G. Kaelin (2014) Phosphorylation of ETS1 by src family kinases prevents its recognition by the COP1 tumor suppressor. *Cancer Cell,* 26**,** 222-234.

Lulli, V., P. Romania, O. Morsilli, M. Gabbianelli, A. Pagliuca, S. Mazzeo, U. Testa, C. Peschle & G. Marziali (2006) Overexpression of Ets-1 in human hematopoietic progenitor cells blocks erythroid and promotes megakaryocytic differentiation. *Cell Death Differ,* 13**,** 1064-74.

Luo, H., Q. Li, J. O'Neal, F. Kreisel, M. M. Le Beau & M. H. Tomasson (2005) c-Myc rapidly induces acute myeloid leukemia in mice without evidence of lymphoma-associated antiapoptotic mutations. *Blood,* 106**,** 2452-61.

Macauley, M. S., W. J. Errington, M. Schårpf, C. D. Mackereth, A. G. Blaszczak, B. J. Graves & L. P. McIntosh (2006) Beads-on-a-string, characterization of Ets-1 sumoylated within its flexible N-terminal sequence. *Journal of Biological Chemistry,* 281**,** 4164-4172.

Maillard, I., U. Koch, A. Dumortier, O. Shestova, L. Xu, H. Sai, S. E. Pross, J. C. Aster, A. Bhandoola, F. Radtke & W. S. Pear (2008) Canonical notch signaling is dispensable for the maintenance of adult hematopoietic stem cells. *Cell Stem Cell,* 2**,** 356-66.

Majérus, M. A., F. Bibollet-ruche, J. B. Telliez, B. Wasylyk & B. Bailleul (1992) Serum, AP-1 and Ets-1 stimulate the human Ets-1 promoter. *Nucleic Acids Research,* 20**,** 2699-2703.

Malecki, M. J., C. Sanchez-Irizarry, J. L. Mitchell, G. Histen, M. L. Xu, J. C. Aster & S. C. Blacklow (2006) Leukemia-associated mutations within the NOTCH1 heterodimerization domain fall into at least two distinct mechanistic classes. *Mol Cell Biol,* 26**,** 4642-51.

Maniaci, C., S. J. Hughes, A. Testa, W. Chen, D. J. Lamont, S. Rocha, D. R. Alessi, R. Romeo & A. Ciulli (2017) Homo-PROTACs: bivalent small-molecule dimerizers of the VHL E3 ubiquitin ligase to induce self-degradation. *Nat Commun,* 8**,** 830.

Mansour, M. R., V. Duke, L. Foroni, B. Patel, C. G. Allen, P. J. Ancliff, R. E. Gale & D. C. Linch (2007) Notch-1 mutations are secondary events in some patients with T-cell acute lymphoblastic leukemia. *Clin Cancer Res,* 13**,** 6964-9.

Mansour, M. R., M. L. Sulis, V. Duke, L. Foroni, S. Jenkinson, K. Koo, C. G. Allen, R. E. Gale, G. Buck, S. Richards, E. Paietta, J. M. Rowe, M. S. Tallman, A. H. Goldstone, A. A. Ferrando & D. C. Linch (2009) Prognostic implications of NOTCH1 and FBXW7

mutations in adults with T-cell acute lymphoblastic leukemia treated on the MRC UKALLXII/ECOG E2993 protocol. *J Clin Oncol,* 27**,** 4352-6.
Mao, J. H., I. J. Kim, D. Wu, J. Climent, H. C. Kang, R. DelRosario & A. Balmain (2008) FBXW7 targets mTOR for degradation and cooperates with PTEN in tumor suppression. *Science,* 321**,** 1499-502.
Marcais, A., R. Jeannet, L. Hernandez, J. Soulier, F. Sigaux, S. Chan & P. Kastner (2010) Genetic inactivation of Ikaros is a rare event in human T-ALL. *Leuk Res,* 34**,** 426-9.
Margolin, A. A., T. Palomero, P. Sumazin, A. Califano, A. A. Ferrando & G. Stolovitzky (2009) ChIP-on-chip significance analysis reveals large-scale binding and regulation by human transcription factor oncogenes. *Proc Natl Acad Sci U S A,* 106**,** 244-9.
McCarter, A. C., G. D. Gatta, A. Melnick, E. Kim, C. Sha, Q. Wang, J. K. Nalamolu, Y. Liu, T. M. Keeley, R. Yan, M. Sun, R. Kodgule, N. Kunnath, A. Ambesi-Impiombato, R. Kuick, A. Rao, R. J. H. Ryan, B. L. Kee, L. C. Samuelson, M. C. Ostrowski, A. A. Ferrando & M. Y. Chiang (2020) Combinatorial ETS1-Dependent Control of Oncogenic NOTCH1 Enhancers in T-cell Leukemia. *Blood Cancer Discovery*.
McCarter, A. C., Q. Wang & M. Chiang (2018) Notch in Leukemia. *Adv Exp Med Biol,* 1066**,** 355-394.
McMillan, B. J., B. Zimmerman, E. D. Egan, M. Lofgren, X. Xu, A. Hesser & S. C. Blacklow (2017) Structure of human POFUT1, its requirement in ligand-independent oncogenic Notch signaling, and functional effects of Dowling-Degos mutations. *Glycobiology,* 27**,** 777-786.
Medyouf, H., X. Gao, F. Armstrong, S. Gusscott, Q. Liu, A. L. Gedman, L. H. Matherly, K. R. Schultz, F. Pflumio, M. J. You & A. P. Weng (2010) Acute T-cell leukemias remain dependent on Notch signaling despite PTEN and INK4A/ARF loss. *Blood,* 115**,** 1175-84.
Mendes, R. D., L. M. Sarmento, K. Cante-Barrett, L. Zuurbier, J. G. Buijs-Gladdines, V. Povoa, W. K. Smits, M. Abecasis, J. A. Yunes, E. Sonneveld, M. A. Horstmann, R. Pieters, J. T. Barata & J. P. Meijerink (2014) PTEN microdeletions in T-cell acute lymphoblastic leukemia are caused by illegitimate RAG-mediated recombination events. *Blood,* 124**,** 567-78.
Mertz, J. A., A. R. Conery, B. M. Bryant, P. Sandy, S. Balasubramanian, D. A. Mele, L. Bergeron & R. J. Sims (2011) Targeting MYC dependence in cancer by inhibiting BET bromodomains. *Proceedings of the National Academy of Sciences,* 108**,** 16669.
Miele, L. & S. Artavanis-Tsakonas. 2018. *Targeting Notch in Cancer From the Fruit Fly to the Clinic*. Springer.
Minuzzo, S., V. Agnusdei, I. Pusceddu, M. Pinazza, L. Moserle, M. Masiero, E. Rossi, M. Crescenzi, T. Hoey, M. Ponzoni, A. Amadori & S. Indraccolo (2015) DLL4 regulates NOTCH signaling and growth of T acute lymphoblastic leukemia cells in NOD/SCID mice. *Carcinogenesis,* 36**,** 115-21.
Moellering, R. E., M. Cornejo, T. N. Davis, C. Del Bianco, J. C. Aster, S. C. Blacklow, A. L. Kung, D. G. Gilliland, G. L. Verdine & J. E. Bradner (2009) Direct inhibition of the NOTCH transcription factor complex. *Nature,* 462**,** 182-8.
Moisan, J., R. Grenningloh, E. Bettelli, M. Oukka & I. C. Ho Ets-1 is a negative regulator of Th17 differentiation.
Morin, R. D., M. Mendez-Lago, A. J. Mungall, R. Goya, K. L. Mungall, R. D. Corbett, N. A. Johnson, T. M. Severson, R. Chiu, M. Field, S. Jackman, M. Krzywinski, D. W. Scott, D. L. Trinh, J. Tamura-Wells, S. Li, M. R. Firme, S. Rogic, M. Griffith, S. Chan, O.

Yakovenko, I. M. Meyer, E. Y. Zhao, D. Smailus, M. Moksa, S. Chittaranjan, L. Rimsza, A. Brooks-Wilson, J. J. Spinelli, S. Ben-Neriah, B. Meissner, B. Woolcock, M. Boyle, H. McDonald, A. Tam, Y. Zhao, A. Delaney, T. Zeng, K. Tse, Y. Butterfield, I. Birol, R. Holt, J. Schein, D. E. Horsman, R. Moore, S. J. Jones, J. M. Connors, M. Hirst, R. D. Gascoyne & M. A. Marra (2011) Frequent mutation of histone-modifying genes in non-Hodgkin lymphoma. *Nature,* 476**,** 298-303.

Mouly, E., K. Chemin, H. V. Nguyen, M. Chopin, L. Mesnard, M. Leite-de-Moraes, O. Burlen-defranoux, A. Bandeira & J.-C. Bories (2010) The Ets-1 transcription factor controls the development and function of natural regulatory T cells. *The Journal of experimental medicine,* 207**,** 2113-2125.

Mullard, A. 2019. Arvinas's PROTACs pass first safety and PK analysis. In *Nat Rev Drug Discov*, 895. England.

Muthusamy, N., K. Barton & J. M. Leiden (1995) Defective activation and survival of T cells lacking the Ets-1 transcription factor. *Nature,* 377**,** 639-42.

Nagaleekar, V. K., S. A. Diehl, I. Juncadella, C. Charland, N. Muthusamy, S. Eaton, L. Haynes, L. A. Garrett-Sinha, J. Anguita & M. Rincón (2008) IP3 receptor-mediated Ca2+ release in naive CD4 T cells dictates their cytokine program. *Journal of Immunology,* 181**,** 8315-8322.

Nagarajan, P., S. S. Chin, D. Wang, S. Liu, S. Sinha & L. A. Garrett-Sinha (2010) Ets1 blocks terminal differentiation of keratinocytes and induces expression of matrix metalloproteases and innate immune mediators. *J Cell Sci,* 123**,** 3566-75.

Nakayama, T., M. Ito, A. Ohtsuru, S. Naito, M. Nakashima, J. A. Fagin, S. Yamashita & I. Sekine (1996) Expression of the Ets-1 proto-oncogene in human gastric carcinoma: Correlation with tumor invasion. *American Journal of Pathology,* 149**,** 1931-1939.

Nhili, R., P. Peixoto, S. Depauw, S. Flajollet, X. Dezitter, M. M. Munde, M. A. Ismail, A. Kumar, A. A. Farahat, C. E. Stephens, M. Duterque-Coquillaud, W. David Wilson, D. W. Boykin & M. H. David-Cordonnier (2013) Targeting the DNA-binding activity of the human ERG transcription factor using new heterocyclic dithiophene diamidines. *Nucleic Acids Res,* 41**,** 125-38.

Nie, L., M. Xu, A. Vladimirova & X. H. Sun (2003) Notch-induced E2A ubiquitination and degradation are controlled by MAP kinase activities. *Embo j,* 22**,** 5780-92.

Nishida, T., M. Terashima & K. Fukami (2006) PIASy-mediated repression of the Ets-1 is independent of its sumoylation. *Biochem Biophys Res Commun,* 345**,** 1536-46.

O'Neil, J., J. Calvo, K. McKenna, V. Krishnamoorthy, J. C. Aster, C. H. Bassing, F. W. Alt, M. Kelliher & A. T. Look (2006) Activating Notch1 mutations in mouse models of T-ALL. *Blood,* 107**,** 781-5.

O'Neil, J., J. Grim, P. Strack, S. Rao, D. Tibbitts, C. Winter, J. Hardwick, M. Welcker, J. P. Meijerink, R. Pieters, G. Draetta, R. Sears, B. E. Clurman & A. T. Look (2007) FBW7 mutations in leukemic cells mediate NOTCH pathway activation and resistance to gamma-secretase inhibitors. *J Exp Med,* 204**,** 1813-24.

Oikawa, M., M. Abe, H. Kurosawa, W. Hida, K. Shirato & Y. Sato (2001) Hypoxia induces transcription factor ETS-1 via the activity of hypoxia-lnducible factor-1. *Biochemical and Biophysical Research Communications,* 289**,** 39-43.

Oliveira, M. L., P. Akkapeddi, D. Ribeiro, A. Melão & J. T. Barata (2019) IL-7R-mediated signaling in T-cell acute lymphoblastic leukemia: An update. *Advances in Biological Regulation,* 71**,** 88-96.

Ozaki, I., G. Zhao, T. Mizuta, Y. Ogawa, T. Hara, S. Kajihara, A. Hisatomi, T. Sakai & K. Yamamoto (2002) Hepatocyte growth factor induces collagenase (matrix metalloproteinase-1) via the transcription factor Ets-1 in human hepatic stellate cell line. *Journal of Hepatology,* 36**,** 169-178.

Paganin, M. & A. Ferrando (2011) Molecular pathogenesis and targeted therapies for NOTCH1-induced T-cell acute lymphoblastic leukemia. *Blood Rev,* 25**,** 83-90.

Pajcini, K. V., L. Xu, L. Shao, J. Petrovic, K. Palasiewicz, Y. Ohtani, W. Bailis, C. Lee, G. B. Wertheim, R. Mani, N. Muthusamy, Y. Li, J. P. P. Meijerink, S. C. Blacklow, R. B. Faryabi, S. Cherry & W. S. Pear (2017) MAFB enhances oncogenic Notch signaling in T cell acute lymphoblastic leukemia. *Sci Signal,* 10.

Pal, A., M. Dziubinski, M. P. Di Magliano, D. M. Simeone, S. Owens, D. Thomas, L. Peterson, H. Potu, M. Talpaz & N. J. Donato (2018) Usp9x Promotes Survival in Human Pancreatic Cancer and Its Inhibition Suppresses Pancreatic Ductal Adenocarcinoma In Vivo Tumor Growth. *Neoplasia,* 20**,** 152-164.

Palii, C. G., C. Perez-Iratxeta, Z. Yao, Y. Cao, F. Dai, J. Davison, H. Atkins, D. Allan, F. J. Dilworth, R. Gentleman, S. J. Tapscott & M. Brand (2011) Differential genomic targeting of the transcription factor TAL1 in alternate haematopoietic lineages. *Embo j,* 30**,** 494-509.

Palomero, T., W. K. Lim, D. T. Odom, M. L. Sulis, P. J. Real, A. Margolin, K. C. Barnes, J. O'Neil, D. Neuberg, A. P. Weng, J. C. Aster, F. Sigaux, J. Soulier, A. T. Look, R. A. Young, A. Califano & A. A. Ferrando (2006a) NOTCH1 directly regulates c-MYC and activates a feed-forward-loop transcriptional network promoting leukemic cell growth. *Proc Natl Acad Sci U S A,* 103**,** 18261-6.

Palomero, T., K. McKenna, O. N. J, I. Galinsky, R. Stone, K. Suzukawa, E. Stiakaki, M. Kalmanti, E. A. Fox, M. A. Caligiuri, J. C. Aster, A. T. Look & A. A. Ferrando (2006b) Activating mutations in NOTCH1 in acute myeloid leukemia and lineage switch leukemias. *Leukemia,* 20**,** 1963-6.

Palomero, T., M. L. Sulis, M. Cortina, P. J. Real, K. Barnes, M. Ciofani, E. Caparros, J. Buteau, K. Brown, S. L. Perkins, G. Bhagat, A. M. Agarwal, G. Basso, M. Castillo, S. Nagase, C. Cordon-Cardo, R. Parsons, J. C. Zuniga-Pflucker, M. Dominguez & A. A. Ferrando (2007) Mutational loss of PTEN induces resistance to NOTCH1 inhibition in T-cell leukemia. *Nat Med,* 13**,** 1203-10.

Papayannidis, C., D. J. DeAngelo, W. Stock, B. Huang, M. N. Shaik, R. Cesari, X. Zheng, J. M. Reynolds, P. A. English, M. Ozeck, J. C. Aster, F. Kuo, D. Huang, P. D. Lira, K. R. McLachlan, K. A. Kern, G. Garcia-Manero & G. Martinelli (2015) A Phase 1 study of the novel gamma-secretase inhibitor PF-03084014 in patients with T-cell acute lymphoblastic leukemia and T-cell lymphoblastic lymphoma. *Blood Cancer J,* 5**,** e350.

Pasqualucci, L., V. Trifonov, G. Fabbri, J. Ma, D. Rossi, A. Chiarenza, V. A. Wells, A. Grunn, M. Messina, O. Elliot, J. Chan, G. Bhagat, A. Chadburn, G. Gaidano, C. G. Mullighan, R. Rabadan & R. Dalla-Favera (2011) Analysis of the coding genome of diffuse large B-cell lymphoma. *Nat Genet,* 43**,** 830-7.

Pear, W., Y. Yashiro-Ohtani, J. Petrovic, S. Yu, V. Mercado, L. Xu, R. Faryabi, X. S. Liu, J. Aster & G. Zang (2016) Modular domains within a super enhancer determine drug resistance in T-cell acute lymphoblastic leukemia. *Experimental Hematology,* 44**,** S25.

Pear, W. S., J. C. Aster, M. L. Scott, R. P. Hasserjian, B. Soffer, J. Sklar & D. Baltimore (1996) Exclusive development of T cell neoplasms in mice transplanted with bone marrow expressing activated Notch alleles. *J Exp Med,* 183**,** 2283-91.

Pei, H., J. S. Yordy, Q. Leng, Q. Zhao, D. K. Watson & R. Li (2003) EAPII interacts with ETS1 and modulates its transcriptional function. *Oncogene,* 22**,** 2699-2709.

Peterson, L. F., H. Sun, Y. Liu, H. Potu, M. Kandarpa, M. Ermann, S. M. Courtney, M. Young, H. D. Showalter, D. Sun, A. Jakubowiak, S. N. Malek, M. Talpaz & N. J. Donato (2015) Targeting deubiquitinase activity with a novel small-molecule inhibitor as therapy for B-cell malignancies. *Blood,* 125**,** 3588-97.

Phuchareon, J., F. McCormick, D. W. Eisele & O. Tetsu (2015) EGFR inhibition evokes innate drug resistance in lung cancer cells by preventing Akt activity and thus inactivating Ets-1 function. *Proceedings of the National Academy of Sciences of the United States of America,* 112**,** E3855-E3863.

Pikman, Y., G. Alexe, G. Roti, A. S. Conway, A. Furman, E. S. Lee, A. E. Place, S. Kim, C. Saran, R. Modiste, D. M. Weinstock, M. Harris, A. L. Kung, L. B. Silverman & K. Stegmaier (2017) Synergistic Drug Combinations with a CDK4/6 Inhibitor in T-cell Acute Lymphoblastic Leukemia. *Clin Cancer Res,* 23**,** 1012-1024.

Pinnell, N., R. Yan, H. J. Cho, T. Keeley, M. J. Murai, Y. Liu, A. S. Alarcon, J. Qin, Q. Wang, R. Kuick, K. S. Elenitoba-Johnson, I. Maillard, L. C. Samuelson, T. Cierpicki & M. Y. Chiang (2015a) The PIAS-like Coactivator Zmiz1 Is a Direct and Selective Cofactor of Notch1 in T Cell Development and Leukemia. *Immunity,* 43**,** 870-883.

--- (2015b) The PIAS-like Coactivator Zmiz1 Is a Direct and Selective Cofactor of Notch1 in T Cell Development and Leukemia. *Immunity,* 43**,** 870-83.

Piovan, E., J. Yu, V. Tosello, D. Herranz, A. Ambesi-Impiombato, A. C. Da Silva, M. Sanchez-Martin, A. Perez-Garcia, I. Rigo, M. Castillo, S. Indraccolo, J. R. Cross, E. de Stanchina, E. Paietta, J. Racevskis, J. M. Rowe, M. S. Tallman, G. Basso, J. P. Meijerink, C. Cordon-Cardo, A. Califano & A. A. Ferrando (2013) Direct reversal of glucocorticoid resistance by AKT inhibition in acute lymphoblastic leukemia. *Cancer Cell,* 24**,** 766-76.

Plotnik, J. P., J. A. Budka, M. W. Ferris & P. C. Hollenhorst (2014) ETS1 is a genome-wide effector of RAS/ERK signaling in epithelial cells. *Nucleic Acids Res,* 42**,** 11928-40.

Pognonec, P., K. E. Boulukos, J. C. Gesquière, D. Stéhelin & J. Ghysdael (1988) Mitogenic stimulation of thymocytes results in the calcium-dependent phosphorylation of c-ets-1 proteins. *The EMBO journal,* 7**,** 977-983.

Polansky, J. K., L. Schreiber, C. Thelemann, L. Ludwig, M. Krüger, R. Baumgrass, S. Cording, S. Floess, A. Hamann & J. Huehn (2010) Methylation matters: binding of Ets-1 to the demethylated Foxp3 gene contributes to the stabilization of Foxp3 expression in regulatory T cells. *Journal of molecular medicine (Berlin, Germany),* 88**,** 1029-1040.

Potu, H., L. F. Peterson, M. Kandarpa, A. Pal, H. Sun, A. Durham, P. W. Harms, P. C. Hollenhorst, U. Eskiocak, M. Talpaz & N. J. Donato (2017) Usp9x regulates Ets-1 ubiquitination and stability to control NRAS expression and tumorigenicity in melanoma. *Nat Commun,* 8**,** 14449.

Pui, C.-H., D. Campana, D. Pei, W. P. Bowman, J. T. Sandlund, S. C. Kaste, R. C. Ribeiro, J. E. Rubnitz, S. C. Raimondi, M. Onciu, E. Coustan-Smith, L. E. Kun, S. Jeha, C. Cheng, S. C. Howard, V. Simmons, A. Bayles, M. L. Metzger, J. M. Boyett, W. Leung, R. Handgretinger, J. R. Downing, W. E. Evans & M. V. Relling (2009) Treating Childhood

Acute Lymphoblastic Leukemia without Cranial Irradiation. *New England Journal of Medicine,* 360**,** 2730-2741.

Pui, J. C., D. Allman, L. Xu, S. DeRocco, F. G. Karnell, S. Bakkour, J. Y. Lee, T. Kadesch, R. R. Hardy, J. C. Aster & W. S. Pear (1999) Notch1 expression in early lymphopoiesis influences B versus T lineage determination. *Immunity,* 11**,** 299-308.

Puzovic, V., I. Brcic, I. Ranogajec & J. Jakic-Razumovic (2014) Prognostic values of ETS-1, MMP-2 and MMP-9 expression and co-expression in breast cancer patients. *Neoplasma,* 61**,** 439-446.

Qian, L., W. Zhang, B. Lei, A. He, L. Ye, X. Li & X. Dong (2016) MicroRNA-101 regulates T-cell acute lymphoblastic leukemia progression and chemotherapeutic sensitivity by targeting Notch1. *Oncol Rep,* 36**,** 2511-2516.

Quinlan, A. R. & I. M. Hall (2010) BEDTools: a flexible suite of utilities for comparing genomic features. *Bioinformatics,* 26**,** 841-2.

Rabault, B. & J. Ghysdael (1994) Calcium-induced phosphorylation of ETS1 inhibits its specific DNA binding activity. *Journal of Biological Chemistry,* 269**,** 28143-28151.

Radtke, I., C. G. Mullighan, M. Ishii, X. Su, J. Cheng, J. Ma, R. Ganti, Z. Cai, S. Goorha, S. B. Pounds, X. Cao, C. Obert, J. Armstrong, J. Zhang, G. Song, R. C. Ribeiro, J. E. Rubnitz, S. C. Raimondi, S. A. Shurtleff & J. R. Downing (2009) Genomic analysis reveals few genetic alterations in pediatric acute myeloid leukemia. *Proc Natl Acad Sci U S A,* 106**,** 12944-9.

Raetz, E. A. & D. T. Teachey (2016) T-cell acute lymphoblastic leukemia. *Hematology. American Society of Hematology. Education Program,* 2016**,** 580-588.

Rahman, S., M. Magnussen, T. E. Leon, N. Farah, Z. Li, B. J. Abraham, K. Z. Alapi, R. J. Mitchell, T. Naughton, A. K. Fielding, A. Pizzey, S. Bustraan, C. Allen, T. Popa, K. Pike-Overzet, L. Garcia-Perez, R. E. Gale, D. C. Linch, F. J. T. Staal, R. A. Young, A. T. Look & M. R. Mansour (2017) Activation of the LMO2 oncogene through a somatically acquired neomorphic promoter in T-cell acute lymphoblastic leukemia. *Blood,* 129**,** 3221-3226.

Rakowski, L. A., D. D. Garagiola, C. M. Li, M. Decker, S. Caruso, M. Jones, R. Kuick, T. Cierpicki, I. Maillard & M. Y. Chiang (2013) Convergence of the ZMIZ1 and NOTCH1 pathways at C-MYC in acute T lymphoblastic leukemias. *Cancer Res,* 73**,** 930-41.

Rakowski, L. A., E. A. Lehotzky & M. Y. Chiang (2011) Transient Responses to NOTCH and TLX1/HOX11 Inhibition in T-Cell Acute Lymphoblastic Leukemia/Lymphoma. *PLoS One,* 6**,** e16761.

Ramasamy, S. K., A. P. Kusumbe, L. Wang & R. H. Adams (2014) Endothelial Notch activity promotes angiogenesis and osteogenesis in bone. *Nature,* 507**,** 376-380.

Rameil, P., P. Lecine, J. Ghysdael, F. Gouilleux, B. Kahn-Perles & J. Imbert (2000) IL-2 and long-term T cell activation induce physical and functional interaction between STAT5 and ETS transcription factors in human T cells. *Oncogene,* 19**,** 2086-97.

Ramírez, F., D. P. Ryan, B. Grüning, V. Bhardwaj, F. Kilpert, A. S. Richter, S. Heyne, F. Dündar & T. Manke (2016) deepTools2: a next generation web server for deep-sequencing data analysis. *Nucleic Acids Research,* 44**,** W160-W165.

Rao, S. S., J. O'Neil, C. D. Liberator, J. S. Hardwick, X. Dai, T. Zhang, E. Tyminski, J. Yuan, N. E. Kohl, V. M. Richon, L. H. Van der Ploeg, P. M. Carroll, G. F. Draetta, A. T. Look, P. R. Strack & C. G. Winter (2009) Inhibition of NOTCH signaling by gamma secretase

inhibitor engages the RB pathway and elicits cell cycle exit in T-cell acute lymphoblastic leukemia cells. *Cancer Res,* 69**,** 3060-8.

Real, P. J., V. Tosello, T. Palomero, M. Castillo, E. Hernando, E. de Stanchina, M. L. Sulis, K. Barnes, C. Sawai, I. Homminga, J. Meijerink, I. Aifantis, G. Basso, C. Cordon-Cardo, W. Ai & A. Ferrando (2009) Gamma-secretase inhibitors reverse glucocorticoid resistance in T cell acute lymphoblastic leukemia. *Nat Med,* 15**,** 50-8.

Reizis, B. & P. Leder (2002) Direct induction of T lymphocyte-specific gene expression by the mammalian Notch signaling pathway. *Genes Dev,* 16**,** 295-300.

Rich, B. E., J. Campos-Torres, R. I. Tepper, R. W. Moreadith & P. Leder (1993) Cutaneous lymphoproliferation and lymphomas in interleukin 7 transgenic mice. *J Exp Med,* 177**,** 305-16.

Robinson, J. T., H. Thorvaldsdóttir, W. Winckler, M. Guttman, E. S. Lander, G. Getz & J. P. Mesirov (2011) Integrative genomics viewer. *Nat Biotechnol,* 29**,** 24-6.

Roderick, J. E., J. Tesell, L. D. Shultz, M. A. Brehm, D. L. Greiner, M. H. Harris, L. B. Silverman, S. E. Sallan, A. Gutierrez, A. T. Look, J. Qi, J. E. Bradner & M. A. Kelliher (2014) c-Myc inhibition prevents leukemia initiation in mice and impairs the growth of relapsed and induction failure pediatric T-ALL cells. *Blood,* 123**,** 1040-50.

Ross-Innes, C. S., R. Stark, A. E. Teschendorff, K. A. Holmes, H. R. Ali, M. J. Dunning, G. D. Brown, O. Gojis, I. O. Ellis, A. R. Green, S. Ali, S.-F. Chin, C. Palmieri, C. Caldas & J. S. Carroll (2012) Differential oestrogen receptor binding is associated with clinical outcome in breast cancer. *Nature,* 481**,** 389-393.

Rossi, F., K. M. McNagny, C. Logie, A. F. Stewart & T. Graf (1996) Excision of Ets by an inducible site-specific recombinase causes differentiation of Myb–Ets-transformed hematopoietic progenitors. *Current Biology,* 6**,** 866-872.

Rothenberg, E. V., J. Ungerback & A. Champhekar (2016) Forging T-Lymphocyte Identity: Intersecting Networks of Transcriptional Control. *Adv Immunol,* 129**,** 109-74.

Rothhammer, T., J. C. Hahne, A. Florin, I. Poser, F. Soncin, N. Wernert & A. K. Bosserhoff (2004) The Ets-1 transcription factor is involved in the development and invasion of malignant melanoma. *Cellular and Molecular Life Sciences CMLS,* 61**,** 118-128.

Roti, G., A. Carlton, K. N. Ross, M. Markstein, K. Pajcini, A. H. Su, N. Perrimon, W. S. Pear, A. L. Kung, S. C. Blacklow, J. C. Aster & K. Stegmaier (2013) Complementary genomic screens identify SERCA as a therapeutic target in NOTCH1 mutated cancer. *Cancer Cell,* 23**,** 390-405.

Roti, G. & K. Stegmaier (2014) New Approaches to Target T-ALL. *Front Oncol,* 4**,** 170.

Rowe, J. M., G. Buck, A. K. Burnett, R. Chopra, P. H. Wiernik, S. M. Richards, H. M. Lazarus, I. M. Franklin, M. R. Litzow, N. Ciobanu, H. G. Prentice, J. Durrant, M. S. Tallman, A. H. Goldstone, Ecog & M. N. A. L. W. Party (2005) Induction therapy for adults with acute lymphoblastic leukemia: results of more than 1500 patients from the international ALL trial: MRC UKALL XII/ECOG E2993. *Blood,* 106**,** 3760-7.

Ryan, R. J., Y. Drier, H. Whitton, M. J. Cotton, J. Kaur, R. Issner, S. Gillespie, C. B. Epstein, V. Nardi, A. R. Sohani, E. P. Hochberg & B. E. Bernstein (2015) Detection of Enhancer-Associated Rearrangements Reveals Mechanisms of Oncogene Dysregulation in B-cell Lymphoma. *Cancer Discov,* 5**,** 1058-71.

Sade, H., S. Krishna & A. Sarin (2004) The anti-apoptotic effect of Notch-1 requires p56lck-dependent, Akt/PKB-mediated signaling in T cells. *J Biol Chem,* 279**,** 2937-44.

Saeki, H., H. Kuwano, H. Kawaguchi, S. Ohno & K. Sugimachi (2000) Expression of Ets-1 transcription factor is correlated with penetrating tumor progression in patients with squamous cell carcinoma of the esophagus. *Cancer,* 89**,** 1670-1676.

Saito, S., Y.-C. Lin, M.-H. Tsai, C.-S. Lin, Y. Murayama, R. Sato & K. K. Yokoyama (2015) Emerging roles of hypoxia-inducible factors and reactive oxygen species in cancer and pluripotent stem cells. *The Kaohsiung Journal of Medical Sciences,* 31**,** 279-286.

Sampath, J., D. Sun, V. J. Kidd, J. Grenet, A. Gandhi, L. H. Shapiro, Q. Wang, G. P. Zambetti & J. D. Schuetz (2001) Mutant p53 Cooperates with ETS and Selectively Up-regulates Human MDR1 Not MRP1. *Journal of Biological Chemistry,* 276**,** 39359-39367.

Sanchez-Irizarry, C., A. C. Carpenter, A. P. Weng, W. S. Pear, J. C. Aster & S. C. Blacklow (2004) Notch subunit heterodimerization and prevention of ligand-independent proteolytic activation depend, respectively, on a novel domain and the LNR repeats. *Mol Cell Biol,* 24**,** 9265-73.

Sanchez-Martin, M., A. Ambesi-Impiombato, Y. Qin, D. Herranz, M. Bansal, T. Girardi, E. Paietta, M. S. Tallman, J. M. Rowe, K. De Keersmaecker, A. Califano & A. A. Ferrando (2017) Synergistic antileukemic therapies in NOTCH1-induced T-ALL. *Proc Natl Acad Sci U S A,* 114**,** 2006-2011.

Sanda, T., L. N. Lawton, M. I. Barrasa, Z. P. Fan, H. Kohlhammer, A. Gutierrez, W. Ma, J. Tatarek, Y. Ahn, M. A. Kelliher, C. H. Jamieson, L. M. Staudt, R. A. Young & A. T. Look (2012) Core transcriptional regulatory circuit controlled by the TAL1 complex in human T cell acute lymphoblastic leukemia. *Cancer Cell,* 22**,** 209-21.

Sawai, C. M., J. Freund, P. Oh, D. Ndiaye-Lobry, J. C. Bretz, A. Strikoudis, L. Genesca, T. Trimarchi, M. A. Kelliher, M. Clark, J. Soulier, S. Chen-Kiang & I. Aifantis (2012) Therapeutic targeting of the cyclin D3:CDK4/6 complex in T cell leukemia. *Cancer Cell,* 22**,** 452-65.

Schnell, S. A., A. Ambesi-Impiombato, M. Sanchez-Martin, L. Belver, L. Xu, Y. Qin, R. Kageyama & A. A. Ferrando (2015) Therapeutic targeting of HES1 transcriptional programs in T-ALL. *Blood,* 125**,** 2806-14.

Schroeter, E. H., J. A. Kisslinger & R. Kopan (1998) Notch-1 signalling requires ligand-induced proteolytic release of intracellular domain. *Nature,* 393**,** 382-6.

Schwickart, M., X. Huang, J. R. Lill, J. Liu, R. Ferrando, D. M. French, H. Maecker, K. O'Rourke, F. Bazan, J. Eastham-Anderson, P. Yue, D. Dornan, D. C. S. Huang & V. M. Dixit (2010) Deubiquitinase USP9X stabilizes MCL1 and promotes tumour cell survival. *Nature,* 463**,** 103-107.

Scripture-Adams, D. D., S. S. Damle, L. Li, K. J. Elihu, S. Qin, A. M. Arias, R. R. Butler, 3rd, A. Champhekar, J. A. Zhang & E. V. Rothenberg (2014) GATA-3 dose-dependent checkpoints in early T cell commitment. *J Immunol,* 193**,** 3470-91.

Seth, A. & T. S. Papas (1990) The c-ets-1 proto-oncogene has oncogenic activity and is positively autoregulated. *Oncogene,* 5**,** 1761-1767.

Seth, A. & D. K. Watson (2005) ETS transcription factors and their emerging roles in human cancer. *Eur J Cancer,* 41**,** 2462-78.

Sharma, V. M., J. A. Calvo, K. M. Draheim, L. A. Cunningham, N. Hermance, L. Beverly, V. Krishnamoorthy, M. Bhasin, A. J. Capobianco & M. A. Kelliher (2006) Notch1 contributes to mouse T-cell leukemia by directly inducing the expression of c-myc. *Mol Cell Biol,* 26**,** 8022-31.

Shiina, M., K. Hamada, T. Inoue-Bungo, M. Shimamura, S. Baba, K. Sato & K. Ogata (2014) Crystallization of the Ets1-Runx1-CBFbeta-DNA complex formed on the TCRalpha gene enhancer. *Acta Crystallogr F Struct Biol Commun,* 70**,** 1380-4.

Shiina, M., K. Hamada, T. Inoue-Bungo, M. Shimamura, A. Uchiyama, S. Baba, K. Sato, M. Yamamoto & K. Ogata (2015) A novel allosteric mechanism on protein-DNA interactions underlying the phosphorylation-dependent regulation of Ets1 target gene expressions. *J Mol Biol,* 427**,** 1655-69.

Shin, H. M., L. M. Minter, O. H. Cho, S. Gottipati, A. H. Fauq, T. E. Golde, G. E. Sonenshein & B. A. Osborne (2006) Notch1 augments NF-kappaB activity by facilitating its nuclear retention. *Embo j,* 25**,** 129-38.

Shochat, C., N. Tal, O. R. Bandapalli, C. Palmi, I. Ganmore, G. te Kronnie, G. Cario, G. Cazzaniga, A. E. Kulozik, M. Stanulla, M. Schrappe, A. Biondi, G. Basso, D. Bercovich, M. U. Muckenthaler & S. Izraeli (2011) Gain-of-function mutations in interleukin-7 receptor-alpha (IL7R) in childhood acute lymphoblastic leukemias. *J Exp Med,* 208**,** 901-8.

Shrivastava, T., K. Mino, N. D. Babayeva, O. I. Baranovskaya, A. Rizzino & T. H. Tahirov (2014) Structural basis of Ets1 activation by Runx1. *Leukemia,* 28**,** 2040-2048.

Sicinska, E., I. Aifantis, L. Le Cam, W. Swat, C. Borowski, Q. Yu, A. A. Ferrando, S. D. Levin, Y. Geng, H. von Boehmer & P. Sicinski (2003) Requirement for cyclin D3 in lymphocyte development and T cell leukemias. *Cancer Cell,* 4**,** 451-61.

Sieweke, M. H., H. Tekotte, J. Frampton & T. Graf (1996) MafB is an interaction partner and repressor of Ets-1 that inhibits erythroid differentiation. *Cell,* 85**,** 49-60.

Smith, S., R. Tripathi, C. Goodings, S. Cleveland, E. Mathias, J. A. Hardaway, N. Elliott, Y. Yi, X. Chen, J. Downing, C. Mullighan, D. A. Swing, L. Tessarollo, L. Li, P. Love, N. A. Jenkins, N. G. Copeland, M. A. Thompson, Y. Du & U. P. Dave (2014) LIM domain only-2 (LMO2) induces T-cell leukemia by two distinct pathways. *PLoS One,* 9**,** e85883.

Song, C., C. Gowda, X. Pan, Y. Ding, Y. Tong, B. H. Tan, H. Wang, S. Muthusami, Z. Ge, M. Sachdev, S. G. Amin, D. Desai, K. Gowda, R. Gowda, G. P. Robertson, H. Schjerven, M. Muschen, K. J. Payne & S. Dovat (2015) Targeting casein kinase II restores Ikaros tumor suppressor activity and demonstrates therapeutic efficacy in high-risk leukemia. *Blood,* 126**,** 1813-22.

Song, C., X. Pan, Z. Ge, C. Gowda, Y. Ding, H. Li, Z. Li, G. Yochum, M. Muschen, Q. Li, K. J. Payne & S. Dovat. 2016. Epigenetic regulation of gene expression by Ikaros, HDAC1 and Casein Kinase II in leukemia. In *Leukemia*, 1436-40. England.

Strohmaier, H., C. H. Spruck, P. Kaiser, K. A. Won, O. Sangfelt & S. I. Reed (2001) Human F-box protein hCdc4 targets cyclin E for proteolysis and is mutated in a breast cancer cell line. *Nature,* 413**,** 316-22.

Sulis, M. L., O. Williams, T. Palomero, V. Tosello, S. Pallikuppam, P. J. Real, K. Barnes, L. Zuurbier, J. P. Meijerink & A. A. Ferrando (2008) NOTCH1 extracellular juxtamembrane expansion mutations in T-ALL. *Blood,* 112**,** 733-40.

Sunshine, A., D. Goich, A. Stith, K. Sortino, J. Dalton, S. Metcalfe, E. C. Svensson & L. A. Garrett-Sinha (2019) Ets1 Controls the Development of B Cell Autoimmune Responses in a Cell-Intrinsic Manner. *ImmunoHorizons,* 3**,** 331.

Takai, N., T. Miyazaki, K. Fujisawa, K. Nasu & I. Miyakawa (2000) Expression of c-Ets1 is associated with malignant potential in endometrial carcinoma. *Cancer,* 89**,** 2059-2067.

Takaku, M., S. A. Grimm, T. Shimbo, L. Perera, R. Menafra, H. G. Stunnenberg, T. K. Archer, S. Machida, H. Kurumizaka & P. A. Wade (2016) GATA3-dependent cellular reprogramming requires activation-domain dependent recruitment of a chromatin remodeler. *Genome Biol,* 17**,** 36.

Takanami, I., K. Takeuchi & M. Karuke (2001) Expression of Ets-1 is correlated with urokinase-type plasminogen activator and poor prognosis in pulmonary adenocarcinoma. *Tumor Biology,* 22**,** 205-210.

Tan, Y., E. Sementino, J. Xu, J. Pei, Z. Liu, T. K. Ito, K. Q. Cai, S. Peri, A. J. Klein-Szanto, D. L. Wiest & J. R. Testa (2017) The homeoprotein Dlx5 drives murine T-cell lymphomagenesis by directly transactivating Notch and upregulating Akt signaling. *Oncotarget,* 8**,** 14941-14956.

Tatarek, J., K. Cullion, T. Ashworth, R. Gerstein, J. C. Aster & M. A. Kelliher (2011) Notch1 inhibition targets the leukemia-initiating cells in a Tal1/Lmo2 mouse model of T-ALL. *Blood,* 118**,** 1579-90.

Tetsu, O. & F. McCormick (2017) ETS-targeted therapy: can it substitute for MEK inhibitors? *Clin Transl Med,* 6**,** 16.

Thompson, B. J., S. Buonamici, M. L. Sulis, T. Palomero, T. Vilimas, G. Basso, A. Ferrando & I. Aifantis (2007) The SCFFBW7 ubiquitin ligase complex as a tumor suppressor in T cell leukemia. *J Exp Med,* 204**,** 1825-35.

Tian, G., B. Erman, H. Ishii, S. S. Gangopadhyay & R. Sen (1999) Transcriptional activation by ETS and leucine zipper-containing basic helix-loop-helix proteins. *Molecular and cellular biology,* 19**,** 2946-2957.

Townsend, E. C., M. A. Murakami, A. Christodoulou, A. L. Christie, J. Koster, T. A. DeSouza, E. A. Morgan, S. P. Kallgren, H. Liu, S. C. Wu, O. Plana, J. Montero, K. E. Stevenson, P. Rao, R. Vadhi, M. Andreeff, P. Armand, K. K. Ballen, P. Barzaghi-Rinaudo, S. Cahill, R. A. Clark, V. G. Cooke, M. S. Davids, D. J. DeAngelo, D. M. Dorfman, H. Eaton, B. L. Ebert, J. Etchin, B. Firestone, D. C. Fisher, A. S. Freedman, I. A. Galinsky, H. Gao, J. S. Garcia, F. Garnache-Ottou, T. A. Graubert, A. Gutierrez, E. Halilovic, M. H. Harris, Z. T. Herbert, S. M. Horwitz, G. Inghirami, A. M. Intlekofer, M. Ito, S. Izraeli, E. D. Jacobsen, C. A. Jacobson, S. Jeay, I. Jeremias, M. A. Kelliher, R. Koch, M. Konopleva, N. Kopp, S. M. Kornblau, A. L. Kung, T. S. Kupper, N. R. LeBoeuf, A. S. LaCasce, E. Lees, L. S. Li, A. T. Look, M. Murakami, M. Muschen, D. Neuberg, S. Y. Ng, O. O. Odejide, S. H. Orkin, R. R. Paquette, A. E. Place, J. E. Roderick, J. A. Ryan, S. E. Sallan, B. Shoji, L. B. Silverman, R. J. Soiffer, D. P. Steensma, K. Stegmaier, R. M. Stone, J. Tamburini, A. R. Thorner, P. van Hummelen, M. Wadleigh, M. Wiesmann, A. P. Weng, J. U. Wuerthner, D. A. Williams, B. M. Wollison, A. A. Lane, A. Letai, M. M. Bertagnolli, J. Ritz, M. Brown, H. Long, J. C. Aster, M. A. Shipp, J. D. Griffin & D. M. Weinstock (2016) The Public Repository of Xenografts Enables Discovery and Randomized Phase II-like Trials in Mice. *Cancer Cell,* 30**,** 183.

Tran, I. T., A. R. Sandy, A. J. Carulli, C. Ebens, J. Chung, G. T. Shan, V. Radojcic, A. Friedman, T. Gridley, A. Shelton, P. Reddy, L. C. Samuelson, M. Yan, C. W. Siebel & I. Maillard (2013) Blockade of individual Notch ligands and receptors controls graft-versus-host disease. *The Journal of Clinical Investigation,* 123**,** 1590-1604.

Trapnell, C., D. G. Hendrickson, M. Sauvageau, L. Goff, J. L. Rinn & L. Pachter (2013) Differential analysis of gene regulation at transcript resolution with RNA-seq. *Nat Biotechnol,* 31**,** 46-53.

Trimarchi, T., E. Bilal, P. Ntziachristos, G. Fabbri, R. Dalla-Favera, A. Tsirigos & I. Aifantis (2014) Genome-wide mapping and characterization of Notch-regulated long noncoding RNAs in acute leukemia. *Cell,* 158**,** 593-606.

Trinquand, A., A. Tanguy-Schmidt, R. Ben Abdelali, J. Lambert, K. Beldjord, E. Lengline, N. De Gunzburg, D. Payet-Bornet, L. Lhermitte, H. Mossafa, V. Lheritier, J. Bond, F. Huguet, A. Buzyn, T. Leguay, J. Y. Cahn, X. Thomas, Y. Chalandon, A. Delannoy, C. Bonmati, S. Maury, B. Nadel, E. Macintyre, N. Ifrah, H. Dombret & V. Asnafi (2013) Toward a NOTCH1/FBXW7/RAS/PTEN-based oncogenetic risk classification of adult T-cell acute lymphoblastic leukemia: a Group for Research in Adult Acute Lymphoblastic Leukemia study. *J Clin Oncol,* 31**,** 4333-42.

Uren, A. G., J. Kool, K. Matentzoglu, J. de Ridder, J. Mattison, M. van Uitert, W. Lagcher, D. Sie, E. Tanger, T. Cox, M. Reinders, T. J. Hubbard, J. Rogers, J. Jonkers, L. Wessels, D. J. Adams, M. van Lohuizen & A. Berns (2008) Large-scale mutagenesis in p19(ARF)- and p53-deficient mice identifies cancer genes and their collaborative networks. *Cell,* 133**,** 727-41.

van Es, J. H., M. E. van Gijn, O. Riccio, M. van den Born, M. Vooijs, H. Begthel, M. Cozijnsen, S. Robine, D. J. Winton, F. Radtke & H. Clevers (2005) Notch/gamma-secretase inhibition turns proliferative cells in intestinal crypts and adenomas into goblet cells. *Nature,* 435**,** 959-63.

Vanden Bempt, M., S. Demeyer, M. Broux, J. De Bie, S. Bornschein, N. Mentens, R. Vandepoel, E. Geerdens, E. Radaelli, B. C. Bornhauser, A. E. Kulozik, J. P. Meijerink, J. P. Bourquin, C. E. de Bock & J. Cools (2018) Cooperative Enhancer Activation by TLX1 and STAT5 Drives Development of NUP214-ABL1/TLX1-Positive T Cell Acute Lymphoblastic Leukemia. *Cancer Cell,* 34**,** 271-285 e7.

VanDussen, K. L., A. J. Carulli, T. M. Keeley, S. R. Patel, B. J. Puthoff, S. T. Magness, I. T. Tran, I. Maillard, C. Siebel, A. Kolterud, A. S. Grosse, D. L. Gumucio, S. A. Ernst, Y. H. Tsai, P. J. Dempsey & L. C. Samuelson (2012) Notch signaling modulates proliferation and differentiation of intestinal crypt base columnar stem cells. *Development,* 139**,** 488-97.

Vilimas, T., J. Mascarenhas, T. Palomero, M. Mandal, S. Buonamici, F. Meng, B. Thompson, C. Spaulding, S. Macaroun, M. L. Alegre, B. L. Kee, A. Ferrando, L. Miele & I. Aifantis (2007) Targeting the NF-kappaB signaling pathway in Notch1-induced T-cell leukemia. *Nat Med,* 13**,** 70-7.

Vilotti, S., M. Biagioli, R. Foti, M. Dal Ferro, Z. S. Lavina, L. Collavin, G. Del Sal, S. Zucchelli & S. Gustincich (2012) The PML nuclear bodies-associated protein TTRAP regulates ribosome biogenesis in nucleolar cavities upon proteasome inhibition. *Cell Death and Differentiation,* 19**,** 488-500.

Walunas, T. L., B. Wang, C. R. Wang & J. M. Leiden (2000) Cutting edge: the Ets1 transcription factor is required for the development of NK T cells in mice. *J Immunol,* 164**,** 2857-60.

Wang, D., S. A. John, J. L. Clements, D. H. Percy, K. P. Barton & L. A. Garrett-Sinha (2005) Ets-1 deficiency leads to altered B cell differentiation, hyperresponsiveness to TLR9 and autoimmune disease. *Int Immunol,* 17**,** 1179-91.

Wang, H., C. Zang, L. Taing, K. L. Arnett, Y. J. Wong, W. S. Pear, S. C. Blacklow, X. S. Liu & J. C. Aster (2014a) NOTCH1-RBPJ complexes drive target gene expression through dynamic interactions with superenhancers. *Proc Natl Acad Sci U S A,* 111**,** 705-10.

Wang, H., J. Zou, B. Zhao, E. Johannsen, T. Ashworth, H. Wong, W. S. Pear, J. Schug, S. C. Blacklow, K. L. Arnett, B. E. Bernstein, E. Kieff & J. C. Aster (2011) Genome-wide analysis reveals conserved and divergent features of Notch1/RBPJ binding in human and murine T-lymphoblastic leukemia cells. *Proc Natl Acad Sci U S A,* 108**,** 14908-13.

Wang, J. H., A. Nichogiannopoulou, L. Wu, L. Sun, A. H. Sharpe, M. Bigby & K. Georgopoulos (1996) Selective defects in the development of the fetal and adult lymphoid system in mice with an Ikaros null mutation. *Immunity,* 5**,** 537-49.

Wang, Q., R. Yan, N. Pinnell, A. C. McCarter, Y. Oh, Y. Liu, C. Sha, N. F. Garber, Y. Chen, Q. Wu, C. J. Ku, I. Tran, A. Serna Alarcon, R. Kuick, J. D. Engel, I. Maillard, T. Cierpicki & M. Y. Chiang (2018) Stage-specific roles for Zmiz1 in Notch-dependent steps of early T-cell development. *Blood,* 132**,** 1279-1292.

Wang, S., R. K. Kollipara, N. Srivastava, R. Li, P. Ravindranathan, E. Hernandez, E. Freeman, C. G. Humphries, P. Kapur, Y. Lotan, L. Fazli, M. E. Gleave, S. R. Plymate, G. V. Raj, J.-T. Hsieh & R. Kittler (2014b) Ablation of the oncogenic transcription factor ERG by deubiquitinase inhibition in prostate cancer. *Proceedings of the National Academy of Sciences,* 111**,** 4251.

Wang, X., S. Feng, J. Fan, X. Li, Q. Wen & N. Luo (2016) New strategy for renal fibrosis: Targeting Smad3 proteins for ubiquitination and degradation. *Biochem Pharmacol,* 116**,** 200-9.

Wang, X., Y. Qiao, I. A. Asangani, B. Ateeq, A. Poliakov, M. Cieslik, S. Pitchiaya, B. Chakravarthi, X. Cao, X. Jing, C. X. Wang, I. J. Apel, R. Wang, J. C. Tien, K. M. Juckette, W. Yan, H. Jiang, S. Wang, S. Varambally & A. M. Chinnaiyan (2017a) Development of Peptidomimetic Inhibitors of the ERG Gene Fusion Product in Prostate Cancer. *Cancer Cell,* 31**,** 532-548.e7.

Wang, Z., Y. Hu, D. Xiao, J. Wang, C. Liu, Y. Xu, X. Shi, P. Jiang, L. Huang, P. Li, H. Liu & G. Qing (2017b) Stabilization of Notch1 by the Hsp90 Chaperone Is Crucial for T-Cell Leukemogenesis. *Clin Cancer Res,* 23**,** 3834-3846.

Wasylyk, C., S. E. Schlumberger, P. Criqui-Filipe & B. Wasylyk (2002) Sp100 interacts with ETS-1 and stimulates its transcriptional activity. *Molecular and Cellular Biology,* 22**,** 2687-2702.

Watanabe, D., H. Takagi, K. Suzuma, I. Suzuma, H. Oh, H. Ohashi, S. Kemmochi, A. Uemura, T. Ojima, E. Suganami, N. Miyamoto, Y. Sato & Y. Honda (2004) Transcription Factor Ets-1 Mediates Ischemia- and Vascular Endothelial Growth Factor-Dependent Retinal Neovascularization. *American Journal of Pathology,* 164**,** 1827-1835.

Wei, G., B. J. Abraham, R. Yagi, R. Jothi, K. Cui, S. Sharma, L. Narlikar, D. L. Northrup, Q. Tang, W. E. Paul, J. Zhu & K. Zhao (2011) Genome-wide analyses of transcription factor GATA3-mediated gene regulation in distinct T cell types. *Immunity,* 35**,** 299-311.

Wei, G., R. Srinivasan, C. Z. Cantemir-Stone, S. M. Sharma, R. Santhanam, M. Weinstein, N. Muthusamy, A. K. Man, R. G. Oshima, G. Leone & M. C. Ostrowski (2009) Ets1 and Ets2 are required for endothelial cell survival during embryonic angiogenesis. *Blood,* 114**,** 1123-30.

Wei, G. H., G. Badis, M. F. Berger, T. Kivioja, K. Palin, M. Enge, M. Bonke, A. Jolma, M. Varjosalo, A. R. Gehrke, J. Yan, S. Talukder, M. Turunen, M. Taipale, H. G. Stunnenberg, E. Ukkonen, T. R. Hughes, M. L. Bulyk & J. Taipale (2010) Genome-wide analysis of ETS-family DNA-binding in vitro and in vivo. *EMBO J,* 29**,** 2147-60.

Wei, W., J. Jin, S. Schlisio, J. W. Harper & W. G. Kaelin, Jr. (2005) The v-Jun point mutation allows c-Jun to escape GSK3-dependent recognition and destruction by the Fbw7 ubiquitin ligase. *Cancer Cell,* 8**,** 25-33.

Welcker, M., A. Orian, J. Jin, J. E. Grim, J. W. Harper, R. N. Eisenman & B. E. Clurman (2004) The Fbw7 tumor suppressor regulates glycogen synthase kinase 3 phosphorylation-dependent c-Myc protein degradation. *Proc Natl Acad Sci U S A,* 101**,** 9085-90.

Wendorff, A. A., U. Koch, F. T. Wunderlich, S. Wirth, C. Dubey, J. C. Bruning, H. R. MacDonald & F. Radtke (2010) Hes1 is a critical but context-dependent mediator of canonical Notch signaling in lymphocyte development and transformation. *Immunity,* 33**,** 671-84.

Weng, A. P., A. A. Ferrando, W. Lee, J. P. t. Morris, L. B. Silverman, C. Sanchez-Irizarry, S. C. Blacklow, A. T. Look & J. C. Aster (2004) Activating mutations of NOTCH1 in human T cell acute lymphoblastic leukemia. *Science,* 306**,** 269-71.

Weng, A. P., J. M. Millholland, Y. Yashiro-Ohtani, M. L. Arcangeli, A. Lau, C. Wai, C. Del Bianco, C. G. Rodriguez, H. Sai, J. Tobias, Y. Li, M. S. Wolfe, C. Shachaf, D. Felsher, S. C. Blacklow, W. S. Pear & J. C. Aster (2006) c-Myc is an important direct target of Notch1 in T-cell acute lymphoblastic leukemia/lymphoma. *Genes Dev,* 20**,** 2096-109.

Weng, A. P., Y. Nam, M. S. Wolfe, W. S. Pear, J. D. Griffin, S. C. Blacklow & J. C. Aster (2003) Growth suppression of pre-T acute lymphoblastic leukemia cells by inhibition of notch signaling. *Mol Cell Biol,* 23**,** 655-64.

Wertz, I. E., S. Kusam, C. Lam, T. Okamoto, W. Sandoval, D. J. Anderson, E. Helgason, J. A. Ernst, M. Eby, J. Liu, L. D. Belmont, J. S. Kaminker, K. M. O'Rourke, K. Pujara, P. B. Kohli, A. R. Johnson, M. L. Chiu, J. R. Lill, P. K. Jackson, W. J. Fairbrother, S. Seshagiri, M. J. Ludlam, K. G. Leong, E. C. Dueber, H. Maecker, D. C. Huang & V. M. Dixit (2011) Sensitivity to antitubulin chemotherapeutics is regulated by MCL1 and FBW7. *Nature,* 471**,** 110-4.

Wilson, L. A., A. Gemin, R. Espiritu & G. Singh (2005) ets-1 is transcriptionally up-regulated by H2O2 via an antioxidant response element. *FASEB Journal,* 19**,** 2085-2087.

Winter, G. E., D. L. Buckley, J. Paulk, J. M. Roberts, A. Souza, S. Dhe-Paganon & J. E. Bradner (2015) Phthalimide conjugation as a strategy for in vivo target protein degradation. *Science,* 348**,** 1376.

Witkowski, M. T., L. Cimmino, Y. Hu, T. Trimarchi, H. Tagoh, M. D. McKenzie, S. A. Best, L. Tuohey, T. A. Willson, S. L. Nutt, M. Busslinger, I. Aifantis, G. K. Smyth & R. A. Dickins (2015) Activated Notch counteracts Ikaros tumor suppression in mouse and human T-cell acute lymphoblastic leukemia. *Leukemia,* 29**,** 1301-11.

Wolfer, A., A. Wilson, M. Nemir, H. R. MacDonald & F. Radtke (2002) Inactivation of Notch1 impairs VDJbeta rearrangement and allows pre-TCR-independent survival of early alpha beta Lineage Thymocytes. *Immunity,* 16**,** 869-79.

Wouters, B. J., M. A. Jorda, K. Keeshan, I. Louwers, C. A. Erpelinck-Verschueren, D. Tielemans, A. W. Langerak, Y. He, Y. Yashiro-Ohtani, P. Zhang, C. J. Hetherington, R. G. Verhaak, P. J. Valk, B. Lowenberg, D. G. Tenen, W. S. Pear & R. Delwel (2007) Distinct gene expression profiles of acute myeloid/T-lymphoid leukemia with silenced CEBPA and mutations in NOTCH1. *Blood,* 110**,** 3706-14.

Wu, Y., C. Cain-Hom, L. Choy, T. J. Hagenbeek, G. P. de Leon, Y. Chen, D. Finkle, R. Venook, X. Wu, J. Ridgway, D. Schahin-Reed, G. J. Dow, A. Shelton, S. Stawicki, R. J. Watts, J. Zhang, R. Choy, P. Howard, L. Kadyk, M. Yan, J. Zha, C. A. Callahan, S. G. Hymowitz

& C. W. Siebel (2010) Therapeutic antibody targeting of individual Notch receptors. *Nature,* 464**,** 1052-7.

Wu, Z. J., R. A. Irizarry, R. Gentleman, F. Martinez-Murillo & F. Spencer (2004) A model-based background adjustment for oligonucleotide expression arrays. *Journal of the American Statistical Association,* 99**,** 909-917.

Xu, W., T. Carr, K. Ramirez, S. McGregor, M. Sigvardsson & B. L. Kee (2013) E2A transcription factors limit expression of Gata3 to facilitate T lymphocyte lineage commitment. *Blood,* 121**,** 1534-42.

Yada, M., S. Hatakeyama, T. Kamura, M. Nishiyama, R. Tsunematsu, H. Imaki, N. Ishida, F. Okumura, K. Nakayama & K. I. Nakayama (2004) Phosphorylation-dependent degradation of c-Myc is mediated by the F-box protein Fbw7. *Embo j,* 23**,** 2116-25.

Yamaguchi, E., T. Nakayama, A. Nanashima, K. Matsumoto, T. Yasutake, I. Sekine & T. Nagayasu (2007) Ets-1 proto-oncogene as a potential predictor for poor prognosis of lung adenocarcinoma. *Tohoku Journal of Experimental Medicine,* 213**,** 41-50.

Yang, B. S., C. A. Hauser, G. Henkel, M. S. Colman, C. Van Beveren, K. J. Stacey, D. A. Hume, R. A. Maki & M. C. Ostrowski (1996) Ras-mediated phosphorylation of a conserved threonine residue enhances the transactivation activities of c-Ets1 and c-Ets2. *Mol Cell Biol,* 16**,** 538-47.

Yang, C., L. H. Shapiro, M. Rivera, A. Kumar & P. K. Brindle (1998) A role for CREB binding protein and p300 transcriptional coactivators in Ets-1 transactivation functions. *Molecular and Cellular Biology,* 18**,** 2218-2229.

Yashiro-Ohtani, Y., Y. He, T. Ohtani, M. E. Jones, O. Shestova, L. Xu, T. C. Fang, M. Y. Chiang, A. M. Intlekofer, S. C. Blacklow, Y. Zhuang & W. S. Pear (2009) Pre-TCR signaling inactivates Notch1 transcription by antagonizing E2A. *Genes Dev,* 23**,** 1665-76.

Yashiro-Ohtani, Y., H. Wang, C. Zang, K. L. Arnett, W. Bailis, Y. Ho, B. Knoechel, C. Lanauze, L. Louis, K. S. Forsyth, S. Chen, Y. Chung, J. Schug, G. A. Blobel, S. A. Liebhaber, B. E. Bernstein, S. C. Blacklow, X. S. Liu, J. C. Aster & W. S. Pear (2014a) Long-range enhancer activity determines Myc sensitivity to Notch inhibitors in T cell leukemia. *Proc Natl Acad Sci U S A*.

--- (2014b) Long-range enhancer activity determines Myc sensitivity to Notch inhibitors in T cell leukemia. *Proc Natl Acad Sci U S A,* 111**,** E4946-53.

Yatim, A., C. Benne, B. Sobhian, S. Laurent-Chabalier, O. Deas, J. G. Judde, J. D. Lelievre, Y. Levy & M. Benkirane (2012) NOTCH1 nuclear interactome reveals key regulators of its transcriptional activity and oncogenic function. *Mol Cell,* 48**,** 445-58.

Yordy, J. S., R. Li, V. I. Sementchenko, H. Pei, R. C. Muise-Helmericks & D. K. Watson (2004) SP100 expression modulates ETS1 transcriptional activity and inhibits cell invasion. *Oncogene,* 23**,** 6654-6665.

Yu, S., D. M. Zhao, R. Jothi & H. H. Xue (2010) Critical requirement of GABPalpha for normal T cell development. *J Biol Chem,* 285**,** 10179-88.

Yu, V. W., B. Saez, C. Cook, S. Lotinun, A. Pardo-Saganta, Y. H. Wang, S. Lymperi, F. Ferraro, M. H. Raaijmakers, J. Y. Wu, L. Zhou, J. Rajagopal, H. M. Kronenberg, R. Baron & D. T. Scadden (2015) Specific bone cells produce DLL4 to generate thymus-seeding progenitors from bone marrow. *J Exp Med,* 212**,** 759-74.

Yuan, T., Y. Yang, J. Chen, W. Li, Q. Zhang, Y. Mi, R. S. Goswami, J. Q. You, D. Lin, M. D. Qian, S. Calin, Y. Liang, R. N. Miranda, G. A. Calin, X. Zhou, L. Ma, P. A. Zweidler-McKay, B. Liu, A. P. Weng, L. J. Medeiros, Y. Zhang & M. J. You (2017) Regulation of

PI3K signaling in T-cell acute lymphoblastic leukemia: a novel PTEN/Ikaros/miR-26b mechanism reveals a critical targetable role for PIK3CD. *Leukemia,* 31**,** 2355-2364.

Zenatti, P. P., D. Ribeiro, W. Li, L. Zuurbier, M. C. Silva, M. Paganin, J. Tritapoe, J. A. Hixon, A. B. Silveira, B. A. Cardoso, L. M. Sarmento, N. Correia, M. L. Toribio, J. Kobarg, M. Horstmann, R. Pieters, S. R. Brandalise, A. A. Ferrando, J. P. Meijerink, S. K. Durum, J. A. Yunes & J. T. Barata (2011) Oncogenic IL7R gain-of-function mutations in childhood T-cell acute lymphoblastic leukemia. *Nat Genet,* 43**,** 932-9.

Zook, E. C., K. Ramirez, X. Guo, G. van der Voort, M. Sigvardsson, E. C. Svensson, Y. X. Fu & B. L. Kee (2016) The ETS1 transcription factor is required for the development and cytokine-induced expansion of ILC2. *J Exp Med,* 213**,** 687-96.

Zuurbier, L., E. F. Petricoin, 3rd, M. J. Vuerhard, V. Calvert, C. Kooi, J. G. Buijs-Gladdines, W. K. Smits, E. Sonneveld, A. J. Veerman, W. A. Kamps, M. Horstmann, R. Pieters & J. P. Meijerink (2012) The significance of PTEN and AKT aberrations in pediatric T-cell acute lymphoblastic leukemia. *Haematologica,* 97**,** 1405-13.

Zweidler-McKay, P. A., D. J. DeAngelo, D. Douer, H. Dombret, O. G. Ottmann, N. Vey, D. A. Thomas, L. Zhu, F. Huang, G. Bajaj & B. S. Fischer (2014) The Safety and Activity of BMS-906024, a Gamma Secretase Inhibitor (GSI) with Anti-Notch Activity, in Patients with Relapsed T-Cell Acute Lymphoblastic Leukemia (T-ALL): Initial Results of a Phase 1 Trial. *Blood,* 124**,** 968-968.